

SRR-CWDA-2010-00093
Revision 2

H-Area Tank Farm Stochastic Fate and Transport Model

August 2012

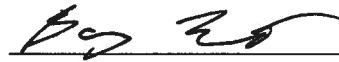
Prepared by: Savannah River Remediation LLC
Closure and Waste Disposal Authority
Aiken, SC 29808



Prepared for U.S. Department of Energy Under Contract No. DE-AC09-09SR22505

APPROVALS

Author:



Barry Lester
Savannah River Remediation LLC
Closure & Waste Disposal Authority

8/2/12
Date

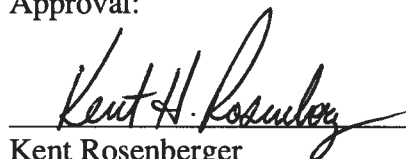
Technical Review:



David Watkins
Savannah River Remediation LLC
Closure & Waste Disposal Authority

8/2/12
Date

Approval:



Kent Rosenberger
Savannah River Remediation LLC
Closure & Waste Disposal Authority

8/3/12
Date

TABLE OF CONTENTS

APPROVALS	2
TABLE OF CONTENTS	3
LIST OF FIGURES	4
LIST OF TABLES	5
ACRONYMS	6
1.0 EXECUTIVE SUMMARY	7
2.0 PURPOSE	8
2.1 Advective-Dispersive Transport Model	8
2.2 Dose Calculator Model	9
3.0 UPDATES TO THE TRANSPORT MODEL TECHNICAL APPROACH	10
3.1 GoldSim Vadose Zone Model	10
3.1.1 Vadose Zone Model Structural Changes	11
4.0 UPDATES TO THE TRANSPORT MODEL INPUTS	27
4.1 General Inputs	27
4.1.1 Species	27
4.2 HTF Source Inputs	34
4.2.1 Waste Tanks	34
4.2.2 Ancillary Equipment Inventories	47
4.3 Vadose Zone Inputs	54
4.4 Saturated Zone Inputs	56
4.4.1 Saturated Zone Darcy Velocity	56
4.4.2 Saturated Zone Geometry and Other Spatial Relationships	57
4.5 Material Properties	61
4.5.1 Adsorption	61
4.5.2 Physical Properties	68
5.0 DOSE CALCULATOR MODEL APPROACH	69
6.0 Dose Calculator Model Inputs	70
6.1 Updated Transfer Factors	70
7.0 MODEL BENCHMARKING	76
7.1 Case A (HTF Base Case)	77
7.1.1 Mass Releases to the Saturated Zone	77
7.1.2 100-Meter Well Locations	81
7.1.3 Total Dose Time Histories	92
7.1.4 Inadvertent Human Intrusion Case	95
8.0 REFERENCES	97
APPENDIX A	99
APPENDIX B	134

LIST OF FIGURES

Figure 3.1-1: Flow Chart Depicting Type III, IIIA, and IV Tanks.....	12
Figure 3.1-2: Flow Chart Depicting Type I and II Tanks.....	13
Figure 3.1-3: Typical Type I Tank Modeling Dimensions.....	17
Figure 3.1-4: Typical Type II Tank Modeling Dimensions.....	18
Figure 3.1-5: Sample Control File for <i>ReadFlowFields.dll</i>	21
Figure 3.1-6: PORFLOW Generated Stream Traces from Waste Tanks along with Hypothetical 1-Meter and 100-Meter Boundaries.....	26
Figure 4.4-1: PORFLOW Stream Traces with Hypothetical 100-Meter Boundary and Associated GoldSim Well Locations.....	57
Figure 4.4-2: Plume Formed by the Release of a Conservative Constituent from Tank 16.....	60
Figure 7.1-1: Plume Formed by a Pulse-Type Release of a Conservative Constituent from Tank 9.....	83
Figure 7.1-2: Plume Formed by a Pulse-Type Release of a Conservative Constituent from Tank 12.....	84
Figure 7.1-3: Plume Formed by a Pulse-Type Release of a Conservative Constituent from Tank 15.....	85
Figure 7.1-4: Plume Formed by a Pulse-Type Release of a Conservative Constituent from Tank 24.....	86
Figure 7.1-5: Plume Formed by a Pulse-Type Release of a Conservative Constituent from Tank 29.....	87
Figure 7.1-6: Plume Formed by a Pulse-Type Release of a Conservative Constituent from Tank 40.....	88
Figure 7.1-7: Plume Formed by a Pulse-Type Release of a Conservative Constituent from Tank 49.....	89
Figure 7.1-8: Plume Formed by a Steady Release of a Conservative Constituent from Tank 13.....	90
Figure 7.1-9: Plume Formed by Steady Release of Conservative Constituent from Tank 9.....	91
Figure 7.1-10: Comparison between PORFLOW and GoldSim Total Dose Results for Case A, Sector A.....	93
Figure 7.1-11: Comparison between PORFLOW and GoldSim Total Dose Results for Case A, Sector B.....	93
Figure 7.1-12: Comparison between PORFLOW and GoldSim Total Dose Results for Case A, Sector C.....	94
Figure 7.1-13: Comparison between PORFLOW and GoldSim Total Dose Results for Case A, Sector E.....	94
Figure 7.1-14: Comparison between PORFLOW and GoldSim Total Dose Results for Case A, Sector F.....	95
Figure 7.1-15: Comparison between PORFLOW and GoldSim Inadvertent Human Intrusion Results.....	96

LIST OF TABLES

Table 3.1-1: Vertical Discretization of the Basemat by Waste Tank Type 15

Table 3.1-2: Vertical Discretization of the UZ by Ancillary Equipment Source 16

Table 3.1-3: Instruction Data Passed to ReadFlowFields.dll 20

Table 3.1-4: Data Extracted from the Flow Field Files 20

Table 3.1-5: Liner Failure Times 22

Table 3.1-6: Parametric Cases (No Fast Flow Zones) 22

Table 3.1-7: Parametric Cases (Partial Fast Flow Zones) 23

Table 3.1-8: Parametric Cases (Full Fast Flow Zones) 23

Table 3.1-9: Inadvertent Intruder Analysis Wells 26

Table 4.1-1: GoldSim Model Species List 27

Table 4.1-2: Calculated Solubilities of Radionuclides of Interest 29

Table 4.1-3: Calculated Solubilities and Controlling Phases in Submerged Waste Tanks 31

Table 4.1-4: Probability Distributions for Various Phases Controlling Reduced Region II
Solubility 32

Table 4.1-5: Probability Distributions for Various Phases Controlling Oxidized Region II
Solubility 33

Table 4.1-6: Probability Distributions for Various Phases Controlling Oxidized Region III
Solubility 33

Table 4.1-7: Pore Volume Distribution for Chemical Condition Step Change 34

Table 4.2-1: HTF Estimated Radiological Inventory (Ci) at HTF Closure (2032) 36

Table 4.2-2: HTF Estimated Chemical Inventory (kg) at HTF Closure 40

Table 4.2-3: Type I Tank Annulus Floor Radiological Inventories 41

Table 4.2-4: Type II Tank Sand Pad Radiological Inventory 43

Table 4.2-5: Type II Annulus Floor Radiological Inventories 45

Table 4.2-6: Annulus Floor Inventories for Nonradioactive Species 47

Table 4.2-7: Sand Pad Inventories for Nonradioactive Species 47

Table 4.2-8: Radiological Ancillary Equipment Inventory: HTF Pump Tank and CTS Tank 48

Table 4.2-9: Radiological Ancillary Equipment Inventory: Evaporators 50

Table 4.2-10: Radiological Ancillary Equipment Inventory: Ancillary Piping Group 52

Table 4.2-11: Non-Radionuclide Ancillary Equipment Inventory: HTF Pump Tank and CTS
Tank 53

Table 4.2-12: Non-Radionuclide Ancillary Equipment Inventory: Evaporators 53

Table 4.2-13: Non-Radionuclide Ancillary Equipment Inventory: Ancillary Piping Group 54

Table 4.3-1: Flow Data Input Files 54

Table 4.4-1: Distance Traveled from Waste Tanks to 100-Meter Boundary 58

Table 4.4-2: Distance Traveled from Ancillary Equipment to 100-Meter Boundary 59

Table 4.5-1: Recommended K_d Values for Cementitious Reduced Regions 62

Table 4.5-2: Recommended K_d Values for Cementitious Oxidized Regions 64

Table 4.5-3: Recommended K_d Values for the Backfill, Vadose Zone and Saturated Zone 66

Table 4.5-4: Annulus Floor Inventories for Nonradioactive Species 68

Table 6.1-1: Triangular Distributions for Feed to Meat Transfer Factors 70

Table 6.1-2: Triangular Distributions for Feed to Milk Transfer Factors 72

Table 6.1-3: Triangular Distributions for Water to Finfish Transfer Factors 74

ACRONYMS

CZ	Contamination Zone
DLL	Dynamic Link Library
HTF	H-Area Tank Farm
IHI	Inadvertent Human Intruder
MOP	Member of Public
NRC	Nuclear Regulatory Commission
PA	Performance Assessment
SZ	Saturated Zone
UZ	Unsaturated Zone

1.0 EXECUTIVE SUMMARY

This report documents a set of revisions to the *H-Area Tank Farm (HTF) Stochastic Fate and Transport Model* (SRR-CWDA-2010-00093, Rev. 1) used in the *Performance Assessment (PA) for the H-Area Tank Farm at the Savannah River Site*, (SRR-CWDA-2010-00128, Rev. 0). The updated model will be used in simulations associated with the development of the HTF PA Rev. 1. Note that within this report, the *HTF Stochastic Fate and Transport Model* (SRR-CWDA-2010-00093, Rev. 2) will also be referred to as the HTF Stochastic Model or simply the HTF GoldSim Model. The revisions to the HTF GoldSim Model reflect changes made to the HTF PORFLOW-based compliance model as well as updates in the structure of the HTF GoldSim Model allowing the model to more rigorously represent the waste tanks, auxiliary sources (e.g., ancillary equipment), and the saturated zone (SZ). The HTF GoldSim Model is an object-oriented probabilistic model designed to evaluate parameter sensitivity and the influence of parameter uncertainty for radionuclide and nonradionuclide (chemical) contaminants located within HTF for potential migration to the accessible environment. For each realization of a Monte Carlo or Latin Hypercube sampling of data, the model calculates the member of public (MOP) doses along a 100-meter boundary surrounding the HTF waste tanks and associated ancillary equipment. The model also calculates doses to inadvertent intruder well drilling adjacent to specific waste tanks. In addition, the software can be used to calculate doses based on concentrations generated by the HTF PORFLOW Model. The advective-dispersive transport submodel used in the HTF stochastic Model is an abstraction of the fully 3-D HTF PORFLOW Model, which provides the computational efficiency needed for multi-realization runs.

Sections 3 and 4 of this report discuss the changes made to the advective-dispersive radionuclide transport submodel, and Sections 5 and 6 of this report discuss the changes made to the dose module.

The final section (Section 7.0) of the report documents the benchmark testing performed to show that the abstraction provides a valid surrogate for the fully 3-D model. During the testing, results from the HTF PORFLOW Model and the HTF GoldSim Model were compared, to evaluate how well the abstraction approximates the trends produced in the fully 3-D model simulation results. The benchmark testing was performed using Case A configuration results. Case A is the HTF Base Case for waste tank operational closure (hereinafter the HTF Base Case will be referred to as Case A).

2.0 PURPOSE

The HTF Stochastic Model is an object-oriented probabilistic model designed to evaluate parameter sensitivity and the influence of parameter uncertainty on the potential for the radiological and chemical waste constituent migration to the accessible environment after HTF facility closure. The accessible environment (for the purpose of compliance) is the area outside of the 100-meter perimeter surrounding the HTF waste tanks and ancillary equipment. In addition, the model evaluates an inadvertent human intruder (IHI) scenario that assumes that the intruder digs a well within 1 meter of a waste tank. The HTF GoldSim Model is comprised of two submodels, 1) an abstraction of the HTF PORFLOW Model, and 2) a dose calculator. The abstraction approximates the process of radionuclide transport from waste tanks and ancillary equipment sources in a manner that allows sensitivity and uncertainty analyses to be performed in a time-efficient manner, while still allowing the influence of parameters on the transport processes to be examined. The model also includes a dose calculator, which evaluates dose at points of compliance based on the concentrations generated by the transport abstraction module or generated by the HTF PORFLOW Model. The updated HTF Stochastic Model was developed using GoldSim (Version 10.5) software (see GTG-2010d for further software details).

2.1 Advective-Dispersive Transport Model

The HTF GoldSim Model solves the general equations for transport of dissolved radionuclides and chemical species within the engineered barrier (the waste tank structure) and the natural barrier (the unsaturated zone, UZ and saturated zone, SZ). The governing equation for 1-D advective-dispersive transport of a dissolved species in a unidirectional flow field is as follows (Equation 2-1):

(Eq. 2-1)

$$\frac{\partial(\phi RC)}{\partial t} = D \frac{\partial^2 C}{\partial l^2} - v \frac{\partial C}{\partial l} - \phi R \lambda C + \sum_{i=1}^{Np} \phi R \lambda_{pi} C_{pi}$$

where:

C	=	solute concentration (m/L ³),
R	=	retardation coefficient
ϕ	=	effective porosity
t	=	time (T)
D	=	dispersion coefficient, $\nu\alpha$ (L ² /T)
ν	=	Darcy velocity (L/T)
α	=	dispersivity (L)
λ	=	decay coefficient (T ⁻¹)
λ_{pi}	=	decay coefficient of the i^{th} parent (T ⁻¹)
Np	=	number of parent species

and:

l	=	transport pathway coordinate, (L)
-----	---	-----------------------------------

The transport module of the HTF GoldSim Model simulates the transport of non-conservative species subject to sorption and either simple decay or ingrowth along decay chains. The model also takes into consideration the influence of solubility control within the contamination zone (CZ). Other processes controlling the mass release from the waste tank structures include; time-dependent physical and chemical degradation of concrete zones and steel liner failure. The releases from ancillary equipment sources are approximated by releasing the inventory directly into the UZ at a specific time. The influence of dispersion (which is represented by the first term on the right-hand side of Equation 2-1), is not explicitly considered in the waste tank structure or UZ. Numerical dispersion associated with mixing cell discretization as discussed in GTG-2010d does influence the releases from the UZ. In the SZ, dispersion is explicitly simulated using GoldSim analytical-solution based pipe elements. The use of GoldSim pipe elements represents a change from SRR-CWDA-2010-00093, Rev 1 of the HTF Stochastic Model, which uses a 1-D string of GoldSim mixing cells to define radionuclide transport in the S,. Changes to the structure of the radionuclide transport model used in the HTF Stochastic Model are documented in Section 3. Changes to the data used to describe radionuclide transport are described in Section 4.

2.2 Dose Calculator Model

In addition to simulating radionuclide transport, the HTF GoldSim Model is designed to calculate receptor doses to a MOP or inadvertent intruder, at points of compliance based on 1) the results from the transport abstraction module, 2) based on output from the HTF PORFLOW Model or 3) based on estimated soil concentrations. The dose calculations are abstracted from conceptualizations of possible exposure pathways.

Changes to the structure of the dose calculator are described in Section 5. Changes to parameters used in the dose calculator are documented in Section 6.

3.0 UPDATES TO THE TRANSPORT MODEL TECHNICAL APPROACH

This section describes the updates to the approach taken in the development of the original HTF GoldSim Model that differentiates SRR-CWDA-2010-00093, Rev 2 from SRR-CWDA-2010-00093, Rev 1. The first part of Section 3 describes changes to the vadose zone model. The vadose zone model evaluates radionuclide transport through the waste tank structure, ancillary equipment and down through the UZ where applicable (waste tanks and ancillary equipment are sometimes partially or fully submerged). The second part of Section 3 describes changes to the SZ model.

3.1 GoldSim Vadose Zone Model

The vadose zone model is comprised of the engineered barrier (either the waste tank and surrounding structures or the ancillary equipment) and the UZ beneath the engineered barrier. The vadose zone portion of the HTF GoldSim Model is an abstraction of the quasi 3-D (radial) waste tank models simulated by the PORFLOW compliance model. The abstraction is based on compartmentalization of the engineered barrier into simplified 1-D legs comprised of GoldSim mixing cells. Each leg is comprised of one or more mixing cells linked in series. The waste tank structure comprised of several groups of cells, representing the reducing grout, the CZ, the liners, the concrete basemat, the sand pads, and the grout annulus. Note that certain design elements, such as the concrete roof, and wall and annulus above the grout, are not represented in the HTF GoldSim Model but are represented in the HTF PORFLOW Model. The UZ beneath the waste tanks (for non-submerged waste tanks) and containing the ancillary equipment is also simulated using sets of linked mixing cells.

The cell pathway elements used in the HTF GoldSim Model are discrete, well-mixed environmental compartments or “mixing cells” used to describe the environmental system being simulated. [GTG-2010e] A cell pathway element represents a specific volume of reference fluid (water for the HTF Stochastic Model) and mass of solid(s). Within the cell, complete mixing takes place so there is no spatial differentiation of concentration within any phase. The dissolved species migrate between cells, via advection or diffusion. The transport module of the HTF Stochastic utilizes the GoldSim cell pathway elements to represent the transport pathways within the waste tank structure and the UZ, where applicable. In the case of the HTF waste tanks, the system is comprised of the engineered barrier (waste tank structure) and part of the natural barrier (UZ). In the case of the HTF ancillary equipment sources, the system is comprised of a single source cell with a time-dependent instantaneous release, and upper natural barrier (UZ).

The GoldSim cell-pathway elements are particularly amenable to simulating the transport processes within the waste tanks because the HTF GoldSim Model is designed to evaluate the fate and transport of radionuclide decay chains and can consider the influence of solubility controls on isotopes as well as sorption on the radionuclide transport process. GoldSim allows for two types of mass links between cells, advective links, and diffusive links. The UZ cells are linked together via advective links only. The UZ cells links are also uncoupled (normal) which minimizes the computational effort. The waste tank structure which is explicitly comprised of the reducing grout, CZ, sand pads (for Type II tanks), steel liners, concrete basemat, and the lower 5-feet of annular grout and the wall (for Type I and II tanks), utilizes both advective and

diffusive links. The diffusive links are important because molecular diffusion controls the transport process in early time before the liners fail, when the flow rates are quite small. One important diffusive process is the upward diffusion from the CZ into the overlying waste tank grout where the storage capacity delays the release of radionuclides. In addition, upward diffusion in the annulus grout can provide a pathway to the wall accelerating the release of radionuclides to the UZ. Note that this latter diffusive process is only considered important in Type I and Type II tanks where the liner has not failed, and where an initial source of radionuclides is assumed in the annulus layer (Type I and Type II tanks) and in the primary sand pad (Type II tanks only).

3.1.1 Vadose Zone Model Structural Changes

Several updates to the vadose zone model have been implemented in the SRR-CWDA-2010-00093, Rev 2 HTF GoldSim Model to allow the model to describe more rigorously the radionuclide transport from the source to the SZ and to evaluate more rigorously the influence of changes in the flow fields. One major structural change implemented was the separation of the waste-tank release model into two models. One model for waste tank types where the mass releases are completely controlled by the liners (Types III, IIIA, and IV), and a second separate transport model for waste tank types where mass can be released from sand pads and the annulus prior to liner failure (Types I and II). The latter waste tank model used to evaluate radionuclide transport in Type III, IIIA, and IV tanks does not contain the cell pathways representing the sand pads, annulus, and wall. Other changes to the structure of the vadose zone model includes: 1) updating the number of cells used to represent specific legs of the pathways, 2) allowing for upward flow in the abbreviated annulus, 3) implementing the logic to allow for stochastic sampling of flow fields, 4) replacing the 1-D string of mixing cells used to simulate transport in the SZ by analytic pipe elements, and 5) superposing the influence of mass releases from upgradient waste tanks on concentrations at inadvertent intruder wells located adjacent to specified waste tanks.

3.1.1.1 Implementation of a Second Waste Tank Release Model

The original HTF Transport Model consisted of a single waste-tank release model with logical controls used to determine whether the annulus and wall sections of the model and sections of basemat below them would be active for the specified waste tank being analyzed in the looping environment. For organizational purposes, it was decided to create two submodels. This bifurcation split the model into a simple submodel used to evaluate Type III, IIIA, and IV tanks, which did not contain the annulus and wall sections of the model and sections of basemat below them. In addition, the UZ section of the model was updated to allow for the use of a greater number of UZ cells. This addition was not needed in the alternative submodel that was only used to represent submerged or partially submerged waste tanks (Type I and II). A flow chart of the structure of the model used to evaluate Type III, IIIA, and IV tanks is presented in Figure 3.1-1. A flow chart of the structure of the model used to evaluate the submerged Type I tanks, and partially submerged Type II tanks is presented in Figure 3.1-2.

Figure 3.1-1: Flow Chart Depicting Type III, IIIA, and IV Tanks

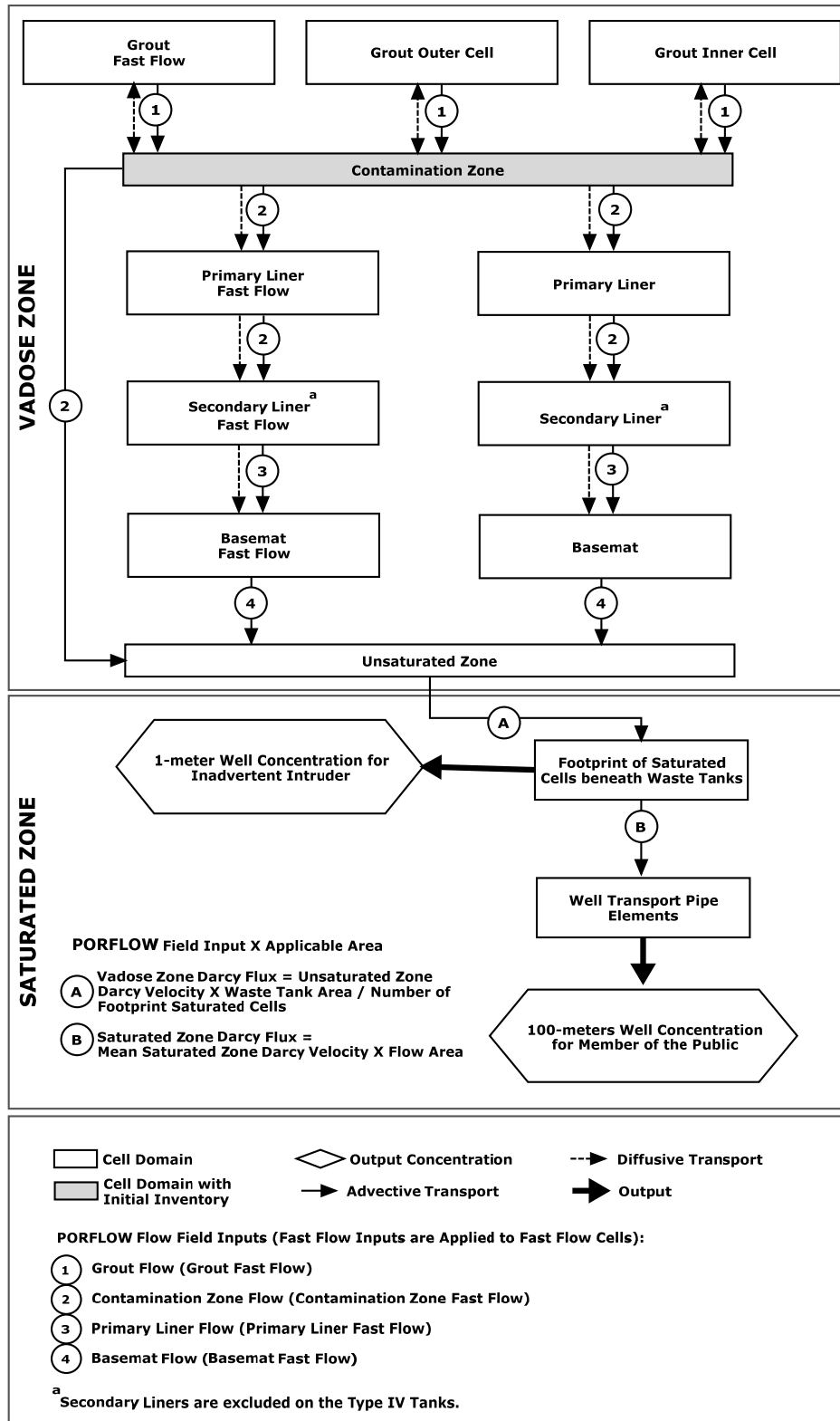
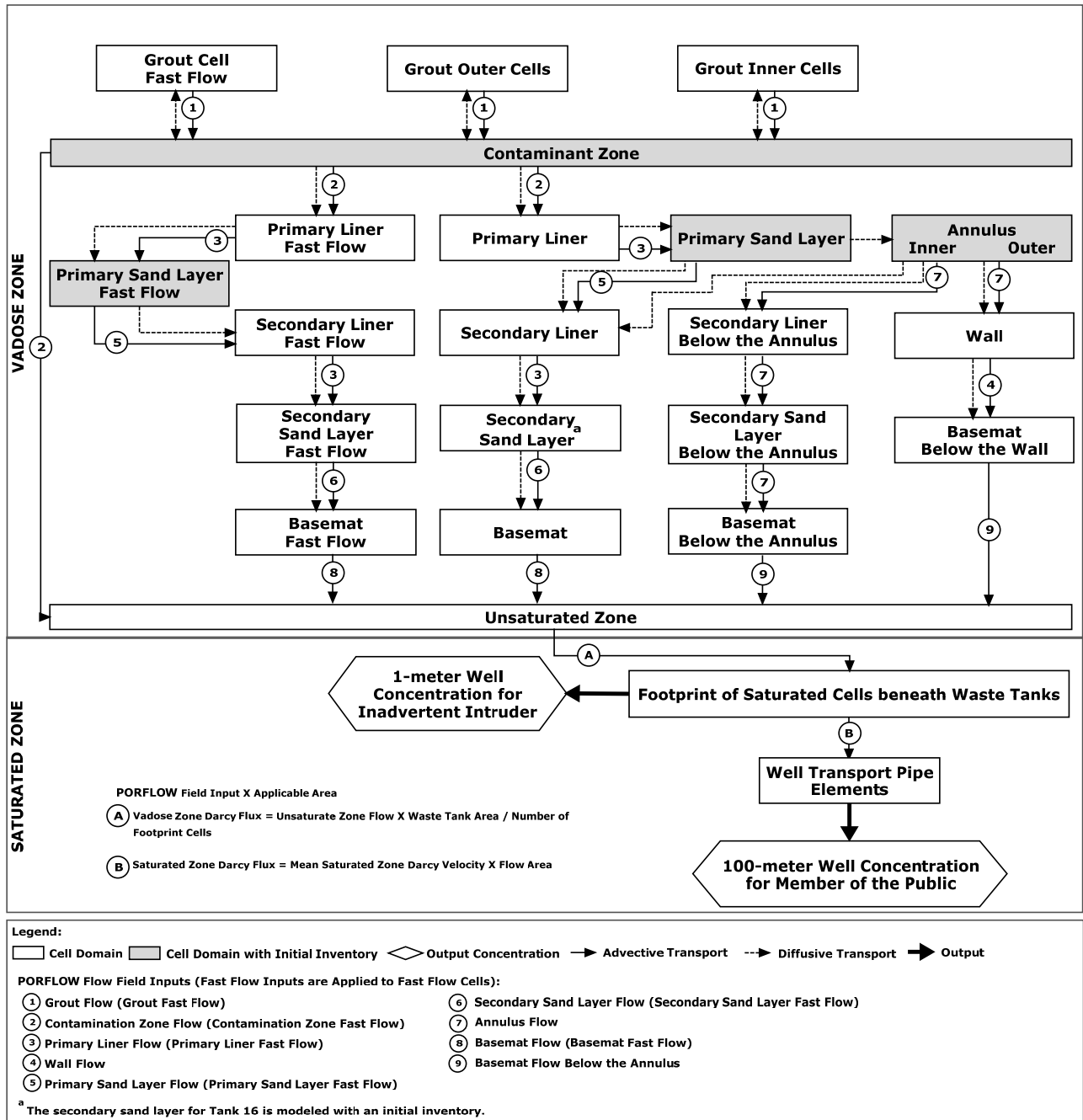


Figure 3.1-2: Flow Chart Depicting Type I and II Tanks



3.1.1.2 *Rediscretization of Vadose Zone Model Sections*

In order to better approximate the radionuclide transport process in the vadose zone model, the sets of mixing cells were rearranged in the waste tank grout, basemat, annulus, and UZ segments of the model. The discretization of the linked mixing zone pathways served two purposes. The first was to allow the user to reduce the degree of numerical dispersion to allow for a better match with PORFLOW results. The second was to allow the model to consider the influence of upward flow in the waste tank grout on the effective storage of radionuclides within the waste tank grout.

3.1.1.2.1 Rediscretization of the Waste Tank Grout Cells

The waste-tank grout cells were discretized to help provide a more rigorous evaluation of the transport processes within the zone. The two main considerations given to discretizing the waste tank grout were the excessive degree of numerical dispersion seen in the zone and the lack of ability to evaluate the influence of upward flow in the waste tank grout, which is especially important when considering the Type IV tanks.

In order to reduce the effects of numerical dispersion, the vertical linkage of cells from top to bottom was increased from a string of 10 cells to a string of 20 cells. The upper 10 cells were assembled in a container called *GroutTop* and the lower 10 cells were assembled in a container called *GroutBoundary*. The lower 10 cells have the same vertical spacing as that used in the lower 10 cells of the HTF PORFLOW Models waste tank grout. The upper 10 cells represent the rest of the waste tank grout and have spacing that increases upwards geometrically. The reason for using this pattern was to allow the updated HTF GoldSim Model to define more accurately the influence of the waste tank grout for radionuclides with a large sorption coefficient. The radionuclides with large sorption coefficients tend to be highly sorbed in a small layer just above the CZ and the previous coarser discretization overestimated the spatial spreading due diffusion and numerical dispersion associated with advection.

In addition to discretizing the mixing cells vertically, a third column of cells was added to the waste tank grout. This breaks the waste tank grout into three concentric cylinders, an inner cylinder, an outer cylinder, and an outermost cylinder representing the fast-flow zone. The addition of the outer cylinder allows the model to consider more accurately the effects of upward flow in the waste-tank grout on the storage of radionuclides within the grout. The influence of upward flow in the waste tank grout is especially important when considering the Type IV tanks.

3.1.1.2.2 Rediscretization of the Basemat Cells

The basemat cells were also discretized to help provide a more rigorous evaluation of the transport processes within the basemat. Note that the basemat is divided into four cylindrical zones defined outward from the center of the waste tank as the fast-flow zone at the center of waste tank foot print, a cylinder that underlies the rest of the waste tank footprint, a third cylinder that underlies the annulus, and a fourth cylinder that underlies the wall. The vertical discretization of the basemat is the same for all four of its segments. The main reason for discretizing the basemat was to minimize the excessive

degree of numerical dispersion seen when simulating the transport of highly sorbing species such as Np-237.

In order to reduce the effects of numerical dispersion, the vertical linkage of cells from top to bottom was increased from a string of 5 cells to a string of up to 30 cells. The model gives the user the capability to choose the number of cells (in groups of five) that represent the basemat for each waste tank type. The choice of the number of cells presently used in the SRR-CWDA-2010-00093, Rev. 2 HTF GoldSim Model to represent the basemat is based on the benchmarking analysis comparing the updated HTF GoldSim Model with HTF PORFLOW Model results (see Table 3.1-1).

Table 3.1-1: Vertical Discretization of the Basemat by Waste Tank Type

Waste Tank Type	Number of Cells
Type I	30
Type I (no liner)	30
Type II	30
Type II (no liner)	30
Type III	30
Type IIIA	25
Type IIIA (West)	25
Type IV	5

Note Type IV tanks use only 5 cells. This difference is consistent with the smaller number of cells used in the discretization of the HTF PORFLOW Model.

3.1.1.2.3 Rediscrretization of the UZ Cells

The UZ cells were also rediscrretized to help decrease the amount of numerical dispersion associated with the number of cells. The rediscrretization of the UZ was performed for both the waste tank release and the ancillary equipment release scenarios.

For waste tank releases, the number of UZ cells was doubled from 10 to 20. Note that this increase applies to only the non-submerged cells. The partially and fully submerged cells still use a set of 10 cells of 0.0001-foot total thickness to represent the non-existent UZ.

For the ancillary equipment releases, the UZ was rediscrretized in a manner that was consistent with the discretization used in the HTF PORFLOW Model. A flexible discretization system allowing the UZ to be discretized into as many as 60 cells was implemented. To simplify the logic, the discretization allows for the use of multiple sets of 10 cells using from 1 to 6 sets. The number of cells representing the UZ for each ancillary equipment source is presented in Table 3.1-2.

Table 3.1-2 Vertical Discretization of the UZ by Ancillary Equipment Source

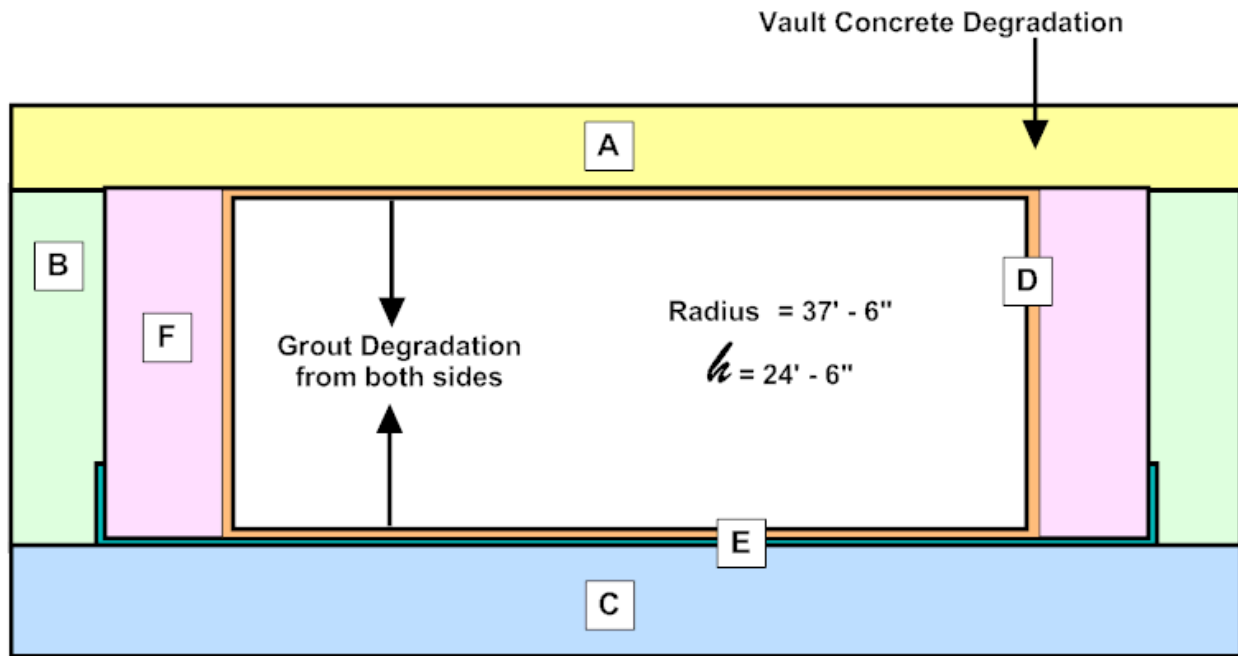
Ancillary Equipment Source	HTF GoldSim Model UZ Cells	HTF PORFLOW Model UZ Cells
HPT 2	10	9
HPT 3	10	9
HPT 4	10	9
HPT 5	10	13
HPT 6	10	13
HPT 7	10	9
HPT 8	10	9
HPT 9	10	9
HPT 10	10	9
E242-H	40	36
E242-16H	50	46
E242-25H	30	25
Transfer-Line 1	40	36
Transfer-Line 2	10	8
Transfer-Line 3	40	36
Transfer-Line 4	10	11
CTS (new)	20	21
CTS (old)	20	21

3.1.1.3 Implementation of Upward Flow in the Annulus

The abstraction of the annulus/vertical-liner/wall system used for Type I and Type II tanks in the HTF GoldSim Model (SRR-CWDA-2010-00093, Rev. 1) considers only the segments of the annulus and wall that are located below the vertical liner separating the two zones (see Figures 3.1-3 and 3.1-4). It is assumed that the transport between the annulus and wall takes place in a small area just above the liner prior to liner failure. Therefore, prior to liner failure flow and diffusion take place between the top of the abbreviated annulus and wall zones. After liner failure, it is assumed that the major process controlling vertical transport is downward flow in the wall and annulus and transfer of mass between the annulus and wall is small enough to be neglected. In the original HTF Transport model, movement of radionuclides within the annulus was controlled by diffusion, prior to liner failure, and by downward flow after liner failure. In this updated model, the advection associated with a water circulation pattern within the volume of the annulus below the secondary liner is allowed to influence mixing within the annulus. Because advection associated with a circulation cell in the annulus can cause upward movement of radionuclides in the annulus, advection is also considered in an ad hoc manner. Within the annulus, an abstraction of the circulation pattern seen in the HTF PORFLOW Model prior to liner failure is applied. The abstraction is implemented by dividing the annulus into two concentric cylinders, which represent an inner and outer zone. When the PORFLOW velocities averaging process is applied to two zones, vertically downward flow occurs in the inner zone and vertically upward flow in the outer zone prior to liner failure. The upward flow is applied to the

annulus prior to liner failure and downward flow based on averaging the flow rate over both zones is used after failure. Since a rigorous determination of how much mass leaves the annulus and enters the wall due to advection cannot be made, the upward flow rate is weighted based upon an analysis comparing GoldSim and PORFLOW peak results prior to liner failure. A multiplier of 0.08 provided a reasonable fit.

Figure 3.1-3: Typical Type I Tank Modeling Dimensions

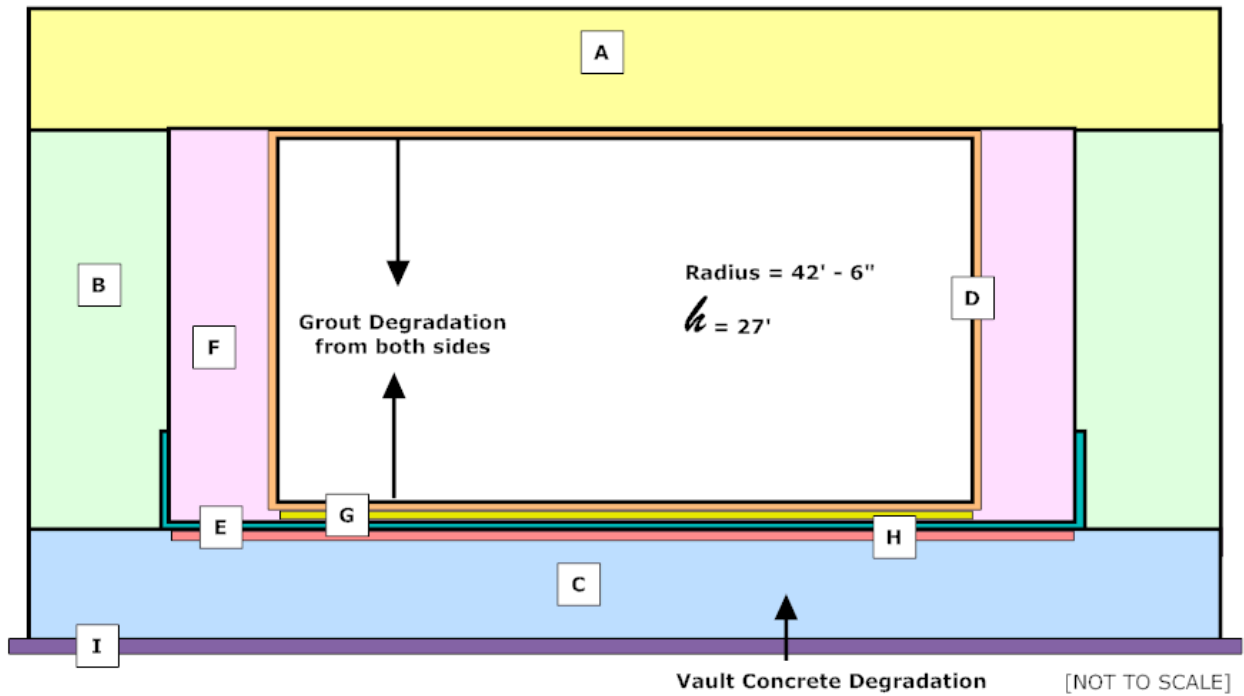


[NOT TO SCALE]

LABEL	THICKNESS
A Concrete Roof	22"
B Concrete Wall	22"
C Concrete Basemat	30"
D Primary Liner	0.5"
E Secondary Liner	5' high and 0.5" thick
F Grouted Annulus	30"

[SRR-CWDA-2010-00128]

Figure 3.1-4: Typical Type II Tank Modeling Dimensions



LABEL	THICKNESS
A Concrete Roof	45"
B Concrete Wall	33"
C Concrete Basemat	42"
D Primary Liner	0.5"
E Secondary Liner	5' high and 0.5" thick
F Grouted Annulus	30.625"
G Primary Liner Sand Bed	1"
H Secondary Liner Sand Bed	1"
I Concrete Working Slab	6"

[SRR-CWDA-2010-00128]

3.1.1.4 Stochastic Sampling of Flow Fields

One major weakness in the original HTF Transport model was that although the model allowed for consideration of uncertainty in most parameters controlling the transport of radionuclides within the engineered barrier and UZ beneath it, the model did not explicitly account for changes in flow fields within the engineered barrier and UZ. To overcome this weakness, SRR-CWDA-2010-00093, Rev 2 model was updated to allow the model to read in flow data from external files containing PORFLOW generated time series assembled in table form. In addition, a set of flow fields and associated data for 72 possible flow scenarios was generated using the HTF PORFLOW Model and assembled in a single file from which the HTF GoldSim Model reads the data associated with the flow scenario that best fits the parameters it has chosen for a specific realization. The logic implemented for the sampling process is discussed in this section and the data used with this new implementation is discussed in Section 4.

The update of the HTF Stochastic Model has been redesigned to read in flow data as opposed to having the flow data copied into data elements, where the data resides until it is updated and replaced. The process of reading in the data is performed using a Dynamic Link Library (DLL) containing a FORTRAN based function that accepts instructions from the HTF GoldSim Model and returns the data needed, which it reads from an external file as per the instructions. The DLL, "ReadFlowFields.dll" (B-SQP-C-00003), is integrated into the HTF Stochastic Fate and Transport Model using GoldSim External elements. Instructions are passed to the DLL through the External element interface. The instructions and there variable names are listed in Table 3.1-3. The instructions passed to the DLL include:

1. the location of the desired table in the file containing the desired data
2. the location of the data file name in the control file
3. the number of dependent variables in the table from which the data is to be read
4. a file extension number for the control file (set to zero if not used)
5. the number of columns containing the Darcy velocity, volumetric flows and saturations to be returned to the GoldSim model (time series data)
6. the position of the infiltration data in the list of outputs to be read
7. a variable name and column number for each data parcel to be read

For more detailed instructions on the data column locations see Table 3.1-3. ReadFlowFields.dll will then return either 1-D tables of time versus dependent variable or scalar variables to the GoldSim-based model. The data passed back from the DLL to the HTF GoldSim Model (as listed in Table 3.1-4) include time series of zone-based Darcy velocities, volumetric flows, saturations, and infiltration rates, as well as scalar values of zone-based pore volumes, pH-based transition times, E_h -based transition times, and cross-flow rates for fully or partially submerged waste tanks.

Table 3.1-3: Instruction Data Passed to ReadFlowFields.dll

Number	Variable Name	Variable Meaning
1	<i>LocNumber</i>	The location of the desired table in a file of ordered 2-D tables each table representing a PORFLOW flow simulation.
2	File Number	The position of the required input file name in a ReadFlowFields.dll control file
3	<i>szTable</i>	The number of dependent-variable columns in the referenced table
4	<i>FileExt</i>	File extension number if desired (normally set to zero)
5	<i>NTimeD</i>	The number of the columns containing Darcy velocity, volumetric flows and saturations to be returned to the HTF GoldSim Model
6	<i>InfilIndex</i>	The position of the infiltration data in the output returned to the HTF GoldSim Model
7 thru the number of variables -1	Variable Names	The position of dependent-variable column in the referenced table for each 1-D table or scalar variable to be returned is found (note that the column number is based on the dependent variables only so that the first three columns representing the run index and time are not considered in determining the position of the columns)
Final Line	Blank	A zero indicating that no more data is requested

Table 3.1-4: Data Extracted from the Flow Field Files

Data	Form	Units
Darcy Velocities	1-D Table	cm/yr
Volumetric Flows	1-D Table	cm ³ /yr
Saturations	1-D Table	N/A
Pore Volumes	Scalar	cm ³
pH Transition Times	Scalar	yr
Eh Transition Times	Scalar	yr
Infiltration Rate	1-D Table	cm/yr
Cross Flow Rate	Scalar	cm/yr

The control file used in the model must be named *ReadFlowFiles.in* or *ReadFlowFilesXX.in* where *XX* is the file extension number passed through the External function interface (see Table 3.1-3). A sample control file is presented in Figure 3.1-5 (the sample file is the file used in the benchmarking study described below). Line by line this control file contains:

1. the number of flow data files that can be chosen from
2. a file name for each flow data file
3. the number of descriptive lines found at the top of the data file (not including the descriptive lines described below)
4. the number of descriptive lines preceding each table (this number is the same for each table)
5. the number of time-specific rows in each table (this number is the same for each table)

Figure 3.1-5: Sample Control File for *ReadFlowFields.dll*

```
6                ! number of data files to be read
GoldSim_StochasticFlowFields.txt    !
GoldSim_CaseAFlowFields.txt        !
GoldSim_CaseBFlowFields.txt        !
GoldSim_CaseCFlowFields.txt        !
GoldSim_CaseDFlowFields.txt        !
GoldSim_CaseEFlowFields.txt        !
0                ! number of lines in the top-of-file header
1                ! number of rows in the header for each data table
40               ! number of rows in each data table
```

Note there are six data files listed in this control file. The first file contains the flow data for stochastic runs and the other five files contain the flow data for Cases A through E. Note the first file contains 72×4 (288) tables for 72 parametric samples and 4 waste tank types (Type I, Type II, Type IIIA, and Type IV). Type III and IIIA-West are not included because there results are so similar to the Type IIIA results. The other files each contain 8 tables representing the 8 included waste tank types (Type I, Type I no-liner, Type II, Type II no-liner, Type IIIA, Type IIIA West, and Type IV).

In addition to the file name data, the control file includes the number of text lines at the top of each file, and the number of header lines for each flow data table within a file. The final number in the control file is the number of rows (time steps) in each table.

The flow-field tables included in the file, *GoldSim_StochasticFlowFields.txt*, are based on a parametric study performed using the HTF PORFLOW model. The flow parametric study was based on the Case A scenario with the following attributes varied:

- 3 fast flow configurations (none, partial, full)
- 4 liner failure times (time zero, early, moderate, late)
- 3 cementitious material degradation rates (fast, nominal, and slow)
- 2 infiltration cases (nominal, no-cap)

The "partial" fast flow path will breach the roof and grout, but not the basemat/floor (as in Cases B and C). The "full" fast flow path will breach the roof, grout, and basemat/floor (as in Cases D and E). The HTF Stochastic Fate and Transport Model is designed to sample for configuration based on five cases (Cases A through E). For compatibility, when the sampled configuration is Case A, the first fast-flow configuration (none) is used. When the sampled configuration is either Case B or Case C, the second fast-flow configuration (partial) is used and when the sampled configuration is Case D or E, the third fast-flow configuration (full) is used.

The parametric study also included the four liner-failure times presented in Table 3.1-5. Since the HTF Stochastic Model, sampling procedure chooses a specific failure time. That specific time dictates which set of flow data based on the liner failure times presented in Table 3.1-5 is used. The criteria for choosing the liner failure time from Table 3.1-5 is based on which time in the table (for the specified waste tank type), the sampled time is closest to. In the HTF GoldSim Model simulation, the sampled liner failure time is used. Since the liner failure times differ, the flow data time series from the parametric study data is scaled from time-zero to the liner failure time to fit the time span from time-zero to the sampled liner failure time. The component of the time series following liner failure is then shifted so that it

is consistent with the sampled time failure (scaling is not considered). In this way, the influence of liner failure time can be evaluated and a degree of consistency between liner failure time and degradation is imposed.

Table 3.1-5: Liner Failure Times

Fast Flow Path:	None				Partial and Full			
	Type I Liner Failure Year	Type II Liner Failure Year	Type III/IIIA Liner Failure Year	Type IV Liner Failure Year	Type I Liner Failure Year	Type II Liner Failure Year	Type III/IIIA Liner Failure Year	Type IV Liner Failure Year
0	0	0	0	0	0	0	0	0
Early	2,100	2,506	3,100	500	100	100	100	75
Moderate	11,397	12,687	12,751	3,638	1,142	2,506	2,077	1,000
Late	15,000	14,500	14,500	8,000	11,000	12,000	12,000	3,638

Uncertainty in the concrete and grout degradation rates is also considered by use of a scaling factor. The three cementitious material degradation rates considered are Case A degradation times, fast (Case A degradation times divided by two), and slow (Case A degradation times multiplied by two).

The other parameter evaluated in the parametric study is the infiltration rate. A "no-cap" infiltration rate of 16.45 in/yr for all time was used as an alternative to the nominal infiltration curve.

The parametric cases from which the flow fields are sampled are listed below in Tables 3.1-6 to 3.1-8.

Table 3.1-6: Parametric Cases (No Fast Flow Zones)

Flow Run	Fast Flow	Liner Failure (see table)	Infiltration Rate (in/yr)	Hydraulic Conductivity Curve
1	None (Case A)	0	Nominal (11.67)	Normal degradation
2	None (Case A)	Early	Nominal (11.67)	Normal degradation
3	None (Case A)	Moderate	Nominal (11.67)	Normal degradation
4	None (Case A)	Late	Nominal (11.67)	Normal degradation
5	None (Case A)	0	Nominal (11.67)	Faster degradation
6	None (Case A)	Early	Nominal (11.67)	Faster degradation
7	None (Case A)	Moderate	Nominal (11.67)	Faster degradation
8	None (Case A)	Late	Nominal (11.67)	Faster degradation
9	None (Case A)	0	Nominal (11.67)	Slower degradation
10	None (Case A)	Early	Nominal (11.67)	Slower degradation
11	None (Case A)	Moderate	Nominal (11.67)	Slower degradation
12	None (Case A)	Late	Nominal (11.67)	Slower degradation
13	None (Case A)	0	No cap (16.45)	Normal degradation
14	None (Case A)	Early	No cap (16.45)	Normal degradation
15	None (Case A)	Moderate	No cap (16.45)	Normal degradation
16	None (Case A)	Late	No cap (16.45)	Normal degradation
17	None (Case A)	0	No cap (16.45)	Faster degradation

18	None (Case A)	Early	No cap (16.45)	Faster degradation
19	None (Case A)	Moderate	No cap (16.45)	Faster degradation
20	None (Case A)	Late	No cap (16.45)	Faster degradation
21	None (Case A)	0	No cap (16.45)	Slower degradation
22	None (Case A)	Early	No cap (16.45)	Slower degradation
23	None (Case A)	Moderate	No cap (16.45)	Slower degradation
24	None (Case A)	Late	No cap (16.45)	Slower degradation

Table 3.1-7: Parametric Cases (Partial Fast Flow Zones)

Flow Run	Fast Flow (Case)	Liner Failure (see table)	Infiltration Rate (in/yr)	Hydraulic Conductivity Curve
25	Partial (Case B and C)	0	Nominal (11.67)	Normal degradation
26	Partial (Case B and C)	Early	Nominal (11.67)	Normal degradation
27	Partial (Case B and C)	Moderate	Nominal (11.67)	Normal degradation
28	Partial (Case B and C)	Late	Nominal (11.67)	Normal degradation
29	Partial (Case B and C)	0	Nominal (11.67)	Faster degradation
30	Partial (Case B and C)	Early	Nominal (11.67)	Faster degradation
31	Partial (Case B and C)	Moderate	Nominal (11.67)	Faster degradation
32	Partial (Case B and C)	Late	Nominal (11.67)	Faster degradation
33	Partial (Case B and C)	0	Nominal (11.67)	Slower degradation
34	Partial (Case B and C)	Early	Nominal (11.67)	Slower degradation
35	Partial (Case B and C)	Moderate	Nominal (11.67)	Slower degradation
36	Partial (Case B and C)	Late	Nominal (11.67)	Slower degradation
37	Partial (Case B and C)	0	No cap (16.45)	Normal degradation
38	Partial (Case B and C)	Early	No cap (16.45)	Normal degradation
39	Partial (Case B and C)	Moderate	No cap (16.45)	Normal degradation
40	Partial (Case B and C)	Late	No cap (16.45)	Normal degradation
41	Partial (Case B and C)	0	No cap (16.45)	Faster degradation
42	Partial (Case B and C)	Early	No cap (16.45)	Faster degradation
43	Partial (Case B and C)	Moderate	No cap (16.45)	Faster degradation
44	Partial (Case B and C)	Late	No cap (16.45)	Faster degradation
45	Partial (Case B and C)	0	No cap (16.45)	Slower degradation
46	Partial (Case B and C)	Early	No cap (16.45)	Slower degradation
47	Partial (Case B and C)	Moderate	No cap (16.45)	Slower degradation
48	Partial (Case B and C)	Late	No cap (16.45)	Slower degradation

Table 3.1-8: Parametric Cases (Full Fast Flow Zones)

Flow Run	Fast Flow (Case)	Liner Failure (see table)	Infiltration Rate (in/yr)	Hydraulic Conductivity Curve
49	Full (Cases D and E)	0	Nominal (11.67)	Normal degradation
50	Full (Cases D and E)	Early	Nominal (11.67)	Normal degradation
51	Full (Cases D and E)	Moderate	Nominal (11.67)	Normal degradation
52	Full (Cases D and E)	Late	Nominal (11.67)	Normal degradation
53	Full (Cases D and E)	0	Nominal (11.67)	Faster degradation
54	Full (Cases D and E)	Early	Nominal (11.67)	Faster degradation

55	Full (Cases D and E)	Moderate	Nominal (11.67)	Faster degradation
56	Full (Cases D and E)	Late	Nominal (11.67)	Faster degradation
57	Full (Cases D and E)	0	Nominal (11.67)	Slower degradation
58	Full (Cases D and E)	Early	Nominal (11.67)	Slower degradation
59	Full (Cases D and E)	Moderate	Nominal (11.67)	Slower degradation
60	Full (Cases D and E)	Late	Nominal (11.67)	Slower degradation
61	Full (Cases D and E)	0	No cap (16.45)	Normal degradation

Table 3.1-8: Parametric Cases (Full Fast Flow Zones) (Continued)

Flow Run	Fast Flow (Case)	Liner Failure (see table)	Infiltration Rate (in/yr)	Hydraulic Conductivity Curve
62	Full (Cases D and E)	Early	No cap (16.45)	Normal degradation
63	Full (Cases D and E)	Moderate	No cap (16.45)	Normal degradation
64	Full (Cases D and E)	Late	No cap (16.45)	Normal degradation
65	Full (Cases D and E)	0	No cap (16.45)	Faster degradation
66	Full (Cases D and E)	Early	No cap (16.45)	Faster degradation
67	Full (Cases D and E)	Moderate	No cap (16.45)	Faster degradation
68	Full (Cases D and E)	Late	No cap (16.45)	Faster degradation
69	Full (Cases D and E)	0	No cap (16.45)	Slower degradation
70	Full (Cases D and E)	Early	No cap (16.45)	Slower degradation
71	Full (Cases D and E)	Moderate	No cap (16.45)	Slower degradation
72	Full (Cases D and E)	Late	No cap (16.45)	Slower degradation

3.1.1.5 Saturate Zone Pipe Elements

In SRR-CWDA-2010-00093, Rev 1 of the HTF Stochastic Model, the 1-D string of 50 GoldSim mixing cells used to define radionuclide transport in the SZ has been replaced by a set of three analytic pipe elements linked in series. The change from mixing cells to pipe elements allows the user to simulate the effects of dispersion in a more straightforward manner (i.e., not changing the number of cells) and not be limited by the number of cells in the choice of longitudinal dispersivity. Since the SZ properties and flow rates do not change over time, the use of pipes is appropriate. The choice of three pipes instead of a single pipe allows the user to experiment with spatially based changes in transport parameters if desired. The use of a string of footprint cells to feed the SZ model is no longer needed, and the mass flux boundary condition is defined by the output from an integrator element that provides the boundary condition for the pipe element in the form of a cumulative mass release curve. The SZ directly below the waste tank is now represented by the upgradient portion of the first pipe. Note that the footprint cells are still used in the IHI analysis presented below in Section 3.1.1.6.

3.1.1.6 Inadvertent Human Intruder Analysis

In the Inadvertent Intruder analysis, the inadvertent intruder dose calculations are based on the 1-meter drinking water well concentrations. In PORFLOW calculations, the concentrations used for the Inadvertent Intruder dose calculations are located at a 1-meter perimeter boundary that surrounds HTF (see Figure 3.1-6). In the HTF GoldSim Model, the inadvertent intruder analysis is performed by choosing one of seven possible well locations defined by yellow squares in Figure 3.1-6 and evaluating the concentration at that location. The well locations and their adjacent waste tanks are identified in Table 3.1-9, along with the PORFLOW grid locations. In addition, the updated HTF GoldSim Model also considers contributions from upgradient waste tanks to the specified wells. For waste tanks likely to influence concentrations at the specified wells, GoldSim pipe-models are used to evaluate the contributions to the wells. Lists of the upgradient waste tanks contributing to each of the specified wells are presented in Table 3.1-9. For the present model, the well analyzed is Well 3 (Table 3.1-9), which is adjacent to Tank 12. This choice is based on a comparison of

Case A PORFLOW dose results at the seven wells, which showed Well 3 to have the highest dose.

Figure 3.1-6: PORFLOW Generated Stream Traces from Waste Tanks along with Hypothetical 1-Meter and 100-Meter Boundaries

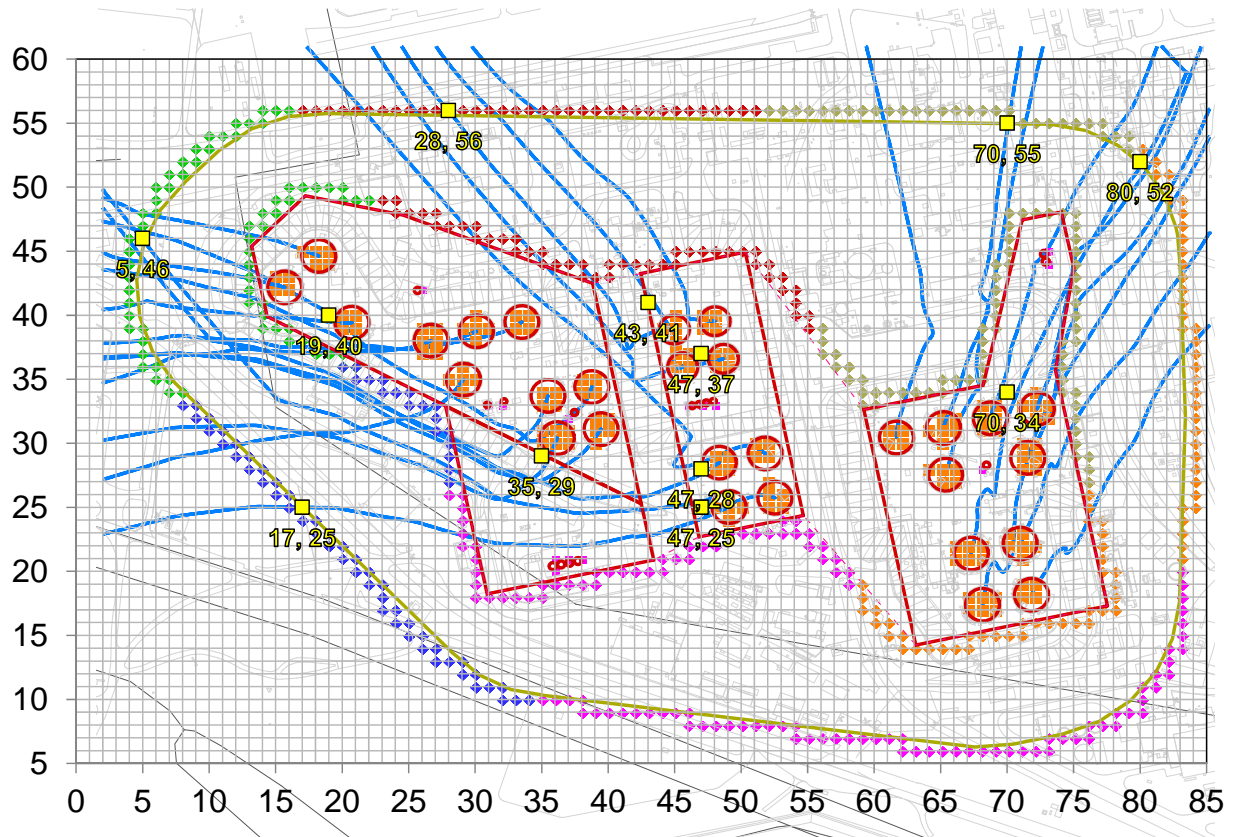


Table 3.1-9: Inadvertent Intruder Analysis Wells

Well Number	Adjacent Waste Tank Number	HTF PORFLOW Model Grid Location (X-Index, Y-Index)	Upgradient Waste Tanks Contributing to Well Concentration
1	40	70, 31	38, 39, 41, 42, 43, 48, 49, 50, 51
2	9	43, 41	10, 11, 12, 14
3	12	47, 37	10, 14
4	13	47, 26	14, 15, 16
5	15	47, 25	13, 14, 16
6	22	35, 29	13, 14, 15, 16, 21, 23, 24, 29, 30, 31
7	35	19, 40	10, 11, 12, 13, 14, 15, 16, 21, 22, 23, 24, 29, 30, 32

4.0 UPDATES TO THE TRANSPORT MODEL INPUTS

This section describes the updates to any input parameters used in the SRR-CWDA-2010-00093, Rev 2 HTF GoldSim Model that have changed from SRR-CWDA-2010-00093, Rev 1 HTF Stochastic Model.

4.1 General Inputs

The General Input Container in the HTF GoldSim Model contains 1) commonly used constants, 2) the species list and basic species data (e.g., half-life), 3) the reference fluid element and its basic properties such as solubilities, and 4) the input data controlling the temporal changes in transport parameters. The commonly used constants are not discussed in this section.

4.1.1 Species

To reduce the calculation time, most of the chemical species evaluated in the HTF Stochastic Model of SRR-CWDA-2010-00093, Rev. 1 were removed from the species list. The two exceptions were nickel and selenium, which were kept to allow for consideration of the influence of the chemical inventory on the solubility calculations. The species list for HTF Stochastic Model from SRR-CWDA-2010-00093, Rev 1, is presented in Table 4.1-1 along with their atomic weight, half-life, daughter products, and the daughter product stoichiometry.

Table 4.1-1: GoldSim Model Species List

Species ID	Atomic Weight	Half-Life (yr)	Radioactive	Daughter 1 (Stoichiometry)	Daughter 2 (Stoichiometry)
Ac-227	227	2.18E+01	Y	Pb (1)	N/A
Ag-108m	108	4.38E+02	Y	Cd (0.0845)	N/A
Al-26	26	7.17E+05	Y	N/A	N/A
Am-241	241	4.32E+02	Y	Np-237 (1)	N/A
Am-242m	242	1.41E+02	Y	Pu-242 (0.1722)	Pu-238 (0.8278)
Am-243	243	7.37E+03	Y	Pu-239 (1)	N/A
Bi-210m	210	3.04E+06	Y	Pb (1)	N/A
C-14	14	5.70E+03	Y	N/A	N/A
Ca-41	41	1.02E+05	Y	N/A	N/A
Cf-249	249	3.51E+02	Y	Cm-245 (1)	N/A
Cf-251	251	8.98E+02	Y	Cm-247 (1)	N/A
Cl-36	36	3.01E+05	Y	N/A	N/A
Cm-243	243	2.91E+01	Y	Pu-239 (1)	Am-243 (0.8278)
Cm-244	244	1.81E+01	Y	Pu-240 (1)	N/A
Cm-245	245	8.50E+03	Y	Pu-241 (1)	N/A
Cm-246	246	4.76E+03	Y	Pu-242 (0.9997)	N/A
Cm-247	247	1.56E+07	Y	Am-243	N/A
Cm-248	248	3.48E+05	Y	Pu-244 (0.9161)	N/A
Co-60	60	5.27E+00	Y	Ni (1)	N/A
Cs-135	135	2.30E+06	Y	Ba (1)	N/A
Cs-137	137	3.00E+01	Y	Ba (1)	N/A
Eu-152	152	1.35E+01	Y	Gd-152 (0.721)	N/A

Table 4.1-1: GoldSim Model Species List (Continued)

Species ID	Atomic Weight	Half-Life (yr)	Radioactive	Daughter 1 (Stoichiometry)	Daughter 2 (Stoichiometry)
Eu-154	154	8.59E+00	Y	N/A	N/A
Eu-155	155	4.75E+00	Y	N/A	N/A
Gd-152	152	1.08E+14	Y	N/A	N/A
H-3	3	1.23E+01	Y	N/A	N/A
I-129	129	1.57E+07	Y	N/A	N/A
K-40	40	1.25E+09	Y	N/A	N/A
Lu-174	174	3.31E+00	Y	N/A	N/A
Mo-93	93	4.00E+03	Y	Nb-93m (1)	N/A
Nb-93m	93	1.61E+01	Y	N/A	N/A
Nb-94	94	2.03E+04	Y	N/A	N/A
Ni-59	59	7.60E+04	Y	N/A	N/A
Ni-63	63	1.00E+02	Y	Cu (1)	N/A
Np-237	237	2.14E+06	Y	U-233 (1)	N/A
Pa-231	231	3.28E+04	Y	Ac-227 (1)	N/A
Pb-210	210	2.22E+01	Y	Pb (1)	N/A
Pd-107	107	6.50E+06	Y	Ag (1)	N/A
Pt-193	193	5.00E+01	Y	N/A	N/A
Pu-238	238	8.77E+01	Y	U-234 (1)	N/A
Pu-239	239	2.41E+04	Y	U-235 (1)	N/A
Pu-240	240	6.56E+03	Y	U-236 (1)	N/A
Pu-241	241	1.43E+01	Y	Am-241 (0.999975)	Np-237 (0.000025)
Pu-242	242	3.75E+05	Y	U-238 (1)	N/A
Pu-244	244	8.00E+07	Y	Pu-240 (0.9988)	N/A
Ra-226	226	1.60E+03	Y	Pb-210 (1)	N/A
Ra-228	228	5.75E+00	Y	Pb (1)	N/A
Se-79	79	2.95E+05	Y	N/A	N/A
Sm-147	147	1.06E+11	Y	N/A	N/A
Sm-151	151	9.00E+01	Y	N/A	N/A
Sn-126	126	2.30E+05	Y	N/A	N/A
Sr-90	90	2.89E+01	Y	N/A	N/A
Tc-99	99	2.11E+05	Y	N/A	N/A
Th-229	229	7.34E+03	Y	N/A	N/A
Th-230	230	7.54E+04	Y	Ra-226 (1)	N/A
Th-232	232	1.41E+10	Y	Ra-228 (1)	N/A
U-232	232	6.89E+01	Y	Pb (1)	N/A
U-233	233	1.59E+05	Y	Th-229 (1)	N/A
U-234	234	2.46E+05	Y	Th-230 (1)	N/A
U-235	235	7.04E+08	Y	Pa-231 (1)	N/A
U-236	236	2.34E+07	Y	Th-232 (1)	N/A
U-238	238	4.47E+09	Y	U-234 (1)	N/A
Zr-93	93	1.53E+06	Y	Nb-93m (1)	N/A
Ni	58.69	N/A	N/A	N/A	N/A
Se	78.96	N/A	N/A	N/A	N/A

[SRR-CWDA-2010-00093, Rev 1]

4.1.1.1 Solubilities

The waste solubility values in the HTF Stochastic Fate and Transport model control the release of solubility controlled radionuclides and non-radioactive species from the CZ above the primary liner. The values determine the maximum combined concentration in the waste cell water of all isotopes of a solubility-controlled element. Many of these values were updated, in SRNL-STI-2012-00404, Rev 0. The values used in HTF Stochastic Model from SRR-CWDA-2010-00093, Rev 2 are based on these updated values. Table 4.1-2 shows the updated baseline solubility values and controlling phases for all of the elements of interest at each of the chemical states of interest. Table 4.1-3 shows the baseline solubility values and controlling phases for the submerged waste tanks. For most of the solubility-controlled species, uncertainty in choice of the solubility-controlling phase (which is the largest uncertainty in calculating solubilities) was addressed primarily through conservatism in choice of the controlling phase. For those solubility controlled radionuclides which have in the past shown been of most concern (plutonium, uranium, neptunium and technetium), probability distributions based on controlling phases were assigned for Region II conditions (Reduced and Oxidized). Tables 4.1-4, 4.1-5, and 4.1-6 present updated distributions for Reduced Region II, Oxidized Region II, and Oxidizing Region III based on different phases for plutonium, uranium, neptunium and technetium, where the probabilities are weighted to account for the possibility of different phases. In addition, the possibility of iron co-precipitation controlling was factored into the plutonium, neptunium, technetium, and uranium probabilities. The probabilities chosen are based on observations in the literature, thermodynamic stability, etc. [SRNL-STI-2012-00404, Rev 0]

Table 4.1-2: Calculated Solubilities of Radionuclides of Interest

	Oxidized Region II		Oxidized Region III		Reduced Region II	
	Controlling Phase	Solubility (mol/L)	Controlling Phase	Solubility (mol/L)	Controlling Phase	Solubility (mol/L)
Ac	Ac(OH) _{3(am)}	1.1E-09	Ac(OH) _{3(am)}	5.9E-08	Ac(OH) _{3(am)}	1.1E-09
Am	Am(OH) _{3(am)}	1.1E-09	Am(OH) _{3(am)}	6.2E-08	Am(OH) _{3(am)}	1.1E-09
Ba	BaSO ₄ (barite)	3.0E-05	BaSO ₄ (barite)	1.3E-05	BaSO ₄ (barite)	4.5E-05
Bk	short half-life	Modeled as instantaneous release	short half-life	Modeled as instantaneous release	short half-life	Modeled as instantaneous release
C	CaCO ₃ (calcite)	1.8E-06	CaCO ₃ (calcite)	9.7E-04	CaCO ₃ (calcite)	1.8E-06
Cf	small inventory	Modeled as instantaneous release	small inventory	Modeled as instantaneous release	small inventory	Modeled as instantaneous release
Cm	Cm(OH) _{3(am)}	1.1E-09	CmCO ₃ OH_0.5H ₂ O _(c)	1.6E-09	Cm(OH) _{3(am)}	1.1E-09
Co	no solubility control	Modeled as instantaneous release	no solubility control	Modeled as instantaneous release	CoS(beta)	3.2E-02

Table 4.1-2: Calculated Solubilities of Radionuclides of Interest (Continued)

	Oxidized Region II		Oxidized Region III		Reduced Region II	
	Controlling Phase	Solubility (mol/L)	Controlling Phase	Solubility (mol/L)	Controlling Phase	Solubility (mol/L)
Cs	no solubility control	Modeled as instantaneous release	no solubility control	Modeled as instantaneous release	no solubility control	Modeled as instantaneous release
Eu	Eu(OH) _{3(am)}	8.3E-07	EuOHCO _{3(cr)}	2.8E-08	Eu(OH) _{3(am)}	8.4E-07
I	no solubility control	Modeled as instantaneous release	no solubility control	Modeled as instantaneous release	no solubility control	Modeled as instantaneous release
Nb	no solubility control	Modeled as instantaneous release	no solubility control	Modeled as instantaneous release	no solubility control	Modeled as instantaneous release
Ni	Ni(OH) ₂ (beta)	9.7E-08	NiCO ₃ (c)	1.2E-05	NiS _(c) alpha	9.7E-08
Np	NpO _{2(am,hyd)}	2.5E-07	NpO _{2(am,hyd)}	1.7E-06	NpO _{2(am,hyd)}	9.9E-10
Pa	no solubility control	Modeled as instantaneous release	no solubility control	Modeled as instantaneous release	no solubility control	Modeled as instantaneous release
Pu	PuO _{2(am,hyd)}	3.2E-11	PuO _{2(am,hyd)}	3.2E-11	PuO _{2(am,hyd)}	3.2E-11
Ra	RaSO ₄	3.0E-05	RaSO ₄	1.3E-05	RaSO ₄	3.0E-05
Rh	short half-life	Modeled as instantaneous release	short half-life	Modeled as instantaneous release	short half-life	Modeled as instantaneous release
Se	no solubility control	Modeled as instantaneous release	no solubility control	Modeled as instantaneous release	FeSe _{2(cr)}	2.2E-05
Sm	Sm(OH) _{3(am)}	1.1E-09	SmCO ₃ OH _{0.5H₂O} (c)	1.6E-09	Sm(OH) _{3(am)}	1.1E-09
Sn	SnO _{2(am)}	4.3E-04	SnO _{2(am)}	6.9E-07	SnO _{2(am)}	4.3E-04
Sr	SrCO ₃	2.8E-03	SrCO ₃	1.4E-04	SrCO ₃	2.9E-03
Tc	no solubility limit	Modeled as instantaneous release	no solubility limit	Modeled as instantaneous release	TcO ₂ .1.6H ₂ O	1.1E-08
Te	short half-life	Modeled as instantaneous release	short half-life	Modeled as instantaneous release	short half-life	Modeled as instantaneous release
Th	ThO _{2(am,hyd,aged)}	1.3E-09	ThO _{2(am,hyd,aged)}	1.3E-09	ThO _{2(am,hyd,aged)}	1.3E-09
U	UO ₃ .2H ₂ O	5.1E-05	UO ₃ .2H ₂ O	4.3E-06	UO _{2(am,hyd)}	4.6E-09
Y	Y(OH) _{3(c)}	3.7E-13	Y(OH) _{3(c)}	1.7E-09	Y(OH) _{3(c)}	3.7E-13

[SRNL-STI-2012-00404, Rev. 0]

Table 4.1-3: Calculated Solubilities and Controlling Phases in Submerged Waste Tanks

	Submerged Condition A		Submerged Condition C		Submerged Condition D	
	Controlling Phase	Solubility (mol/L)	Controlling Phase	Solubility (mol/L)	Controlling Phase	Solubility (mol/L)
Ac	No solubility control	Modeled as instantaneous release	Ac(OH)3(am)	1.8E-07	Ac(OH)3(am)	1.6E-07
Am	AMOHCO3	2.8E-04	AmCO3OH·0.5 H2O	3.8E-09	AmCO3OH·0.5H2O	4.0E-09
Ba	Witherite (BaCO3)	2.6E-05	BaSO4	6.7E-06	BaSO4	1.9E-05
Bk	Short Half-life	Modeled as instantaneous release	Short Half-life	Modeled as instantaneous release	Short Half-life	Modeled as instantaneous release
C	No solubility control	Modeled as instantaneous release	CaCO3	3.9E-04	CaCO3	3.7E-04
Cf	Small inventory	Modeled as instantaneous release	Small inventory	Modeled as instantaneous release	Small inventory	Modeled as instantaneous release
Cm	Cm(OH)3	2.8E-04	CmCO3OH·0.5 H2O	3.8E-09	CmCO3OH·0.5H2O	3.9E-09
Co	No solubility control	Modeled as instantaneous release	beta-CoS	1.3E-04	No solubility control	Modeled as instantaneous release
Cs	No solubility control	Modeled as instantaneous release	No solubility control	Modeled as instantaneous release	No solubility control	Modeled as instantaneous release
Eu	Eu2(CO3)3 8H2O	2.3E-03	EuOHCO3(c)	3.5E-08	EuOHCO3(c)	3.7E-08
I	No solubility control	Modeled as instantaneous release	No solubility control	Modeled as instantaneous release	No solubility control	Modeled as instantaneous release
Nb	No solubility control	Modeled as instantaneous release	No solubility control	Modeled as instantaneous release	No solubility control	Modeled as instantaneous release
Ni	No solubility control	Modeled as instantaneous release	alpha-NiS	6.3E-11	beta-Ni(OH)2	6.3E-07
Np	NpO2(am,hyd)	2.5E-05	NpO2(am,hyd)	9.9E-10	NpO2(am,hyd)	1.8E-05
Pa	No solubility control	Modeled as instantaneous release	No solubility control	Modeled as instantaneous release	No solubility control	Modeled as instantaneous release
Pu	PuO2(am,hyd)	2.4E-10	PuO2(am,hyd)	3.3E-11	PuO2(am,hyd)	3.2E-11
Ra	RaSO4	2.5E-05	RaSO4	6.8E-06	RaSO4	1.9E-05
Rh	Short half-life	Modeled as instantaneous release	Short half-life	Modeled as instantaneous release	Short half-life	Modeled as instantaneous release

**Table 4.1-3: Calculated Solubilities and Controlling Phases in Submerged Waste Tanks
(Continued)**

	Submerged Condition A		Submerged Condition C		Submerged Condition D	
	Controlling Phase	Solubility (mol/L)	Controlling Phase	Solubility (mol/L)	Controlling Phase	Solubility (mol/L)
Se	No solubility control	Modeled as instantaneous release	FeS2	5.1E-08	No solubility control	Modeled as instantaneous release
Sm	SmCO3OH·0.5 H2O	2.5E-04	SmCO3OH 0.5H2O	3.7E-09	SmCO3OH·0.5 H2O	3.8E-09
Sn	SnO2(am)	3.5E-08	SnO2(am)	2.6E-07	SnO2(am)	2.7E-07
Sr	No solubility control	Modeled as instantaneous release	SrCO3	9.9E-04	SrCO3	9.8E-04
Tc	No solubility control	Modeled as instantaneous release	TcO2·1.6H2O	4.0E-09	No solubility control	Modeled as instantaneous release
Te	No solubility control	Modeled as instantaneous release	No solubility control	Modeled as instantaneous release	No solubility control	Modeled as instantaneous release
Th	ThO2(am,aged)	1.7E-05	ThO2(am,aged)	1.3E-09	ThO2(am,aged)	1.3E-09
U	UO3·2H2O	4.3E-05	UO2(am)	4.5E-09	UO3·2H2O	1.8E-06
Y	No Solubility Control	Modeled as instantaneous release	Y(OH)3	1.4E-08	Y(OH)3	1.3E-08

Condition A: Porewater = Groundwater

Condition C: Porewater = Mixture 0.9 Groundwater + 0.1 Reduced Region II Porewater

Condition D: Porewater = Mixture 0.9 Groundwater + 0.1 Oxidized Region II Porewater

[SRNL-STI-2012-00404 Rev. 0]

Table 4.1-4: Probability Distributions for Various Phases Controlling Reduced Region II Solubility

Element	Controlling Phase	Solubility (mol/L)	Probability ^b
Plutonium	PuO _{2(am,hyd)}	3.2E-11	0.5
	Fe co-precipitation ^a	7.6E-13	0.5
Neptunium	NpO _{2(am,hyd)}	9.9E-10	0.5
	Fe co-precipitation ^a	4.6E-15	0.5
Technetium	TcO ₂ ·1.6H ₂ O	1.1E-08	0.5
	Fe co-precipitation ^a	1.1E-14	0.5
Uranium	UO _{2(am,hyd)}	4.6E-09	0.5
	Fe co-precipitation ^a	2.4E-12	0.5

[SRNL-STI-2012-00404 Rev. 0]

a Reduced Region II iron co-precipitation values (from SRNL-STI-2012-00404 Rev. 0) assumed to be controlling 50 % of the time.

b Probabilities modified from source table to include iron co-precipitation

Table 4.1-5: Probability Distributions for Various Phases Controlling Oxidized Region II Solubility

Element	Controlling Phase	Solubility (mol/L)	Probability ^b
Plutonium	PuO _{2(am,hyd)}	3.2E-11	0.5
	Fe co-precipitation ^a	7.4E-12	0.5
Neptunium	NpO _{2(am,hyd)}	2.5E-07	0.5
	Fe co-precipitation ^a	4.4E-14	0.5
Technetium	no solubility limit	Modeled as instantaneous release	0.5
	Fe co-precipitation ^a	1.1E-13	0.5
Uranium	UO ₃ ·2H ₂ O	5.1E-05	0.5
	Fe co-precipitation ^a	2.3E-11	0.5

[SRNL-STI-2012-00404 Rev. 0]

^a Oxidized Region II Fe co-precipitation values (from SRNL-STI-2012-00404 Rev. 0) assumed to be controlling 50 % of the time.

^b Probabilities modified from source table to include Fe co-precipitation

^c -1 is an indicator of no solubility control in GoldSim stochastic elements

Table 4.1-6: Probability Distributions for Various Phases Controlling Oxidized Region III Solubility

Element	Controlling Phase	Solubility (mol/L)	Probability ^b
Plutonium	PuO _{2(am,hyd)}	3.2E-11	0.5
	Fe co-precipitation ^a	1.5E-13	0.5
Neptunium	NpO _{2(am,hyd)}	1.7E-06	0.5
	Fe co-precipitation ^a	8.8E-16	0.5
Technetium	no solubility limit	Modeled as instantaneous release	0.5
	Fe co-precipitation ^a	2.1E-15	0.5
Uranium	UO ₃ ·2H ₂ O	4.3E-06	0.5
	Fe co-precipitation ^a	4.5E-13	0.5

[SRNL-STI-2012-00404 Rev. 0]

^a Oxidized Region II Fe co-precipitation values (from SRNL-STI-2012-00404, Rev. 0) assumed to be controlling 50 % of the time.

^b Probabilities modified from source table to include Fe co-precipitation

^c -1 is an indicator of no solubility control in GoldSim stochastic elements

4.1.1.2 Transition Times

The transition times for chemistry-based changes in waste solubility and K_d values are calculated in the HTF GoldSim Model by counting the number of pore volumes of water that have flowed through the zone for which the transition times are being calculated and comparing the number of pore volumes to specified numbers of pore volumes. There are two chemical environment transitions considered, the first based on E_h and the second based on pH. The specified number of pore volumes used to calculate the occurrence of changes in chemistry has been updated since the development of the original HTF Stochastic Model and

the new values as presented in SRNL-STI-2012-00404 Rev. 0 have been implemented in the HTF GoldSim Model in SRR-CWDA-2010-00093, Rev 2. The specified pore volumes controlling the transition times are defined by triangular distributions with the most likely value used for deterministic runs. Separate values and associated distributions are used for non-submerged and submerged conditions. For fully submerged waste tanks (Type I), only the submerged values are used. For the partially submerged Type II tanks, the submerged values are used for zones beneath the primary liner, and non-submerged values are used for zones above the primary liner. For all other waste tank types, only the non-submerged values are used. The values used in HTF Stochastic Model of SRR-CWDA-2010-00093, Rev 2 are presented in Table 4.1-7.

Table 4.1-7: Pore Volume Distribution for Chemical Condition Step Change

Waste Tank Position	Transition ^a	Number of Pore Volumes Required		
		Deterministic (Most Likely)	Triangular Distribution	
			Minimum	Maximum
Non Submerged	Reduced Region II to Oxidized Region II (Step 1)	523	366	680
	Oxidized Region II to Oxidized Region III (Step 2)	2,119	1,060	3,179
Submerged	Condition C ^b to Condition D ^b (Step 1)	1,787	1,251	2,323
	Condition D ^b to Oxidized Region III (Step 2)	2,442	1,221	3,663

From SRNL-STI-2012-00404, Rev 0

a Step 1 = +/- 30 % of most likely; Step 2 = +/- 50 % of most likely

b Where Condition C =water flowing into the CZ is small fraction of groundwater mixed with the Reduced Region II grout pore fluid, and Condition D = water flowing into CZ is small fraction of groundwater mixed with Oxidizing Region II grout pore fluid.

4.2 HTF Source Inputs

In SRR-CWDA-2010-00093, Rev 2, of the HTF Stochastic Model, the source terms have been updated as described in SRR-CWDA-2010-00023, Rev. 3. The HTF source inputs include the inventories both the waste tanks and the ancillary equipment.

4.2.1 Waste Tanks

The HTF source inputs for the waste tanks include the inventories, the engineered structure geometry, the waste-tank configuration statistics, and the waste tank-type classification.

4.2.1.1 Inventory

The waste tank inventories, which have been updated, include values for the CZ, the sand pads, and the annulus. In addition, the CZ values have species dependent distributions used in the stochastic analyses.

4.2.1.1.1 Waste Tank Inventory Deterministic Values

For each waste tank the updated deterministic values for the radionuclide inventories in the CZ, are presented in Table 4.2-1. The deterministic values for the nonradioactive species inventories in the CZ, for each waste tank are presented in Table 4.2-2. For the annulus floor, the deterministic radionuclide inventories for the Type I tanks (Tank 9, Tank 10, Tank 11, and Tank 12) are presented in Table 4.2-3. For the primary and secondary sand pads, the deterministic radionuclide inventories for the Type II Tanks (Tank 13, Tank 14, Tank 15, and Tank 16) are presented in Table 4.2-4. For the annulus floor, the deterministic radionuclide inventories for the Type II Tanks (Tank 13, Tank 14, Tank 15, and Tank 16) are presented in Table 4.2-5. The Type I and Type II tank deterministic inventory values for the nonradioactive species in the annulus floor are presented in Table 4.2-6. The Type II tank deterministic inventory values for the nonradioactive species, in the primary and secondary sand pads, are presented in Table 4.2-7. Note that Tank 16 is the only waste tank with a secondary sand pad inventory. The initial estimates are taken from SRR-CWDA-2010-00023, Rev. 3, which also provides a description of the method and justification used to generate the initial inventory estimates used in the various waste tank components.

Table 4.2-1: HTF Estimated Radiological Inventory (Ci) at HTF Closure (2032)

Tank	Ac-227	Al-26	Am-241	Am-242m	Am-243	Ba-137m	C-14	Cf-249	Cf-251	Cl-36	Cm-243	Cm-244	Cm-245
9	1.0E+00	1.0E+00	7.0E+02	1.0E+00	3.0E+00	7.4E+02	1.0E+00	1.0E+00	1.0E+00	2.1E-03	1.0E+00	2.0E+01	1.0E+00
10	1.0E+00	1.0E+00	7.0E+02	1.0E+00	3.0E+00	7.4E+02	1.0E+00	1.0E+00	1.0E+00	2.1E-03	1.0E+00	2.0E+01	1.0E+00
11	1.0E+00	1.0E+00	7.0E+02	1.0E+00	3.0E+00	7.4E+02	1.0E+00	1.0E+00	1.0E+00	2.1E-03	1.0E+00	2.0E+01	1.0E+00
12	1.0E+00	1.0E+00	7.0E+02	1.0E+00	3.0E+00	7.4E+02	1.0E+00	1.0E+00	1.0E+00	2.1E-03	1.0E+00	2.0E+01	1.0E+00
13	1.0E+00	1.0E+00	7.0E+02	1.0E+00	3.0E+00	7.4E+02	1.0E+00	1.0E+00	1.0E+00	2.1E-03	1.0E+00	2.0E+01	1.0E+00
14	1.0E+00	1.0E+00	7.0E+02	1.0E+00	3.0E+00	7.4E+02	1.0E+00	1.0E+00	1.0E+00	2.1E-03	1.0E+00	2.0E+01	1.0E+00
15	1.0E+00	1.0E+00	7.0E+02	1.0E+00	3.0E+00	7.4E+02	1.0E+00	1.0E+00	1.0E+00	2.1E-03	1.0E+00	2.0E+01	1.0E+00
16	1.0E+00	1.0E+00	8.1E+01	1.0E+00	1.0E+00	1.2E+02	1.0E+00	1.0E+00	1.0E+00	5.3E-04	1.0E+00	2.4E+00	1.0E+00
21	1.0E+00	1.0E+00	5.0E+00	1.0E+00	1.0E+00	2.3E+03	1.0E+00	1.0E+00	1.0E+00	2.1E-03	1.0E+00	4.6E+00	1.0E+00
22	1.0E+00	1.0E+00	5.0E+00	1.0E+00	1.0E+00	2.3E+03	1.0E+00	1.0E+00	1.0E+00	2.1E-03	1.0E+00	4.6E+00	1.0E+00
23	1.0E+00	1.0E+00	5.0E+00	1.0E+00	1.0E+00	2.3E+03	1.0E+00	1.0E+00	1.0E+00	2.1E-03	1.0E+00	4.6E+00	1.0E+00
24	1.0E+00	1.0E+00	5.0E+00	1.0E+00	1.0E+00	2.3E+03	1.0E+00	1.0E+00	1.0E+00	2.1E-03	1.0E+00	4.6E+00	1.0E+00
29	1.0E+00	1.0E+00	1.1E+03	1.0E+00	1.0E+00	5.2E+03	1.0E+00	1.0E+00	1.0E+00	2.1E-03	1.0E+00	2.2E+03	1.0E+00
30	1.0E+00	1.0E+00	1.1E+03	1.0E+00	1.0E+00	5.2E+03	1.0E+00	1.0E+00	1.0E+00	2.1E-03	1.0E+00	2.2E+03	1.0E+00
31	1.0E+00	1.0E+00	1.1E+03	1.0E+00	1.0E+00	5.2E+03	1.0E+00	1.0E+00	1.0E+00	2.1E-03	1.0E+00	2.2E+03	1.0E+00
32	1.0E+00	1.0E+00	1.1E+03	1.0E+00	1.0E+00	5.2E+03	1.0E+00	1.0E+00	1.0E+00	2.1E-03	1.0E+00	2.2E+03	1.0E+00
35	1.0E+00	1.0E+00	1.1E+03	1.0E+00	1.0E+00	5.2E+03	1.0E+00	1.0E+00	1.0E+00	2.1E-03	1.0E+00	2.2E+03	1.0E+00
36	1.0E+00	1.0E+00	1.1E+03	1.0E+00	1.0E+00	5.2E+03	1.0E+00	1.0E+00	1.0E+00	2.1E-03	1.0E+00	2.2E+03	1.0E+00
37	1.0E+00	1.0E+00	1.1E+03	1.0E+00	1.0E+00	5.2E+03	1.0E+00	1.0E+00	1.0E+00	2.1E-03	1.0E+00	2.2E+03	1.0E+00
38	1.0E+00	1.0E+00	1.1E+03	1.0E+00	1.0E+00	5.2E+03	1.0E+00	1.0E+00	1.0E+00	2.1E-03	1.0E+00	2.2E+03	1.0E+00
39	1.0E+00	1.0E+00	1.1E+03	1.0E+00	1.0E+00	5.2E+03	1.0E+00	1.0E+00	1.0E+00	2.1E-03	1.0E+00	2.2E+03	1.0E+00
40	1.0E+00	1.0E+00	1.1E+03	1.0E+00	1.0E+00	5.2E+03	1.0E+00	1.0E+00	1.0E+00	2.1E-03	1.0E+00	2.2E+03	1.0E+00
41	1.0E+00	1.0E+00	1.1E+03	1.0E+00	1.0E+00	5.2E+03	1.0E+00	1.0E+00	1.0E+00	2.1E-03	1.0E+00	2.2E+03	1.0E+00
42	1.0E+00	1.0E+00	1.1E+03	1.0E+00	1.0E+00	5.2E+03	1.0E+00	1.0E+00	1.0E+00	2.1E-03	1.0E+00	2.2E+03	1.0E+00
43	1.0E+00	1.0E+00	1.1E+03	1.0E+00	1.0E+00	5.2E+03	1.0E+00	1.0E+00	1.0E+00	2.1E-03	1.0E+00	2.2E+03	1.0E+00
48	1.0E+00	1.0E+00	1.1E+03	1.0E+00	1.0E+00	5.2E+03	1.0E+00	1.0E+00	1.0E+00	2.1E-03	1.0E+00	2.2E+03	1.0E+00
49	1.0E+00	1.0E+00	1.1E+03	1.0E+00	1.0E+00	5.2E+03	1.0E+00	1.0E+00	1.0E+00	2.1E-03	1.0E+00	2.2E+03	1.0E+00
50	1.0E+00	1.0E+00	1.1E+03	1.0E+00	1.0E+00	5.2E+03	1.0E+00	1.0E+00	1.0E+00	2.1E-03	1.0E+00	2.2E+03	1.0E+00
51	1.0E+00	1.0E+00	1.1E+03	1.0E+00	1.0E+00	5.2E+03	1.0E+00	1.0E+00	1.0E+00	2.1E-03	1.0E+00	2.2E+03	1.0E+00

Table 4.2-1: HTF Estimated Radiological Inventory (Ci) at HTF Closure (2032) (Continued)

Tank	Cm-247	Cm-248	Co-60	Cs-135	Cs-137	Eu-152	Eu-154	H-3	I-129	K-40	Nb-94	Ni-59	Ni-63	Np-237
9	1.0E+00	1.0E+00	1.0E+00	5.4E-03	7.9E+02	2.1E+01	2.9E+02	1.0E+00	2.8E-04	1.1E-03	1.1E-01	8.6E+00	6.3E+02	2.1E-01
10	1.0E+00	1.0E+00	1.0E+00	5.4E-03	7.9E+02	2.1E+01	2.9E+02	1.0E+00	2.8E-04	1.1E-03	1.1E-01	8.6E+00	6.3E+02	2.1E-01
11	1.0E+00	1.0E+00	1.0E+00	5.4E-03	7.9E+02	2.1E+01	2.9E+02	1.0E+00	2.8E-04	1.1E-03	1.1E-01	8.6E+00	6.3E+02	2.1E-01
12	1.0E+00	1.0E+00	1.0E+00	5.4E-03	7.9E+02	2.1E+01	2.9E+02	1.0E+00	2.8E-04	1.1E-03	1.1E-01	8.6E+00	6.3E+02	2.1E-01
13	1.0E+00	1.0E+00	1.0E+00	5.4E-03	7.9E+02	2.1E+01	2.9E+02	1.0E+00	2.8E-04	1.1E-03	1.1E-01	8.6E+00	6.3E+02	2.1E-01
14	1.0E+00	1.0E+00	1.0E+00	5.4E-03	7.9E+02	2.1E+01	2.9E+02	1.0E+00	2.8E-04	1.1E-03	1.1E-01	8.6E+00	6.3E+02	2.1E-01
15	1.0E+00	1.0E+00	1.0E+00	5.4E-03	7.9E+02	2.1E+01	2.9E+02	1.0E+00	2.8E-04	1.1E-03	1.1E-01	8.6E+00	6.3E+02	2.1E-01
16	1.0E+00	1.0E+00	1.0E+00	9.9E-04	1.3E+02	1.0E+00	3.3E+01	1.0E+00	5.3E-05	2.6E-04	2.6E-02	1.0E+00	1.1E+02	2.2E-02
21	1.0E+00	1.0E+00	1.0E+00	2.3E-02	2.4E+03	1.0E+00	8.3E+00	1.0E+00	2.1E-04	1.1E-03	1.1E-01	1.0E+00	9.1E+00	1.3E-02
22	1.0E+00	1.0E+00	1.0E+00	2.3E-02	2.4E+03	1.0E+00	8.3E+00	1.0E+00	2.1E-04	1.1E-03	1.1E-01	1.0E+00	9.1E+00	1.3E-02
23	1.0E+00	1.0E+00	1.0E+00	2.3E-02	2.4E+03	1.0E+00	8.3E+00	1.0E+00	2.1E-04	1.1E-03	1.1E-01	1.0E+00	9.1E+00	1.3E-02
24	1.0E+00	1.0E+00	1.0E+00	2.3E-02	2.4E+03	1.0E+00	8.3E+00	1.0E+00	2.1E-04	1.1E-03	1.1E-01	1.0E+00	9.1E+00	1.3E-02
29	1.0E+00	1.0E+00	1.0E+00	7.1E-03	5.5E+03	3.8E+01	9.2E+02	1.0E+00	6.7E-03	1.1E-03	1.1E-01	1.0E+00	7.9E+02	4.0E-01
30	1.0E+00	1.0E+00	1.0E+00	7.1E-03	5.5E+03	3.8E+01	9.2E+02	1.0E+00	6.7E-03	1.1E-03	1.1E-01	1.0E+00	7.9E+02	4.0E-01
31	1.0E+00	1.0E+00	1.0E+00	7.1E-03	5.5E+03	3.8E+01	9.2E+02	1.0E+00	6.7E-03	1.1E-03	1.1E-01	1.0E+00	7.9E+02	4.0E-01
32	1.0E+00	1.0E+00	1.0E+00	7.1E-03	5.5E+03	3.8E+01	9.2E+02	1.0E+00	6.7E-03	1.1E-03	1.1E-01	1.0E+00	7.9E+02	4.0E-01
35	1.0E+00	1.0E+00	1.0E+00	7.1E-03	5.5E+03	3.8E+01	9.2E+02	1.0E+00	6.7E-03	1.1E-03	1.1E-01	1.0E+00	7.9E+02	4.0E-01
36	1.0E+00	1.0E+00	1.0E+00	7.1E-03	5.5E+03	3.8E+01	9.2E+02	1.0E+00	6.7E-03	1.1E-03	1.1E-01	1.0E+00	7.9E+02	4.0E-01
37	1.0E+00	1.0E+00	1.0E+00	7.1E-03	5.5E+03	3.8E+01	9.2E+02	1.0E+00	6.7E-03	1.1E-03	1.1E-01	1.0E+00	7.9E+02	4.0E-01
38	1.0E+00	1.0E+00	1.0E+00	7.1E-03	5.5E+03	3.8E+01	9.2E+02	1.0E+00	6.7E-03	1.1E-03	1.1E-01	1.0E+00	7.9E+02	4.0E-01
39	1.0E+00	1.0E+00	1.0E+00	7.1E-03	5.5E+03	3.8E+01	9.2E+02	1.0E+00	6.7E-03	1.1E-03	1.1E-01	1.0E+00	7.9E+02	4.0E-01
40	1.0E+00	1.0E+00	1.0E+00	7.1E-03	5.5E+03	3.8E+01	9.2E+02	1.0E+00	6.7E-03	1.1E-03	1.1E-01	1.0E+00	7.9E+02	4.0E-01
41	1.0E+00	1.0E+00	1.0E+00	7.1E-03	5.5E+03	3.8E+01	9.2E+02	1.0E+00	6.7E-03	1.1E-03	1.1E-01	1.0E+00	7.9E+02	4.0E-01
42	1.0E+00	1.0E+00	1.0E+00	7.1E-03	5.5E+03	3.8E+01	9.2E+02	1.0E+00	6.7E-03	1.1E-03	1.1E-01	1.0E+00	7.9E+02	4.0E-01
43	1.0E+00	1.0E+00	1.0E+00	7.1E-03	5.5E+03	3.8E+01	9.2E+02	1.0E+00	6.7E-03	1.1E-03	1.1E-01	1.0E+00	7.9E+02	4.0E-01
48	1.0E+00	1.0E+00	1.0E+00	7.1E-03	5.5E+03	3.8E+01	9.2E+02	1.0E+00	6.7E-03	1.1E-03	1.1E-01	1.0E+00	7.9E+02	4.0E-01
49	1.0E+00	1.0E+00	1.0E+00	7.1E-03	5.5E+03	3.8E+01	9.2E+02	1.0E+00	6.7E-03	1.1E-03	1.1E-01	1.0E+00	7.9E+02	4.0E-01
50	1.0E+00	1.0E+00	1.0E+00	7.1E-03	5.5E+03	3.8E+01	9.2E+02	1.0E+00	6.7E-03	1.1E-03	1.1E-01	1.0E+00	7.9E+02	4.0E-01
51	1.0E+00	1.0E+00	1.0E+00	7.1E-03	5.5E+03	3.8E+01	9.2E+02	1.0E+00	6.7E-03	1.1E-03	1.1E-01	1.0E+00	7.9E+02	4.0E-01

Table 4.2-1: HTF Estimated Radiological Inventory (Ci) at HTF Closure (2032) (Continued)

Tank	Pa-231	Pd-107	Pt-193	Pu-238	Pu-239	Pu-240	Pu-241	Pu-242	Pu-244	Ra-226	Ra-228	Se-79	Sm-151	Sn-126
9	2.1E-03	2.1E-01	2.1E-01	6.5E+03	8.0E+01	5.0E+01	7.6E+02	1.0E+00	1.0E+00	2.1E-02	2.1E+00	4.8E+00	1.1E+04	4.6E+00
10	2.1E-03	2.1E-01	2.1E-01	6.5E+03	8.0E+01	5.0E+01	7.6E+02	1.0E+00	1.0E+00	2.1E-02	2.1E+00	4.8E+00	1.1E+04	4.6E+00
11	2.1E-03	2.1E-01	2.1E-01	6.5E+03	8.0E+01	5.0E+01	7.6E+02	1.0E+00	1.0E+00	2.1E-02	2.1E+00	4.8E+00	1.1E+04	4.6E+00
12	2.1E-03	2.1E-01	2.1E-01	6.5E+03	8.0E+01	5.0E+01	7.6E+02	1.0E+00	1.0E+00	2.1E-02	2.1E+00	4.8E+00	1.1E+04	4.6E+00
13	2.1E-03	2.1E-01	2.1E-01	6.5E+03	8.0E+01	5.0E+01	7.6E+02	1.0E+00	1.0E+00	2.1E-02	2.1E+00	4.8E+00	1.1E+04	4.6E+00
14	2.1E-03	2.1E-01	2.1E-01	6.5E+03	8.0E+01	5.0E+01	7.6E+02	1.0E+00	1.0E+00	2.1E-02	2.1E+00	4.8E+00	1.1E+04	4.6E+00
15	2.1E-03	2.1E-01	2.1E-01	6.5E+03	8.0E+01	5.0E+01	7.6E+02	1.0E+00	1.0E+00	2.1E-02	2.1E+00	4.8E+00	1.1E+04	4.6E+00
16	5.3E-04	5.3E-02	5.3E-02	2.9E+02	7.7E+00	3.7E+00	2.0E+01	1.0E+00	1.0E+00	5.3E-03	5.3E-01	1.0E+00	1.8E+03	1.0E+00
21	2.1E-03	2.1E-01	2.1E-01	7.2E+01	1.0E+00	3.6E-01	2.1E+00	1.0E+00	1.0E+00	2.1E-02	2.1E+00	1.0E+00	2.4E+02	1.0E+00
22	2.1E-03	2.1E-01	2.1E-01	7.2E+01	1.0E+00	3.6E-01	2.1E+00	1.0E+00	1.0E+00	2.1E-02	2.1E+00	1.0E+00	2.4E+02	1.0E+00
23	2.1E-03	2.1E-01	2.1E-01	7.2E+01	1.0E+00	3.6E-01	2.1E+00	1.0E+00	1.0E+00	2.1E-02	2.1E+00	1.0E+00	2.4E+02	1.0E+00
24	2.1E-03	2.1E-01	2.1E-01	7.2E+01	1.0E+00	3.6E-01	2.1E+00	1.0E+00	1.0E+00	2.1E-02	2.1E+00	1.0E+00	2.4E+02	1.0E+00
29	2.1E-03	2.1E-01	2.1E-01	2.8E+03	2.4E+02	1.5E+02	4.6E+03	1.0E+00	1.0E+00	2.1E-02	2.1E+00	1.0E+00	7.7E+04	1.0E+00
30	2.1E-03	2.1E-01	2.1E-01	2.8E+03	2.4E+02	1.5E+02	4.6E+03	1.0E+00	1.0E+00	2.1E-02	2.1E+00	1.0E+00	7.7E+04	1.0E+00
31	2.1E-03	2.1E-01	2.1E-01	2.8E+03	2.4E+02	1.5E+02	4.6E+03	1.0E+00	1.0E+00	2.1E-02	2.1E+00	1.0E+00	7.7E+04	1.0E+00
32	2.1E-03	2.1E-01	2.1E-01	1.5E+04	2.4E+02	1.5E+02	4.6E+03	1.0E+00	1.0E+00	2.1E-02	2.1E+00	1.0E+00	7.7E+04	1.0E+00
35	2.1E-03	2.1E-01	2.1E-01	2.8E+03	2.4E+02	1.5E+02	4.6E+03	1.0E+00	1.0E+00	2.1E-02	2.1E+00	1.0E+00	7.7E+04	1.0E+00
36	2.1E-03	2.1E-01	2.1E-01	2.8E+03	2.4E+02	1.5E+02	4.6E+03	1.0E+00	1.0E+00	2.1E-02	2.1E+00	1.0E+00	7.7E+04	1.0E+00
37	2.1E-03	2.1E-01	2.1E-01	2.8E+03	2.4E+02	1.5E+02	4.6E+03	1.0E+00	1.0E+00	2.1E-02	2.1E+00	1.0E+00	7.7E+04	1.0E+00
38	2.1E-03	2.1E-01	2.1E-01	2.8E+03	2.4E+02	1.5E+02	4.6E+03	1.0E+00	1.0E+00	2.1E-02	2.1E+00	1.0E+00	7.7E+04	1.0E+00
39	2.1E-03	2.1E-01	2.1E-01	1.5E+04	2.4E+02	1.5E+02	4.6E+03	1.0E+00	1.0E+00	2.1E-02	2.1E+00	1.0E+00	7.7E+04	1.0E+00
40	2.1E-03	2.1E-01	2.1E-01	1.5E+04	2.4E+02	1.5E+02	4.6E+03	1.0E+00	1.0E+00	2.1E-02	2.1E+00	1.0E+00	7.7E+04	1.0E+00
41	2.1E-03	2.1E-01	2.1E-01	2.8E+03	2.4E+02	1.5E+02	4.6E+03	1.0E+00	1.0E+00	2.1E-02	2.1E+00	1.0E+00	7.7E+04	1.0E+00
42	2.1E-03	2.1E-01	2.1E-01	1.5E+04	2.4E+02	1.5E+02	4.6E+03	1.0E+00	1.0E+00	2.1E-02	2.1E+00	1.0E+00	7.7E+04	1.0E+00
43	2.1E-03	2.1E-01	2.1E-01	1.5E+04	2.4E+02	1.5E+02	4.6E+03	1.0E+00	1.0E+00	2.1E-02	2.1E+00	1.0E+00	7.7E+04	1.0E+00
48	2.1E-03	2.1E-01	2.1E-01	2.8E+03	2.4E+02	1.5E+02	4.6E+03	1.0E+00	1.0E+00	2.1E-02	2.1E+00	1.0E+00	7.7E+04	1.0E+00
49	2.1E-03	2.1E-01	2.1E-01	2.8E+03	2.4E+02	1.5E+02	4.6E+03	1.0E+00	1.0E+00	2.1E-02	2.1E+00	1.0E+00	7.7E+04	1.0E+00
50	2.1E-03	2.1E-01	2.1E-01	1.5E+04	2.4E+02	1.5E+02	4.6E+03	1.0E+00	1.0E+00	2.1E-02	2.1E+00	1.0E+00	7.7E+04	1.0E+00
51	2.1E-03	2.1E-01	2.1E-01	1.5E+04	2.4E+02	1.5E+02	4.6E+03	1.0E+00	1.0E+00	2.1E-02	2.1E+00	1.0E+00	7.7E+04	1.0E+00

Table 4.2-1: HTF Estimated Radiological Inventory (Ci) at HTF Closure (2032) (Continued)

Tank	Sr-90	Tc-99	Th-229	Th-230	Th-232	U-232	U-233	U-234	U-235	U-236	U-238	Y-90	Zr-93
9	1.4E+04	8.1E+00	2.1E-03	2.1E-02	2.9E-02	2.1E-03	5.9E-01	9.6E-02	2.1E-02	2.1E-02	2.9E-02	1.4E+04	4.0E-01
10	1.4E+04	8.1E+00	2.1E-03	2.1E-02	2.9E-02	2.1E-03	5.9E-01	9.6E-02	2.1E-02	2.1E-02	2.9E-02	1.4E+04	4.0E-01
11	1.4E+04	8.1E+00	2.1E-03	2.1E-02	2.9E-02	2.1E-03	5.9E-01	9.6E-02	2.1E-02	2.1E-02	2.9E-02	1.4E+04	4.0E-01
12	2.2E+03	1.5E+00	5.3E-04	5.3E-03	5.3E-03	5.3E-04	8.7E-02	2.4E-02	5.3E-03	5.3E-03	5.3E-04	2.2E+03	6.3E-02
13	3.1E+02	1.6E-01	2.1E-03	2.1E-02	2.1E-02	2.1E-03	6.0E-02	2.2E-02	2.1E-02	2.1E-02	7.4E-03	3.1E+02	8.8E-03
14	3.1E+02	1.6E-01	2.1E-03	2.1E-02	2.1E-02	2.1E-03	6.0E-02	2.2E-02	2.1E-02	2.1E-02	7.4E-03	3.1E+02	8.8E-03
15	3.1E+02	1.6E-01	2.1E-03	2.1E-02	2.1E-02	2.1E-03	6.0E-02	2.2E-02	2.1E-02	2.1E-02	7.4E-03	3.1E+02	8.8E-03
16	3.1E+02	1.6E-01	2.1E-03	2.1E-02	2.1E-02	2.1E-03	6.0E-02	2.2E-02	2.1E-02	2.1E-02	7.4E-03	3.1E+02	8.8E-03
21	2.0E+04	9.7E+00	2.1E-03	2.1E-02	2.7E-02	2.1E-03	1.3E+00	6.6E-01	2.1E-02	1.1E-01	8.4E-02	2.0E+04	5.7E-01
22	2.0E+04	9.7E+00	2.1E-03	2.1E-02	2.7E-02	2.1E-03	1.3E+00	6.6E-01	2.1E-02	1.1E-01	8.4E-02	2.0E+04	5.7E-01
23	2.0E+04	9.7E+00	2.1E-03	2.1E-02	2.7E-02	2.1E-03	1.3E+00	6.6E-01	2.1E-02	1.1E-01	8.4E-02	2.0E+04	5.7E-01
24	2.0E+04	9.7E+00	2.1E-03	2.1E-02	2.7E-02	2.1E-03	1.3E+00	6.6E-01	2.1E-02	1.1E-01	8.4E-02	2.0E+04	5.7E-01
29	2.0E+04	9.7E+00	2.1E-03	2.1E-02	2.7E-02	2.1E-03	1.3E+00	6.6E-01	2.1E-02	1.1E-01	8.4E-02	2.0E+04	5.7E-01
30	2.0E+04	9.7E+00	2.1E-03	2.1E-02	2.7E-02	2.1E-03	1.3E+00	6.6E-01	2.1E-02	1.1E-01	8.4E-02	2.0E+04	5.7E-01
31	2.0E+04	9.7E+00	2.1E-03	2.1E-02	2.7E-02	2.1E-03	1.3E+00	6.6E-01	2.1E-02	1.1E-01	8.4E-02	2.0E+04	5.7E-01
32	2.0E+04	9.7E+00	2.1E-03	2.1E-02	2.7E-02	2.1E-03	1.3E+00	6.6E-01	2.1E-02	1.1E-01	8.4E-02	2.0E+04	5.7E-01
35	2.0E+04	9.7E+00	2.1E-03	2.1E-02	2.7E-02	2.1E-03	1.3E+00	6.6E-01	2.1E-02	1.1E-01	8.4E-02	2.0E+04	5.7E-01
36	2.0E+04	9.7E+00	2.1E-03	2.1E-02	2.7E-02	2.1E-03	1.3E+00	6.6E-01	2.1E-02	1.1E-01	8.4E-02	2.0E+04	5.7E-01
37	2.0E+04	9.7E+00	2.1E-03	2.1E-02	2.7E-02	2.1E-03	1.3E+00	6.6E-01	2.1E-02	1.1E-01	8.4E-02	2.0E+04	5.7E-01
38	2.0E+04	9.7E+00	2.1E-03	2.1E-02	2.7E-02	2.1E-03	1.3E+00	6.6E-01	2.1E-02	1.1E-01	8.4E-02	2.0E+04	5.7E-01
39	2.0E+04	9.7E+00	2.1E-03	2.1E-02	2.7E-02	2.1E-03	1.3E+00	6.6E-01	2.1E-02	1.1E-01	8.4E-02	2.0E+04	5.7E-01
40	2.0E+04	9.7E+00	2.1E-03	2.1E-02	2.7E-02	2.1E-03	1.3E+00	6.6E-01	2.1E-02	1.1E-01	8.4E-02	2.0E+04	5.7E-01
41	2.0E+04	9.7E+00	2.1E-03	2.1E-02	2.7E-02	2.1E-03	1.3E+00	6.6E-01	2.1E-02	1.1E-01	8.4E-02	2.0E+04	5.7E-01
42	2.0E+04	9.7E+00	2.1E-03	2.1E-02	2.7E-02	2.1E-03	1.3E+00	6.6E-01	2.1E-02	1.1E-01	8.4E-02	2.0E+04	5.7E-01
43	2.0E+04	9.7E+00	2.1E-03	2.1E-02	2.7E-02	2.1E-03	1.3E+00	6.6E-01	2.1E-02	1.1E-01	8.4E-02	2.0E+04	5.7E-01
48	1.4E+04	8.1E+00	2.1E-03	2.1E-02	2.9E-02	2.1E-03	5.9E-01	9.6E-02	2.1E-02	2.1E-02	2.9E-02	1.4E+04	4.0E-01
49	1.4E+04	8.1E+00	2.1E-03	2.1E-02	2.9E-02	2.1E-03	5.9E-01	9.6E-02	2.1E-02	2.1E-02	2.9E-02	1.4E+04	4.0E-01
50	1.4E+04	8.1E+00	2.1E-03	2.1E-02	2.9E-02	2.1E-03	5.9E-01	9.6E-02	2.1E-02	2.1E-02	2.9E-02	1.4E+04	4.0E-01
51	2.2E+03	1.5E+00	5.3E-04	5.3E-03	5.3E-03	5.3E-04	8.7E-02	2.4E-02	5.3E-03	5.3E-03	5.3E-04	2.2E+03	6.3E-02

[Table 3.3-1, SRR-CWDA-2010-00023, Rev 3]

Table 4.2-2: HTF Estimated Chemical Inventory (kg) at HTF Closure

Waste Tank	Ni	Se
9	6.3E+01	1.1E-02
10	6.3E+01	1.1E-02
11	6.3E+01	1.1E-02
12	1.1E-01	1.1E-02
13	4.6E+01	1.1E-02
14	4.6E+01	1.1E-02
15	4.6E+01	1.1E-02
16	4.6E+01	1.0E-03
21	1.3E+02	2.0E-03
22	1.3E+02	2.0E-03
23	1.3E+02	2.0E-03
24	1.3E+02	2.0E-03
29	1.3E+02	1.2E-02
30	1.3E+02	1.2E-02
31	1.3E+02	1.2E-02
32	1.3E+02	1.2E-02
35	1.3E+02	1.2E-02
36	1.3E+02	1.2E-02
37	1.3E+02	1.2E-02
38	1.3E+02	1.2E-02
39	1.3E+02	1.2E-02
40	1.3E+02	1.2E-02
41	1.3E+02	1.2E-02
42	1.3E+02	1.2E-02
43	1.3E+02	1.2E-02
48	6.3E+01	1.2E-02
49	6.3E+01	1.2E-02
50	6.3E+01	1.2E-02
51	1.1E-01	1.2E-02

[Table 3.3-2, SRR-CWDA-2010-00023, Rev 3]

Table 4.2-3: Type I Tank Annulus Floor Radiological Inventories

Radionuclide	Tank 9 (Ci)	Tank 10 (Ci)	Tank 11 (Ci)	Tank 12 (Ci)
Ac-227	1.0E+00	1.0E+00	1.0E+00	1.0E+00
Ag-108m	0.0E+00	0.0E+00	0.0E+00	0.0E+00
Al-26	1.0E+00	1.0E+00	1.0E+00	1.0E+00
Am-241	7.0E+00	7.0E+00	2.1E-01	2.1E-01
Am-242m	1.0E+00	1.0E+00	1.0E+00	1.0E+00
Am-243	3.0E+00	3.0E+00	3.0E+00	3.0E+00
Bi-210m	0.0E+00	0.0E+00	0.0E+00	0.0E+00
C-14	1.0E+00	1.0E+00	1.0E+00	1.0E+00
Ca-41	0.0E+00	0.0E+00	0.0E+00	0.0E+00
Cf-249	1.0E+00	1.0E+00	1.0E+00	1.0E+00
Cf-251	1.0E+00	1.0E+00	1.0E+00	1.0E+00
Cl-36	1.7E-03	1.7E-03	5.3E-05	5.3E-05
Cm-243	1.0E+00	1.0E+00	1.0E+00	1.0E+00
Cm-244	2.1E-01	2.1E-01	6.4E-03	6.4E-03
Cm-245	1.0E+00	1.0E+00	1.0E+00	1.0E+00
Cm-246	0.0E+00	0.0E+00	0.0E+00	0.0E+00
Cm-247	1.0E+00	1.0E+00	1.0E+00	1.0E+00
Cm-248	1.0E+00	1.0E+00	1.0E+00	1.0E+00
Co-60	1.0E+00	1.0E+00	1.0E+00	1.0E+00
Cs-135	3.2E-03	3.2E-03	9.8E-05	9.8E-05
Cs-137	1.2E+04	1.2E+04	3.7E+02	3.7E+02
Eu-152	2.1E+01	2.1E+01	2.1E+01	2.1E+01
Eu-154	2.9E+00	2.9E+00	8.8E-02	8.8E-02
Eu-155	0.0E+00	0.0E+00	0.0E+00	0.0E+00
Gd-152	0.0E+00	0.0E+00	0.0E+00	0.0E+00
H-3	1.0E+00	1.0E+00	1.0E+00	1.0E+00
I-129	1.7E-04	1.7E-04	5.3E-06	5.3E-06
K-40	8.7E-04	8.7E-04	2.6E-05	2.6E-05
Lu-174	0.0E+00	0.0E+00	0.0E+00	0.0E+00
Mo-93	0.0E+00	0.0E+00	0.0E+00	0.0E+00
Nb-93m	0.0E+00	0.0E+00	0.0E+00	0.0E+00

Table 4.2-3: Type I Tank Annulus Floor Radiological Inventories (Continued)

Radionuclide	Tank 9 (Ci)	Tank 10 (Ci)	Tank 11 (Ci)	Tank 12 (Ci)
Nb-94	8.7E-02	8.7E-02	2.6E-03	2.6E-03
Ni-59	8.6E+00	8.6E+00	8.6E+00	8.6E+00
Ni-63	9.6E+00	9.6E+00	2.9E-01	2.9E-01
Np-237	2.6E-02	2.6E-02	7.9E-04	7.9E-04
Pa-231	1.7E-03	1.7E-03	5.3E-05	5.3E-05
Pb-210	0.0E+00	0.0E+00	0.0E+00	0.0E+00
Pd-107	1.7E-01	1.7E-01	5.3E-03	5.3E-03
Pt-193	1.7E-01	1.7E-01	5.3E-03	5.3E-03
Pu-238	2.5E+01	2.5E+01	7.6E-01	7.6E-01
Pu-239	3.6E+00	3.6E+00	1.1E-01	1.1E-01
Pu-240	4.2E+00	4.2E+00	1.3E-01	1.3E-01
Pu-241	1.3E+01	1.3E+01	3.9E-01	3.9E-01
Pu-242	1.0E+00	1.0E+00	1.0E+00	1.0E+00
Pu-244	1.0E+00	1.0E+00	1.0E+00	1.0E+00
Ra-226	1.7E-02	1.7E-02	5.3E-04	5.3E-04
Ra-228	1.7E+00	1.7E+00	5.3E-02	5.3E-02
Se-79	4.8E+00	4.8E+00	4.8E+00	4.8E+00
Sm-147	0.0E+00	0.0E+00	0.0E+00	0.0E+00
Sm-151	1.5E+02	1.5E+02	4.7E+00	4.7E+00
Sn-126	4.6E+00	4.6E+00	4.6E+00	4.6E+00
Sr-90	7.8E+03	7.8E+03	2.4E+02	2.4E+02
Tc-99	4.9E+00	4.9E+00	1.5E-01	1.5E-01
Th-229	1.7E-03	1.7E-03	5.3E-05	5.3E-05
Th-230	1.7E-02	1.7E-02	5.3E-04	5.3E-04
Th-232	2.4E-02	2.4E-02	7.1E-04	7.1E-04
U-232	1.7E-03	1.7E-03	5.3E-05	5.3E-05
U-233	1.4E-01	1.4E-01	4.3E-03	4.3E-03
U-234	9.1E-02	9.1E-02	2.8E-03	2.8E-03
U-235	2.6E-04	2.6E-04	7.9E-06	7.9E-06
U-236	1.2E-03	1.2E-03	3.6E-05	3.6E-05
U-238	1.0E-03	1.0E-03	3.2E-05	3.2E-05
Zr-93	5.5E-03	5.5E-03	1.7E-04	1.7E-04

[Table 2.5-3, SRR-CWDA-2010-00023, Rev.3]

Table 4.2-4: Type II Tank Sand Pad Radiological Inventory

Radionuclide	Tank 13 (Ci)	Tank 14 (Ci)	Tank 15 (Ci)	Tank 16 (Ci)	
	Primary	Primary	Primary	Primary	Secondary
Ac-227	1.0E+00	1.0E+00	1.0E+00	1.0E+00	1.0E+00
Ag-108m	0.0E+00	0.0E+00	0.0E+00	0.0E+00	0.0E+00
Al-26	1.0E+00	1.0E+00	1.0E+00	1.0E+00	1.0E+00
Am-241	2.1E-01	2.8E+00	2.1E-01	2.8E+00	5.5E-02
Am-242m	1.0E+00	1.0E+00	1.0E+00	1.0E+00	1.0E+00
Am-243	3.0E+00	3.0E+00	3.0E+00	1.0E+00	1.0E+00
Bi-210m	0.0E+00	0.0E+00	0.0E+00	0.0E+00	0.0E+00
C-14	1.0E+00	1.0E+00	1.0E+00	1.0E+00	1.0E+00
Ca-41	0.0E+00	0.0E+00	0.0E+00	0.0E+00	0.0E+00
Cf-249	1.0E+00	1.0E+00	1.0E+00	1.0E+00	1.0E+00
Cf-251	1.0E+00	1.0E+00	1.0E+00	1.0E+00	1.0E+00
Cl-36	5.3E-05	6.9E-04	5.3E-05	6.9E-04	1.4E-05
Cm-243	1.0E+00	1.0E+00	1.0E+00	1.0E+00	1.0E+00
Cm-244	6.4E-03	8.3E-02	6.4E-03	8.3E-02	1.7E-03
Cm-245	1.0E+00	1.0E+00	1.0E+00	1.0E+00	1.0E+00
Cm-246	0.0E+00	0.0E+00	0.0E+00	0.0E+00	0.0E+00
Cm-247	1.0E+00	1.0E+00	1.0E+00	1.0E+00	1.0E+00
Cm-248	1.0E+00	1.0E+00	1.0E+00	1.0E+00	1.0E+00
Co-60	1.0E+00	1.0E+00	1.0E+00	1.0E+00	1.0E+00
Cs-135	9.8E-05	1.3E-03	9.8E-05	1.3E-03	2.6E-05
Cs-137	3.7E+02	4.8E+03	3.7E+02	4.8E+03	9.5E+01
Eu-152	2.1E+01	2.1E+01	2.1E+01	1.0E+00	1.0E+00
Eu-154	8.8E-02	1.1E+00	8.8E-02	1.1E+00	2.3E-02
Eu-155	0.0E+00	0.0E+00	0.0E+00	0.0E+00	0.0E+00
Gd-152	0.0E+00	0.0E+00	0.0E+00	0.0E+00	0.0E+00
H-3	1.0E+00	1.0E+00	1.0E+00	1.0E+00	1.0E+00
I-129	5.3E-06	6.9E-05	5.3E-06	6.9E-05	1.4E-06
K-40	2.6E-05	3.4E-04	2.6E-05	3.4E-04	6.9E-06
Lu-174	0.0E+00	0.0E+00	0.0E+00	0.0E+00	0.0E+00
Mo-93	0.0E+00	0.0E+00	0.0E+00	0.0E+00	0.0E+00
Nb-93m	0.0E+00	0.0E+00	0.0E+00	0.0E+00	0.0E+00

Table 4.2-4: Type II Tank Sand Pad Radiological Inventories (Continued)

Radionuclide	Tank 13 (Ci)	Tank 14 (Ci)	Tank 15 (Ci)	Tank 16 (Ci)	
	Primary	Primary	Primary	Primary	Secondary
Nb-94	2.6E-03	3.4E-02	2.6E-03	3.4E-02	6.9E-04
Ni-59	8.6E+00	8.6E+00	8.6E+00	1.0E+00	1.0E+00
Ni-63	2.9E-01	3.8E+00	2.9E-01	3.8E+00	7.6E-02
Np-237	7.9E-04	1.0E-02	7.9E-04	1.0E-02	2.1E-04
Pa-231	5.3E-05	6.9E-04	5.3E-05	6.9E-04	1.4E-05
Pb-210	0.0E+00	0.0E+00	0.0E+00	0.0E+00	0.0E+00
Pd-107	5.3E-03	6.9E-02	5.3E-03	6.9E-02	1.4E-03
Pt-193	5.3E-03	6.9E-02	5.3E-03	6.9E-02	1.4E-03
Pu-238	7.6E-01	9.8E+00	7.6E-01	9.8E+00	2.0E-01
Pu-239	1.1E-01	1.4E+00	1.1E-01	1.4E+00	2.9E-02
Pu-240	1.3E-01	1.7E+00	1.3E-01	1.7E+00	3.3E-02
Pu-241	3.9E-01	5.1E+00	3.9E-01	5.1E+00	1.0E-01
Pu-242	1.0E+00	1.0E+00	1.0E+00	1.0E+00	1.0E+00
Pu-244	1.0E+00	1.0E+00	1.0E+00	1.0E+00	1.0E+00
Ra-226	5.3E-04	6.9E-03	5.3E-04	6.9E-03	1.4E-04
Ra-228	5.3E-02	6.9E-01	5.3E-02	6.9E-01	1.4E-02
Se-79	4.8E+00	4.8E+00	4.8E+00	1.0E+00	1.0E+00
Sm-147	0.0E+00	0.0E+00	0.0E+00	0.0E+00	0.0E+00
Sm-151	4.7E+00	6.1E+01	4.7E+00	6.1E+01	1.2E+00
Sn-126	4.6E+00	4.6E+00	4.6E+00	1.0E+00	1.0E+00
Sr-90	2.4E+02	3.1E+03	2.4E+02	3.1E+03	6.1E+01
Tc-99	1.5E-01	1.9E+00	1.5E-01	1.9E+00	3.8E-02
Th-229	5.3E-05	6.9E-04	5.3E-05	6.9E-04	1.4E-05
Th-230	5.3E-04	6.9E-03	5.3E-04	6.9E-03	1.4E-04
Th-232	7.1E-04	9.3E-03	7.1E-04	6.9E-03	1.4E-04
U-232	5.3E-05	6.9E-04	5.3E-05	6.9E-04	1.4E-05
U-233	4.3E-03	5.6E-02	4.3E-03	5.6E-02	1.1E-03
U-234	2.8E-03	3.6E-02	2.8E-03	3.6E-02	7.2E-04
U-235	7.9E-06	1.0E-04	7.9E-06	1.0E-04	2.1E-06
U-236	3.6E-05	4.7E-04	3.6E-05	4.7E-04	9.4E-06
U-238	3.2E-05	4.1E-04	3.2E-05	4.1E-04	8.3E-06
Zr-93	1.7E-04	2.2E-03	1.7E-04	2.2E-03	4.3E-05

[Table 2.5-5, SRR-CWDA-2010-00023, Rev. 3]

Table 4.2-5: Type II Annulus Floor Radiological Inventories

Radionuclide	Tank 13 (Ci)	Tank 14 (Ci)	Tank 15 (Ci)	Tank 16 (Ci)
Ac-227	1.0E+00	1.0E+00	1.0E+00	1.0E+00
Ag-108m	0.0E+00	0.0E+00	0.0E+00	0.0E+00
Al-26	1.0E+00	1.0E+00	1.0E+00	1.0E+00
Am-241	2.1E-01	7.0E+00	2.1E-01	7.0E+00
Am-242m	1.0E+00	1.0E+00	1.0E+00	1.0E+00
Am-243	3.0E+00	3.0E+00	3.0E+00	1.0E+00
Bi-210m	0.0E+00	0.0E+00	0.0E+00	0.0E+00
C-14	1.0E+00	1.0E+00	1.0E+00	1.0E+00
Ca-41	0.0E+00	0.0E+00	0.0E+00	0.0E+00
Cf-249	1.0E+00	1.0E+00	1.0E+00	1.0E+00
Cf-251	1.0E+00	1.0E+00	1.0E+00	1.0E+00
Cl-36	5.3E-05	1.7E-03	5.3E-05	1.7E-03
Cm-243	1.0E+00	1.0E+00	1.0E+00	1.0E+00
Cm-244	6.4E-03	2.1E-01	6.4E-03	2.1E-01
Cm-245	1.0E+00	1.0E+00	1.0E+00	1.0E+00
Cm246	0.0E+00	0.0E+00	0.0E+00	0.0E+00
Cm-247	1.0E+00	1.0E+00	1.0E+00	1.0E+00
Cm-248	1.0E+00	1.0E+00	1.0E+00	1.0E+00
Co-60	1.0E+00	1.0E+00	1.0E+00	1.0E+00
Cs-135	9.8E-05	3.2E-03	9.8E-05	3.2E-03
Cs-137	3.7E+02	1.2E+04	3.7E+02	1.2E+04
Eu-152	2.1E+01	2.1E+01	2.1E+01	1.0E+00
Eu-154	8.8E-02	2.9E+00	8.8E-02	2.9E+00
Eu-155	0.0E+00	0.0E+00	0.0E+00	0.0E+00
Gd-152	0.0E+00	0.0E+00	0.0E+00	0.0E+00
H-3	1.0E+00	1.0E+00	1.0E+00	1.0E+00
I-129	5.3E-06	1.7E-04	5.3E-06	1.7E-04
K-40	2.6E-05	8.7E-04	2.6E-05	8.7E-04
Lu-174	0.0E+00	0.0E+00	0.0E+00	0.0E+00
Mo-93	0.0E+00	0.0E+00	0.0E+00	0.0E+00
Nb-93m	0.0E+00	0.0E+00	0.0E+00	0.0E+00

Table 4.2-5: Type II Tank Annulus Floor Radiological Inventories (Continued)

Radionuclide	Tank 13 (Ci)	Tank 14 (Ci)	Tank 15 (Ci)	Tank 16 (Ci)
Nb-94	2.6E-03	8.7E-02	2.6E-03	8.7E-02
Ni-59	8.6E+00	8.6E+00	8.6E+00	1.0E+00
Ni-63	2.9E-01	9.6E+00	2.9E-01	9.6E+00
Np-237	7.9E-04	2.6E-02	7.9E-04	2.6E-02
Pa-231	5.3E-05	1.7E-03	5.3E-05	1.7E-03
Pb-210	0.0E+00	0.0E+00	0.0E+00	0.0E+00
Pd-107	5.3E-03	1.7E-01	5.3E-03	1.7E-01
Pt-193	5.3E-03	1.7E-01	5.3E-03	1.7E-01
Pu-238	7.6E-01	2.5E+01	7.6E-01	2.5E+01
Pu-239	1.1E-01	3.6E+00	1.1E-01	3.6E+00
Pu-240	1.3E-01	4.2E+00	1.3E-01	4.2E+00
Pu-241	3.9E-01	1.3E+01	3.9E-01	1.3E+01
Pu-242	1.0E+00	1.0E+00	1.0E+00	1.0E+00
Pu-244	1.0E+00	1.0E+00	1.0E+00	1.0E+00
Ra-226	5.3E-04	1.7E-02	5.3E-04	1.7E-02
Ra-228	5.3E-02	1.7E+00	5.3E-02	1.7E+00
Se-79	4.8E+00	4.8E+00	4.8E+00	1.0E+00
Sm-147	0.0E+00	0.0E+00	0.0E+00	0.0E+00
Sm-151	4.7E+00	1.5E+02	4.7E+00	1.5E+02
Sn-126	4.6E+00	4.6E+00	4.6E+00	1.0E+00
Sr-90	2.4E+02	7.8E+03	2.4E+02	7.8E+03
Tc-99	1.5E-01	4.9E+00	1.5E-01	4.9E+00
Th-229	5.3E-05	1.7E-03	5.3E-05	1.7E-03
Th-230	5.3E-04	1.7E-02	5.3E-04	1.7E-02
Th-232	7.1E-04	2.4E-02	7.1E-04	1.7E-02
U-232	5.3E-05	1.7E-03	5.3E-05	1.7E-03
U-233	4.3E-03	1.4E-01	4.3E-03	1.4E-01
U-234	2.8E-03	9.1E-02	2.8E-03	9.1E-02
U-235	7.9E-06	2.6E-04	7.9E-06	2.6E-04
U-236	3.6E-05	1.2E-03	3.6E-05	1.2E-03
U-238	3.2E-05	1.0E-03	3.2E-05	1.0E-03
Zr-93	1.7E-04	5.5E-03	1.7E-04	5.5E-03

[Table 2.5-3, SRR-CWDA-2010-00023, Rev. 3]

Table 4.2-6: Annulus Floor Inventories for Nonradioactive Species

Chemical	Tank 9 (kg)	Tank 10 (kg)	Tank 11 (kg)	Tank 12 (kg)	Tank 13 (kg)	Tank 14 (kg)	Tank 15 (kg)	Tank 16 (kg)
Ni	1.4E+00	1.4E+00	4.3E-02	4.3E-02	4.3E-02	1.4E+00	4.3E-02	1.4E+00
Se	4.0E-03	4.0E-03	1.2E-04	1.2E-04	1.2E-04	4.0E-03	1.2E-04	4.0E-03

[Table 2.5-4, SRR-CWDA-2010-00023, Rev. 3]

Table 4.2-7: Sand Pad Inventories for Nonradioactive Species

Chemical	Tank 13 Primary Sand Pad (kg)	Tank 14 Primary Sand Pad (kg)	Tank 15 Primary Sand Pad (kg)	Tank 16 Primary Sand Pad (kg)	Tank 16 Secondary Sand Pad (kg)
Ni	4.3E-02	5.5E-01	4.3E-02	5.5E-01	1.1E-02
Se	1.2E-04	1.6E-03	1.2E-04	1.6E-03	3.1E-05

[Table 2.5-5, SRR-CWDA-2010-00023, Rev. 3]

4.2.1.1.2 Waste Tank Inventory Distribution Values

In the HTF GoldSim Model, the uncertainty in the CZ inventory values is considered by species and waste tank dependent distributions of inventory multipliers. These multipliers were not updated in the new model.

4.2.2 Ancillary Equipment Inventories

The ancillary equipment evaluated in the GoldSim model includes 11 pump tanks, 3 evaporators, and 4 zones of transfer lines or pipes. The 4 zones of transfer lines are outlined in Figure 3.1-6, with the Zone 1 located in the eastern section of the HTF, Zone 2 in the central part of the HTF, Zone 3 in the northwest and zone 4 in the southwest. The updated radionuclide inventories for the pump tanks are presented in Table 4.2-8, the updated radionuclide inventories for the evaporators are presented in Table 4.2-9, and the updated radionuclide inventories for the transfer lines are presented in Table 4.2-10. The updated nonradioactive species inventories for the pump tanks are presented in Table 4.2-11, the updated nonradionuclide inventories for the evaporators are presented in Table 4.2-12, and the updated nonradionuclide inventories for the transfer lines are presented in Table 4.2-13. The methodology and justification for ancillary equipment estimated initial inventories are presented in SRR-CWDA-2010-00023, Rev 3.

Table 4.2-8: Radiological Ancillary Equipment Inventory: HTF Pump Tank and CTS Tank

Radionuclide	HPT and CTS Residual (Ci)
Ac-227	1.00E-11
Ag-108m	0
Al-26	2.30E-06
Am-241	2.50E-02
Am-242m	1.70E-05
Am-243	4.00E-04
Bi-210m	0
C-14	3.20E-07
Ca-41	0
Cf-249	1.70E-14
Cf-251	6.00E-16
Cl-36	4.80E-07
Cm-243	6.00E-06
Cm-244	1.40E-03
Cm-245	1.40E-06
Cm246	0
Cm-247	3.20E-15
Cm-248	3.30E-15
Co-60	4.20E-05
Cs-135	3.10E-06
Cs-137	7.00E-01
Eu-152	9.50E-04
Eu-154	2.10E-03
Eu-155	0
Gd-152	0
H-3	3.00E-05
I-129	3.40E-08
K-40	2.40E-07
Lu-174	0
Mo-93	0
Nb-93m	0

Table 4.2-8: Radiological Ancillary Equipment Inventory: HTF Pump Tank and CTS Tank (Continued)

Radionuclide	HPT and CTS Residual (Ci)
Nb-94	7.2E-08
Ni-59	3.2E-04
Ni-63	2.0E-02
Np-237	1.4E-05
Pa-231	1.1E-10
Pb210	0
Pd-107	4.8E-05
Pt-193	3.6E-05
Pu-238	1.8E-01
Pu-239	3.3E-03
Pu-240	2.0E-03
Pu-241	1.4E-02
Pu-242	5.7E-06
Pu-244	2.6E-08
Ra-226	2.9E-11
Ra-228	1.0E-08
Se-79	1.9E-04
Sm-147	0
Sm-151	1.2E+00
Sn-126	2.2E-04
Sr-90	3.0E+00
Tc-99	3.1E-03
Th-229	2.4E-07
Th-230	3.7E-09
Th-232	1.6E-06
U-232	1.0E-07
U-233	6.4E-05
U-234	1.3E-05
U-235	1.7E-07
U-236	1.3E-06
U-238	1.5E-06
Zr-93	2.5E-04

[Table 4.3-1, SRR-CWDA-2010-00023 Rev.3]

Table 4.2-9: Radiological Ancillary Equipment Inventory: Evaporators

Radionuclide	HPT and CTS Residual (Ci)
Ac-227	0
Ag-108m	0
Al-26	0
Am-241	3.9E-03
Am-242m	0
Am-243	0
Bi-210m	0
C-14	0
Ca-41	0
Cf-249	0
Cf-251	0
Cl-36	0
Cm-243	0
Cm-244	0
Cm-245	0
Cm246	0
Cm-247	0
Cm-248	0
Co-60	3.0E-05
Cs-135	0
Cs-137	5.0E-01
Eu-152	0
Eu-154	0
Eu-155	0
Gd-152	0
H-3	3.0E-06
I-129	0
K-40	0
Lu-174	0
Mo-93	0
Nb-93m	0

Table 4.2-9: Radiological Ancillary Equipment Inventory: Evaporators (Continued)

Radionuclide	HPT and CTS Residual (Ci)
Nb-94	0
Ni-59	0
Ni-63	0
Np-237	3.6E-06
Pa-231	0
Pb210	0
Pd-107	0
Pt-193	0
Pu-238	4.3E-03
Pu-239	1.4E-02
Pu-240	3.1E-03
Pu-241	1.1E-02
Pu-242	4.5E-06
Pu-244	0
Ra-226	0
Ra-228	0
Se-79	7.7E-09
Sm-147	0
Sm-151	0
Sn-126	0
Sr-90	2.8E-02
Tc-99	1.3E-03
Th-229	0
Th-230	0
Th-232	0
U-232	0
U-233	1.1E-05
U-234	7.1E-06
U-235	8.1E-08
U-236	1.4E-07
U-238	7.5E-06
Zr-93	0

[Table 4.4-3, SRR-CWDA-2010-00023, Rev.3]

Table 4.2-10: Radiological Ancillary Equipment Inventory: Ancillary Piping Group

Radionuclide	Units	Group 1	Group 2	Group 3	Group 4
Ac-227	Ci	2.8E-09	1.4E-09	2.9E-09	1.0E-09
Ag-108m	Ci	0	0	0	0
Al-26	Ci	3.2E-04	1.6E-04	3.3E-04	1.2E-04
Am-241	Ci	3.6E+00	1.8E+00	3.8E+00	1.3E+00
Am-242m	Ci	2.6E-03	1.3E-03	2.7E-03	9.7E-04
Am-243	Ci	5.7E-02	2.8E-02	5.9E-02	2.1E-02
Bi-210m	Ci	0	0	0	0
C-14	Ci	4.6E-05	2.3E-05	4.8E-05	1.7E-05
Ca-41	Ci	0	0	0	0
Cf-249	Ci	2.5E-12	1.2E-12	2.6E-12	9.2E-13
Cf-251	Ci	8.6E-14	4.3E-14	9.0E-14	3.2E-14
Cl-36	Ci	6.7E-05	3.4E-05	7.0E-05	2.5E-05
Cm-243	Ci	1.4E-03	7.0E-04	1.4E-03	5.2E-04
Cm-244	Ci	4.6E-01	2.3E-01	4.8E-01	1.7E-01
Cm-245	Ci	1.9E-04	9.6E-05	2.0E-04	7.1E-05
Cm-246	Ci	0	0	0	0
Cm-247	Ci	4.4E-13	2.2E-13	4.6E-13	1.7E-13
Cm-248	Ci	4.6E-13	2.3E-13	4.8E-13	1.7E-13
Co-60	Ci	9.7E-02	4.9E-02	1.0E-01	3.6E-02
Cs-135	Ci	4.4E-04	2.2E-04	4.5E-04	1.6E-04
Cs-137	Ci	1.6E+02	8.0E+01	1.7E+02	5.9E+01
Eu-152	Ci	4.0E-01	2.0E-01	4.1E-01	1.5E-01
Eu-154	Ci	1.6E+00	8.3E-01	1.7E+00	6.1E-01
Eu-155	Ci	0	0	0	0
Gd-152	Ci	0	0	0	0
H-3	Ci	1.4E-02	7.0E-03	1.4E-02	5.2E-03
I-129	Ci	4.7E-06	2.4E-06	4.9E-06	1.8E-06
K-40	Ci	3.4E-05	1.7E-05	3.5E-05	1.2E-05
Lu-174	Ci	0	0	0	0
Mo93	Ci	0	0	0	0
Nb93m	Ci	0	0	0	0
Nb-94	Ci	1.0E-05	5.1E-06	1.1E-05	3.8E-06
Ni-59	Ci	4.5E-02	2.2E-02	4.7E-02	1.7E-02
Ni-63	Ci	3.2E+00	1.6E+00	3.4E+00	1.2E+00
Np-237	Ci	1.9E-03	9.8E-04	2.0E-03	7.2E-04
Pa-231	Ci	1.5E-08	7.7E-09	1.6E-08	5.7E-09
Pb-210	Ci	0	0	0	0
Pd-107	Ci	6.7E-03	3.4E-03	7.0E-03	2.5E-03
Pt-193	Ci	6.7E-03	3.4E-03	7.0E-03	2.5E-03
Pu-238	Ci	2.9E+01	1.5E+01	3.1E+01	1.1E+01
Pu-239	Ci	4.7E-01	2.4E-01	4.9E-01	1.7E-01
Pu-240	Ci	2.8E-01	1.4E-01	2.9E-01	1.0E-01
Pu-241	Ci	5.7E+00	2.9E+00	5.9E+00	2.1E+00

**Table 4.2-10: Radiological Ancillary Equipment Inventory: Ancillary Piping Group
(Continued)**

Radionuclide	Units	Group 1	Group 2	Group 3	Group 4
Pu-242	Ci	8.0E-04	4.0E-04	8.4E-04	3.0E-04
Pu-244	Ci	3.7E-06	1.8E-06	3.8E-06	1.4E-06
Ra-226	Ci	4.2E-09	2.1E-09	4.4E-09	1.6E-09
Ra-228	Ci	1.8E-05	9.1E-06	1.9E-05	6.8E-06
Se-79	Ci	2.7E-02	1.4E-02	2.8E-02	1.0E-02
Sm147	Ci	0	0	0	0
Sm-151	Ci	2.1E+02	1.0E+02	2.2E+02	7.7E+01
Sn-126	Ci	3.2E-02	1.6E-02	3.3E-02	1.2E-02
Sr-90	Ci	7.1E+02	3.6E+02	7.3E+02	2.6E+02
Tc-99	Ci	3.9E-01	2.0E-01	4.1E-01	1.5E-01
Th-229	Ci	3.3E-05	1.7E-05	3.5E-05	1.2E-05
Th-230	Ci	5.2E-07	2.6E-07	5.4E-07	1.9E-07
Th-232	Ci	2.2E-04	1.1E-04	2.3E-04	8.3E-05
U-232	Ci	1.8E-05	9.2E-06	1.9E-05	6.8E-06
U-233	Ci	9.0E-03	4.5E-03	9.4E-03	3.3E-03
U-234	Ci	1.9E-03	9.4E-04	2.0E-03	7.0E-04
U-235	Ci	2.4E-05	1.2E-05	2.5E-05	9.0E-06
U-236	Ci	1.9E-04	9.3E-05	1.9E-04	6.9E-05
U-238	Ci	2.2E-04	1.1E-04	2.3E-04	8.1E-05
Zr-93	Ci	3.5E-02	1.7E-02	3.6E-02	1.3E-02

[Derived from values presented in Table 4.2-3 of SRR-CWDA-2010-00023, Rev 3]

**Table 4.2-11: Non-Radionuclide Ancillary Equipment Inventory: HTF Pump Tank and
CTS Tank**

Chemical	HPT and CTS (kg)
Ni	9.5E-03
Se	1.2E-05

[Table 4.3-2, SRR-CWDA-2010-00023,
Rev 3]

Table 4.2-12: Non-Radionuclide Ancillary Equipment Inventory: Evaporators

Chemical	Inventory in Evaporator Vessel (kg)
Ni	3.0E-03
Se	2.0E-05

[Table 4.4-4, SRR-CWDA-2010-00023, Rev 3]

Table 4.2-13: Non-Radionuclide Ancillary Equipment Inventory: Ancillary Piping Group

Chemical	Units	Group 1	Group 2	Group 3	Group 4
Ni	kg	1.3E+00	6.7E-01	1.4E+00	5.0E-01
Se	kg	1.6E-03	8.2E-04	1.7E-03	6.1E-04

[Derived from values presented in Table 4.2-4 of SRR-CWDA-2010-00023, Rev 3]

4.3 Vadose Zone Inputs

The major inputs for the vadose zone include the flow rates through the vadose zone and the geometry of the portion of the vadose zone included in the model. Note that the flow rates through the waste tank structure are also included in this section.

4.3.1.1 Vadose Zone Flow Rates

4.3.1.1.1 Waste Tank Flow Rates

As discussed in Section 3.1.1.4, SRR-CWDA-2010-00093, Rev 1 of the HTF Stochastic Model has been redesigned to read in flow data as opposed to having the flow data copied into data elements, where the data resides until it is updated and replaced. In addition, besides reading in flow data for the basic configurations, Case A, Case B, Case C, Case D, and Case E, the model can sample from a set of flow data sets that were generated by PORFLOW for a parametric study (see Table 3.1-6). Each of the four waste tank types (Types I, II, III/IIIA, and IV), has 72 data sets that can be sampled from. The input files and attributes are listed in Table 4.3-1. The data extracted from these data files includes time series of spatially averaged vertical Darcy velocities, volumetric flow rates, saturations, and infiltration rates. In addition, scalar parameters such as pore volumes, transition times, and cross-flow rates are also extracted from these files.

Table 4.3-1: Flow Data Input Files

File Name	File Attributes	Number of Tables
<i>GoldSim_StochasticFlowFields.txt</i>	Contains tables of flow data from 72 parametric combinations for 4 waste tank types	288
<i>GoldSim_CaseAFlowFields.txt</i>	Contains tables of flow data for the Case A configuration for all 8 waste tank types	8
<i>GoldSim_CaseBFlowFields.txt</i>	Contains tables of flow data for the Case B configuration for all 8 waste tank types	8
<i>GoldSim_CaseCFlowFields.txt</i>	Contains tables of flow data for the Case C configuration for all 8 waste tank types	8
<i>GoldSim_CaseDFlowFields.txt</i>	Contains tables of flow data for the Case D configuration for all 8 waste tank types	8
<i>GoldSim_CaseEFlowFields.txt</i>	Contains tables of flow data for the Case E configuration for all 8 waste tank types	8

4.3.1.1.2 Chemical Transition Times

Waste tank reducing grout, CZ, annulus, wall, and basemat (both under the CZ and under the wall) chemical transition times are independently solved for the HTF GoldSim Model based upon structure pore volumes and associated volumetric flow rates (or vertical Darcy velocities) derived from the HTF PORFLOW Model. To evaluate the number of pore volumes of water that passed through waste tank reducing grout and/or CZ (to determine chemical environment transition times) the volumetric rate of water passing through the waste tank grout or CZ is utilized along with the associated pore volume. For the non-submerged waste tanks (Type III/IIIA and IV) and partially submerged waste tanks (Type II), volumetric flow rates taken directly from the PORFLOW runs are used. For submerged waste tanks (Type I), the volumetric rates are based on an effective flow rate V_{eff} , which is a function of the vertical Darcy velocity, the time dependent infiltration rate, and a horizontal flow component estimated to be 480 cm/yr ($V_{crossflow}$). The effective flow rate (Equation 4.3-1) can be expressed as:

(Eq. 4.3-1)

$$V_{eff} = V_{down} + V_{down} V_{crossflow} / I = V_{down} (1 + V_{crossflow} / I)$$

Equation 4.3-1, is used for both partially and fully submerged waste tanks, when calculating transition times for basemat segments,

In the original HTF GoldSim Model, the chemical transition times for the annulus, wall, and the basemat beneath the wall were taken from the HTF PORFLOW Model input, but are solved for directly in the updated model. This change was necessitated by the more comprehensive manner in which the HTF GoldSim Model samples and rescales flow fields. The HTF Stochastic Model from SRR-CWDA-2010-00093, Rev 2 also differs in several ways from PORFLOW when it comes to calculating the transition times. The calculations for the annulus and the waste tank wall, the pore volumes used to derive the transition times differ between the two models. The SRR-CWDA-2010-00093, Rev 2 HTF PORFLOW Model utilizes the full annulus and wall pore volumes for generating its chemical transition times and the updated HTF GoldSim Model considers only the pore volumes of the abbreviated sections of the annulus and wall that are located beneath the secondary liner. In addition, the volumetric flow rates (or vertical Darcy velocities for submerged zone calculations) for the updated HTF PORFLOW Model are based upon the full volume of the annulus and wall, and the volumetric flow rates or vertical Darcy velocities are based on averaging over the abbreviated space in the updated HTF GoldSim Model calculations. The differences in the transition times represent slight differences in the conceptual models between the SRR-CWDA-2010-00093, Rev. 1 and Rev. 2 models, which are reflected in results presented in Section 7.

4.3.1.1.3 Ancillary Equipment Flow Rates

The vadose zone flow rates used in the update HTF GoldSim Model for the ancillary equipment are also based on spatially averaged downward components of PORFLOW generated Darcy velocities for the combined backfill and UZ. Because the updated flow model showed only a small change in the streamtraces, flow rates for the ancillary equipment were not updated.

4.4 Saturated Zone Inputs

For waste tank releases, the SZ modeling domain begins at the upgradient edge of the waste tank and extends to the 100-meter boundary depicted in Figure 3.1-6. Data inputs specific to the SZ include: 1) data that describes the flow fields controlling the transport of mass released from the waste tanks and ancillary equipment and 2) data describing the geometry of the SZ and the spatial relationships between the sources (waste tanks and ancillary equipment) and the 100-meter boundary. Updates to these inputs, implemented in SRR-CWDA-2010-00093, Rev. 1 of the HTF Stochastic Model, are described below.

4.4.1 Saturated Zone Darcy Velocity

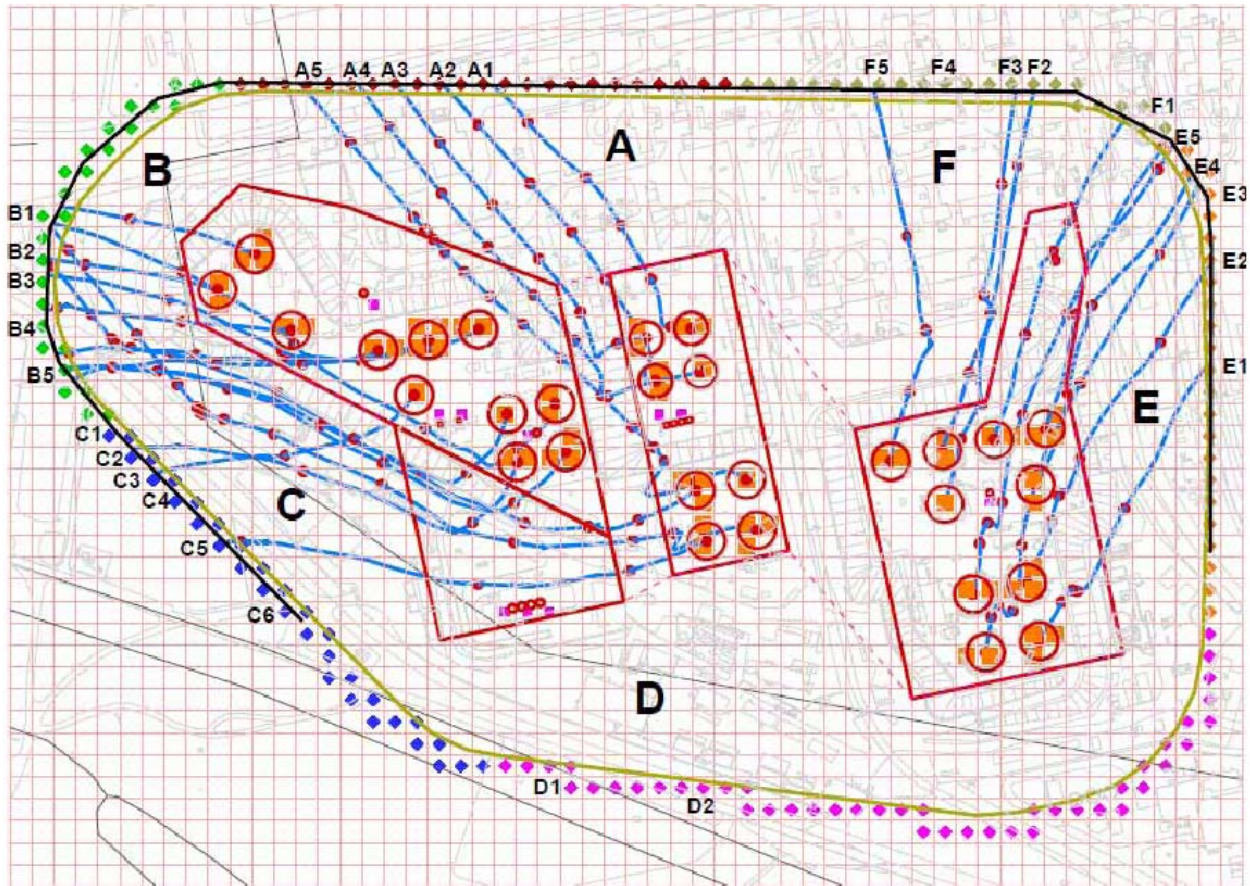
Groundwater flow in the SZ is approximated as a unidirectional flow field of constant Darcy velocity. The flow velocity is derived from a PORFLOW simulation where stream traces were generated based on a particle released at the center of each source (waste tank or ancillary equipment). The particle's path length to the 100-meter boundary from the stream trace simulation and the time it took for the peak value of the breakthrough curves to reach the boundary were translated into averaged transport velocities. Darcy velocities were in turn derived from the transport velocities and the SZ porosity used as shown in Equation 4.4-1:

(Eq. 4.4-1)

$$DarcyVelocity = TransportVelocity \times Porosity$$

Although the PORFLOW SZ model grid was updated, the change in spatially averaged Darcy velocities was not considered large enough to warrant updating the HTF GoldSim Model. One change that was made to the handling of SZ flow in the updated HTF GoldSim Model is the consideration of flow rates at the contact between particle tracking lines and the 100-meter boundary (see Figure 4.4-1) to determine the dilution effects at the 100-meter boundary. In the updated model, the original spatially averaged Darcy velocities are used to determine the transport time to the 100-meter boundary, and flow rates at the 100-meter boundary from the new PORFLOW flow model, are used to determine the degree of dilution at the boundary. Note that the dots along the stream traces represent the particles location at 10-year intervals.

Figure 4.4-1: PORFLOW Stream Traces with Hypothetical 100-Meter Boundary and Associated GoldSim Well Locations



4.4.2 Saturated Zone Geometry and Other Spatial Relationships

As noted in Section 3.1.1.5, in SRR-CWDA-2010-00093, Rev. 1 of the HTF Stochastic Model, the 1-D string of 50 GoldSim mixing cells used to define radionuclide transport in the SZ was replaced by a set of three analytic pipe elements linked in series. In the SRR-CWDA-2010-00093, Rev. 1 model, the SZ modeling domain begins at the downgradient edge of the waste tank and extends to the 100-meter boundary. In the updated model, this is no longer necessary and the SZ modeling domain includes the SZ beneath the waste tank and extends to the 100-meter boundary.

4.4.2.1 Saturated Zone Geometry

4.4.2.1.1 Saturated Zone Pathway Lengths

The SZ transport pathway lengths based on the PORFLOW stream trace analysis have not been updated from the original model. The only change to these distances is that the radius of simulated waste tank is now be added to the pathway length. The pathway length for each waste tank release, starting from the center of the waste tank, is presented in Table 4.4-1. Similarly, the pathway lengths, starting from the center of each ancillary equipment source are presented in Table 4.4-2.

Table 4.4-1: Distance Traveled from Waste Tanks to 100-Meter Boundary

Tank ID	Distance Traveled (ft)
Tank 9	908.9
Tank 10	764.4
Tank 11	1,046.0
Tank 12	974.4
Tank 13	1,720.8
Tank 14	1,546.6
Tank 15	1,138.2
Tank 16	1,967.9
Tank 21	1,283.9
Tank 22	1,001.9
Tank 23	1,373.7
Tank 24	1,156.4
Tank 29	1,037.6
Tank 30	863.3
Tank 31	712.4
Tank 32	637.5
Tank 35	565.2
Tank 36	396.7
Tank 37	457.5
Tank 38	889.5
Tank 39	866.4
Tank 40	817.1
Tank 41	738.0
Tank 42	987.3
Tank 43	818.3
Tank 48	1,191.4
Tank 49	873.5
Tank 50	1,263.5
Tank 51	801.0

[SRR-CWA-2010-00093, Rev. 1]

Table 4.4-2: Distance Traveled from Ancillary Equipment to 100-Meter Boundary

Ancillary Equipment ID	Distance Traveled (ft)
HPT2	1,300.3
HPT3	1,267.2
HPT4	1,244.5
HPT5	381.0
HPT6	364.3
HPT7	494.2
HPT8	517.0
HPT9	542.1
HPT10	570.6
E242_H	1,245.2
E242_16H	936.3
E242_25H	740.4
HTF_T_Line1	956.0
HTF_T_Line2	1,231.9
HTF_T_Line3	877.2
HTF_T_Line4	624.9
CTSO	711.2
CTSN	809.9

[SRR-CWA-2010-00093, Rev. 1]

4.4.2.1.2 Saturated Zone Thickness

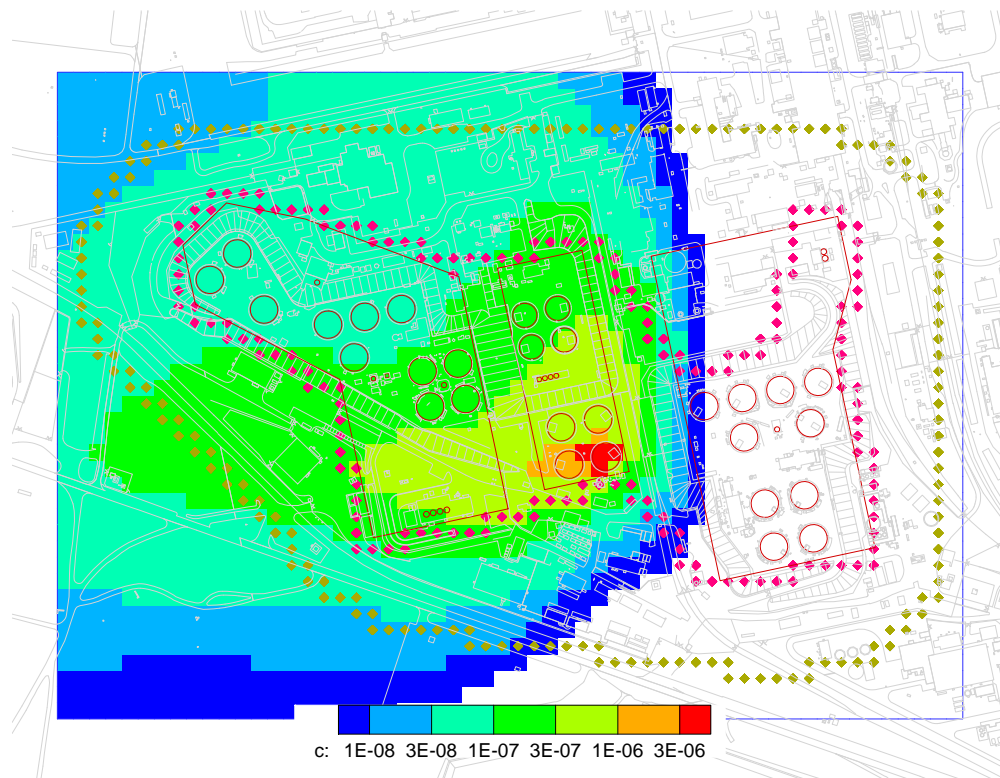
In the original HTF GoldSim Model, the saturated thickness was based on estimates for the lower aquifer zone of the Upper Three Runs Aquifer presented in Table 7 of SRNL-STI-2010-00148 Rev. 0. The deterministic value used in the model was 60 feet and the stochastic distribution used was a triangular distribution with a minimum value of 55 feet, a maximum value of 80 feet, and a most likely value of 60 feet. In SRR-CWDA-2010-00093, Rev. 1 model, the saturated thickness has been updated to include both the upper and lower aquifer zones. The deterministic value used in the model is 130 feet and the stochastic distribution used was a triangular distribution with a minimum value of 110 feet, a maximum value of 170 feet, and a most likely value of 130 feet. These new values are taken from estimated values presented in Table 7 of SRNL-STI-2010-00148 Rev. 0. Cross-sectional plots of concentrations from the updated HTF PORFLOW Model indicate that some plumes from the waste tank releases, especially for the eastern Type IIIA tanks, are spread into both zones.

4.4.2.1.3 Saturated Zone Dispersivity

For consistency with the HTF PORFLOW Modeling effort, the longitudinal dispersivity used in the HTF GoldSim Model has been updated to 3.16 meters, the same as used in the HTF PORFLOW Model. To simulate the spreading associated with a typical plume, the horizontal transverse is usually set to a fraction of the longitudinal dispersivity (0.316 meters for the updated HTF PORFLOW Model), but in the updated HTF GoldSim Model, the horizontal, transverse dispersivity is also used to help compensate for

transverse spreading due to the flow fields. The spreading is associated with the occurrence of a groundwater divide, and directional changes in flow directions with depth. The degree to which spreading can occur in the HTF can be easily seen in the PORFLOW simulation of a conservative species release from Tank 16 (Figure 4.4-2). To capture the large degree of spreading associated with the spatial variability in the flow fields in the HTF, the transverse dispersivity is set to 0.948 meter for the western waste tanks. Since the plumes emanating from the eastern Type IIIA tanks do not show the degree of spreading associated with the eastern waste tank plumes, the HTF GoldSim Model uses 0.316 meter for the transverse dispersivity, the same value that is used in the updated HTF PORFLOW Model. For the western waste tank releases, the updated HTF GoldSim Model uses the same vertical dispersivity (0.0316 meter) as used in the updated HTF PORFLOW Model. For the waste tank releases from the eastern Type IIIA tanks, the HTF GoldSim Model uses a vertical dispersivity of 0.0695 meter, which helps capture the degree of vertical spreading seen in the updated HTF PORFLOW Model results.

Figure 4.4-2: Plume Formed by the Release of a Conservative Constituent from Tank 16



Note: Units on scale bar are mole per liter and the concentrations were produced by a hypothetical constant source of 1 mol/yr.

4.5 Material Properties

The material properties that are discussed in this section include the K_d s, which describe the affinity of specific radionuclides to sorbing onto the different materials used in constructing the waste-tank structures or found naturally at the site. They also include the site-specific physical parameters such as porosity and bulk density.

4.5.1 Adsorption

In the GoldSim model multiple segments, within the waste tank structure (the reducing grout above the CZ, the basemat, the grouted-annulus zone, and the sand pads) play a role in retarding contaminant transport of species subject to sorption. Sorption also takes place in the vadose zone and SZ soils beneath the waste tanks and ancillary equipment. The effectiveness of each zone in retarding the transport of different species is tied to the assigned K_d values, which vary for different elements and depend on the time-variant chemical states of the zone. Table 4.5-1 contains the old and updated median K_d values in the cementitious zones for the Reduced Region II and Reduced Region III chemical environments. Table 4.5-2 contains the old and updated median K_d values in the cementitious zones for the Oxidized Region II and Oxidized Region III chemical environments. Table 4.5-3 contains the old and new median K_d values used in the backfill, vadose zone, and SZ, for all of the elements of interest. The vadose zone values are also used in the sand pads. Note that for the vadose zone and sand pads, the K_d values used are dependent on the chemical state of water leaching from the reducing grout. The leachate impacted K_d values used in the HTF GoldSim Model have not been updated. The distributions for the K_d values used in the HTF GoldSim Modeling are based on the approach described in SRNL-STI-2009-00473, which has not changed.

Table 4.5-1: Recommended K_d Values for Cementitious Reduced Regions

Element	Region II		Region III	
	Old	New	Old	New
Ac	7,000	7,000	1,000	1,000
Ag	5,000	5,000	1,000	1,000
Al	7,000	7,000	1,000	1,000
Am	7,000	7,000	1,000	1,000
As	1,000	200 ^a	100	100 ^a
At	9	9	4	4
Ba	100	100 ^a	70	70 ^a
Bi	7,000	7,000	1,000	1,000
C	3,000	3,000	300	300
Ca	15	15	5	5
Cd	5,000	5,000	1,000	1,000
Cf	7,000	7,000	1,000	1,000
Cl	10	10	1	1
Cm	7,000	7,000	1,000	1,000
Co	5,000	5,000	2,000	1,000
Cr	1,000	1,000	1,000	1,000
Cs	20	20	10	10
Cu	5,000	5,000	2,000	1,000
Eu	7,000	7,000	1,000	1,000
F	10	10	1	1
Fe	7,000	7,000	1,000	1,000
Fr	20	20	10	10
Gd	7,000	7,000	1,000	1,000
H	0	0	0	0
Hg	5,000	5,000	2,000	1,000
I	9	9	4	4
K	20	20	10	10
Lu	7,000	7,000	1,000	1,000
Mn	100	100	10	10
Mo	300	300	150	150
Nb	1,000	1,000	500	500
Ni	4,000	4,000	400	400
NO2	0	0	0	0
NO3	0	0	0	0
Np	10,000	10,000	5,000	5,000

Table 4.5-1: Recommended K_d Values for Cementitious Reduced Regions (Continued)

Element	Region II		Region III	
	Old	New	Old	New
Pa	10,000	10,000	5,000	5,000
Pb	500	5,000	250	1,000
Pd	4,000	5,000	400	1,000
Po	5,000	5,000	500	500
Pt	5,000	5,000	2,000	1,000
Pu	10,000	10,000	2,000	2,000
Ra	100	100	70	70
Rn	0	0	0	0
Sb	1,000	1,000	100	100
Se	300	300	150	150
Sm	7,000	7,000	1,000	1,000
Sn	5,000	5,000	500	500
Sr	15	15	5	5
Tc	5,000	1,000 ^a	1,000	1,000 ^a
Th	5,000	5,000	500	500
Tl	20	20	10	10
U	2,500	2,500	2,500	2,500
Y	7,000	7,000	1,000	1,000
Zn	5,000	5,000	2,000	1,000
Zr	5,000	5,000	500	500

[From SRNL-STI-2009-00473 unless otherwise noted]

^a From SRNL-STI-2010-00667

Table 4.5-2: Recommended K_d Values for Cementitious Oxidized Regions

Element	Region II		Region III	
	Old	New	Old	New
Ac	6,000	6,000	600	600
Ag	4,000	4,000	400	400
Al	6,000	6,000	600	600
Am	6,000	6,000	600	600
As	1,000	320	100	100
At	15	15	4	4
Ba	100	100	70	70
Bi	6,000	6,000	600	600
C	3,000	3,000	300	300
Ca	15	15	5	5
Cd	4,000	4,000	400	400
Cf	6,000	6,000	600	600
Cl	10	10	1	1
Cm	6,000	6,000	600	600
Co	4,000	4,000	400	400
Cr	10	10	1	1
Cs	20	20	10	10
Cu	4,000	4,000	400	400
Eu	6,000	6,000	600	600
F	10	10	1	1
Fe	6,000	6,000	600	600
Fr	20	20	10	10
Gd	6,000	6,000	600	600
H	0	0	0	0
Hg	300	300	100	100
I	15	15	4	4
K	20	20	10	10
Lu	6,000	6,000	600	600
Mn	100	100	10	10
Mo	300	300	150	150
Nb	1,000	1,000	500	500
Ni	4,000	4,000	400	400
NO2	0	0	0	0
NO3	0	0	0	0
Np	10,000	10,000	5,000	5,000

Table 4.5-2: Recommended K_d Values for Cementitious Oxidized Regions (Continued)

Element	Region II		Region III	
	Old	New	Old	New
Pa	10,000	10,000	5,000	5,000
Pb	300	300	100	100
Pd	4,000	4,000	400	400
Po	300	300	100	100
Pt	4,000	4,000	400	400
Pu	10,000	10,000	2,000	2,000
Ra ^d	100	100	70	70
Rn	0	0	0	0
Sb	1,000	1,000	100	100
Se	300	300	150	150
Sm	6,000	6,000	600	600
Sn	4,000	4,000	2,000	2,000
Sr	15	15	5	5
Tc	0.8	0.8	0.5	0.5
Th	10,000	10,000	2,000	2,000
Tl	20	150	10	150
U	250	1,000 ^a	70	100 ^a
Y	6,000	6,000	600	600
Zn	4,000	4,000	400	400
Zr	10,000	10,000	2,000	2,000

[From SRNL-STI-2009-00473 unless otherwise noted]

^a From SRNL-STI-2010-00493

Table 4.5-3: Recommended K_d Values for the Backfill, Vadose Zone and Saturated Zone

Element	Backfill (mL/g) ^a		Vadose Zone / SZ (mL/g) ^b	
	Old	New	Old	New
Ac	8,500	8,500	1,100	1,100
Ag	150	30 ^d	60	10 ^d
Al	1,300	1,300	1,300	1,300
Am	8,500	8,500	1,100	1,100
As	200	200	100	100
At	0.9	0.9	0.3	0.3
Ba	101 ^c	101 ^d	15 ^c	15 ^d
Bi	8,500	8,500	1,100	1,100
C	400	400	10	10
Ca	17	17	5	5
Cd	30	30	15	15
Cf	8,500	8,500	1,100	1,100
Cl	0	8 ^d	0	1 ^d
Cm	8,500	8,500	1,100	1,100
Co	100	100	40	40
Cr	10	400 ^d	4	1,000 ^d
Cs	50	50	10	10
Cu	70	70	50	50
Eu	8,500	8,500	1,100	1,100
F	0	0	0	0
Fe	400	400	200	200
Fr	50	50	10	10
Gd	8,500	8,500	1,100	1,100
H	0	0	0	0
Hg	1,000	1,000	800	800
I	0.9	0.9	0.3	0.3
K	25	25	5	5
Lu	8,500	8,500	1,100	1,100
Mn	200	200	15	15
Mo	1,000	1,000	1,000	1,000
Nb	0	0	0	0
Ni	30	30	7	7
NO2	0	0	0	0
NO3	0	0	0	0
Np	9	9	3	3

Table 4.5-3: Recommended K_d Values for the Backfill, Vadose Zone and SZ (Continued)

Element	Backfill (mL/g) ^a		Vadose Zone / SZ (mL/g) ^b	
	Old	New	Old	New
Pa	9	9	3	3
Pb	5,000	5,000	2,000	2,000
Pd	30	30	7	7
Po	5,000	5,000	2,000	2,000
Pt	30	30	7	7
Pu	5,950	5,950	290	650 ^f
Ra	185 ^c	185 ^d	25 ^c	25 ^d
Rn	0	0	0	0
Sb	2,500	2,500	2,500	2,500
Se	1,000	1,000	1,000	1,000
Sm	8,500	8,500	1,100	1,100
Sn	5,000	5,000	2,000	2,000
Sr	17	17	5	5
Tc	1.8	1.8	0.6	0.6
Th	2,000	2,000	900	900
Tl	50	70 ^d	10	25 ^d
U	300	400 ^d	200	300 ^d
Y	8,500	8,500	1,100	1,100
Zn	30	30	15	15
Zr	2,000	2,000	900	900

[From SRNL-STI-2009-00473 unless otherwise noted]

- ^a Backfill represented by clayey sediment.
- ^b Vadose/SZ represented by sandy sediment.
- ^c From SRNL-STI-2010-00527
- ^d From SRNL-STI-2010-00493
- ^e From SRNL-STI-2011-00011
- ^f From SRNL-STI-2011-00672

4.5.2 Physical Properties

The physical parameters describing the material that the water flows through include the porosity, bulk density, saturated effective diffusion coefficient, and saturations for each component or material type. The only material with updated properties is the grout.

4.5.2.1 Grout Properties

The basic grout properties were also updated in the new model. The model in SRR-CWDA-2010-00093, Rev. 1 uses an updated set of grout parameters based on the updated grout formula identified as "LP#8-16" in SRNL-STI-2011-00551, Rev 0. The updated properties include porosity, dry bulk density the effective diffusion coefficient, and the saturated hydraulic conductivity. Updated values of these parameters are presented in Table 4.5-4. Note that the effective diffusion coefficients presented in Table 4.5-4 are the initial values that will increase over time as degradation occurs.

Table 4.5-4: Annulus Floor Inventories for Nonradioactive Species

Property	(OLD) Reducing Grout ^a	(NEW) Reducing Grout
Porosity (%)	26.6	21.0
Dry Bulk Density (g/cm ³)	1.84	1.97
Average Particle Density (g/cm ³)	2.51	2.49
Effective Diffusion Coefficient (cm ² /s)	8.0E-07	5.0E-08
Saturated Hydraulic Conductivity (cm/s)	3.6E-08	2.1E-09

[SRR-CWDA-2010-00128, Rev 0, Table 4.2-32, SRNL-STI-2011-00551, Rev 0, Table 3-5]

a HTF PA, Rev. 0

5.0 DOSE CALCULATOR MODEL APPROACH

The transport module of the HTF GoldSim and HTF PORFLOW Models calculate contaminant groundwater dose concentrations to the MOP and the inadvertent with the 100-meter well water, the seepage (e.g., the intersection of the Fourmile Branch and UTR and the land surface), and the 1-meter well water as the primary water sources. The exposure route for inadvertent intruder ingestion assumes the receptor uses a well as drinking water from the 1-meter well for dose calculations, whereas the 100-meter and seepage (or stream) concentrations are used to calculate the dose to the MOP. The contaminant concentrations in these three primary water sources are the inputs to the inadvertent intruder and MOP dose calculations.

Only one change was made to the dose calculator, model approach and that represented the correction of an error that was discovered in a Nuclear Regulatory Commission (NRC) review. [ML121170309] The error corrected pertained to the leaching rate constant (*Lambda_Leach*) used in the HTF GoldSim Model. The irrigation rate used in the leaching rate constant was not adjusted by the fraction of time the vegetation is irrigated (0.2, as presented in SRR-CWDA-2010-00128 Rev. 0, Table 4.6-8).

6.0 DOSE CALCULATOR MODEL INPUTS

Except for the following transfer factor changes, the input data for the dose calculations were not changed from the development of SRR-CWDA-2010-00093, Rev. 1 HTF Stochastic Model. In the updated HTF Stochastic Model, the deterministic transfer factors for feed to meat, feed to milk, and water to finfish were replaced with distributions to reflect the uncertainty in the data.

6.1 Updated Transfer Factors

The distributions for the feed to meat, feed to milk, and water to finfish transfer factors used in SRR-CWDA-2010-00093, Rev. 1 HTF Stochastic Model, are triangular distributions. Table 6.1-1 presents the triangular distributions for the feed to meat transfer factors. Table 6.1-2 presents the triangular distributions for the feed to milk transfer factors. Table 6.1-3 presents the triangular distributions for the water to finfish transfer factors.

Table 6.1-1: Triangular Distributions for Feed to Meat Transfer Factors

Species	Recommended Values of Feed To Meat (d/kg)	Min Values of Feed To Meat (d/kg)	Max Values of Feed To Meat (d/kg)
Ac-227	4.00E-04	2.00E-05	4.00E-04
Ag-108m	3.00E-03	3.00E-03	1.70E-02
Al-26	1.50E-03	5.00E-04	1.50E-03
Am-241	5.00E-04	3.50E-06	5.00E-04
Am-242m	5.00E-04	3.50E-06	5.00E-04
Am-243	5.00E-04	3.50E-06	5.00E-04
Bi-210m	4.00E-04	4.00E-04	2.00E-03
C-14	3.10E-02	3.10E-02	4.89E-02
Ca-41	1.30E-02	7.00E-04	1.30E-02
Cf-249	4.00E-05	4.00E-05	5.00E-03
Cf-251	4.00E-05	4.00E-05	5.00E-03
Cl-36	1.70E-02	1.70E-02	8.00E-02
Cm-243	4.00E-05	3.50E-06	2.00E-04
Cm-244	4.00E-05	3.50E-06	2.00E-04
Cm-245	4.00E-05	3.50E-06	2.00E-04
Cm-246	4.00E-05	3.50E-06	2.00E-04
Cm-247	4.00E-05	3.50E-06	2.00E-04
Cm-248	4.00E-05	3.50E-06	2.00E-04
Co-60	4.30E-04	4.30E-04	3.00E-02
Cs-135	2.20E-02	2.20E-02	5.00E-02
Cs-137	2.20E-02	2.20E-02	5.00E-02
Eu-152	2.00E-05	2.00E-05	5.00E-03
Eu-154	2.00E-05	2.00E-05	5.00E-03
Eu-155	2.00E-05	2.00E-05	5.00E-03
Gd-152	2.00E-05	2.00E-05	3.50E-03
H-3	0.00E+00	0.00E+00	1.20E-02

Table 6.1-1: Triangular Distributions for Feed to Meat Transfer Factors (Continued)

Species	Recommended Values of Feed To Meat (d/kg)	Min Values of Feed To Meat (d/kg)	Max Values of Feed To Meat (d/kg)
I-129	6.70E-03	6.70E-03	4.00E-02
K-40	2.00E-02	2.00E-02	2.00E-02
Lu-174	4.50E-03	2.00E-03	4.50E-03
Mo-93	1.00E-03	1.00E-03	8.00E-03
Nb-93m	2.60E-07	2.60E-07	2.80E-01
Nb-94	2.60E-07	2.60E-07	2.80E-01
Ni-59	5.00E-03	5.00E-03	5.30E-02
Ni-63	5.00E-03	5.00E-03	5.30E-02
Np-237	1.00E-03	5.50E-05	1.00E-03
Pa-231	4.47E-04	5.00E-06	5.00E-03
Pb-210	7.00E-04	3.00E-04	8.00E-04
Pd-107	4.00E-03	2.00E-04	4.00E-03
Pt-193	4.00E-03	2.00E-04	4.00E-03
Pu-238	1.10E-06	1.10E-06	1.00E-04
Pu-239	1.10E-06	1.10E-06	1.00E-04
Pu-240	1.10E-06	1.10E-06	1.00E-04
Pu-241	1.10E-06	1.10E-06	1.00E-04
Pu-242	1.10E-06	1.10E-06	1.00E-04
Pu-244	1.10E-06	1.10E-06	1.00E-04
Ra-226	1.70E-03	2.50E-04	1.70E-03
Ra-228	1.70E-03	2.50E-04	1.70E-03
Se-79	1.50E-02	1.50E-02	1.00E-01
Sm-147	3.16E-04	2.00E-05	5.00E-03
Sm-151	3.16E-04	2.00E-05	5.00E-03
Sn-126	8.00E-02	1.00E-02	8.00E-02
Sr-90	1.30E-03	1.30E-03	1.00E-02
Tc-99	6.32E-03	1.00E-04	4.00E-01
Th-229	2.30E-04	6.00E-06	2.30E-04
Th-230	2.30E-04	6.00E-06	2.30E-04
Th-232	2.30E-04	6.00E-06	2.30E-04
U-232	3.90E-04	2.00E-04	8.00E-04
U-233	3.90E-04	2.00E-04	8.00E-04
U-234	3.90E-04	2.00E-04	8.00E-04
U-235	3.90E-04	2.00E-04	8.00E-04
U-236	3.90E-04	2.00E-04	8.00E-04
U-238	3.90E-04	2.00E-04	8.00E-04
Zr-93	1.20E-06	1.20E-06	3.40E-02

[SRNL-STI-2010-00447, Rev 0, Tables 2-5, PNNL-13421, IAEA-472]

Table 6.1-2: Triangular Distributions for Feed to Milk Transfer Factors

Species	Recommended Values of Feed To Milk (d/L)	Min Values of Feed To Milk (d/L)	Maxi Values of Feed To Milk (d/L)
Ac-227	2.00E-05	2.00E-06	2.06E-05
Ag-108m	1.58E-03	5.00E-05	5.00E-02
A-126	2.06E-04	2.00E-04	2.06E-04
Am-241	4.20E-07	4.2E-07	5.00E-06
Am-242m	4.20E-07	4.2E-07	5.00E-06
Am-243	4.20E-07	4.2E-07	5.00E-06
Bi-210m	5.00E-04	5.00E-04	1.00E-03
C-14	1.20E-02	1.05E-02	1.20E-02
Ca-41	1.00E-02	3.00E-03	1.03E-02
Cf-249	1.50E-06	7.50E-07	2.00E-06
Cf-251	1.50E-06	7.50E-07	2.00E-06
Cl-36	1.70E-02	1.50E-02	2.00E-02
Cm-243	2.00E-05	2.00E-06	2.06E-05
Cm-244	2.00E-05	2.00E-06	2.06E-05
Cm-245	2.00E-05	2.00E-06	2.06E-05
Cm-246	2.00E-05	2.00E-06	2.06E-05
Cm-247	2.00E-05	2.00E-06	2.06E-05
Cm-248	2.00E-05	2.00E-06	2.06E-05
Co-60	1.10E-04	1.10E-04	2.06E-03
Cs-135	4.60E-03	4.60E-03	1.20E-02
Cs-137	4.60E-03	4.60E-03	1.20E-02
Eu-152	3.00E-05	2.00E-05	6.00E-05
Eu-154	3.00E-05	2.00E-05	6.00E-05
Eu-155	3.00E-05	2.00E-05	6.00E-05
Gd-152	3.00E-05	2.00E-05	6.00E-05
H-3	1.50E-02	1.00E-20	1.50E-02
I-129	5.40E-03	5.40E-03	1.20E-02
K-40	7.20E-03	7.00E-03	7.21E-03
Lu-174	2.06E-05	2.00E-05	6.00E-05
Mo-93	1.10E-03	1.10E-03	7.50E-03
Nb-93m	4.10E-07	4.10E-07	2.06E-02
Nb-94	4.10E-07	4.10E-07	2.06E-02
Ni-59	9.50E-04	9.50E-04	2.00E-02
Ni-63	9.50E-04	9.50E-04	2.00E-02
Np-237	5.00E-06	5.00E-06	1.00E-05
Pa-231	5.00E-06	5.00E-06	5.15E-06
Pb-210	1.90E-04	1.90E-04	3.00E-04
Pd-107	1.00E-02	1.00E-04	1.03E-02
Pt-193	5.15E-03	1.00E-04	5.15E-03
Pu-238	1.00E-05	1.00E-07	1.00E-05
Pu-239	1.00E-05	1.00E-07	1.00E-05

Table 6.1-2: Triangular Distributions for Feed to Milk Transfer Factors (Continued)

Species	Recommended Values of Feed To Milk (d/L)	Min Values of Feed To Milk (d/L)	Maxi Values of Feed To Milk (d/L)
Pu240	1.00E-05	1.00E-07	1.00E-05
Pu241	1.00E-05	1.00E-07	1.00E-05
Pu242	1.00E-05	1.00E-07	1.00E-05
Pu244	1.00E-05	1.00E-07	1.00E-05
Ra226	3.80E-04	3.80E-04	1.30E-03
Ra228	3.80E-04	3.80E-04	1.30E-03
Se79	4.00E-03	4.00E-03	4.50E-02
Sm147	3.00E-05	5.00E-06	6.00E-05
Sm151	3.00E-05	5.00E-06	6.00E-05
Sn126	1.00E-03	1.00E-03	2.50E-03
Sr90	1.30E-03	1.30E-03	2.80E-03
Tc99	1.87E-03	2.30E-05	2.50E-02
Th229	5.00E-06	5.00E-06	5.15E-06
Th230	5.00E-06	5.00E-06	5.15E-06
Th232	5.00E-06	5.00E-06	5.15E-06
U232	1.80E-03	4.00E-04	1.80E-03
U233	1.80E-03	4.00E-04	1.80E-03
U234	1.80E-03	4.00E-04	1.80E-03
U235	1.80E-03	4.00E-04	1.80E-03
U236	1.80E-03	4.00E-04	1.80E-03
U238	1.80E-03	4.00E-04	1.80E-03
Zr93	3.60E-06	5.50E-07	3.09E-05

[SRNL-STI-2010-00447, Rev 0, Tables 2-5, PNNL-13421, IAEA-472]

Table 6.1-3: Triangular Distributions for Water to Finfish Transfer Factors

Species	Recommended Values of Water To Finfish (L/kg)	Min Values of Water To Finfish (L/kg)	Max Values of Water To Finfish (L/kg)
Ac227	2.50E+01	1.50E+01	2.50E+01
Ag108m	1.10E+02	2.30E+00	1.10E+02
Al26	5.10E+01	5.10E+01	5.00E+02
Am241	2.40E+02	2.10E+01	2.40E+03
Am242m	2.40E+02	2.10E+01	2.40E+03
Am243	2.40E+02	2.10E+01	2.40E+03
Bi210m	1.50E+01	1.00E+01	1.50E+01
C14	3.00E+00	3.00E+00	5.00E+04
Ca41	1.20E+01	1.20E+01	1.00E+03
Cf249	2.50E+01	2.50E+01	2.50E+01
Cf251	2.50E+01	2.50E+01	2.50E+01
Cl36	4.70E+01	4.70E+01	1.00E+03
Cm243	3.00E+01	2.10E+01	2.50E+02
Cm244	3.00E+01	2.10E+01	2.50E+02
Cm245	3.00E+01	2.10E+01	2.50E+02
Cm246	3.00E+01	2.10E+01	2.50E+02
Cm247	3.00E+01	2.10E+01	2.50E+02
Cm248	3.00E+01	2.10E+01	2.50E+02
Co60	7.60E+01	7.60E+01	3.30E+02
Cs135	3.00E+03	2.00E+03	4.70E+03
Cs137	3.00E+03	2.00E+03	4.70E+03
Eu152	1.30E+02	2.50E+01	1.30E+02
Eu154	1.30E+02	2.50E+01	1.30E+02
Eu155	1.30E+02	2.50E+01	1.30E+02
Gd152	3.00E+01	2.50E+01	3.00E+01
H3	1.00E+00	9.00E-01	1.00E+00
I129	3.00E+01	3.00E+01	5.00E+02
K40	3.20E+03	1.00E+03	1.00E+04
Lu174	2.50E+01	2.50E+01	2.50E+01
Mo93	1.90E+00	1.90E+00	1.00E+01
Nb93m	3.00E+02	2.00E+02	3.00E+04
Nb94	3.00E+02	2.00E+02	3.00E+04
Ni59	2.10E+01	2.10E+01	1.00E+02
Ni63	2.10E+01	2.10E+01	1.00E+02
Np237	2.10E+01	1.00E+01	2.50E+02
Pa231	1.00E+01	1.00E+01	1.13E+01
Pb210	2.50E+01	2.50E+01	3.00E+02
Pd107	1.00E+01	1.00E+01	1.00E+01
Pt193	3.50E+01	3.50E+01	1.00E+02
Pu238	3.00E+01	3.50E+00	4.70E+03
Pu239	3.00E+01	3.50E+00	4.70E+03

Table 6.1-3: Triangular Distributions for Water to Fish Transfer Factors (Continued)

Species	Recommended Values of Water To Finfish (L/kg)	Min Values of Water To Finfish (L/kg)	Max Values of Water To Finfish (L/kg)
Pu240	3.00E+01	3.50E+00	4.70E+03
Pu241	3.00E+01	3.50E+00	4.70E+03
Pu242	3.00E+01	3.50E+00	4.70E+03
Pu244	3.00E+01	3.50E+00	4.70E+03
Ra226	4.00E+00	4.00E+00	7.00E+01
Ra228	4.00E+00	4.00E+00	7.00E+01
Se79	6.00E+03	1.70E+02	6.00E+03
Sm147	3.00E+01	2.50E+01	3.00E+01
Sm151	3.00E+01	2.50E+01	3.00E+01
Sn126	3.00E+03	3.00E+03	3.00E+03
Sr90	2.90E+00	2.90E+00	5.01E+02
Tc99	2.00E+01	1.50E+01	2.00E+01
Th229	6.00E+00	6.00E+00	1.00E+02
Th230	6.00E+00	6.00E+00	1.00E+02
Th232	6.00E+00	6.00E+00	1.00E+02
U232	9.60E-01	9.60E-01	5.00E+01
U233	9.60E-01	9.60E-01	5.00E+01
U234	9.60E-01	9.60E-01	5.00E+01
U235	9.60E-01	9.60E-01	5.00E+01
U236	9.60E-01	9.60E-01	5.00E+01
U238	9.60E-01	9.60E-01	5.00E+01
Zr93	2.20E+01	2.20E+01	3.00E+02

[SRNL-STI-2010-00447, Rev 0, Tables 2-5, PNNL-13421, IAEA-472]

7.0 MODEL BENCHMARKING

The PORFLOW model is a 3-D flow and transport model that was designed to simulate rigorously the potential release of radionuclides and nonradioactive species from waste tanks and associated ancillary equipment located in the HTF and the transport of the released species to downgradient locations. The GoldSim based model is an abstraction of the PORFLOW based model and is designed used in performing sensitivity and uncertainty analyses that would be prohibitive using a computationally intensive model like the PORFLOW based model. In the abstraction, spatially averaged flow rates from the PORFLOW based model, used as input to the HTF GoldSim Model, control the transport of radionuclides and nonradioactive species through a simplified assemblage of the main structural features found in the waste tanks. While 3-D flow can take place within the structural features of the waste tanks, the HTF GoldSim Model is limited to 1-D flow through these features. In the SZ, a complex three-dimensional flow field produced by PORFLOW is represented by 1-D flow along stream traces, produced by PORFLOW, emanating from under the footprint of each waste tank or ancillary equipment source. In the SZ the timing of concentration breakthrough curve peaks generated by PORFLOW (for a conservative tracer) and the stream trace lengths were used to determine the flow velocities rates along the stream traces. The degree of dilution was based on Darcy velocities along the 100-meter boundary.

In order to perform sensitivity and uncertainty analyses using the GoldSim based model, it is first necessary to show that results from the two models (PORFLOW and GoldSim based models), show a sufficient degree of agreement so that the results of the HTF GoldSim Model stochastic simulations can consistently reflect the results that the PORFLOW Model would generate. In other words, it is important that the GoldSim abstraction successfully approximate the basic features of the HTF PORFLOW Model.

In the benchmarking effort, PORFLOW/GoldSim comparisons were performed in four phases. The first phase focused on how well the abstraction model approximates the radionuclide releases from the waste tanks and ancillary equipment. The radionuclide releases to the SZ are used for this comparison, and are referred to below as “vadose zone mass release.” The second phase focused on how well the abstraction model approximated the radionuclide transport behavior in the SZ. The sector-based radionuclide species-specific dose contributions are examined for this task. The sectors used for the comparison were Sectors A, B, C, E, and F. The locations of the sectors are shown in Figure 4.4-1. The third phase compared PORFLOW dose results with total GoldSim dose results, evaluating how well the timing and magnitude of the time histories matched. The fourth phase used a comparison of IHI total dose results, based on concentrations solved for adjacent to Tank 12.

The benchmarking evaluation was conducted for Configuration A (e.g., Case A) results.

The main comparisons used to verify that the HTF GoldSim Model approximates the basic features of the HTF PORFLOW Model is; 1) a comparison of the Case A vadose zone mass releases and 2) a comparison of the Case A 100-meter observation well concentration results. The model comparisons for Case A were conducted using Ra-226, Tc-99, I-129, Cs-135, and Np-237.

In the waste tank benchmarking effort, comparisons were made of mass releases from one or more representative waste tanks for each waste tank type. The number of waste tanks evaluated for each waste tank type was dependent on differences in environment or other considerations. For the Type I tanks, one waste tank without initial damage to the liner (Tank 9) and one waste tank with initial damage to the liner (Tank 12) were evaluated. For the Type II tanks, one waste tank without initial damage to the liner (Tank 13) and one waste tank with initial damage to the liner (Tank 15) were evaluated. In addition, a third waste tank with initial damage to the liner and an inventory in the secondary sand pad (Tank 16). For Type IV and Type III tanks, one waste tank was evaluated for each type (Tank 24 for Type IV tanks and Tank 31 for Type III tanks). For Type IIIA tanks, one from the western side of the HTF (Tank 36) and one from the eastern side (Tank 40) were evaluated. Vadose zone mass release comparisons were also made for the ancillary equipment sources. In the ancillary equipment benchmarking effort, comparisons were made of mass releases from one pump tank (HPT-7), one evaporator (E242-25H), and one of the four waste tank line areas (Zone 3 or HTF-T-Line3).

7.1 Case A (HTF Base Case)

The Case A represents, what is considered to be, the most likely scenario for the time-base degradation of the waste tank structure, including the degradation of the cementitious material and the steel liner. Case A lacks a fast flow path through the grout and basemat, and the liners fail normally. Gradual degradation of the grout and the cementitious material proceed according to Table 1 in SRR-CWDA-2010-00019. In addition, the full reducing capacity of the reducing grout is available to control the chemistry in the CZ.

Because mass releases from the ancillary equipment is handled as a simple release to the UZ or SZ (where no UZ exists) without any alternative scenarios, the comparison of ancillary equipment mass releases is included in this section. Although a comparison of ancillary equipment mass releases to the SZ is expected to show similar results between the two models, the comparison is presented here to show that the HTF GoldSim Model successfully approximates the UZ. Because of the large number of plots involved in the analysis, the plots of the comparisons between PORFLOW and HTF GoldSim Model results for the Case A are assembled in Appendix A.

7.1.1 Mass Releases to the Saturated Zone

To build confidence in the HTF GoldSim Model a comparison of the PORFLOW and HTF GoldSim Models was done. The comparison was done for the model generated mass fluxes that enter the UZ below the Type I tanks (Tanks 9 and 12), the Type II tanks (Tanks 13, 15, and 16), the Type IV tank (Tank 24), the Type III tank (Tank 31), and the Type IIIA tanks (Tanks 36 and 40) in addition to the ancillary equipment.

7.1.1.1 Tank 9

A comparison of PORFLOW and GoldSim mass releases of Ra-226 presented in Figure A.1-1 indicates that the HTF GoldSim Model can produce a good approximation of PORFLOW releases of Ra-226 from Tank 9. Ra-226 was chosen as a benchmarking species because it represents the main dose contributor in the base-case model. It should be noted that because Ra-226 is generated through ingrowth from the Pu-238→U-234→Th-230 chain, the behavior of the parent species might differ to some extent because the HTF GoldSim

Model handles the influence of solubility limits more rigorously than does PORFLOW. For example, in the GoldSim simulations all isotopes of uranium are considered simultaneously in the analysis. In the PORFLOW simulations decay chains, and parts of decay chains are considered separately, so more of the parent product mass can be released from the CZ. [SRS-REG-2007-00002, Section 5.6.2.1.2] Technetium-99 was chosen as a benchmarking species because its transport is strongly controlled by solubility limits, in addition to it being a major dose contributor in the Case A model results. As can be seen in Figure A.1-2, the HTF GoldSim Model does an adequate job of reproducing the trends in the release of Tc-99 to the SZ from Tank 9. Prior to liner failure, the GoldSim Tc-99 release lags behind the PORFLOW release and after the liner failure, the match is quite good. The lag prior to liner failure is associated with the differences in the manner the two models handle transition times in the annulus. The transition times in the HTF PORFLOW Model are based upon the pore volume of the whole annulus and the volumetric flow within that volume. The transition times in the HTF GoldSim Model are based upon the pore volume of the abbreviated annulus and the volumetric flow within that smaller volume (the same is true for the wall). This difference in the volume affected by the flushing process makes the two models somewhat inconsistent when mass release from the annulus is important such as for Type I and Type II tanks. The good comparison of release rates after liner failure indicates that the solubility control associated with the CZ is being accurately approximated in the HTF GoldSim Model. Iodine-129 was chosen as a benchmarking species because its transport is not subject to solubility control and is either slightly sorbed or unsorbed along its transport pathway. Iodine-129 is also a major dose contributor in the Case A model results. Figure A.1-3 (Appendix A) shows that there is a good match between the PORFLOW results and the GoldSim results for I-129 releases from Tank 9. The match is especially good at the higher concentrations and not quite as good at early time. Cesium-135 was chosen as a benchmarking species because its transport is not subject to solubility control and it is more strongly sorbed than I-129 in the UZ. Figure A.1-4 shows that there is a good match between the PORFLOW results and the GoldSim results for Cs-135 releases from Tank 9. The match is especially good at the higher concentrations. Figure A.1-5 presents the Np-237 releases from the two models. For Np-237, the trends are similar, but the match is only fair. Note that Np-237 is one of the species that has parents that are handled differently in GoldSim, which always considers all isotopes of an element in solubility controls. Neptunium-237 is generated through ingrowth from the Cf-249→Cm-245→Pu-241→Am-241→Np-237, Np-237 chain.

7.1.1.2 Tank 12

A comparison of PORFLOW and GoldSim mass releases of Ra-226 presented in Figure A.1-6 indicates that the HTF GoldSim Model can produce a good approximation of PORFLOW releases from Tank 12. As can be seen in Figure A.1-6, there is an early time release of Ra-226 caused by the immediate failure of the steel liner in Tank 12. The early time release of Ra-226 is overestimated to some extent, but the representation is still acceptable, showing the general trends of the release. As can be seen in Figure A.1-7, the HTF GoldSim Model does an adequate job of reproducing the trends in the release of Tc-99 to the SZ from Tank 12. Slight differences associated with transition timing calculations for the annulus and wall can be seen. A very good match after 7,000 years indicates that the solubility control

associated with the contaminant zone is being accurately approximated in the HTF GoldSim Model. Figure A.1-8 depicts a good match between the PORFLOW results and the GoldSim results for I-129 releases from Tank 12. The match is especially good at the higher concentrations. Figure A.1-9 shows that there is a good match between the PORFLOW results and the GoldSim results for Cs-135 releases from Tank 12. The match is especially good at the higher concentrations. Figure A.1-10 presents the Np-237 releases from the two models, and for Np-237, the match is fair.

7.1.1.3 Tank 13

The comparison of PORFLOW and GoldSim mass releases presented in Figures A.1-11 through A.1-15 indicates that for Type II tank releases where the liner remains intact, the HTF GoldSim Model can still generally generate a good approximation of PORFLOW releases. The flow and transport system through the engineered barrier is much more complex for the Type II tanks because of the sand pads (primary and secondary) located beneath the primary and secondary liners. In all of the Type II Tanks, it is assumed that there is some contaminant resides in the sand pads. The mass in the primary sand pad, the sand pad sandwiched between the primary and secondary liners, is capable of migrating out of the engineered barrier prior to liner failure, a process that is seen in the PORFLOW simulations. The exit route is from the sand pad to the annulus and upward through the annulus. Once the mass has migrates above the 5-foot vertical extension of the secondary liner (see Figure 3.1-4), it will leave the system through the wall and the concrete basemat and finally into the SZ. The comparison of PORFLOW and GoldSim mass releases of Ra-226 presented in Figure A.1-11 indicates that the HTF GoldSim Model can produce a very good approximation of PORFLOW releases from Tank 13. As can be seen in Figure A.1-12, the HTF GoldSim Model does an adequate job of reproducing the trends in the release of Tc-99 to the SZ from Tank 13. It can be seen that prior to the transition of the chemical state in the annulus from a reducing to an oxidizing environment, the Tc-99 mass release at very low magnitudes is overestimated in the HTF GoldSim Model, but the trends are similar. As expected, the timing of the transition from a reducing to an oxidizing state in the annulus/wall zone differs between the two models. After the transition from a reducing to an oxidizing state, the two models show very similar behavior. Figure A.1-13 shows a good match between the PORFLOW results and the GoldSim results for I-129 releases from Tank 13 after 10,000 years. The match is especially good at the high peak concentration associated with the liner failure. Figure A.1-14 shows that the match between the PORFLOW results and the GoldSim results for Cs-135 with its higher K_d values is good after 10,000 years with the general trends of the releases still similar and the match very good at the high peak concentration associated with the liner failure. Figure A.1-15 presents the Np-237 releases from the two models. The GoldSim generated release of Np-237 from Tank 13 matches the PORFLOW results quite well.

7.1.1.4 Tank 15

The comparison of PORFLOW and GoldSim mass releases presented in Figures A.1-16 through A.1-20 indicates that for Type II Tank releases where the liner is considered to have failed at the start of the simulation, the HTF GoldSim Model is a good approximation of Type II tank PORFLOW model. The comparison of PORFLOW and GoldSim mass releases of Ra-226 presented in Figure A.1-16 show that the HTF GoldSim Model produced a very good approximation of PORFLOW Ra-226 releases from Tank 15. As can be seen in Figure A.1-17, the HTF GoldSim Model does a good job of reproducing the trends in the release of Tc-99 to the SZ from Tank 15. It can also be seen that the later trends found in the PORFLOW simulations are also reproduced very well. Figures A.1-18 and A.1-19 show that there is a very good correlation between both the I-129 and Cs-135 mass releases generated by PORFLOW and their mass releases given by the HTF GoldSim Model. As can be seen in Figure A.1-20, the GoldSim generated release of Np-237 from Tank 15 shows trends similar to the PORFLOW results.

7.1.1.5 Tank 16

Figures A.1-21 through A.1-25 show a comparison of PORFLOW and GoldSim mass releases from Type II tanks where an initial inventory is assigned to the secondary sand pad as well as the primary sand pad (Tank 16). As can be seen by comparing Figures A.1-21 through A.1-25 to Figures A.1-16 through A.1-20 it can be seen the trends shown in both sets of results are quite similar. The mass release from simulations of the Type II tank the liner fails at the start of the simulation and there is no inventory in the secondary sand pad. Similarly, the mass release for the Type II tank from the HTF GoldSim Model the liner fails at the start of the simulation and there is an inventory in the secondary sand pad. This is a good approximation of the Type II tank PORFLOW model.

7.1.1.6 Tank 24

The comparison of PORFLOW and GoldSim mass releases presented in Figures A.1-26 through A.1-30 shows that for Type IV Tank releases, the HTF GoldSim Model does a good job of approximating the PORFLOW Type IV Tank Model (Tank 24). The comparison of PORFLOW and GoldSim mass releases of Ra-226 presented in Figure A.1-26 shows that he GoldSim results are very similar to PORFLOW generated Ra-226 releases from Tank 24. As can be seen in Figure A.1-27, the HTF GoldSim Model does a good job of reproducing the release of Tc-99 to the SZ from Tank 24. Figures A.1-28 and A.1-29 show that GoldSim does a good job of reproducing the I-129 and Cs-135 mass releases generated by PORFLOW, although the GoldSim peak release is a little more dispersed. As can be seen in Figure A.1-30, the GoldSim generated release of Np-237 from Tank 24 matches the PORFLOW results very well.

7.1.1.7 Tank 31

The comparison of PORFLOW and GoldSim mass releases presented in Figures A.1-31 through A.1-35 shows that for Type III tank releases, the HTF GoldSim Model does a good job of approximating the PORFLOW Type III Tank Model (Tank 31). The comparison of PORFLOW and GoldSim mass releases of Ra-226 presented in Figure A.1-31 shows that the GoldSim results are a very good approximation of PORFLOW generated Ra-226 releases

from Tank 31. As can be seen in Figure A.1-32, the HTF GoldSim Model does a very good job of reproducing solubility-controlled trends in the release of Tc-99 to the SZ from Tank 31. Figures A.1-33 and A.1-34 show that there is a good match between both the I-129 and Cs-135 mass releases generated by PORFLOW and their mass releases given by the HTF GoldSim Model except for the low releases at early times where GoldSim seems to overestimate the release. As can be seen in Figure A.1-35, the GoldSim generated release of Np-237 from Tank 31 is smaller than the PORFLOW results reflecting differences in the solubility models.

7.1.1.8 Tanks 36 and 40

A comparison of PORFLOW and GoldSim mass releases from the eastern Type IIIA Tanks presented in Figures A.1-36 through A.1-40 to releases presented for the Type III Tanks in Figures A.1-31 through A.1-35 shows little difference between the results for the similar waste tank types. Thus for an eastern Type IIIA tank the HTF GoldSim Model does an adequate job of approximating the PORFLOW results. This is also true for the comparison of PORFLOW and GoldSim mass releases for the western Type IIIA Tanks presented in Figures A.1-41 through A.1-44 and the releases presented for the Type III Tanks in Figures A.1-31 through A.1-34. A comparison between Figures A.1-45 and A.1-35 showing HTF PORFLOW Model and HTF GoldSim Model releases of Np-237 from Tanks 40 and 31 respectively, reflect differences due to differences in the inventories of members of the Cf-249→Cm-245→Pu241→Am241→Np-237 decay chain. There are also major differences in the inventories of the isotopes of the member species such as the isotopes of Cm. The difference in ratios of the Cm isotopes in Tank 36 and Tank 40 will dictate that the solubility controls in the HTF GoldSim and PORFLOW Models will be quite different.

7.1.1.9 Ancillary Equipment

Figures A.1-46 through A.1-50 portrays the differences between the PORFLOW and GoldSim, Ra-226, Tc-99, I-129, Cs-135, and Np-237, releases from HPT-7, respectively. Figures A.1-46 shows that the HTF GoldSim Model does a good job of matching the Ra-226 peak, but after the peak, the mass is released at a faster rate in the GoldSim simulation. The GoldSim releases from HPT-7 in Figures A.1-47 through A.1-50 also clearly match the PORFLOW releases very well.

A comparison of PORFLOW and GoldSim mass releases from Transfer-Line Zone 3 presented in Figures A.1-51 through A.1-55 shows that the HTF GoldSim Model does a good job of matching the results from PORFLOW for Ra-226, Tc-99, I-129, Cs-135, and Np-237.

Examinations of PORFLOW and GoldSim mass releases from the evaporator E242-25H presented in Figures A.1-56 through A.1-58 show that the HTF GoldSim Model does a good job of matching the results from PORFLOW for Ra-226, Tc-99, and Np-237. Iodine-129 and Cs-135 mass releases from E242-25H are not presented here because the evaporator had no inventory for the two species.

7.1.2 100-Meter Well Locations

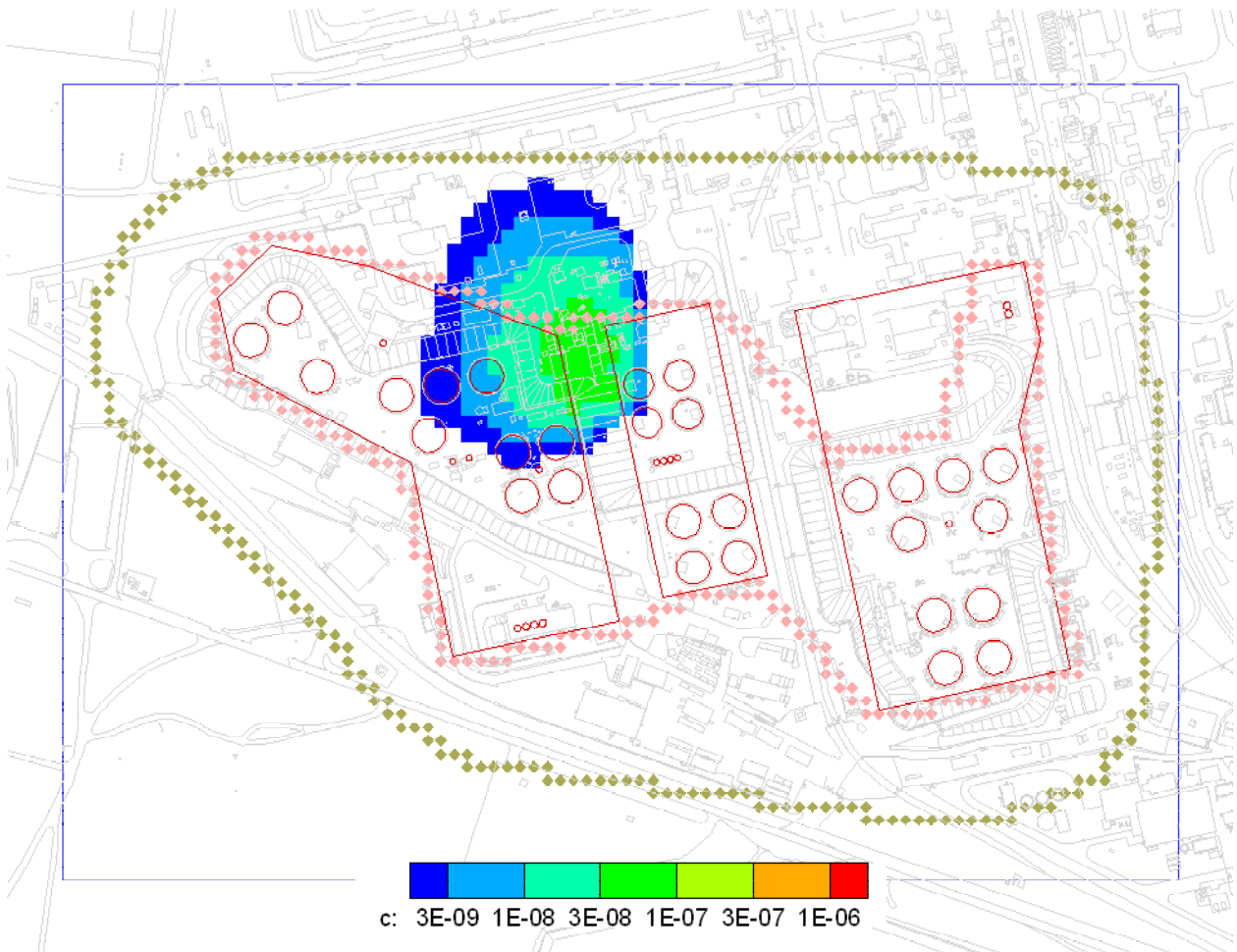
The second phase of the benchmarking process is focused on how well the abstraction model approximated the radionuclide transport behavior in the SZ. The radionuclide dose contributions (in mrem), for Sectors A, B, C, E, and F, were examined for this task. Note

that Sector D is not included because it is never analyzed in the HTF GoldSim Model. Sector D is neglected in the HTF GoldSim Model because the particle traces are oriented in directions that would dictate that the mass reaching Sector D was caused by backwards diffusion. In the HTF PORFLOW Model simulations mass is advected to Sector D, which is a very different conceptual model. The locations of the sectors are presented in Figure 4.4-1. For this exercise, the major species contributing to dose are presented in the comparisons. Note that the definition of major is based on HTF PORFLOW Model results and for specific radionuclides, such as Ni-59, the dose contribution is much lower in the HTF GoldSim Model. This inconsistency in Ni-59 results is a function of the manner in which the two models handle solubility controls. The HTF GoldSim Model considers the influence of non-radionuclide nickel, on the precipitation of Ni-59 and the HTF PORFLOW Model does not. This difference tends to overestimate the dose contribution of Ni-59 in PORFLOW results relative to GoldSim results.

7.1.2.1 Sector A

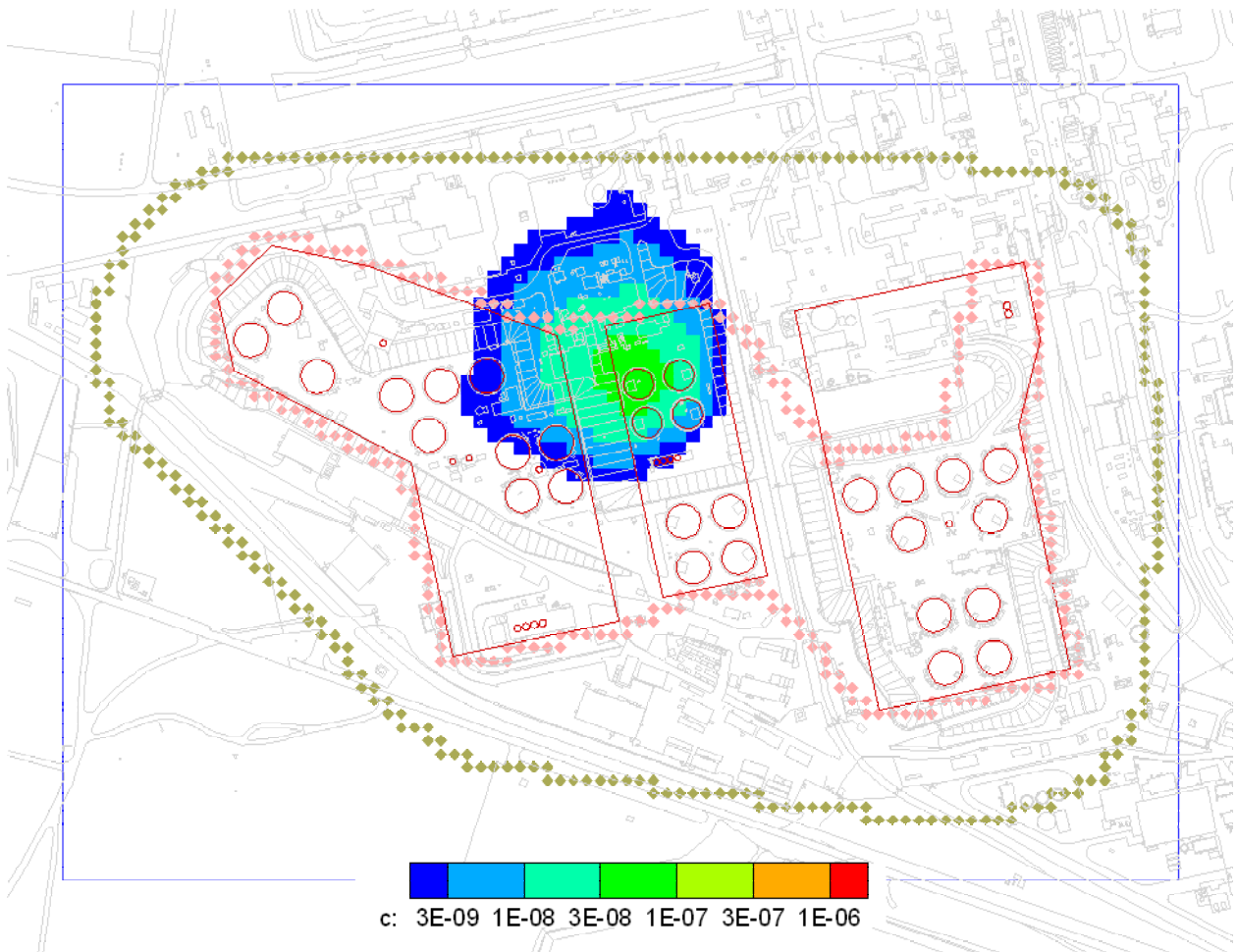
An examination of PORFLOW and HTF GoldSim Model generated dose contributions for Sector A, presented in Figures A.2-1 (PORFLOW results) and A.2-2 (GoldSim results), show that the general trends and peak dose contributions for most of the major dose contributors, are similar for the two models. There are several major differences in the two models that are reflected in the results. The first difference is in the degree of spreading of plumes in the models. By nature, the HTF PORFLOW Model is subject to greater spreading than the HTF GoldSim Model assuming due to the conceptual models. Spreading of the plume in the HTF GoldSim Model is a function of mechanical dispersion. In the HTF PORFLOW Model, the spreading of the plume is a function of a divergent flow field in addition to mechanical dispersion, especially for the westernmost waste tanks (Tank 9 through Tank 37). This can be seen in the plots presented in Figures 7.2-1 through 7.2-5, which are snapshots of plumes generated by PORFLOW for pulse releases of conservative species for several of the western waste tanks. These snapshots indicate that the spreading of the plumes is enhanced by the divergent flow field resulting in plumes that have length to width ratio of less than 3.2, which would be expected when the ratio of longitudinal dispersivity to horizontal transverse dispersivity is 10. In fact, the spreading of a plume based on a pulse-type release from Tank 12 (Figure 7.2-2) is indicative of what would be expected in a system not subject to a divergent flow field if the ratio of longitudinal dispersivity to horizontal transverse dispersivity is unity. Note that in Tanks 15 release, the plume starts out narrow and then widens as it changes direction. In contrast, the plumes in the eastern section of the HTF (Tanks 38 through 51), where the flow field is not quite as divergent, spread as expected for a 10:1 dispersivity ratio (see Figures 7.2-6 through 7.2-7). To help the HTF GoldSim Model more closely approximate the influence of the diverging flow field, the dispersivity ratio for the western waste tank releases was set to 3.3:1. For the eastern waste tanks, the longitudinal dispersivity to horizontal transverse dispersivity was set to 10:1, which is the same as used in the HTF PORFLOW Model simulations.

Figure 7.1-1: Plume Formed by a Pulse-Type Release of a Conservative Constituent from Tank 9



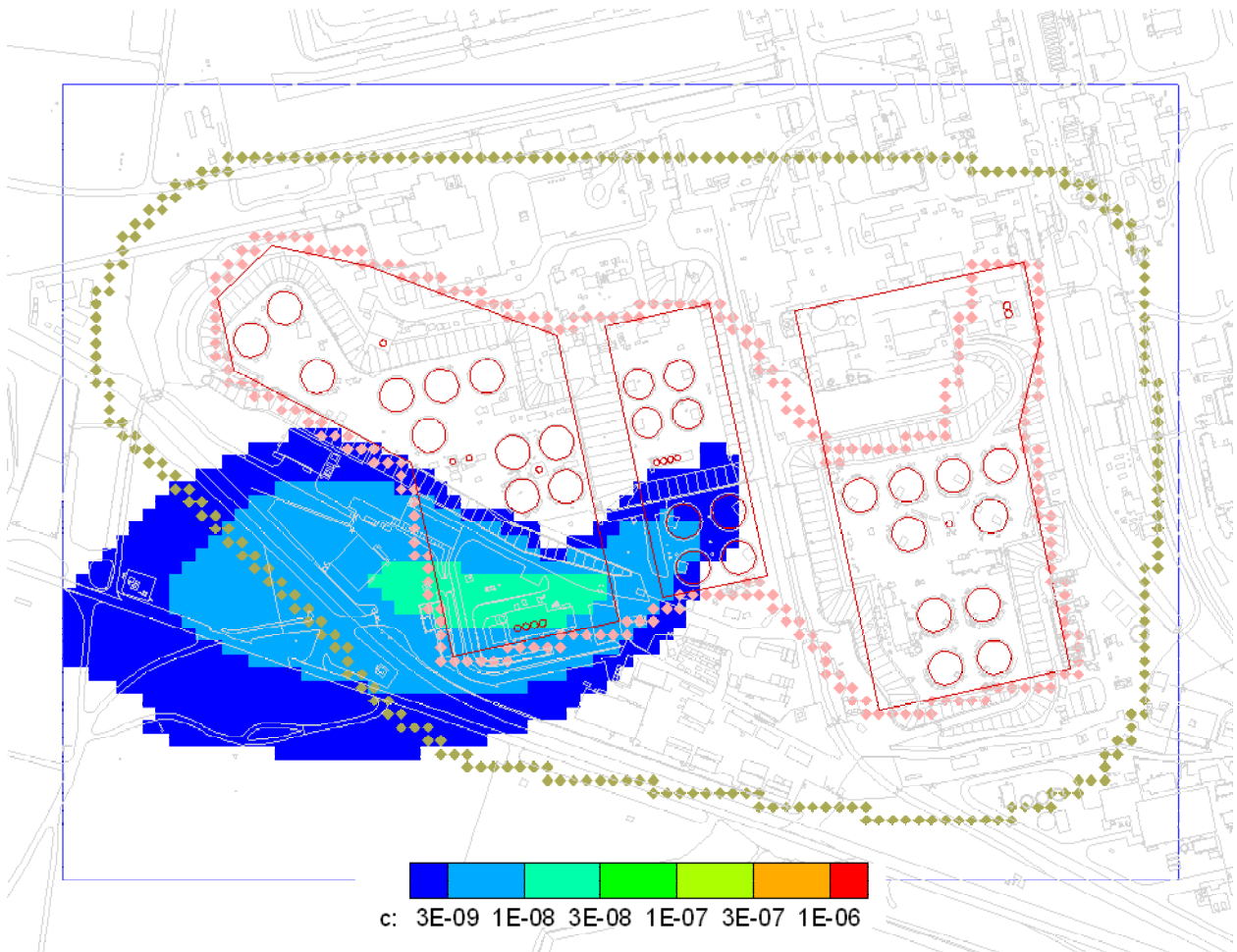
Note: Units on scale bar are in moles divided by liter and the concentrations were produced by a hypothetical constant source of 1 mol/yr.

Figure 7.1-2: Plume Formed by a Pulse-Type Release of a Conservative Constituent from Tank 12



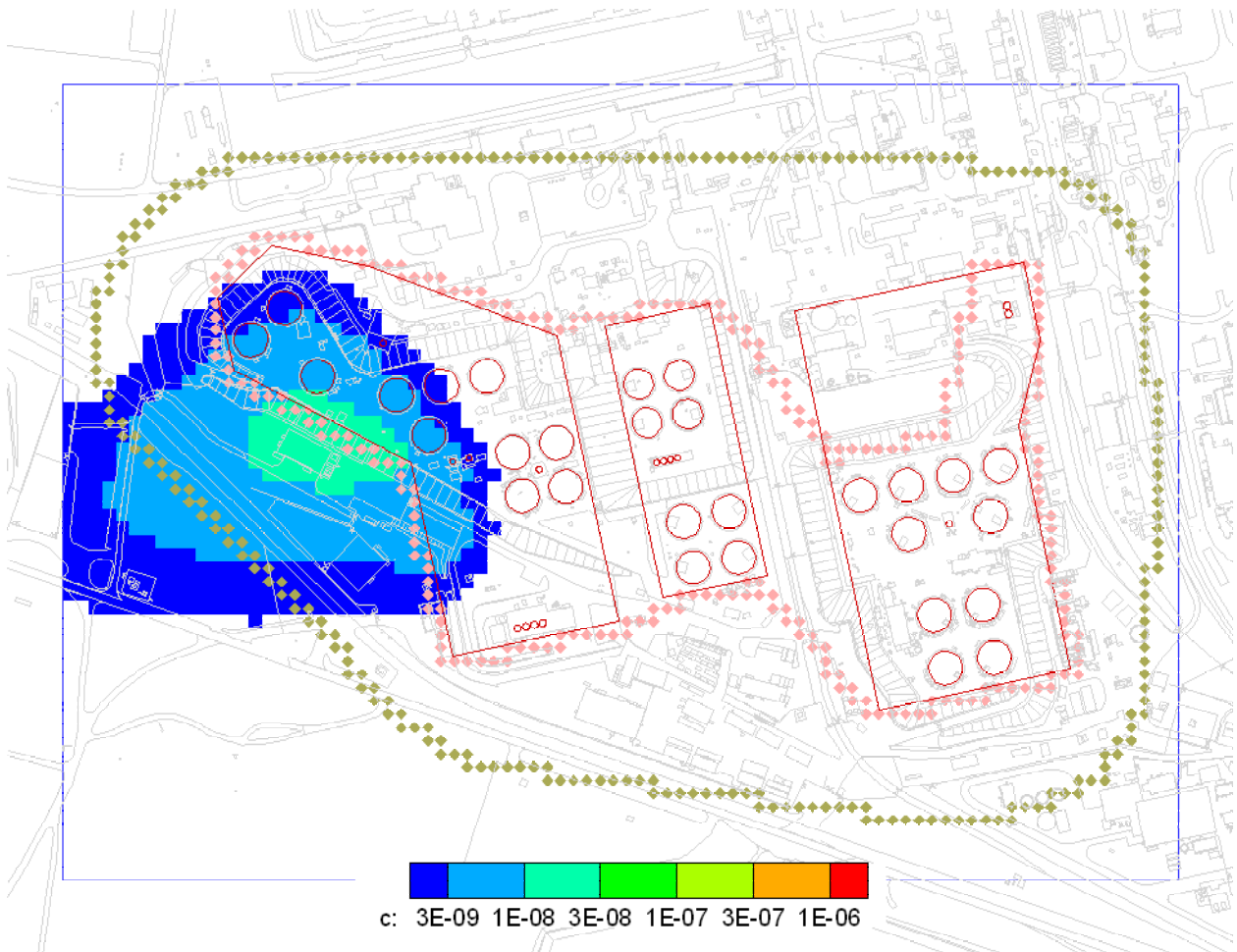
Note: Units on scale bar are in moles divided by liter and the concentrations were produced by a hypothetical constant source of 1 mol/yr.

Figure 7.1-3: Plume Formed by a Pulse-Type Release of a Conservative Constituent from Tank 15



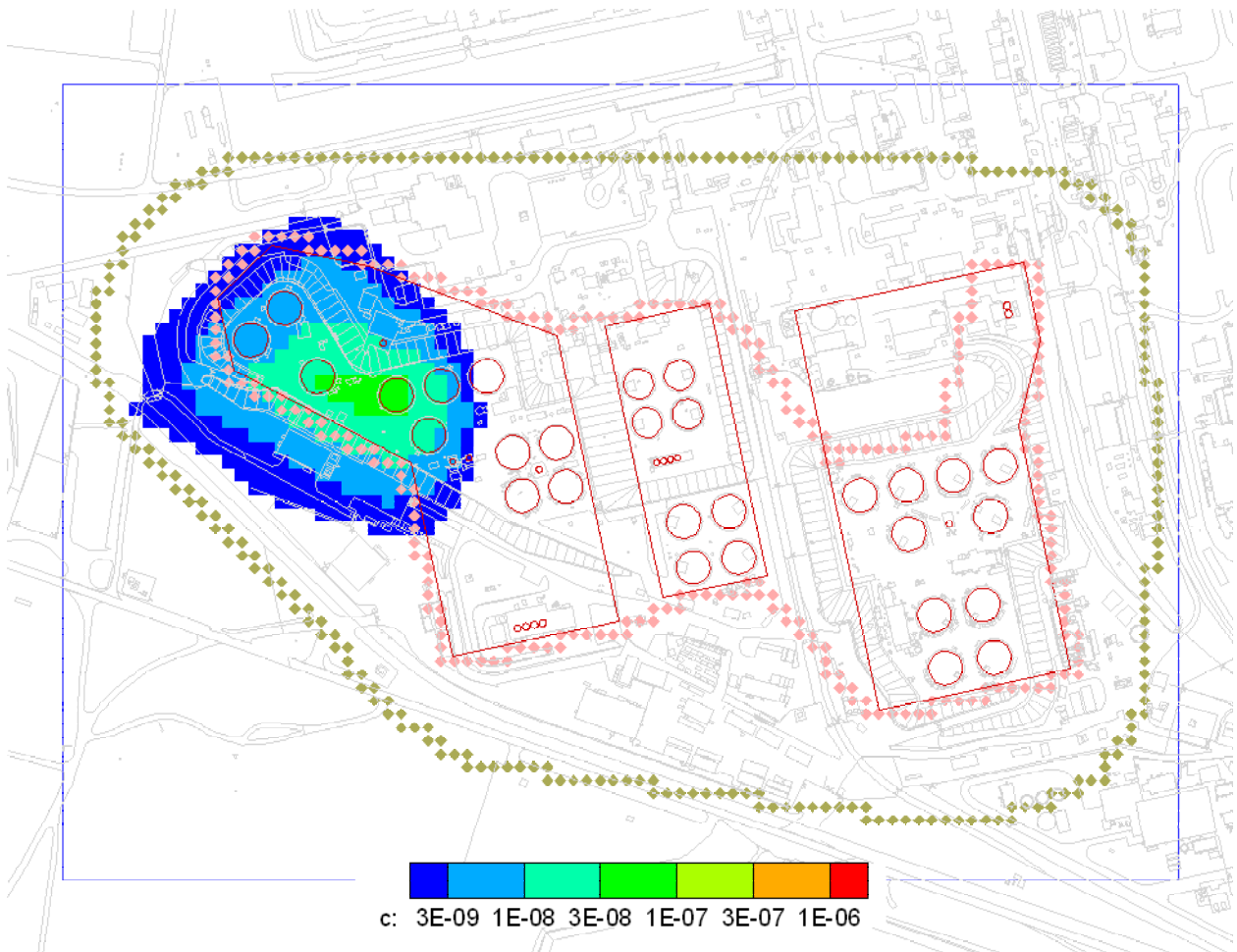
Note: Units on scale bar are in moles divided by liter and the concentrations were produced by a hypothetical constant source of 1 mol/yr.

Figure 7.1-4: Plume Formed by a Pulse-Type Release of a Conservative Constituent from Tank 24



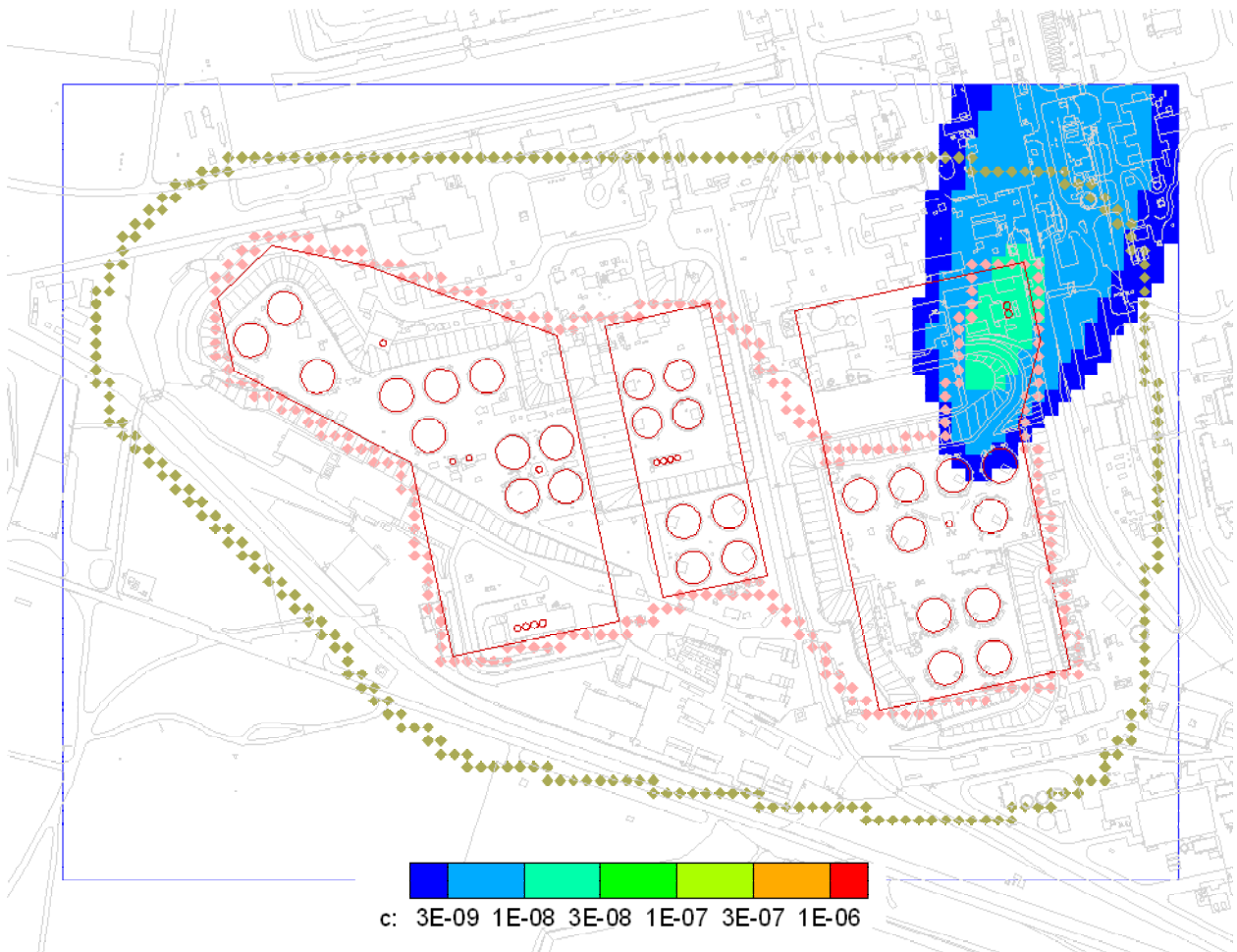
Note: Units on scale bar are in moles divided by liter and the concentrations were produced by a hypothetical constant source of 1 mol/yr.

Figure 7.1-5: Plume Formed by a Pulse-Type Release of a Conservative Constituent from Tank 29



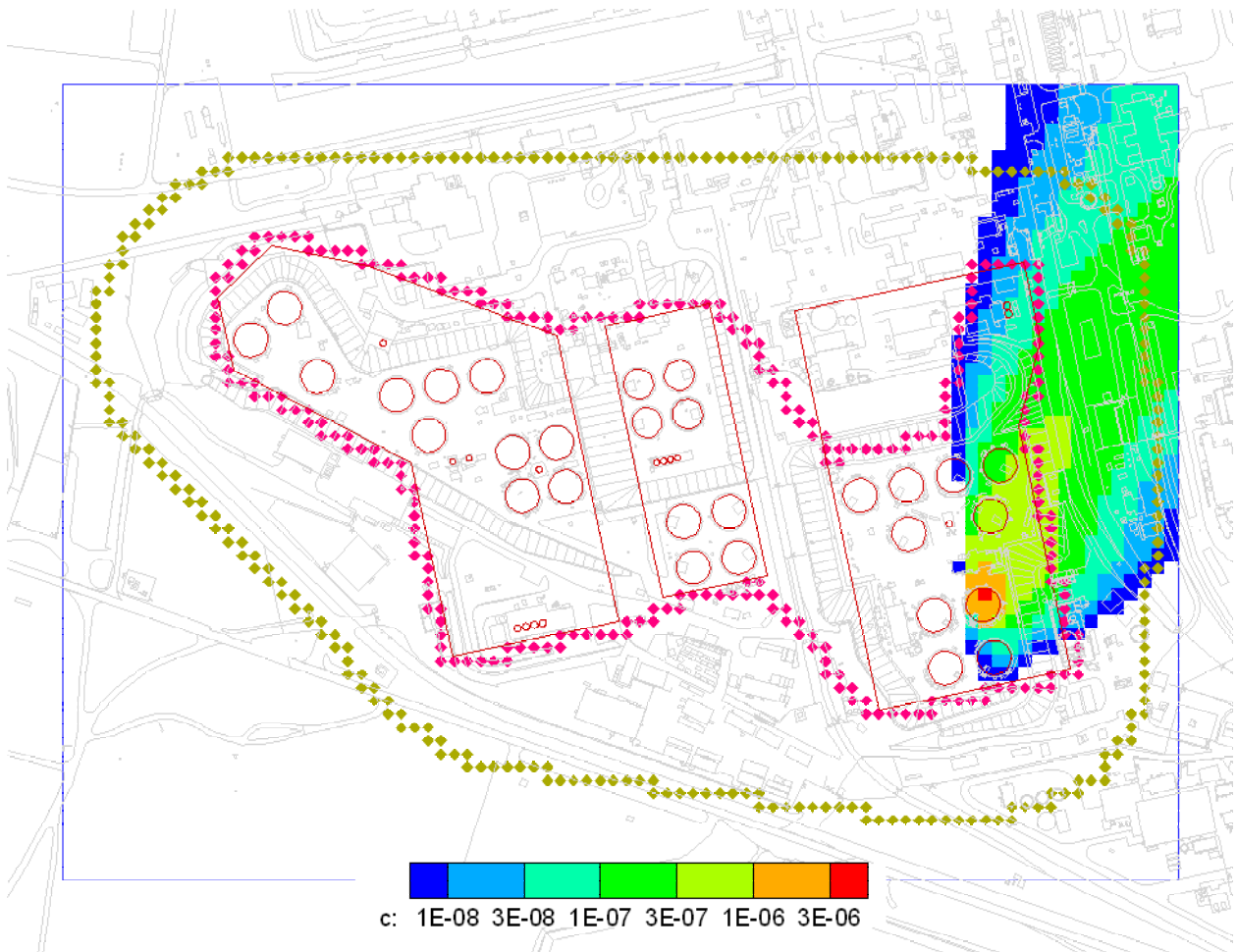
Note: Units on scale bar are in moles divided by liter and the concentrations were produced by a hypothetical constant source of 1 mol/yr.

Figure 7.1-6: Plume Formed by a Pulse-Type Release of a Conservative Constituent from Tank 40



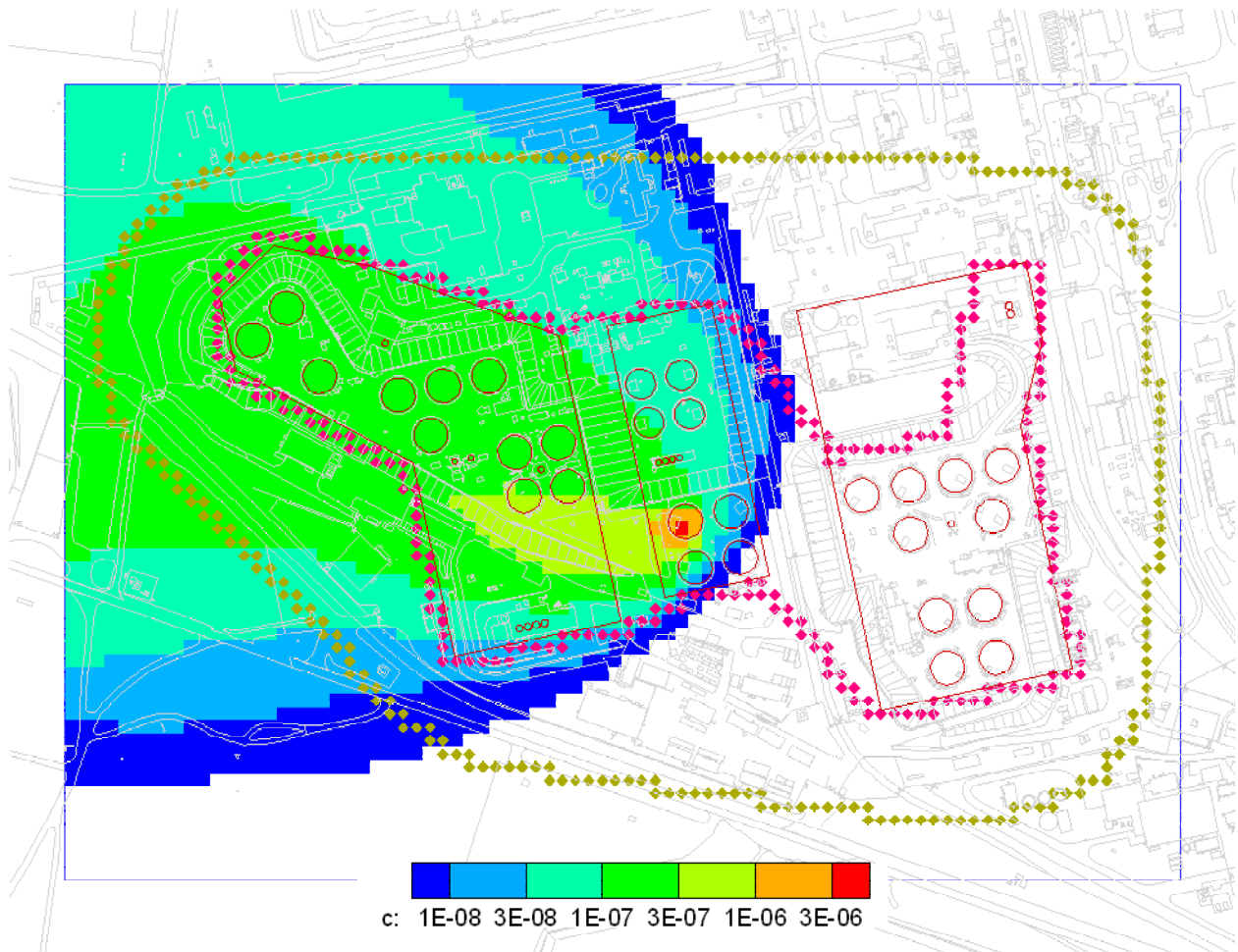
Note: Units on scale bar are in moles divided by liter and the concentrations were produced by a hypothetical constant source of 1 mol/yr.

Figure 7.1-7: Plume Formed by a Pulse-Type Release of a Conservative Constituent from Tank 49



Note: Units on scale bar are in moles divided by liter and the concentrations were produced by a hypothetical constant source of 1 mol/yr.

Figure 7.1-8: Plume Formed by a Steady Release of a Conservative Constituent from Tank 13



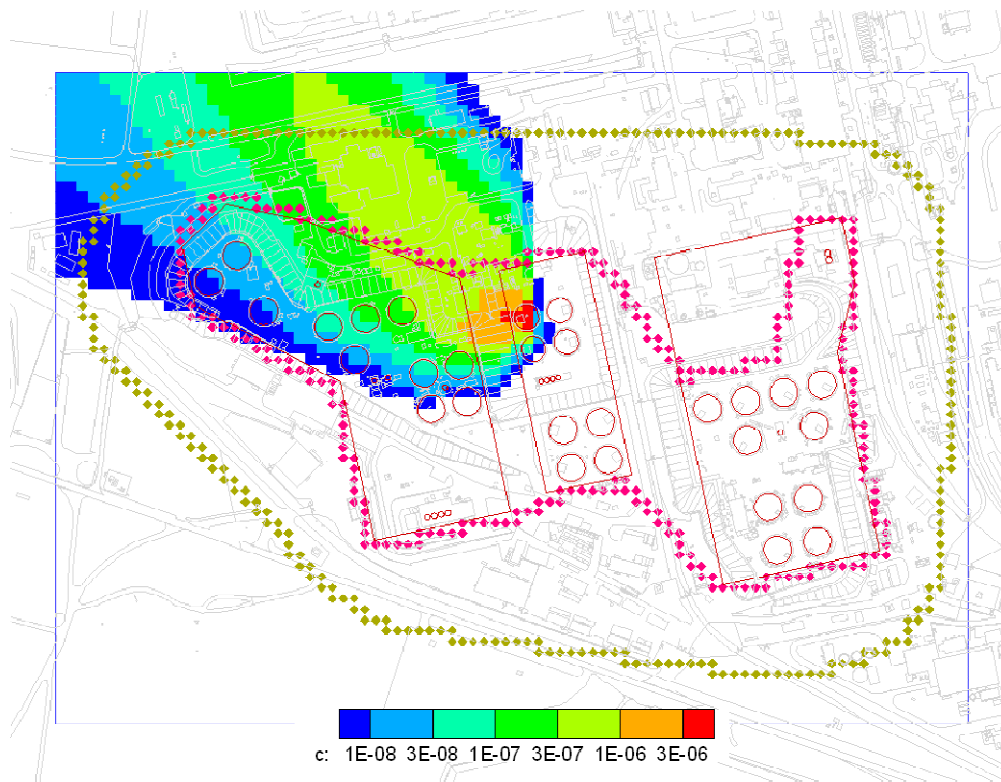
Note: Units on scale bar are in moles divided by liter and the concentrations were produced by a hypothetical constant source of 1 mol/yr.

A second difference in the resultant dose concentrations is a more radical influence of the flow divide in providing mass to Sectors such as Sector A, from waste tanks, that are not likely to influence Sector A based on the streamlines (see Figures 4.4-1). An examination of figures based on steady releases of a conservative radionuclide from several waste tanks indicates this point. As can be seen in Figure 7.2-8, and comparing the plume to the streamline from Tank 13 plotted in Figure 4.4-1, Sector A will be influenced by release from Tanks 13 largely in the PORFLOW simulations than in the GoldSim simulations where only mechanical dispersion provides for spreading. This condition is easily seen when comparing iodine releases in Figures A.2-1 and A.2-2. As can be discerned from the two figures, and comparing them with Figures A.1-3 and A.1-13, there are two I-129 peaks after 10,000 years, showing up in the HTF PORFLOW Model simulation (Figure A.1-3) from Tank 9 and Tank 13 releases. In the HTF GoldSim Model simulation (Figure A.1-13) only the release from Tank 9 shows up at a discernible level.

7.1.2.2 Sector B

PORFLOW and HTF GoldSim Model generated dose contributions for Sector B, presented in Figures A.2-3 (PORFLOW results) and A.2-4 (GoldSim results), show that the general trends and peak dose contributions for most of the major dose contributors, are similar for the two models. As can be seen in the two figures, peak values are generally similar, except near the end of the simulation where the Ra-226 dominated peak value is higher in the GoldSim results. Major differences in the trends include peaks from Tank 9 (i.e., Tc-99 and I-129) that occur in the PORFLOW results and not in the GoldSim results. This difference is a function of where the 100-meter boundary results are solved for in the HTF GoldSim Model versus the HTF PORFLOW Model. The HTF PORFLOW Model discretization generates results all along the 100-meter boundary. The maximum radionuclide concentration at any node in a sector is then used to solve for the dose contribution at that sector. In the HTF GoldSim Model, results at specified points along the 100-meter boundary are used to solve for the dose contribution at each sector. The set of points used are based on their proximity to streamlines and where the highest values are expected. As can be seen by comparing Figure 7.1-9 and Figure 4.4-1 which depicts the 100-meter boundary points used to evaluate the Sector B dose contributions, there is a difference between how the models handle the Tc-99, where the Tank 9 release influences the Sector B results in the HTF PORFLOW Model and not in the HTF GoldSim Model. Although the Tc-99 peak in the HTF PORFLOW Model gives Sector B a higher peak total concentration, the major influence of the Tank 9 release is captured in both the HTF PORFLOW Model and HTF GoldSim Model Sector A results.

Figure 7.1-9: Plume Formed by Steady Release of Conservative Constituent from Tank 9



7.1.2.3 Sector C

PORFLOW and HTF GoldSim Model generated dose contributions for Sector C are presented in Figures A.2-5 (PORFLOW results) and A.2-6 (GoldSim results). A comparison of the two figures shows that the general trends and peak dose contributions, for most of the major dose contributors, are similar in the two models. As can be seen in the two figures, peak values are generally similar, except for Tc-99 contributions between 4,000 and 12,000 years where the influence on dose is negligible. This difference is also due to the evaluation points used in the two models.

7.1.2.4 Sector E

PORFLOW and HTF GoldSim Model generated dose contributions for Sector E, presented in Figures A.2-7 (PORFLOW results) and A.2-8 (GoldSim results), shows that the general trends and peak dose contributions for most of the major dose contributors, are similar for the two models.

7.1.2.5 Sector F

The PORFLOW and HTF GoldSim Model generated dose contributions for Sector F, presented in Figures A.2-9 (PORFLOW results) and A.2-10 (GoldSim results), shows that the general trends and peak dose contributions for most of the major dose contributors, are similar for the two models, but not quite as good as was seen in the Sector E results. This difference is associated with the spreading of releases waste tanks that have streamlines that cross the 100-meter boundary in Sector E (see Figure 7.1-7).

7.1.3 Total Dose Time Histories

An additional check on the appropriateness of the HTF GoldSim Model as a surrogate for the fully three-dimensional HTF PORFLOW Model, is a comparison between total doses generated using PORFLOW and the HTF GoldSim Model. For the Base Case, the comparison between the PORFLOW and GoldSim results presented in Figures 7.1-10 through Figure 7.1-14 show that the HTF GoldSim Model approximates the general trends quite well.

Figure 7.1-10: Comparison between PORFLOW and GoldSim Total Dose Results for Case A, Sector A

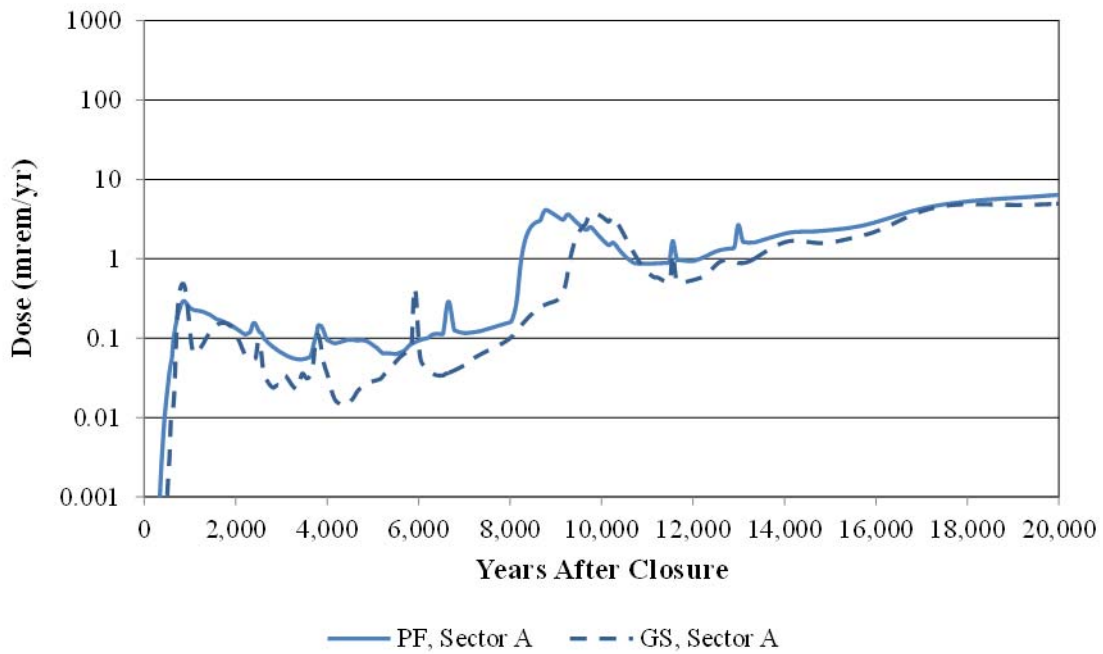


Figure 7.1-11: Comparison between PORFLOW and GoldSim Total Dose Results for Case A, Sector B

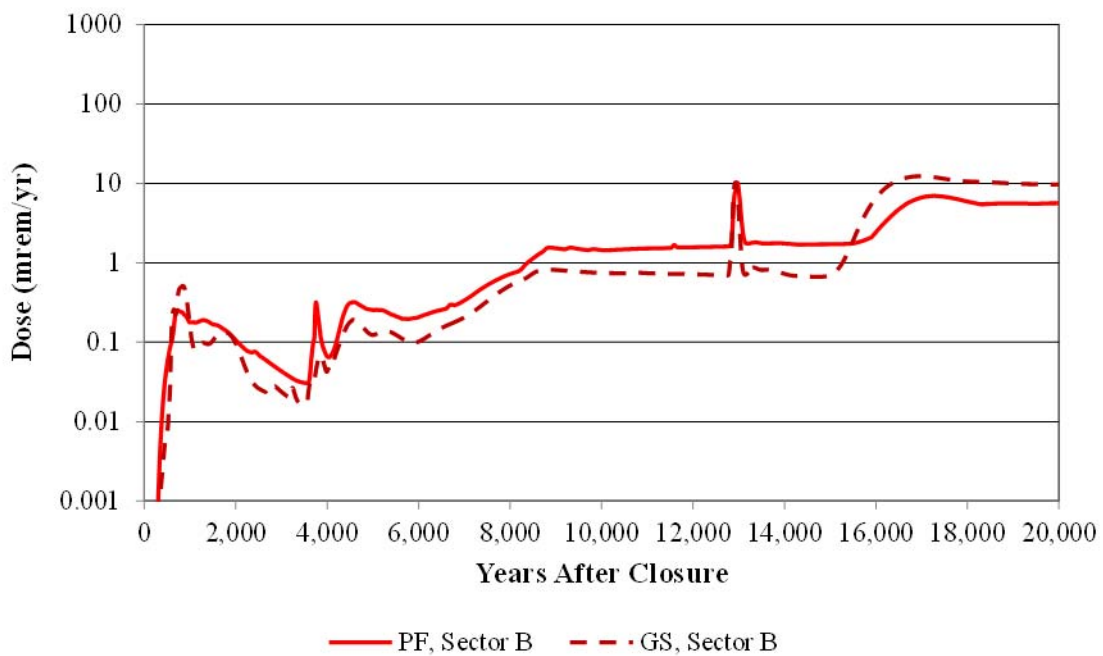


Figure 7.1-12: Comparison between PORFLOW and GoldSim Total Dose Results for Case A, Sector C

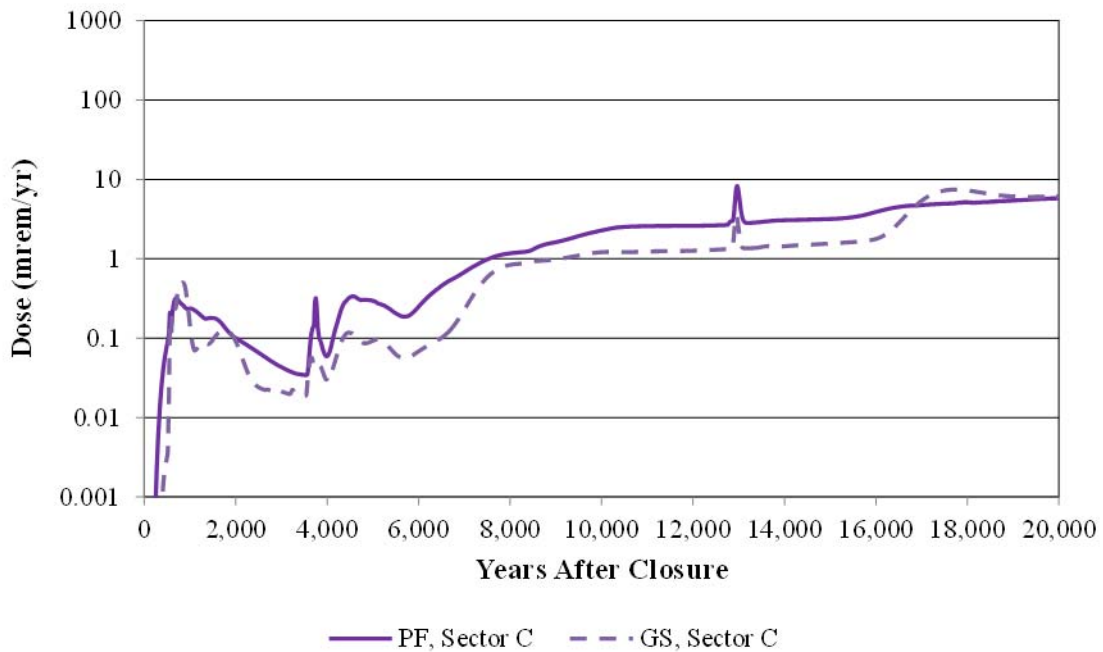


Figure 7.1-13: Comparison between PORFLOW and GoldSim Total Dose Results for Case A, Sector E

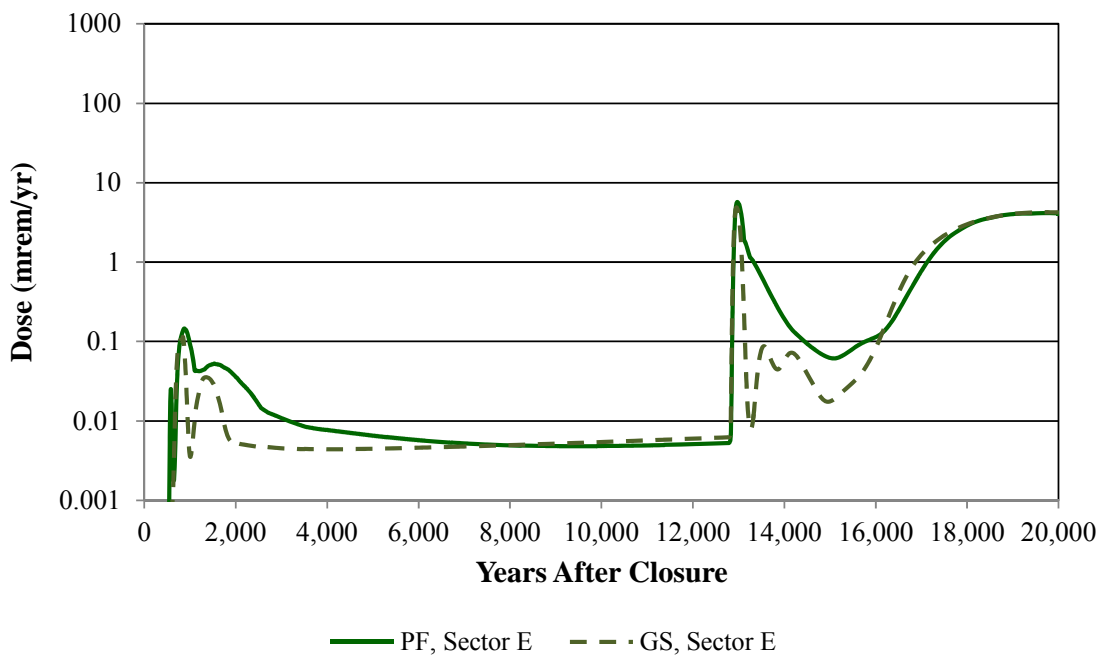
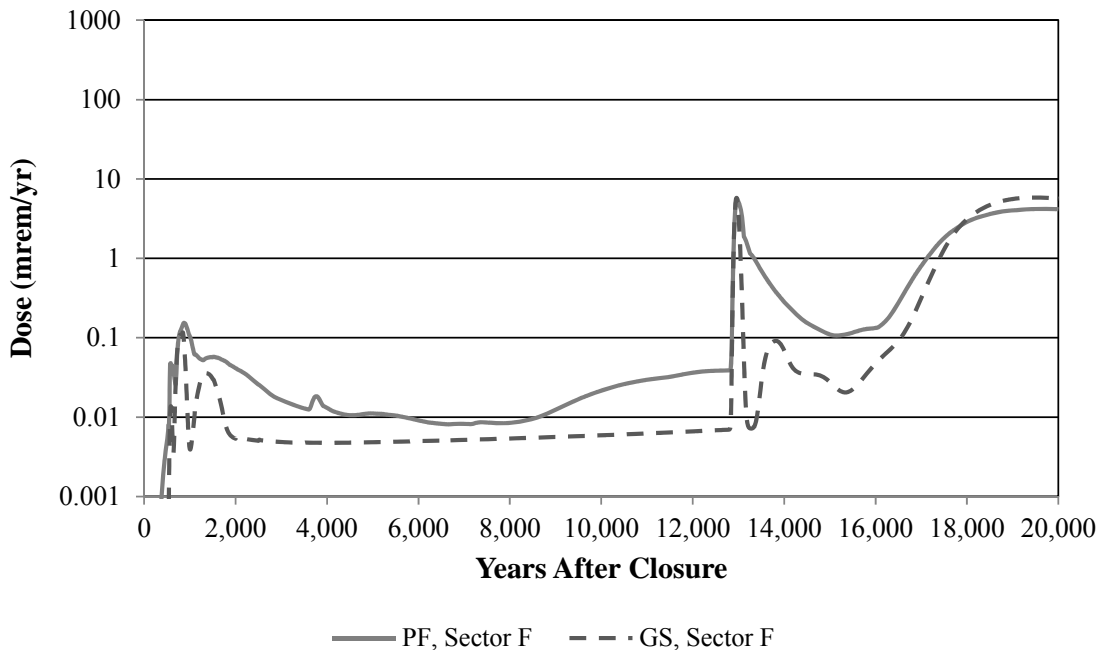


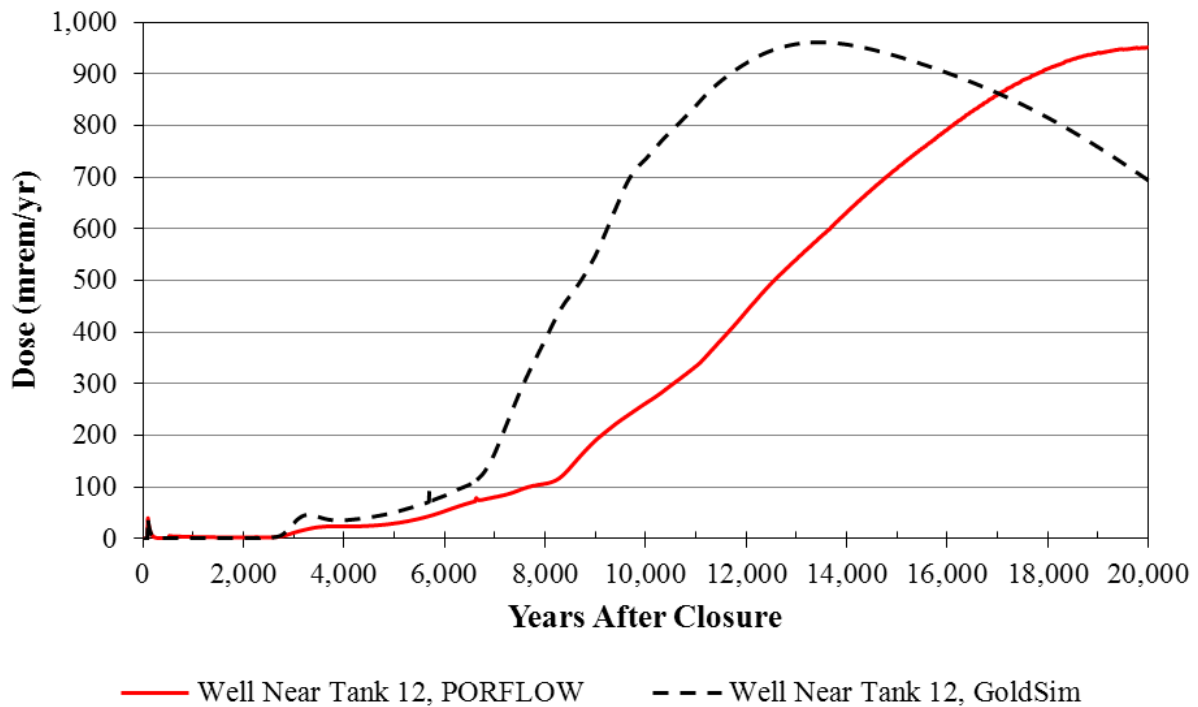
Figure 7.1-14: Comparison between PORFLOW and GoldSim Total Dose Results for Case A, Sector F



7.1.4 Inadvertent Human Intrusion Case

In addition, to 100-meter boundary results, PORFLOW provides 1-meter boundary results for use in the IHI case. The HTF GoldSim Model does not consider a 1-meter boundary but assumes that the intruder drills a well just outside of a waste tank. Based on PORFLOW results adjacent to specified waste tanks (see Section 3.1.1.6 and Table 3.1-9), showing a maximum IHI dose adjacent to Tank 12 (see Figure 3.1-6), the HTF GoldSim Model assumes that the well is drilled next to Tank 12. A comparison, between GoldSim and PORFLOW results for a well drilled next to Tank 12, presented in Figure 7.1-15, shows a peak 10,000-year dose of 735 mrem/yr at a well adjacent to Tank 12. This is about 2.8 times higher than the deterministic PORFLOW result (262 mrem/yr). Over a 20,000-year period, the GoldSim and PORFLOW results for the well drilled next to Tank 12 show a peak dose of 961 mrem/yr within 20,000 years for a well adjacent to Tank 12. This is just 1.7% more than the deterministic PORFLOW result (951 mrem/yr). Although the two models show very similar peak results, there is a large difference in breakthrough times. This large difference in breakthrough times is associated with the influence of horizontal flow in the HTF PORFLOW Model, which lengthens the pathway taken by radionuclides initialized in the annulus as they pass through the basemat into the UZ.

Figure 7.1-15: Comparison between PORFLOW and GoldSim Inadvertent Human Intrusion Results



8.0 REFERENCES

B-SQP-C-00003, *Software Quality Assurance Plan for ReadFlowFields.dll for the Savannah River Site's Liquid Waste Program*, Savannah River Site, Aiken, SC, Rev. 0, July 2012.

GTG-2010d, (Copyright), *GoldSim Contaminant Transport Module User's Guide, Version 5.1*, GoldSim Technology Group LLC, Issaquah, WA, December 2010.

GTG-2010e (Copyright), *User's Guide GoldSim Contaminant Transport Module*, GoldSim Technology Group, Issaquah, WA, Version 6.0, December 2010.

IAEA-472, (Copyright), *Handbook of Parameter Values for the Prediction of Radionuclide Transfer in Terrestrial and Freshwater Environments, Technical Reports Series No. 472*, International Atomic Energy Agency, Vienna, January 2010.

ML121170309, *Technical Evaluation Report For the Revised Performance Assessment for the Saltstone Disposal Facility at the Savannah River Site, South Carolina Final Report*, U.S. Nuclear Regulatory Commission, Washington, DC, Rev. 0, April 2012.

PNNL-13421, Staven, L.H., et al., *A Compendium of Transfer Factors for Agricultural and Animal Products*, Pacific Northwest National Laboratory, Richland, WA, Rev. 0, June 2003.

SRNL-STI-2009-00473, Kaplan, D.I., *Geochemical Data Package for Performance Assessment Calculations Related to the Savannah River Site*, Savannah River Site, Aiken, SC, Rev. 2, March 15, 2010.

SRNL-STI-2010-00148, Jones, et al., *Hydrogeologic Data Summary in Support of the H-Area Tank Farm Performance Assessment*, Savannah River Site, Aiken, SC, Rev. 0, February 2010.

SRNL-STI-2010-00447, Jannik, G.T., et al., *Land and Water Use Characteristics and Human Health Input Parameters for use in Environmental Dosimetry and Risk Assessments at the Savannah River Site*, Savannah River Site, Aiken, SC, Rev. 0, August 6, 2010.

SRNL-STI-2010-00493, Seaman, J.C., and Kaplan, D. I., *Chloride, Chromate, Silver, Thallium, and Uranium Sorption to SRS Soils, Sediments, and Cementitious Materials*, Savannah River Site, Aiken, SC, Rev. 0, September 29, 2010.

SRNL-STI-2010-00527, Powell, B.A., et al., *Iodine, Neptunium, Radium, and Strontium Sorption to Savannah River Site Sediments*, Savannah River Site, Aiken, SC, Rev. 0, September 2010.

SRNL-STI-2010-00667, Almond, P.M., and Kaplan, D.I., *Distribution Coefficients (K_d) Generated From A Core Sample Collected from the Saltstone Disposal Facility*, Savannah River Site, Aiken, SC, Rev. 0, April 2011.

SRNL-STI-2011-00011, Kaplan, D.I., *Estimated Neptunium Sediment Sorption Values as a Function of pH and Measured Barium and Radium K_d Values*, Savannah River Site, Aiken, SC, Rev. 0, January 13, 2011.

SRNL-STI-2011-00551, Stefanko, D.B., and Langton, C.A., *Tanks 18 and 19-F Structural Flowable Grout Fill Material Evaluation and Recommendations*, Savannah River Site, Aiken, SC, Rev. 0, September 2011.

SRNL-STI-2011-00672, Almond, P.M., et al., *Variability of K_d Values in Cementitious Materials and Sediments*, Savannah River Site, Aiken, SC, Rev. 0, January 2012.

SRNL-STI-2012-00404, Denham, M.E., *Evolution of Chemical Conditions and Estimated Solubility Controls on Radionuclides in the Residual Waste Layer During Post-Closure Aging of High-Level Waste Tanks*, Savannah River Site, Aiken, SC, Rev. 0, August 2012.

SRR-CWDA-2010-00019, *H-Area Tank Farm Grout and Concrete Degradation Modeling Information*, Savannah River Site, Aiken, SC, Rev. 0, March 15, 2010.

SRR-CWDA-2010-00023, *H-Tank Farm Waste Tank Closure Inventory for Use in Performance Assessment Modeling*, Savannah River Site, Aiken, SC, Rev. 3, November 2010.

SRR-CWDA-2010-00093, *H-Area Tank Farm Stochastic Fate and Transport Model*, Savannah River Site, Aiken, SC, Rev. 1, November 2010.

SRR-CWDA-2010-00128, *Performance Assessment for the H-Tank Farm at the Savannah River Site*, Savannah River Site, Aiken, SC, Rev. 0, March 2011.

SRS-REG-2007-00002, *Performance Assessment for the F-Tank Farm at the Savannah River Site*, Savannah River Site, Aiken, SC, Rev. 1, March 31, 2010.

APPENDIX A

A.0 Purpose

The purpose of this appendix is to present the benchmarking comparisons between PORFLOW simulation runs and GoldSim deterministic simulation Runs for the base-case (Case A). Comparisons of PORFLOW release results from the vadose zone models (which includes the UZ where applicable) and equivalent GoldSim results are presented in Section A.1. Comparisons of HTF PORFLOW Model generated 100-meter species-specific dose contributions by Sector and equivalent GoldSim results are presented in Section A.2.

A.1 Benchmarking Stage One

The first stage of the GoldSim benchmarking effort consisted of a comparison of PORFLOW generated mass releases to the SZ (mol/yr) with GoldSim releases to the SZ. The benchmarking results for the Base Case (Case A) HTF simulations are presented below.

Figure A.1-1: Ra-226 Release from Tank 9 (Case A)

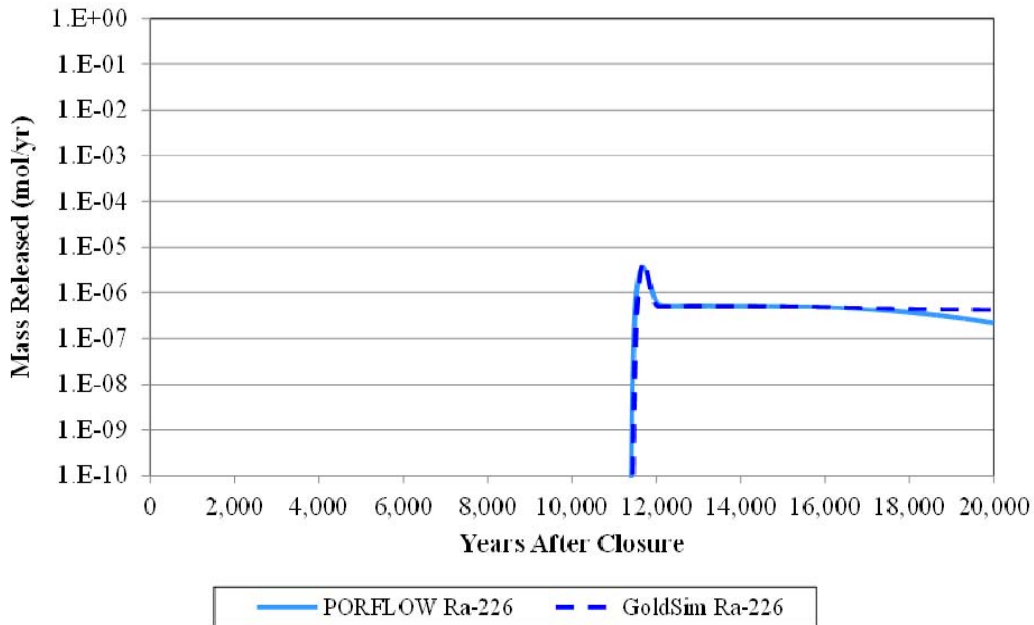


Figure A.1-2: Tc-99 Release from Tank 9 (Case A)

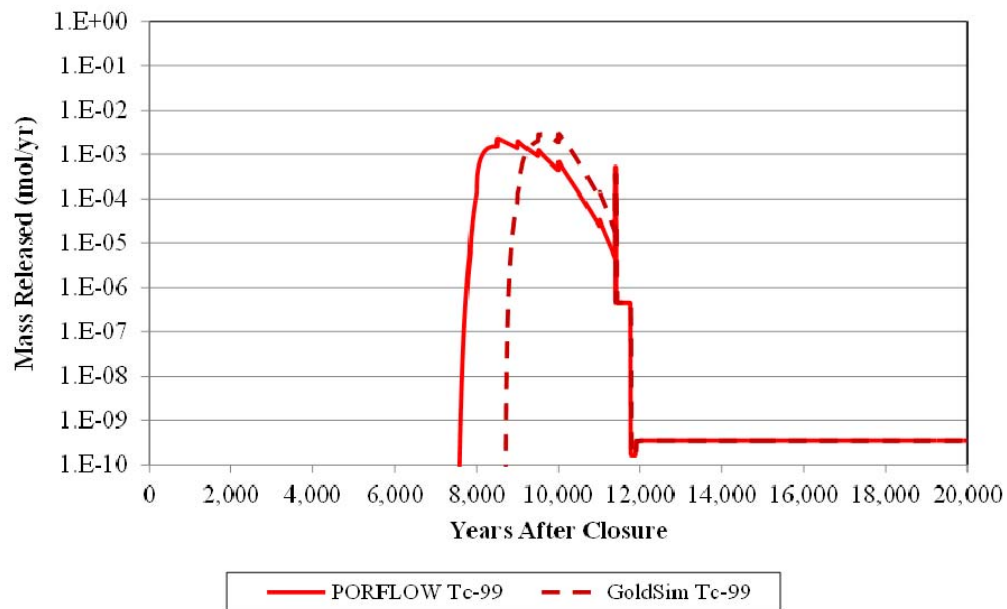


Figure A.1-3: I-129 Release from Tank 9 (Case A)

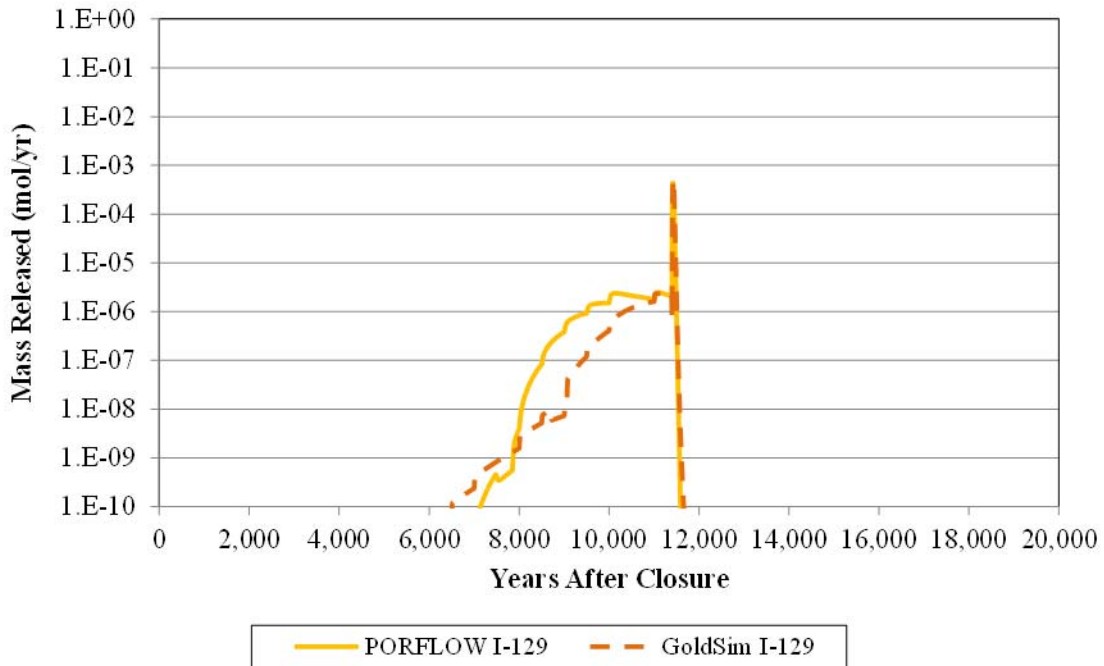


Figure A.1-4: Cs-135 Release from Tank 9 (Case A)

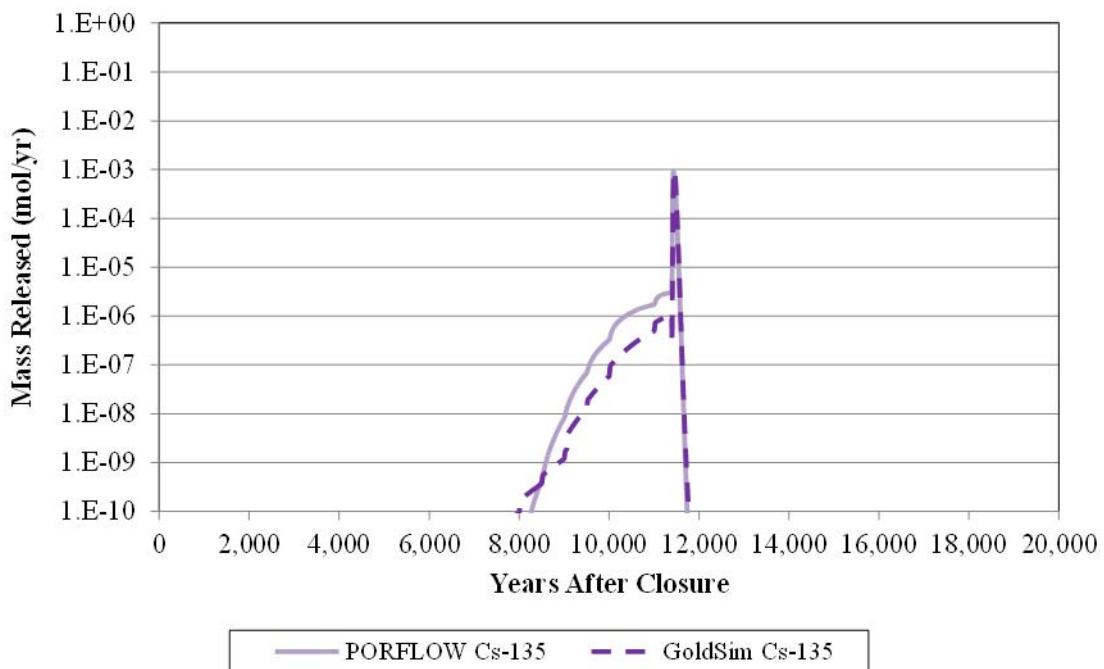


Figure A.1-5: Np-237 Release from Tank 9 (Case A)

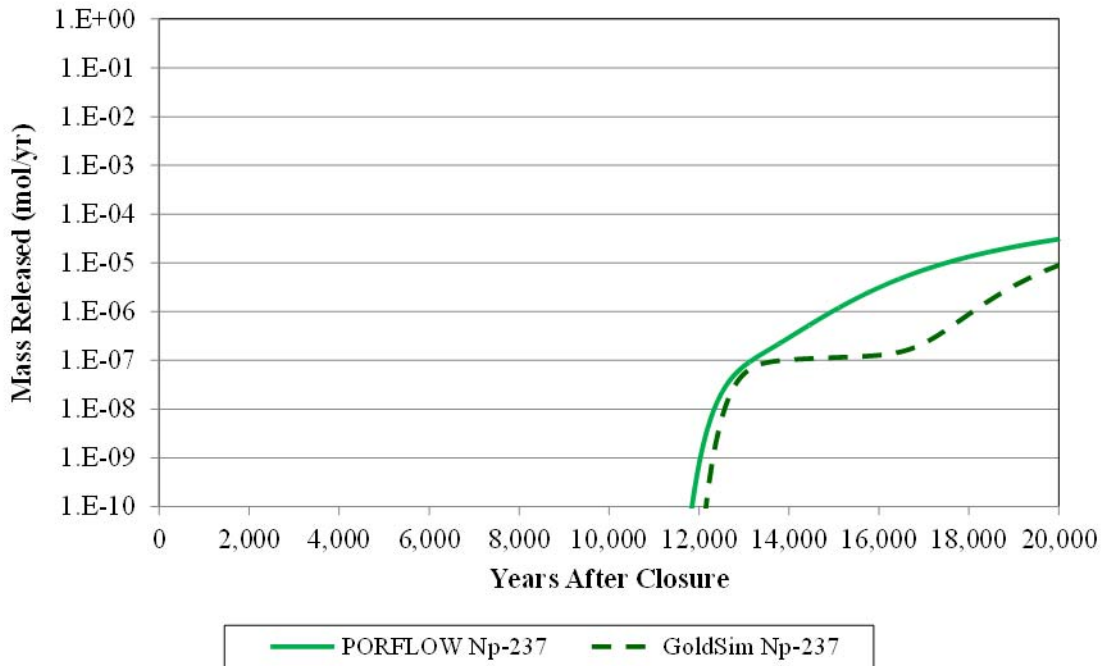


Figure A.1-6: Ra-226 Release from Tank 12 (Case A)

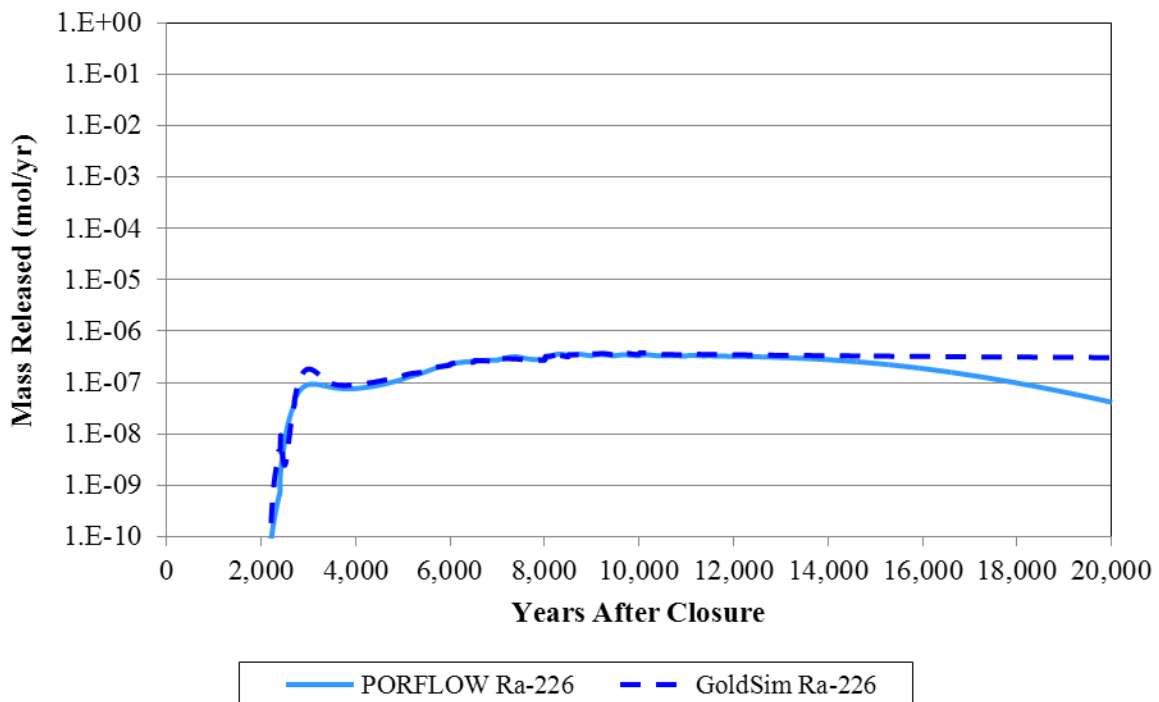


Figure A.1-7: Tc-99 Release from Tank 12 (Case A)

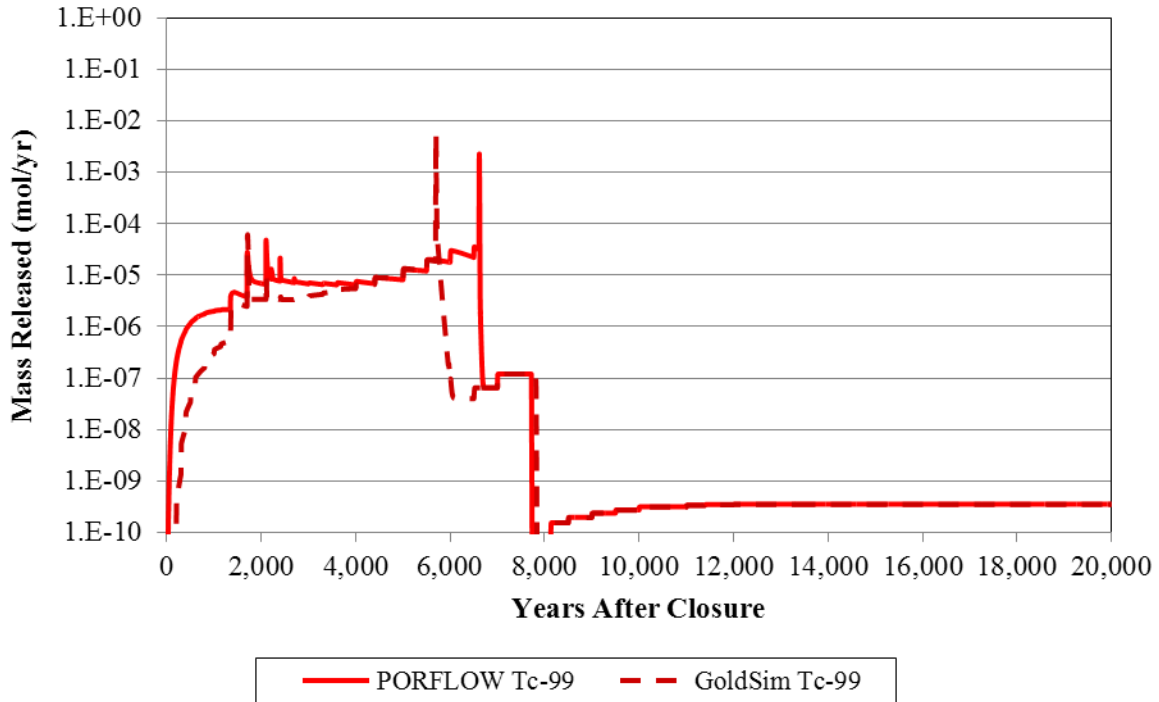


Figure A.1-8: I-129 Release from Tank 12 (Case A)

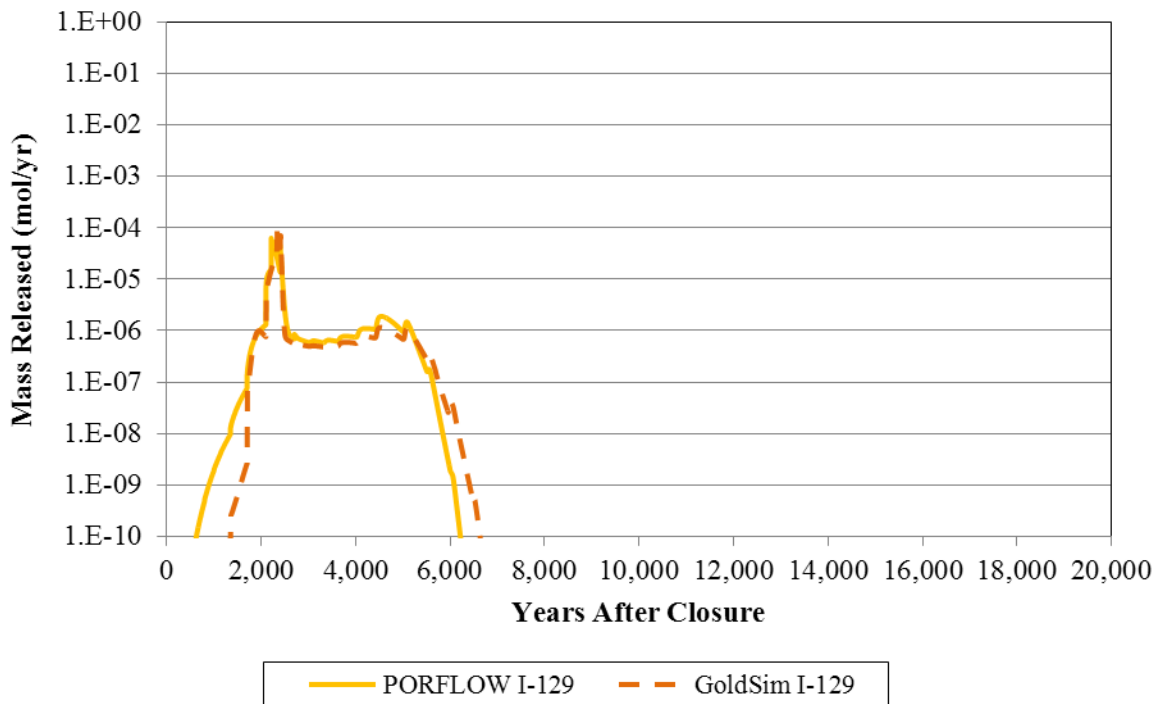


Figure A.1-9: Cs-135 Release from Tank 12 (Case A)

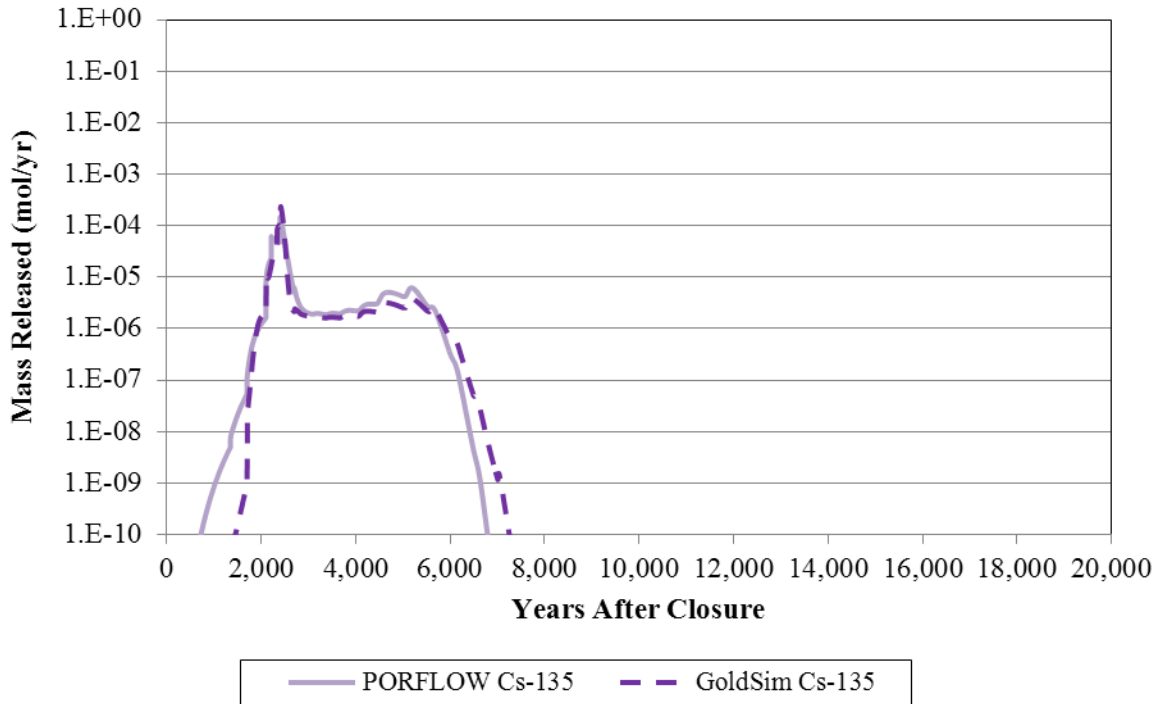


Figure A.1-10: Np-237 Release from Tank 12 (Case A)

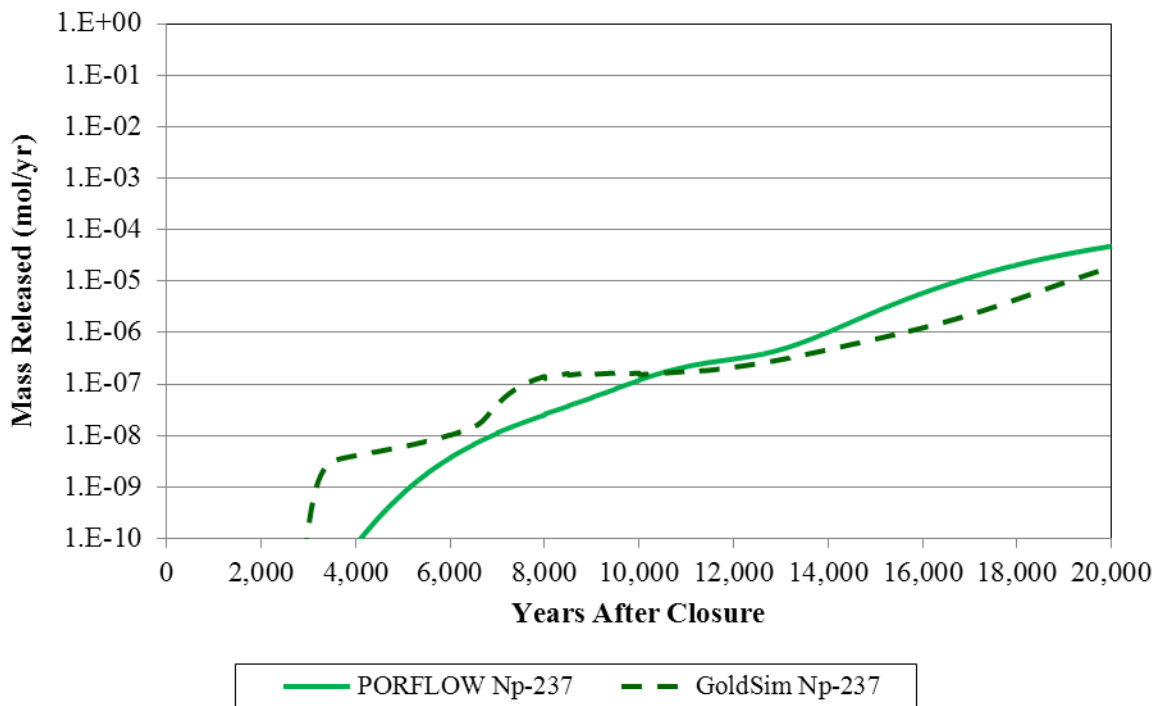


Figure A.1-11: Ra-226 Release from Tank 13 (Case A)

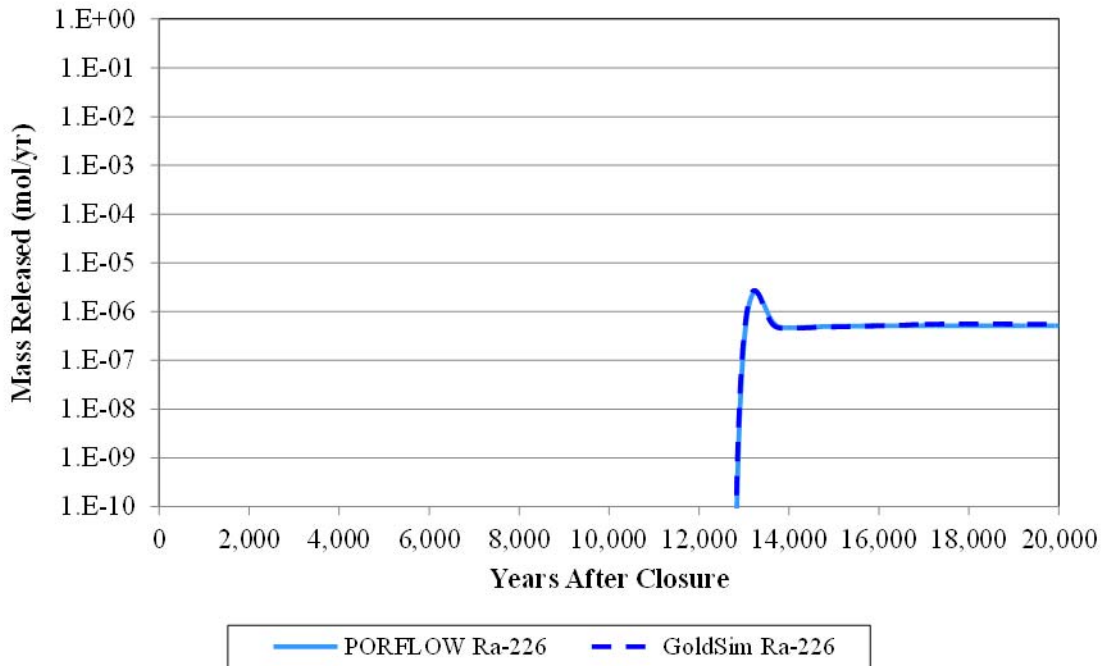


Figure A.1-12: Tc-99 Release from Tank 13 (Case A)

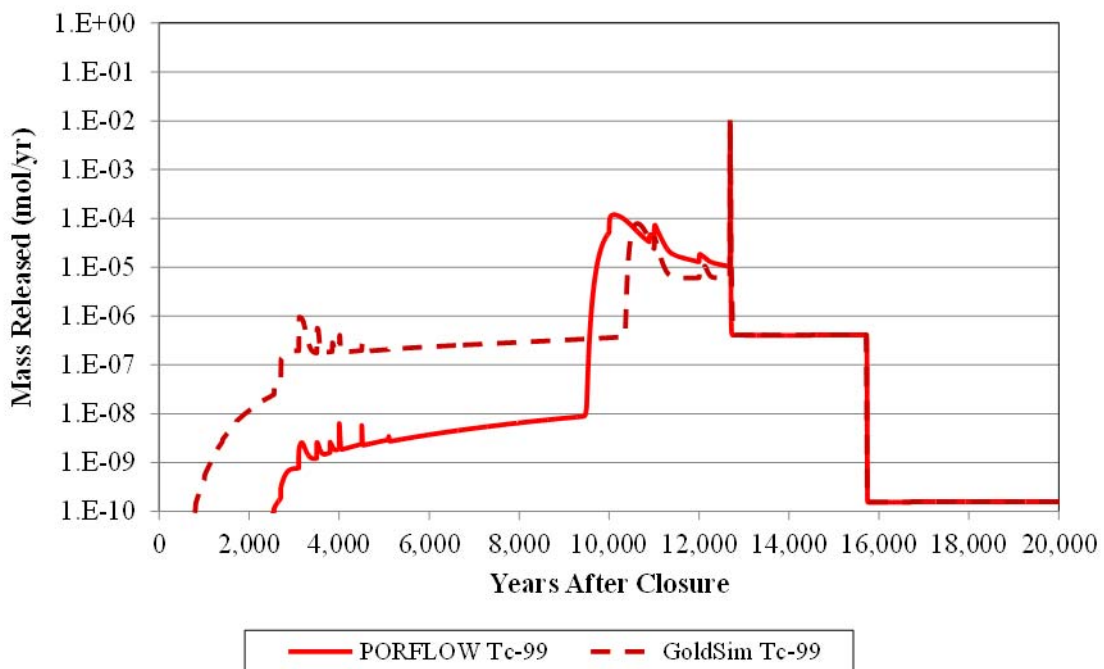


Figure A.1-13: I-129 Release from Tank 13 (Case A)

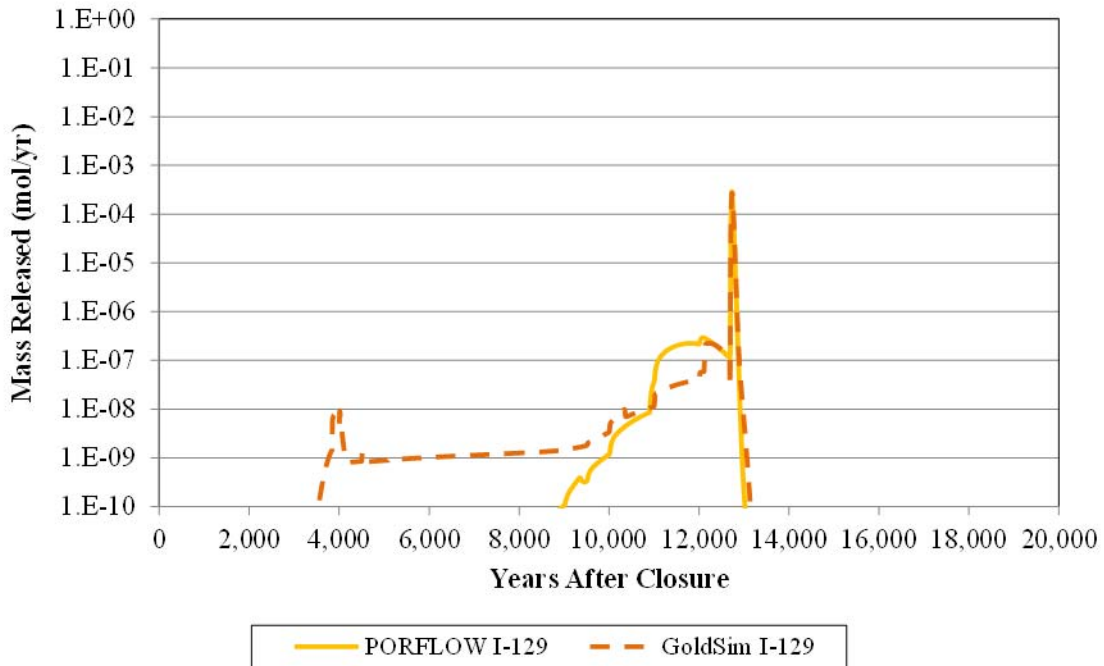


Figure A.1-14: Cs-135 Release from Tank 13 (Case A)

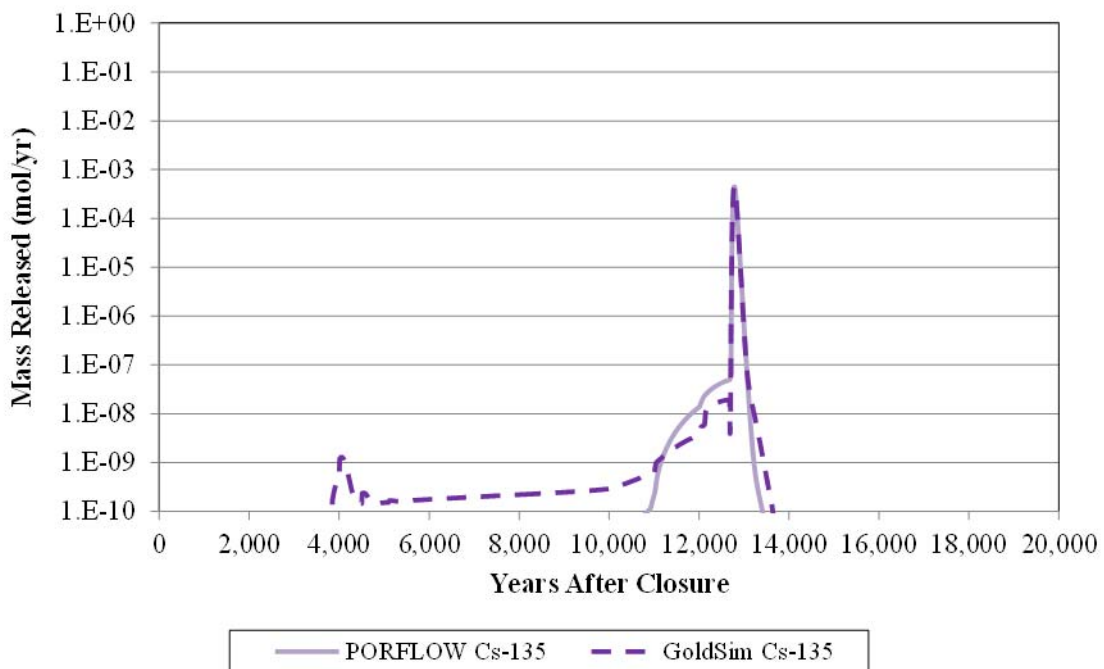


Figure A.1-15: Np-237 Release from Tank 13 (Case A)

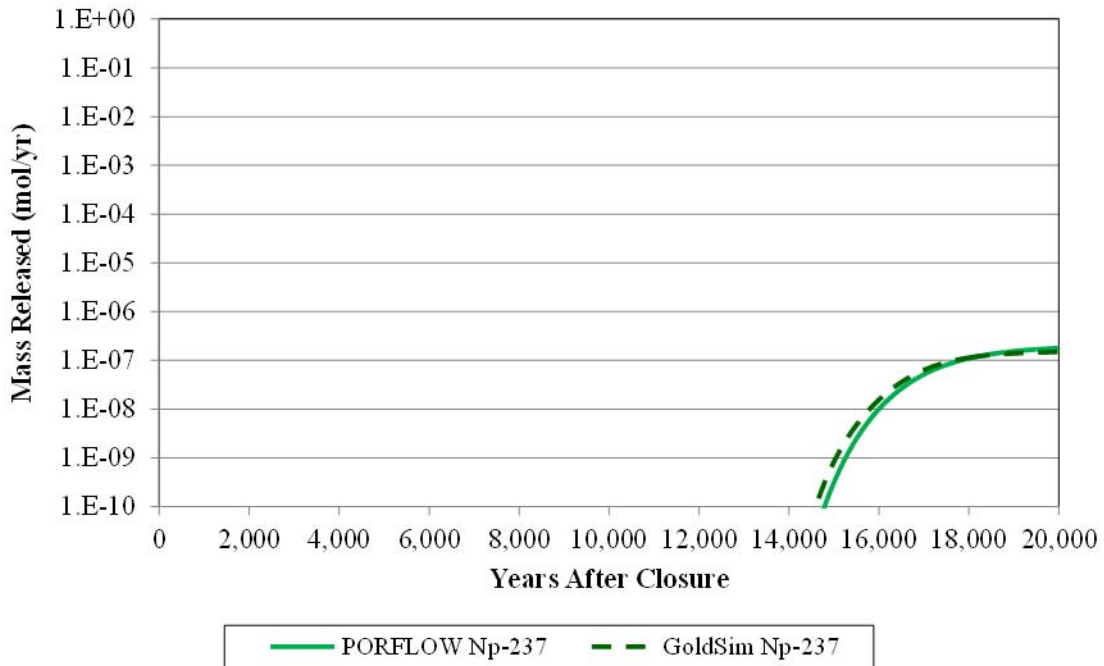


Figure A.1-16: Ra-226 Release from Tank 15 (Case A)

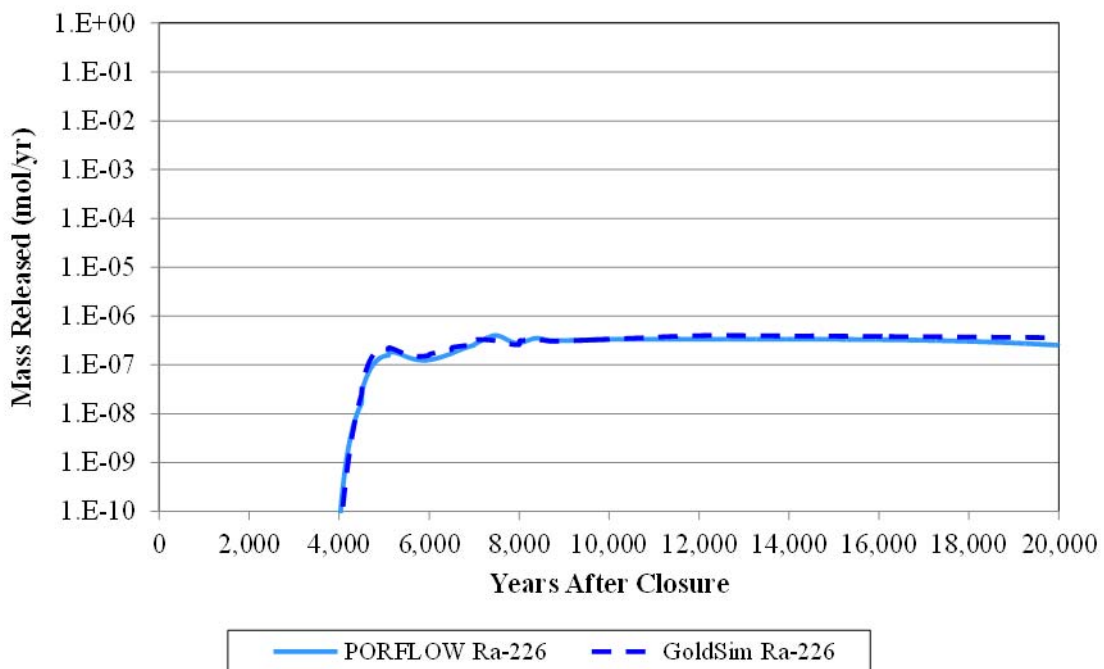


Figure A.1-17: Tc-99 Release from Tank 15 (Case A)

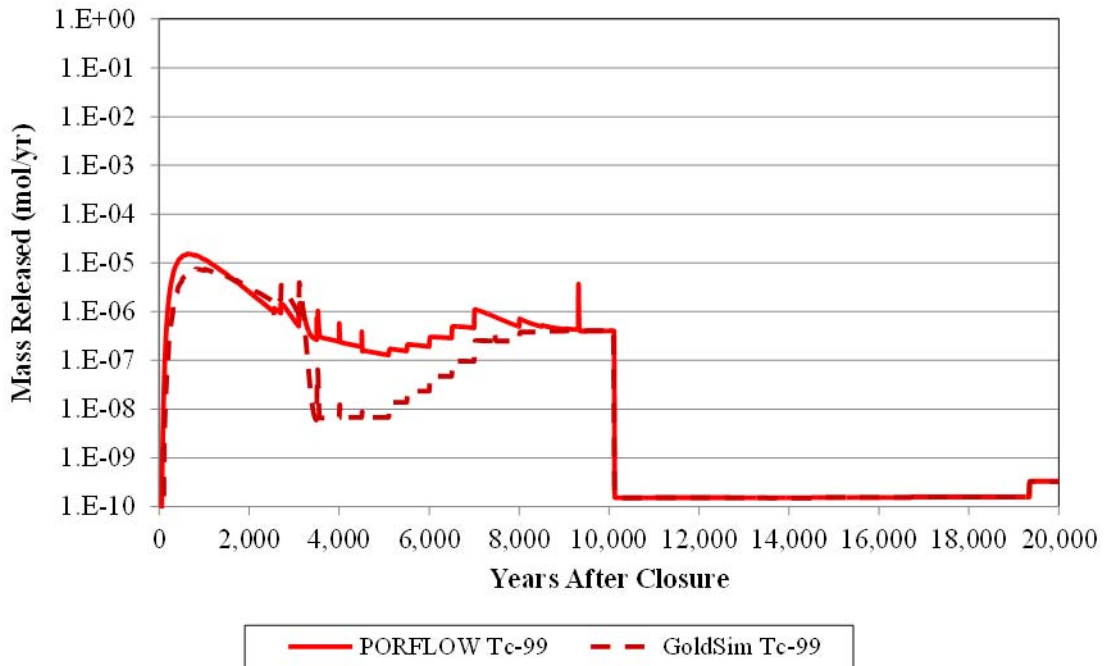


Figure A.1-18: I-129 Release from Tank 15 (Case A)

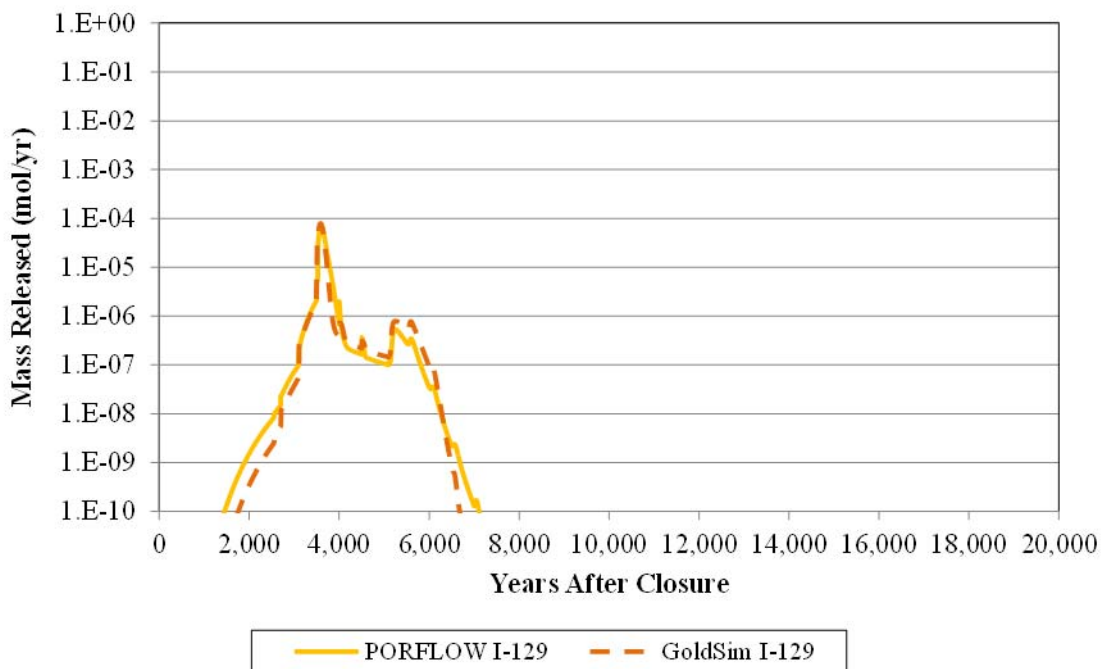


Figure A.1-19: Cs-135 Release from Tank 15 (Case A)

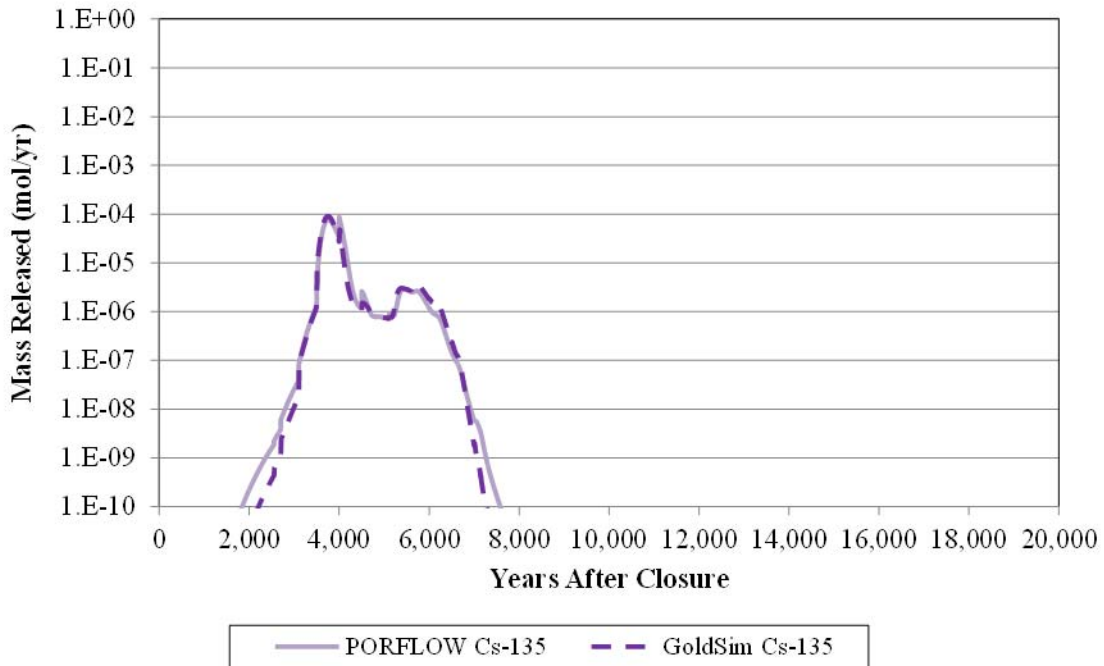


Figure A.1-20: Np-237 Release from Tank 15 (Case A)

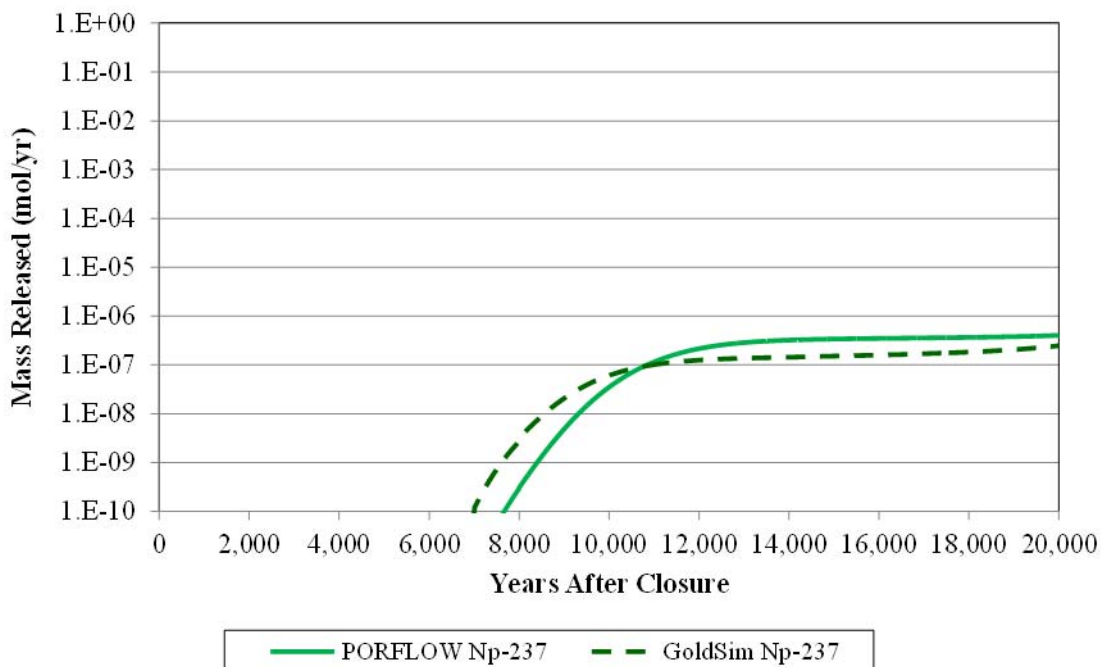


Figure A.1-21: Ra-226 Release from Tank 16 (Case A)

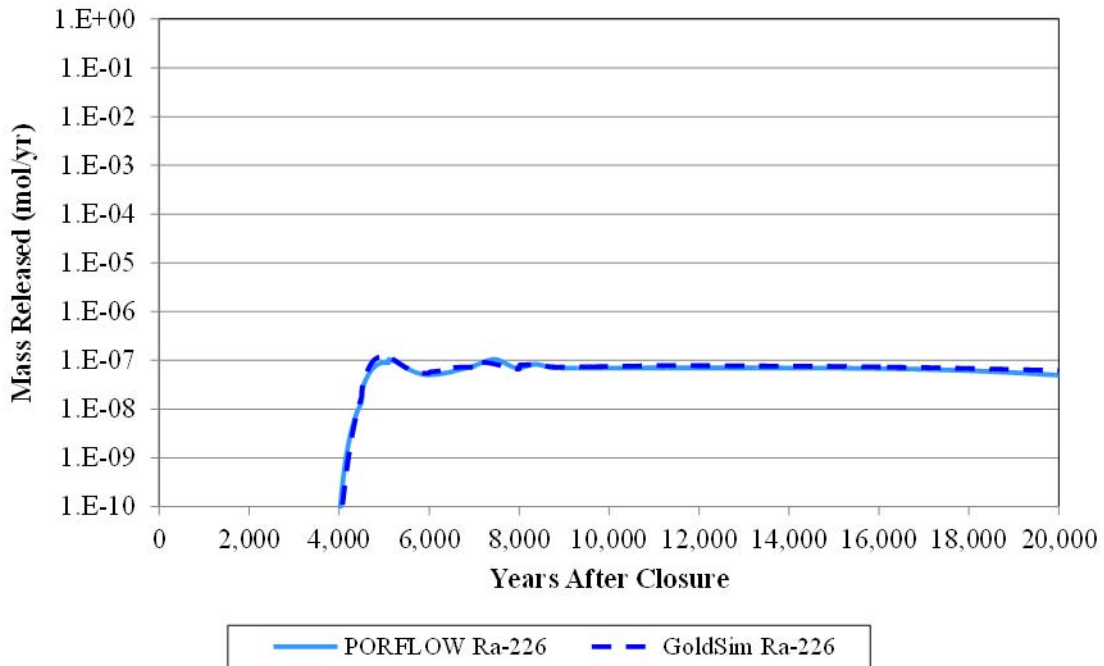


Figure A.1-22: Tc-99 Release from Tank 16 (Case A)

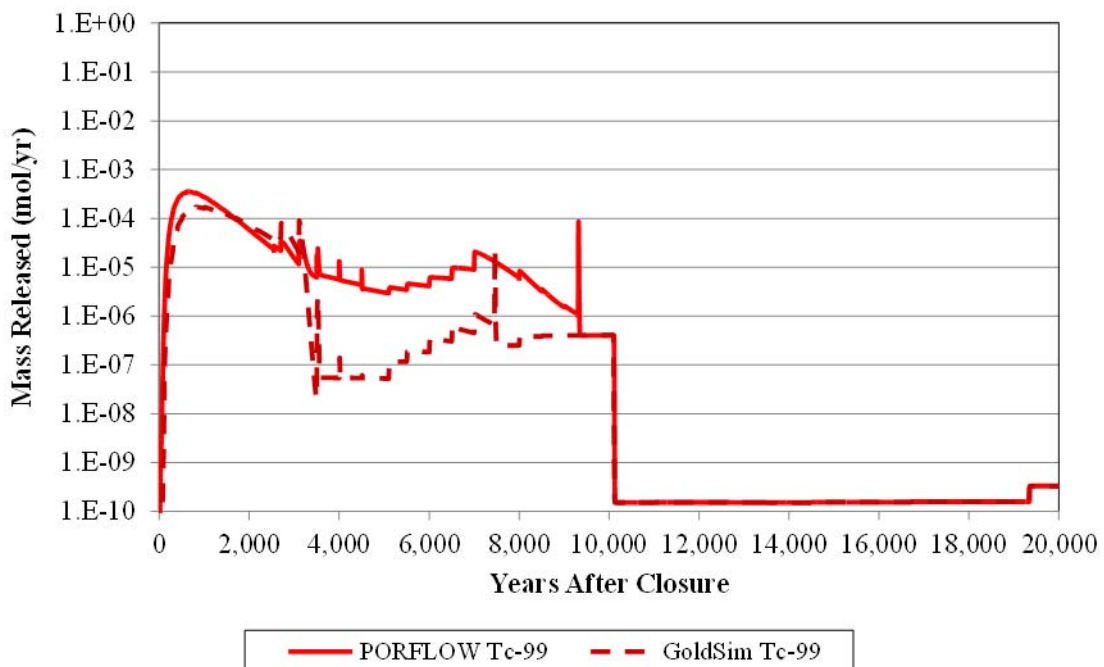


Figure A.1-23: I-129 Release from Tank 16 (Case A)

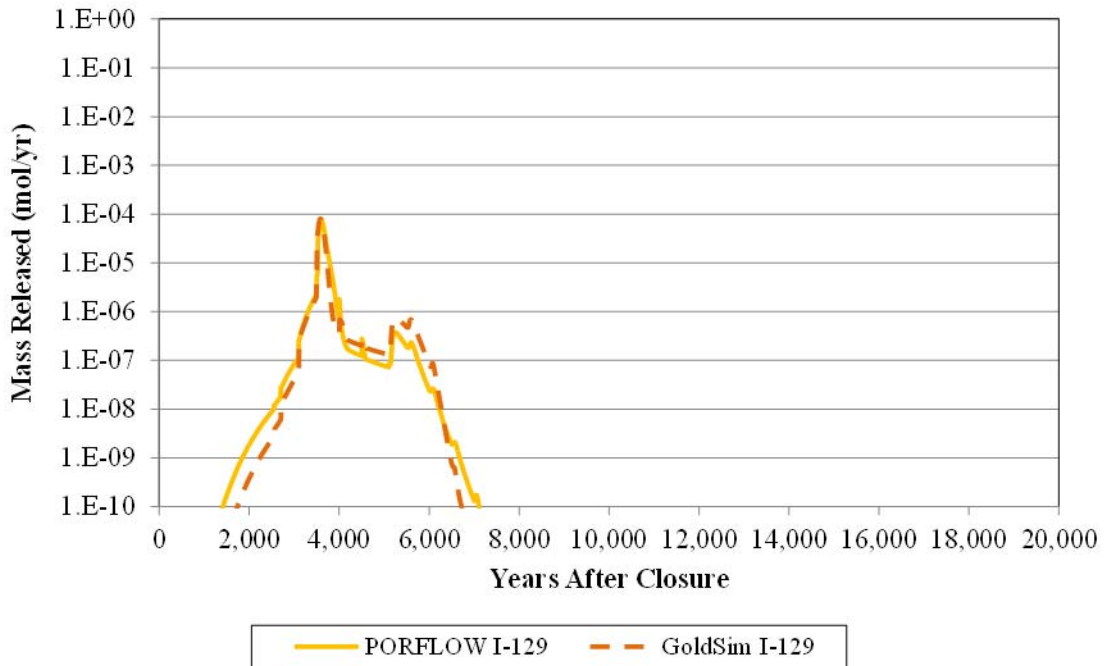


Figure A.1-24: Cs-135 Release from Tank 16 (Case A)

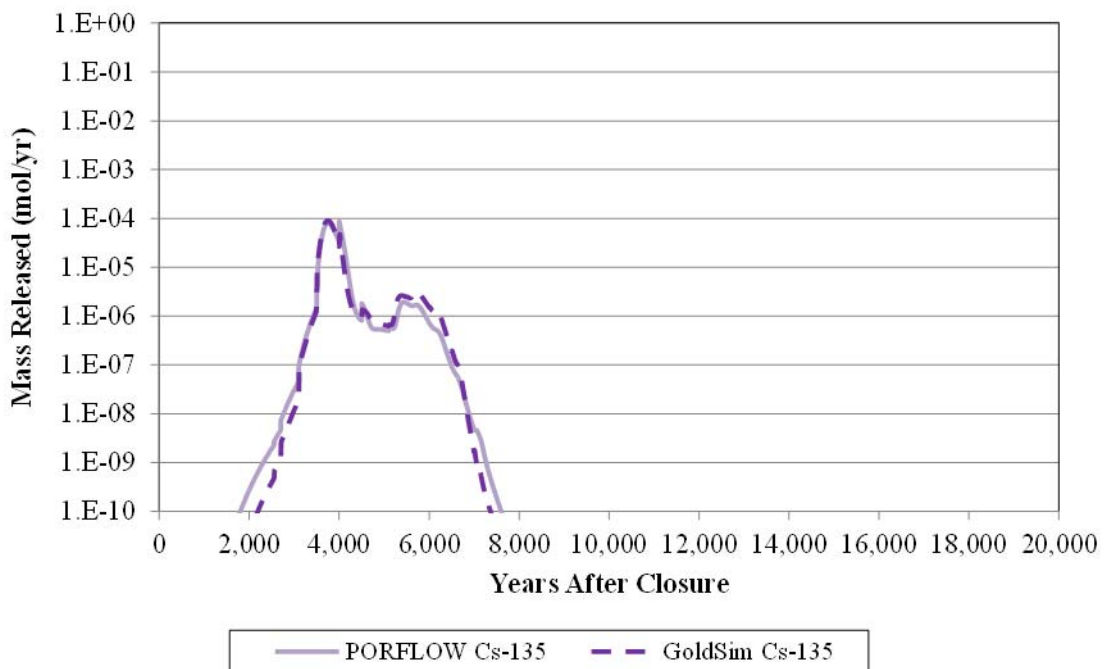


Figure A.1-25: Np-237 Release from Tank 16 (Case A)

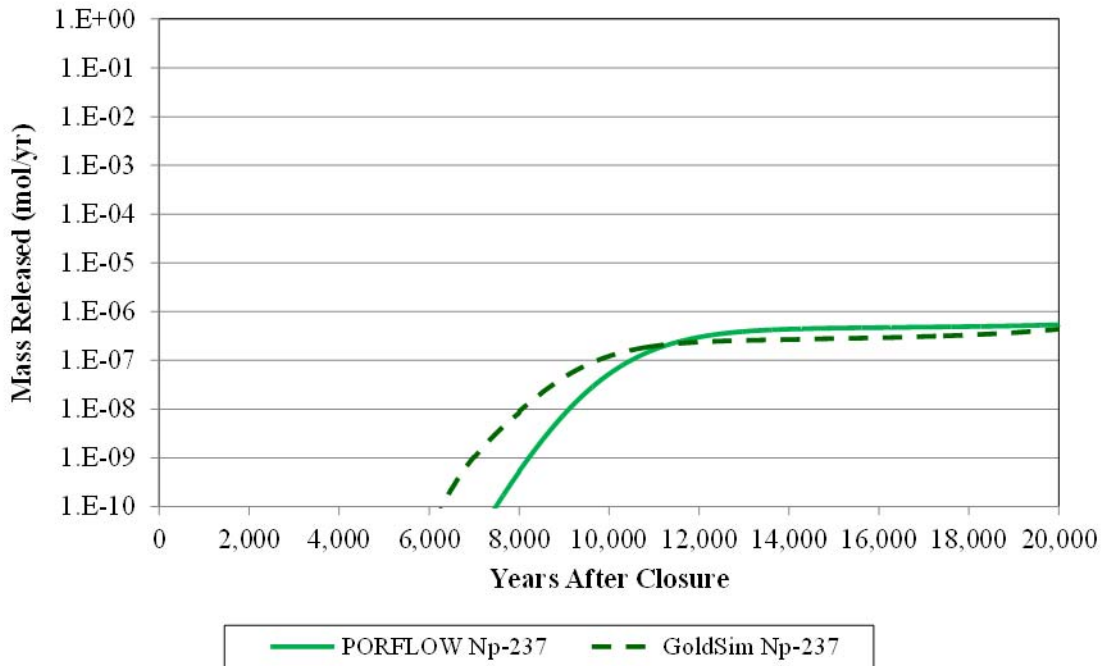


Figure A.1-26: Ra-226 Release from Tank 24 (Case A)

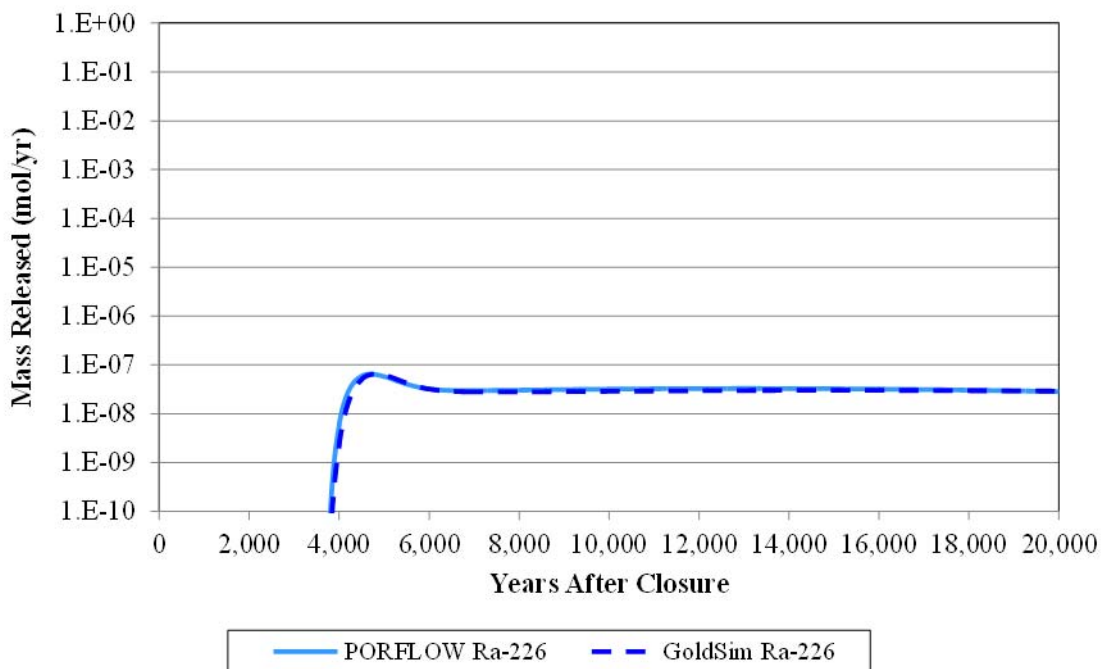


Figure A.1-27: Tc-99 Release from Tank 24 (Case A)

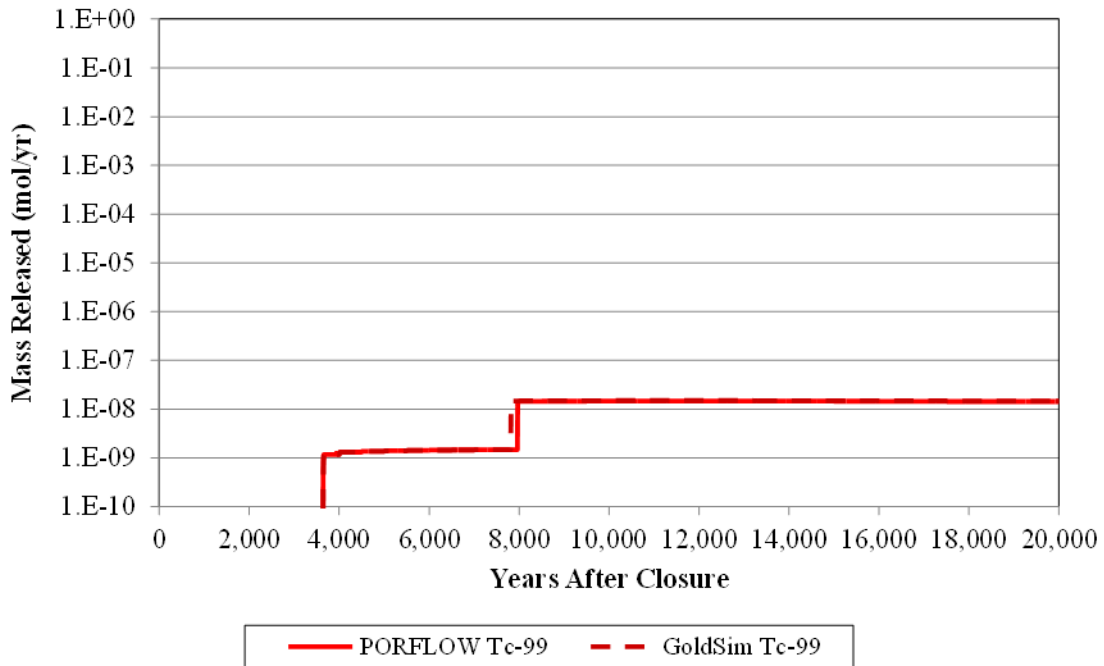


Figure A.1-28: I-129 Release from Tank 24 (Case A)

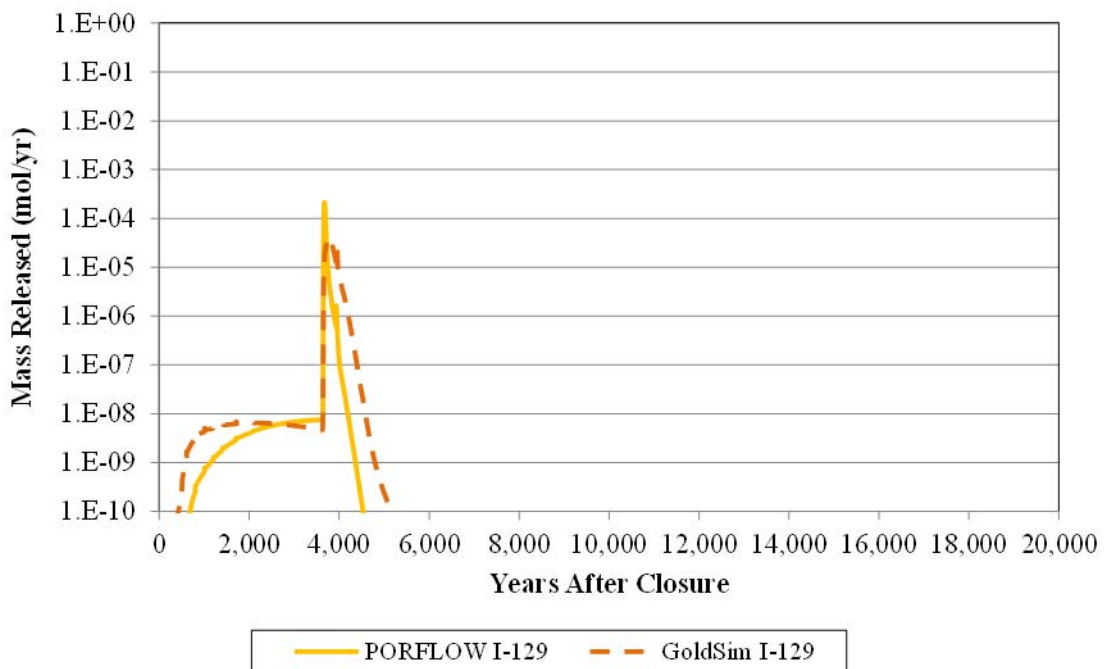


Figure A.1-29: Cs-135 Release from Tank 24 (Case A)

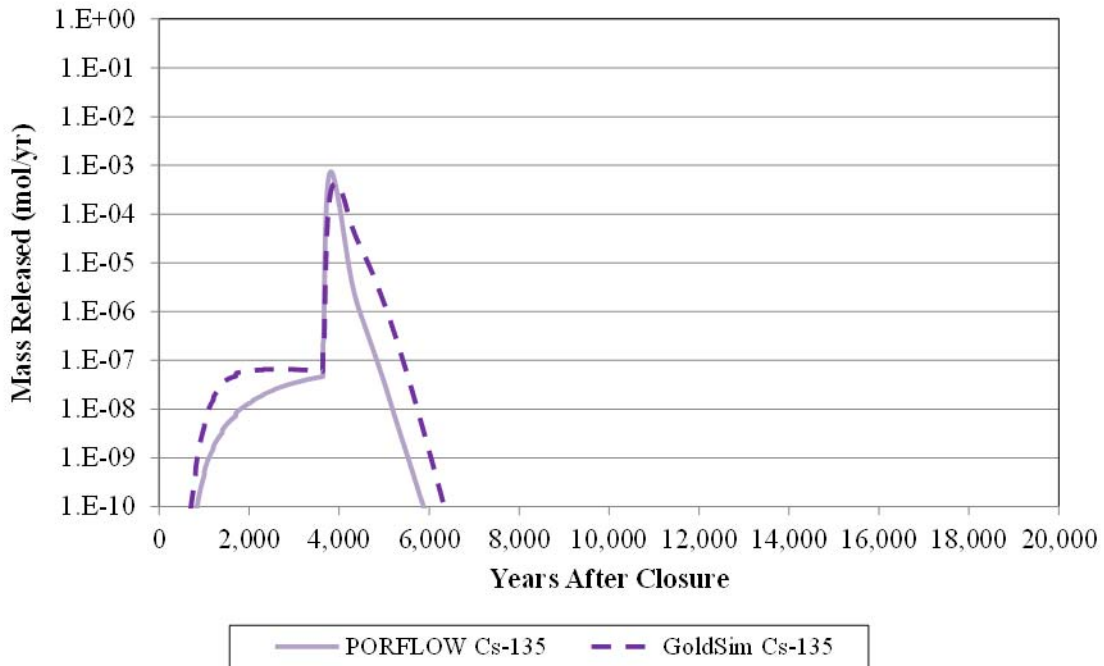


Figure A.1-30: Np-237 Release from Tank 24 (Case A)

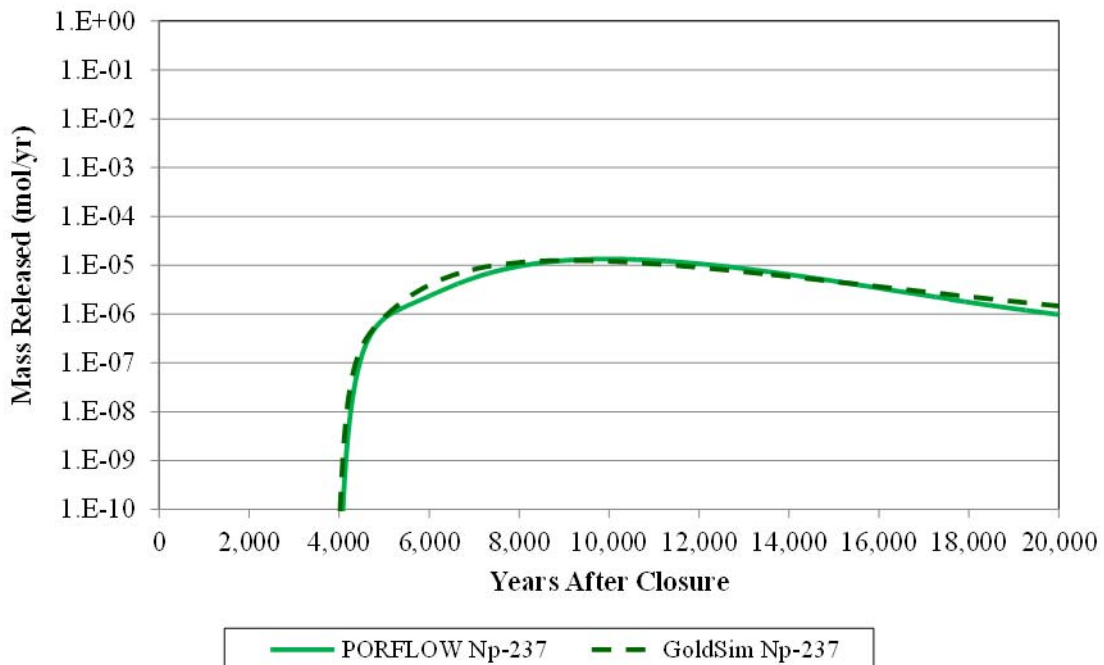


Figure A.1-31: Ra-226 Release from Tank 31 (Case A)

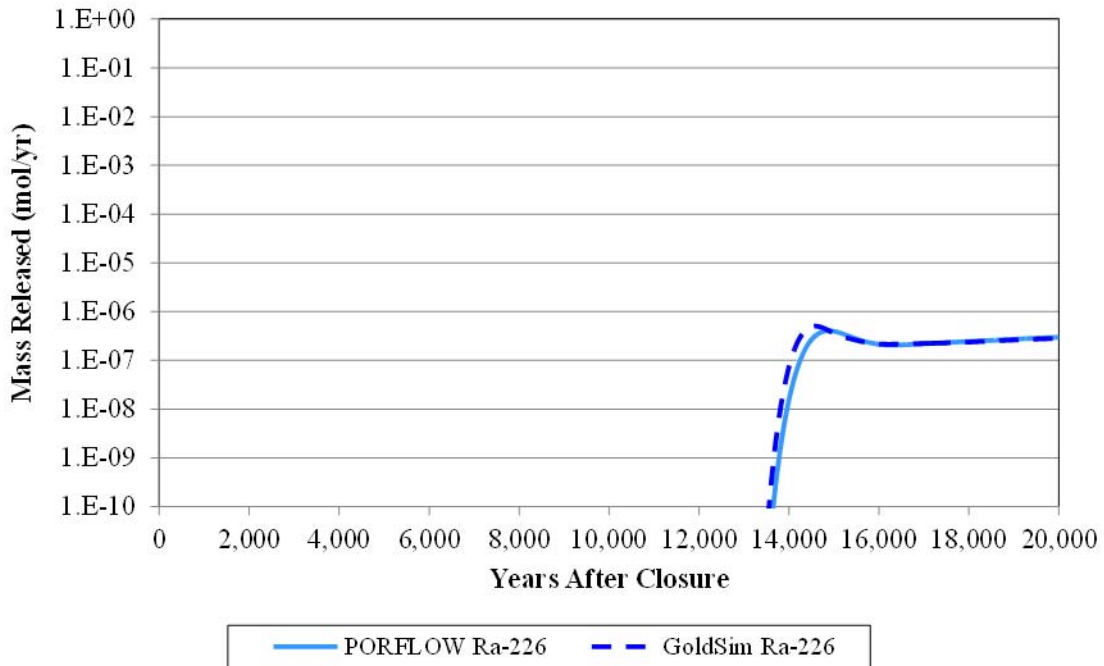


Figure A.1-32: Tc-99 Release from Tank 31 (Case A)

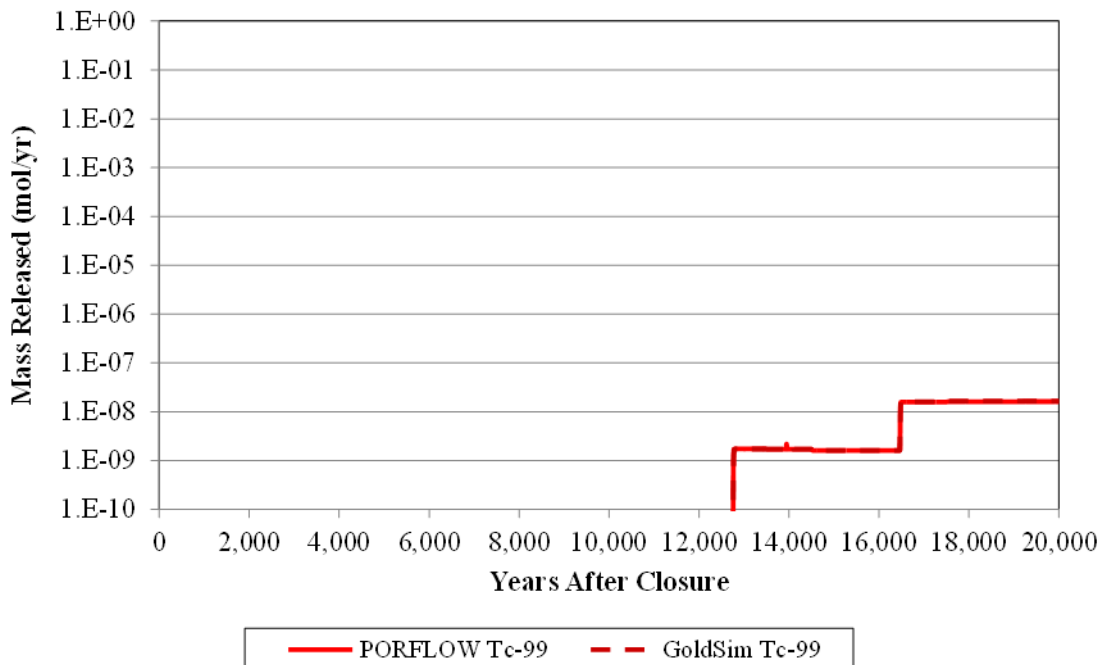


Figure A.1-33: I-129 Release from Tank 31 (Case A)

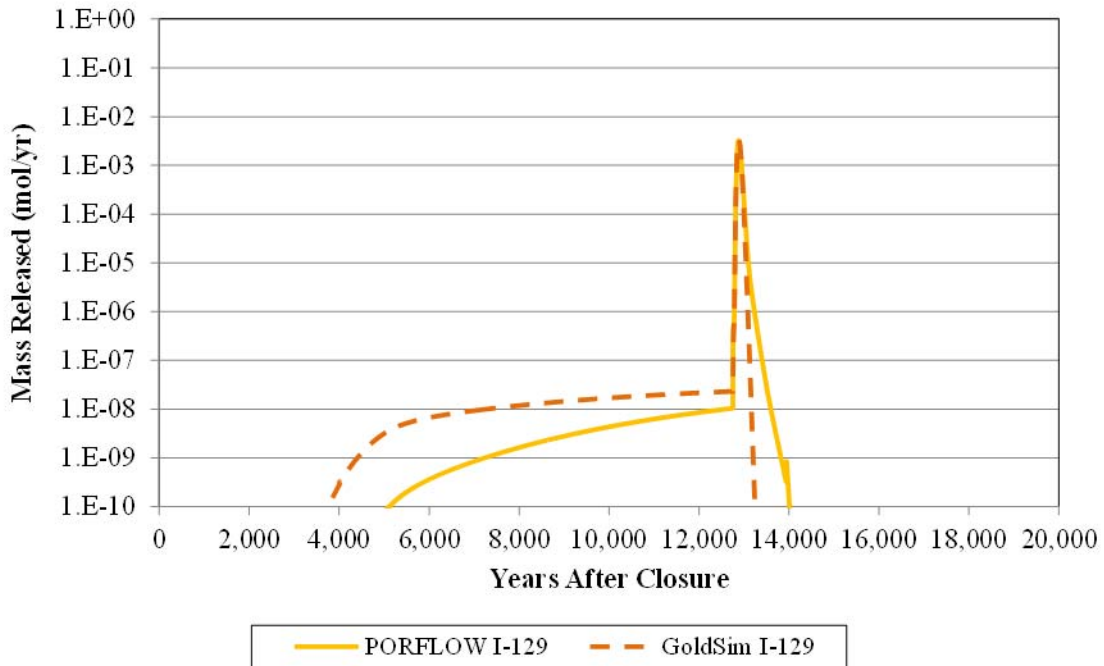


Figure A.1-34: Cs-135 Release from Tank 31 (Case A)

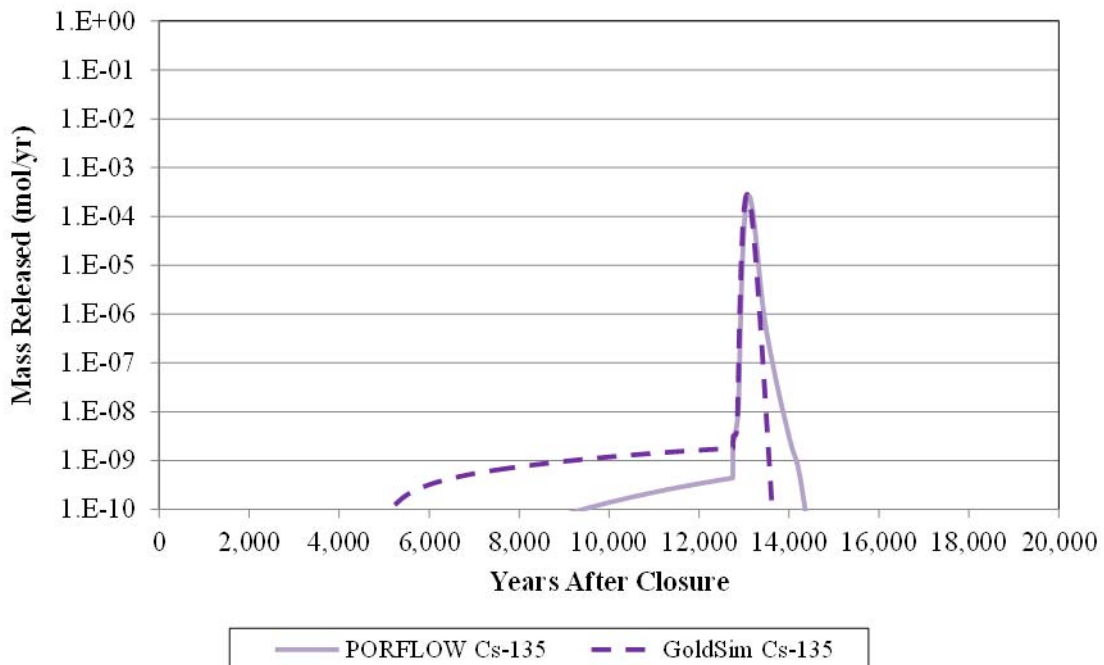


Figure A.1-35: Np-237 Release from Tank 31 (Case A)

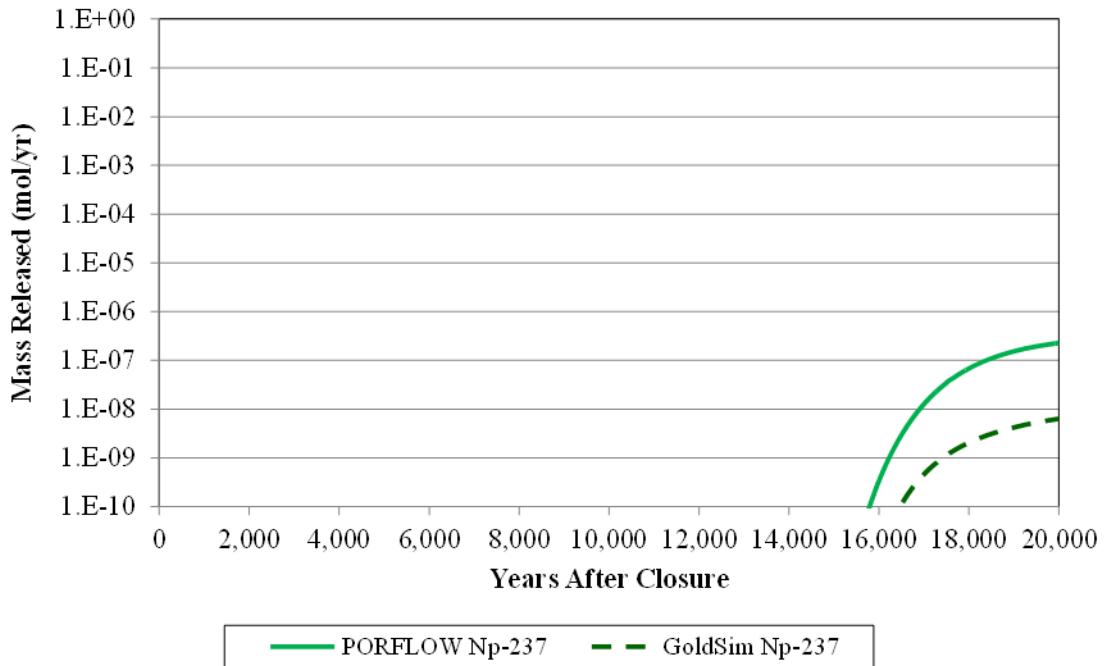


Figure A.1-36: Ra-226 Release from Tank 36 (Case A)

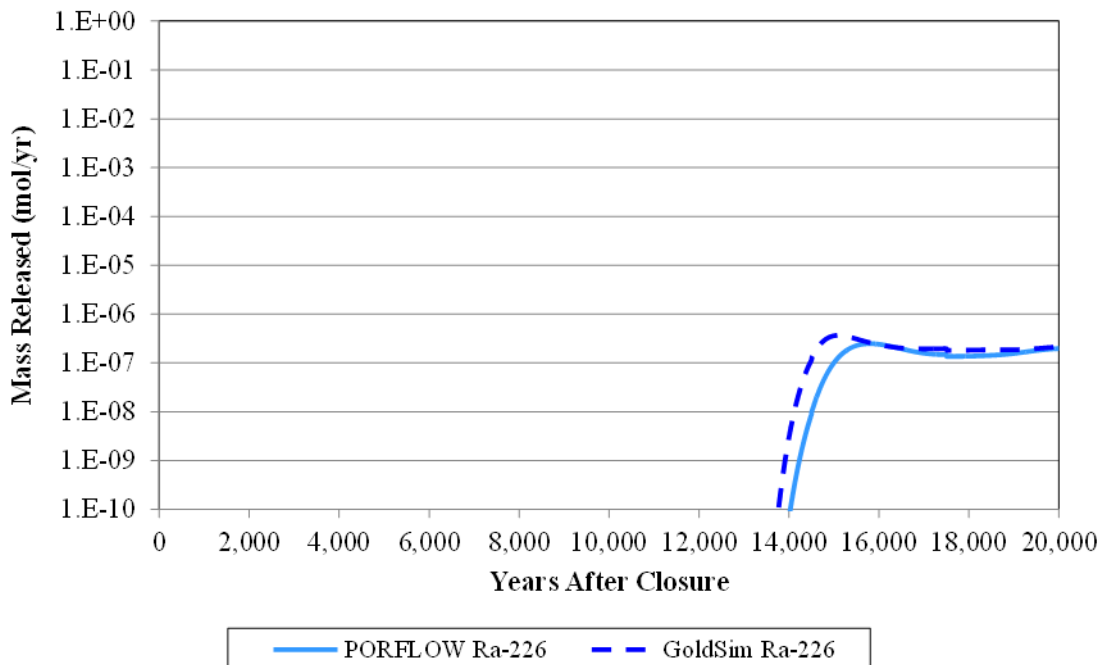


Figure A.1-37: Tc-99 Release from Tank 36 (Case A)

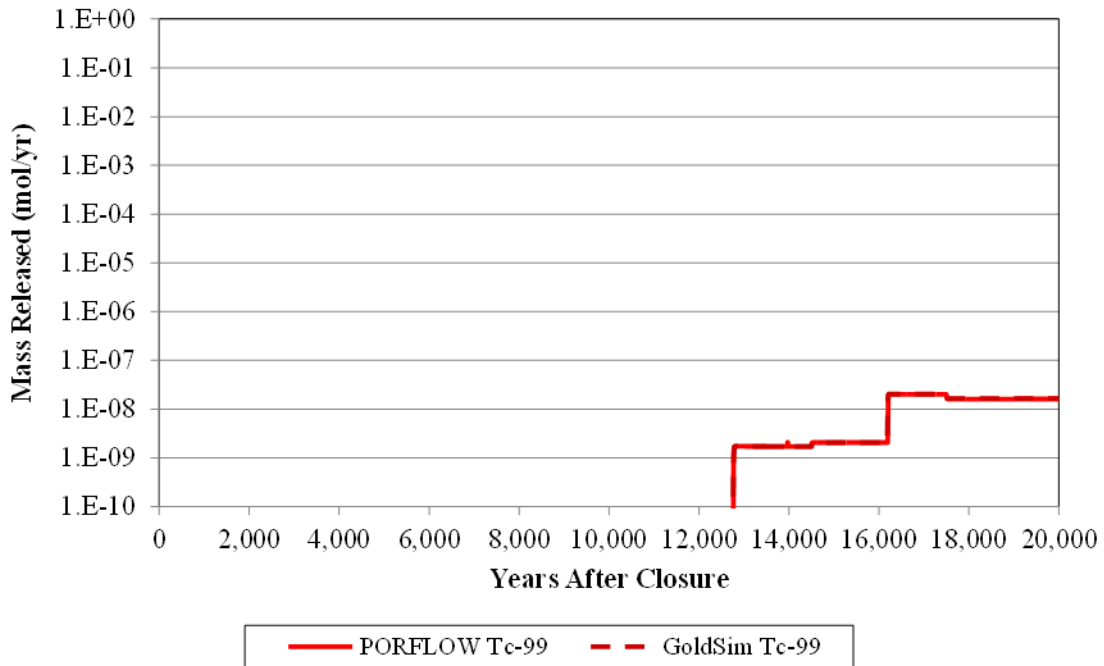


Figure A.1-38: I-129 Release from Tank 36 (Case A)

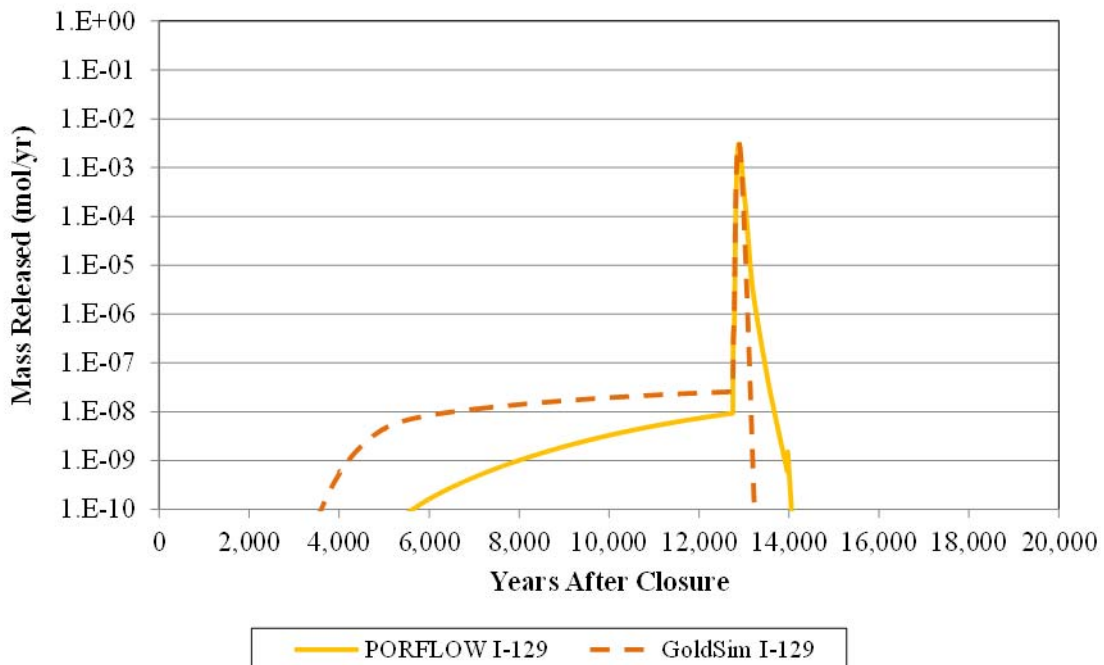


Figure A.1-39: Cs-135 Release from Tank 36 (Case A)

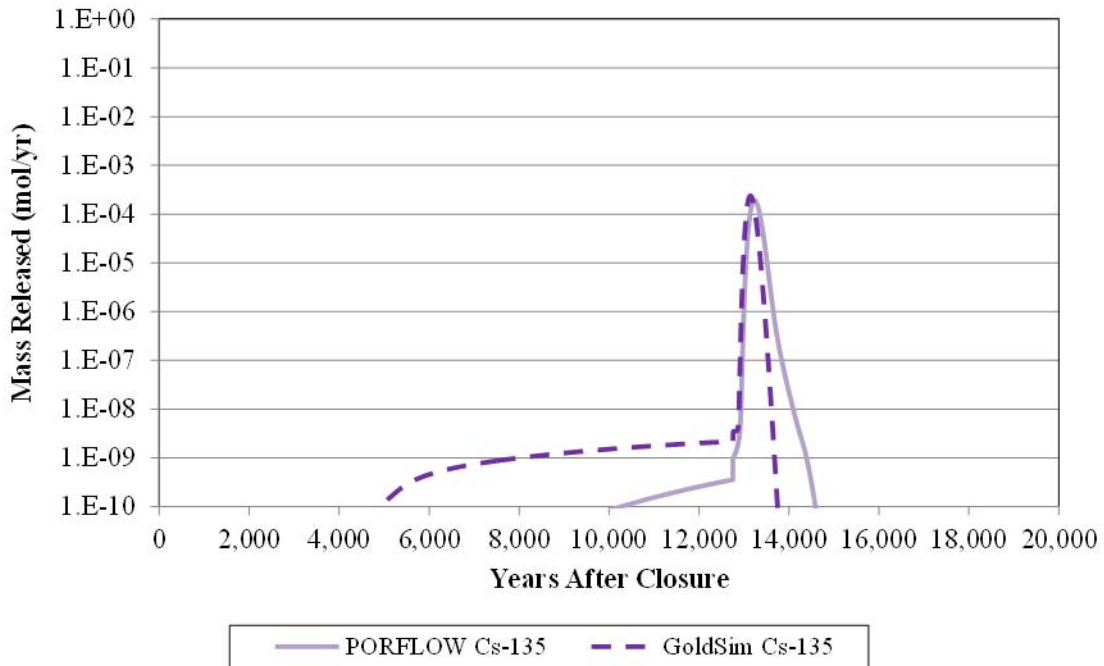


Figure A.1-40: Np-237 Release from Tank 36 (Case A)

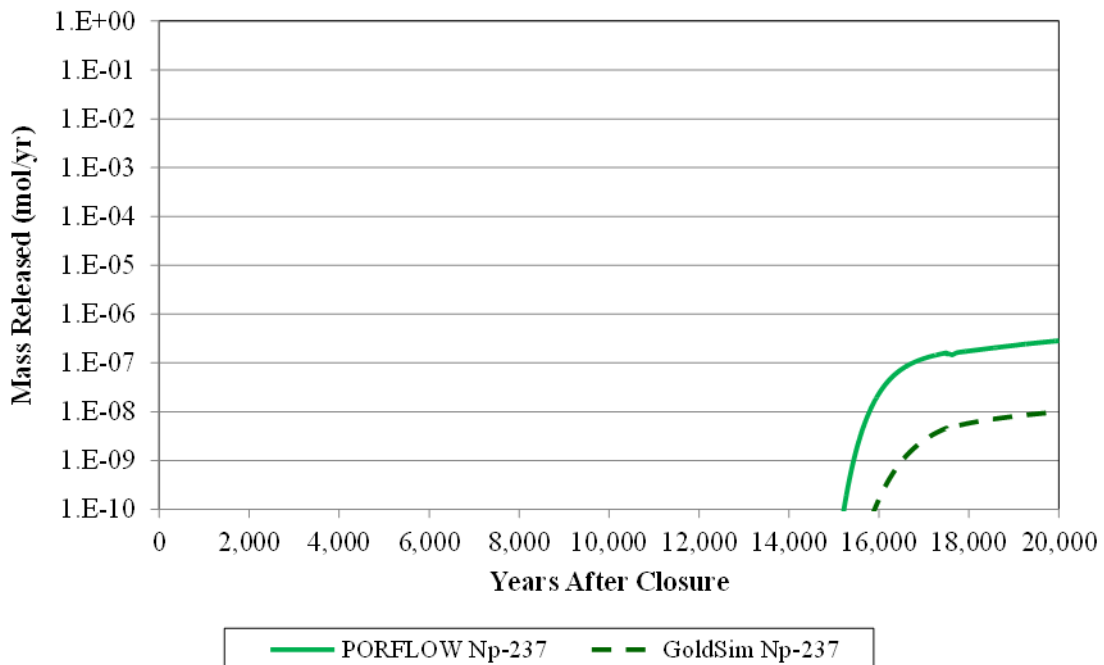


Figure A.1-41: Ra-226 Release from Tank 40 (Case A)

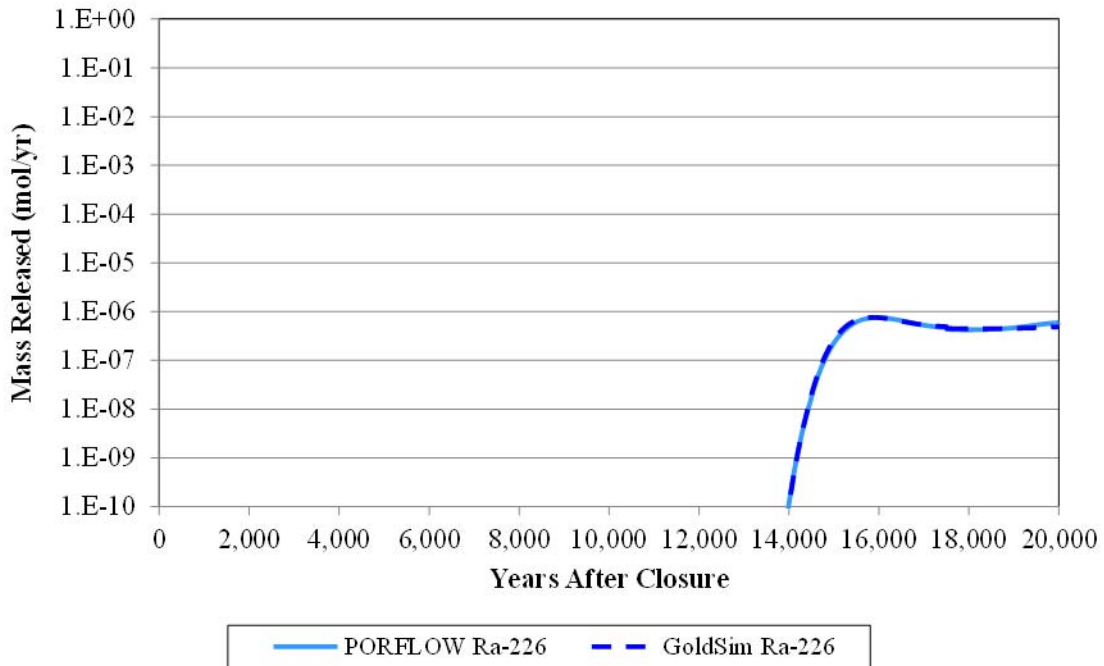


Figure A.1-42: Tc-99 Release from Tank 40 (Case A)

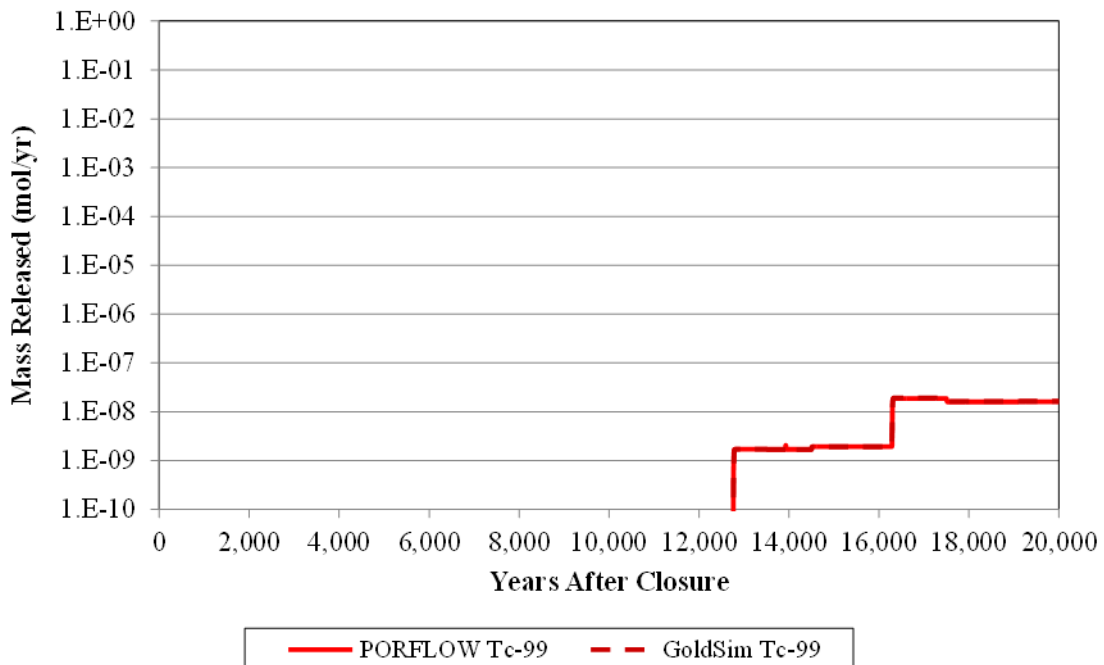


Figure A.1-43: I-129 Release from Tank 40 (Case A)

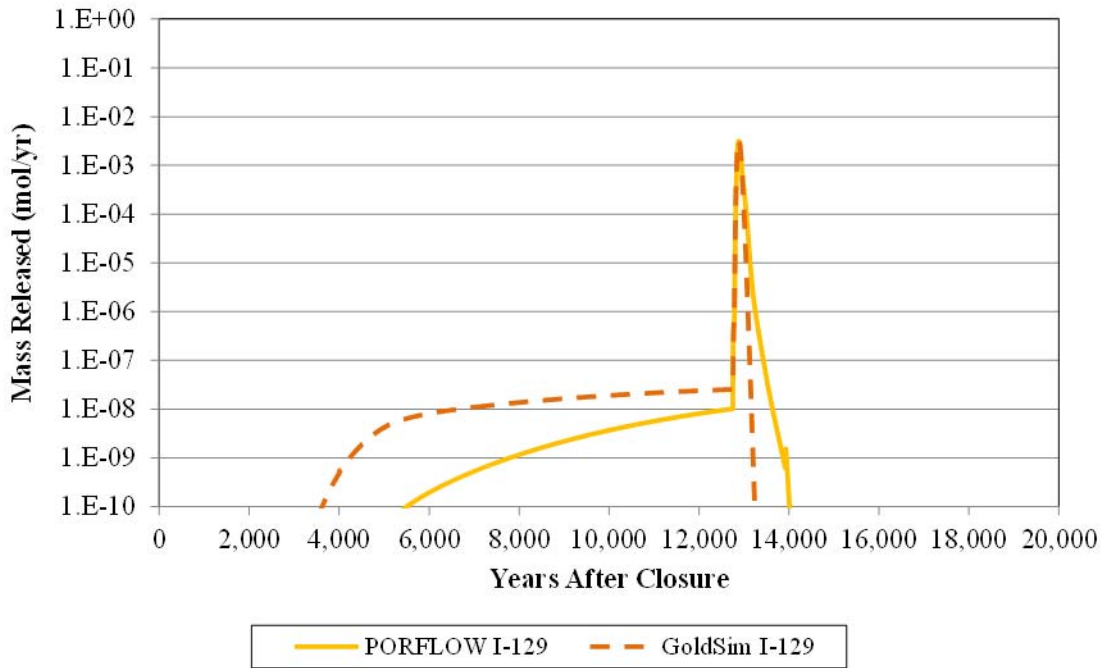


Figure A.1-44: Cs-135 Release from Tank 40 (Case A)

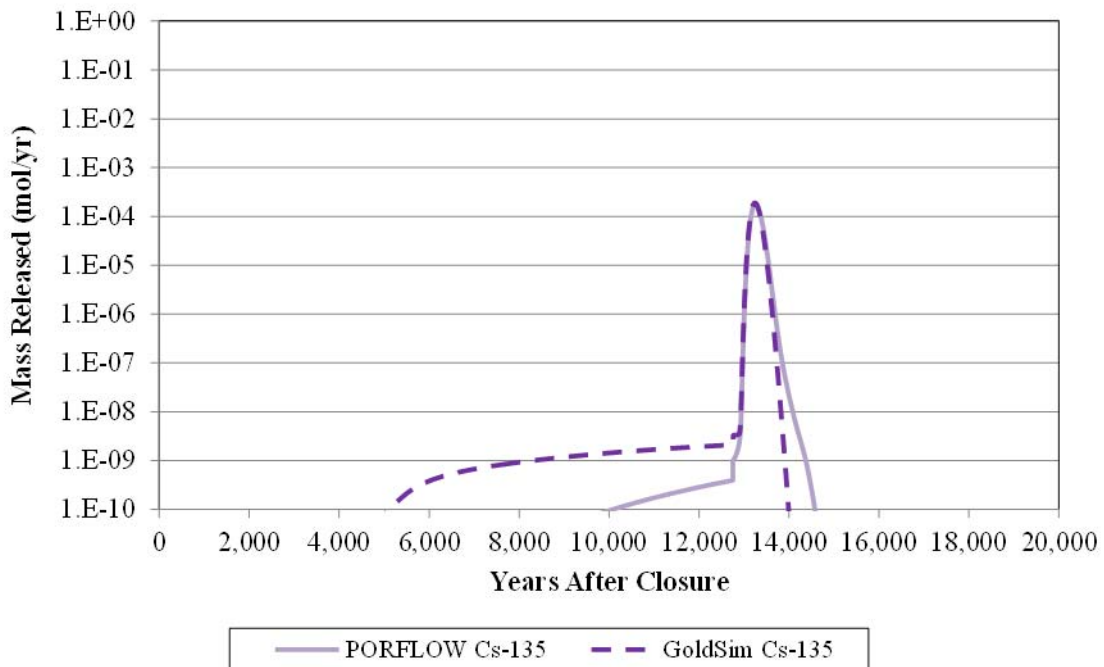


Figure A.1-45: Np-237 Release from Tank 40 (Case A)

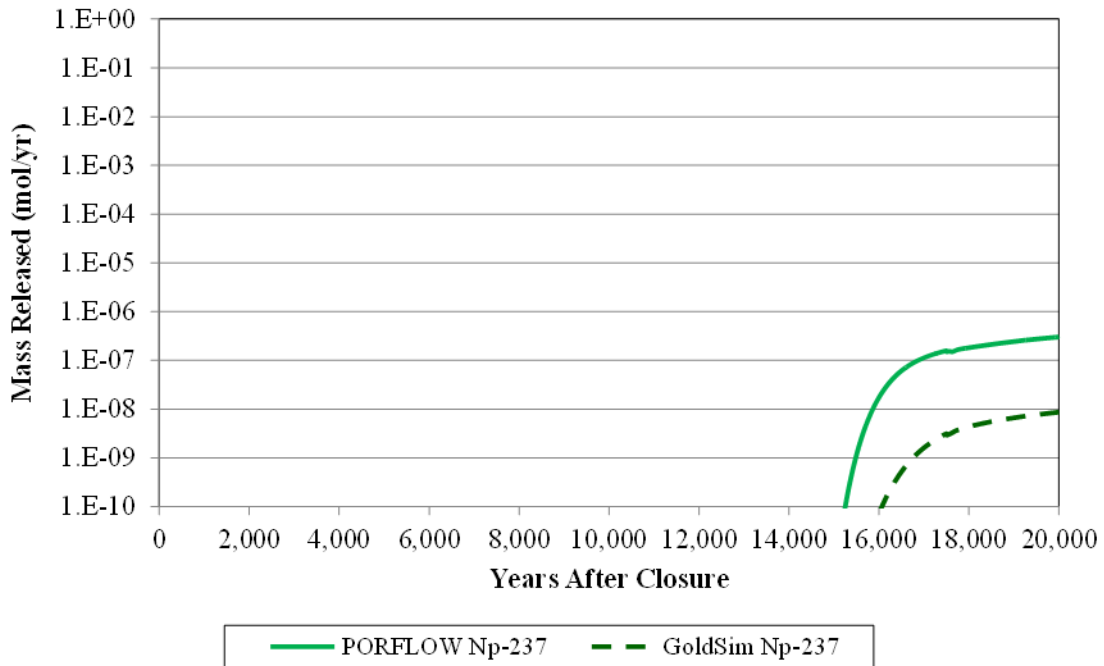


Figure A.1-46: Ra-226 Release from HPT-7 (Case A)

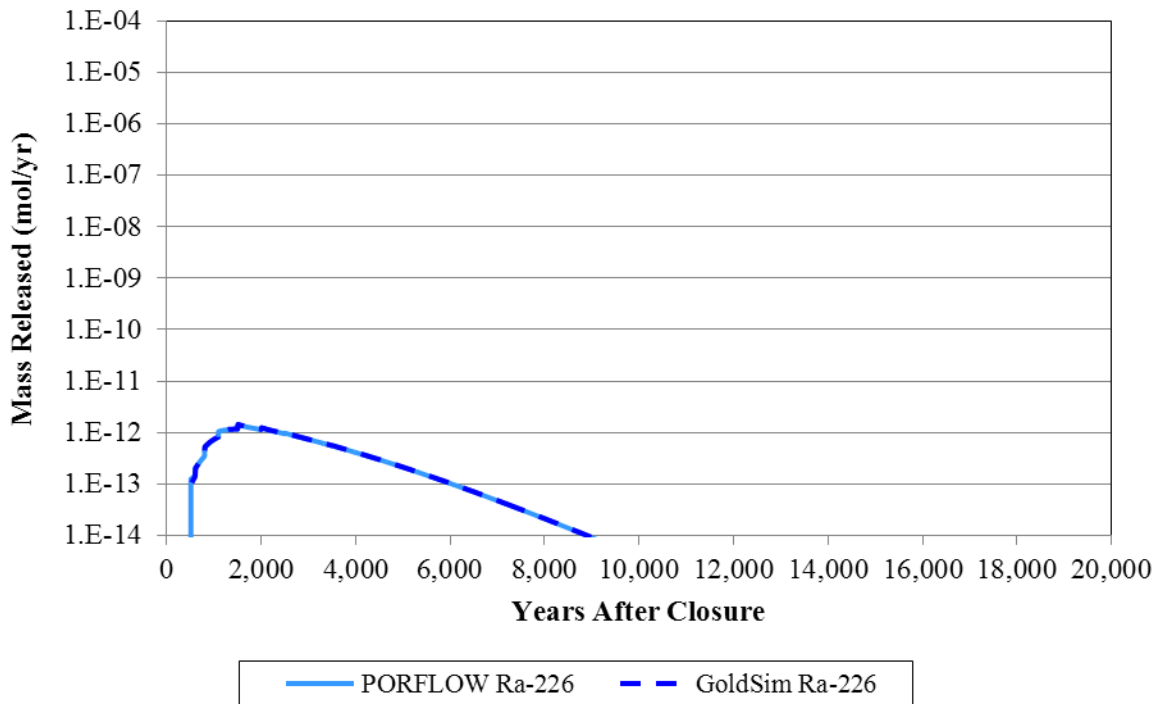


Figure A.1-47: Tc-99 Release from HPT-7 (Case A)

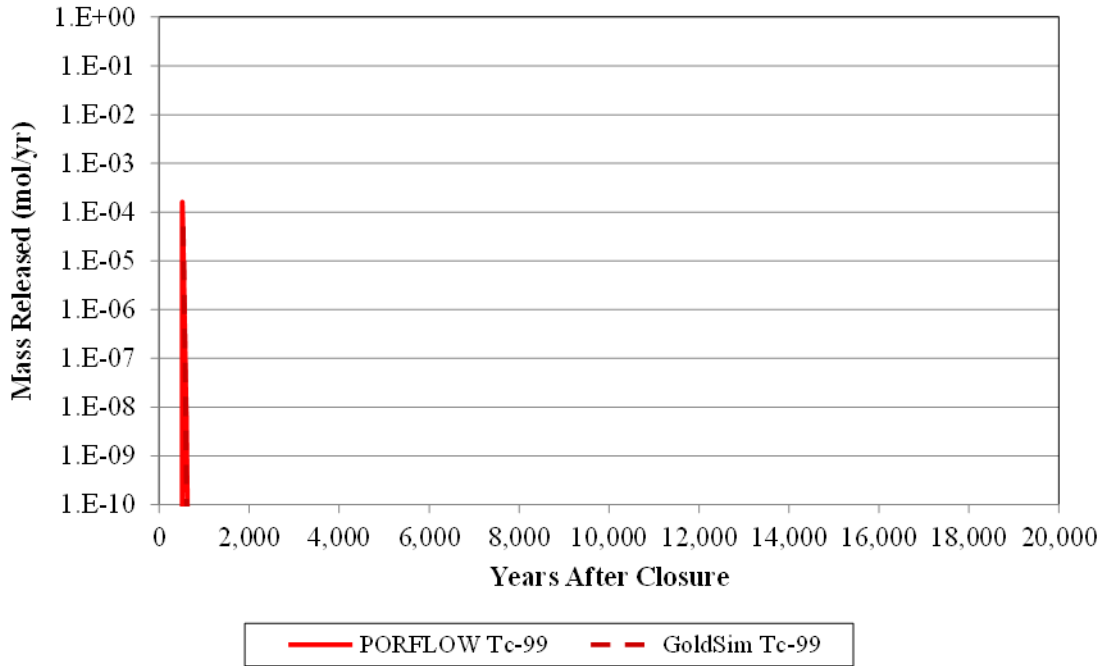


Figure A.1-48: I-129 Release from HPT-7 (Case A)

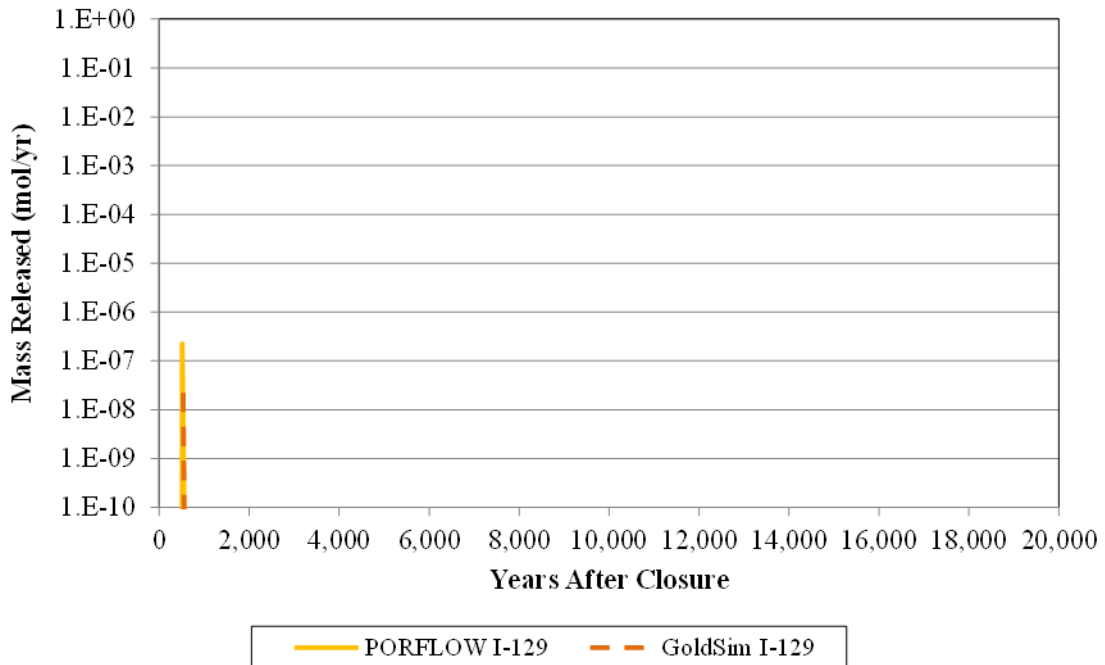


Figure A.1-49: Cs-135 Release from HPT-7 (Case A)

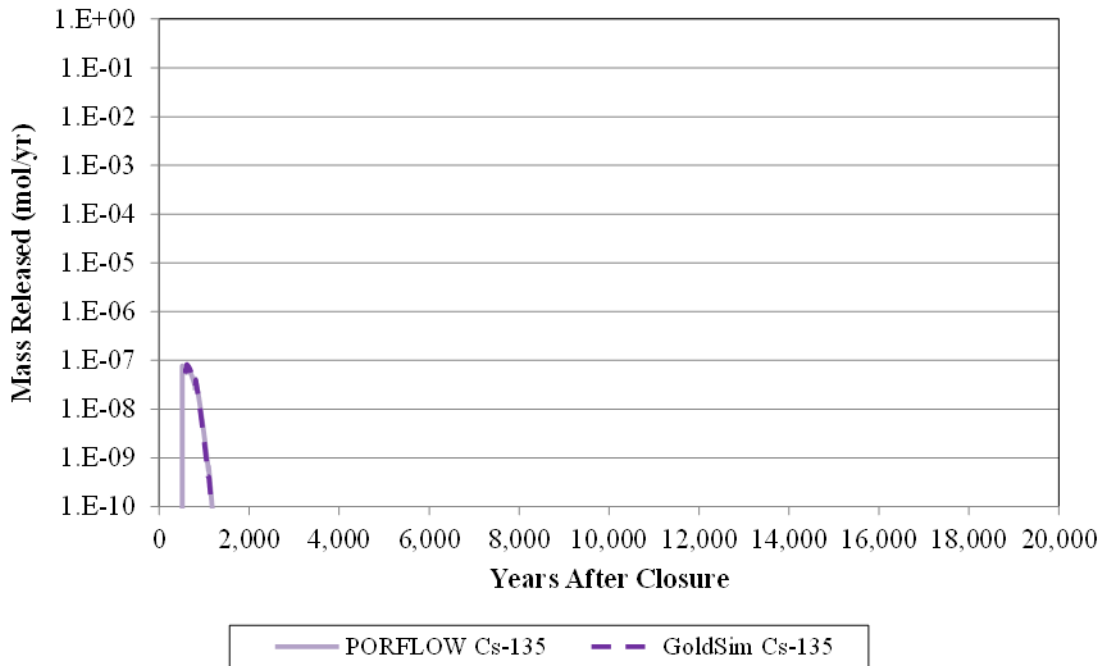


Figure A.1-50: Np-237 Release from HPT-7 (Case A)

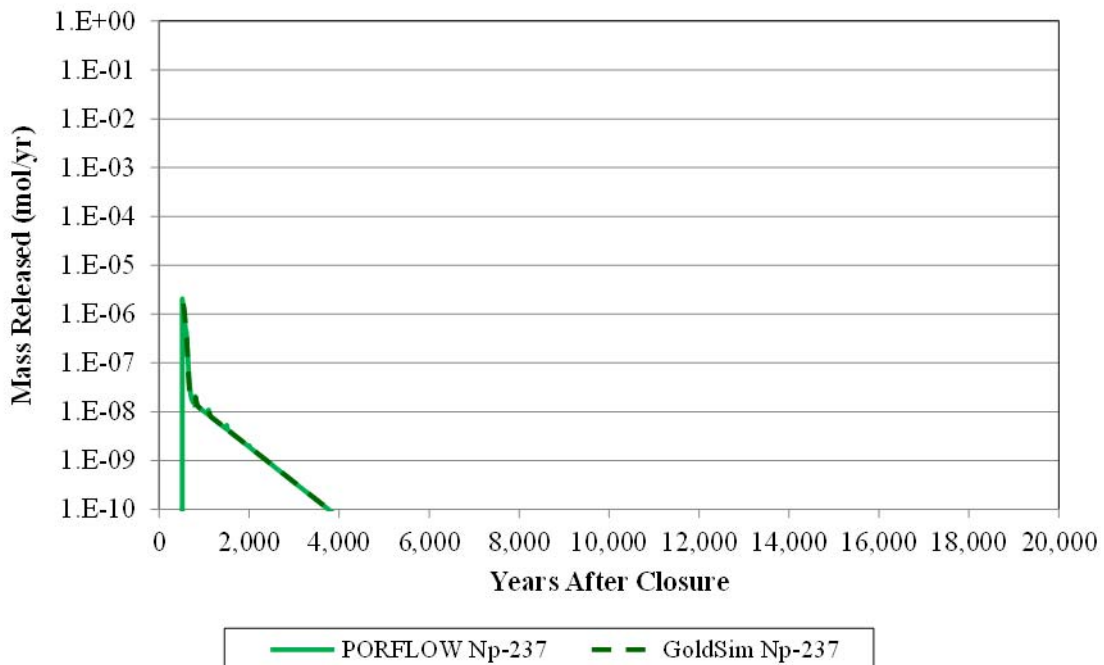


Figure A.1-51: Ra-226 Release from Transfer Line, Zone 3 (Case A)

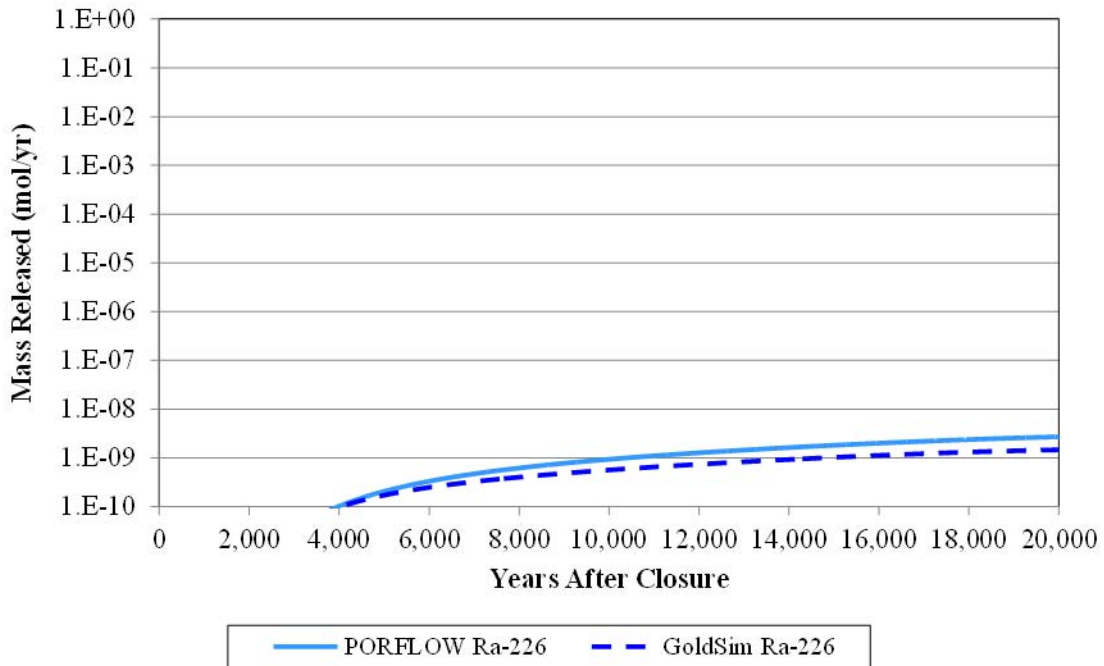


Figure A.1-52: Tc-99 Release from Transfer Line, Zone 3 (Case A)

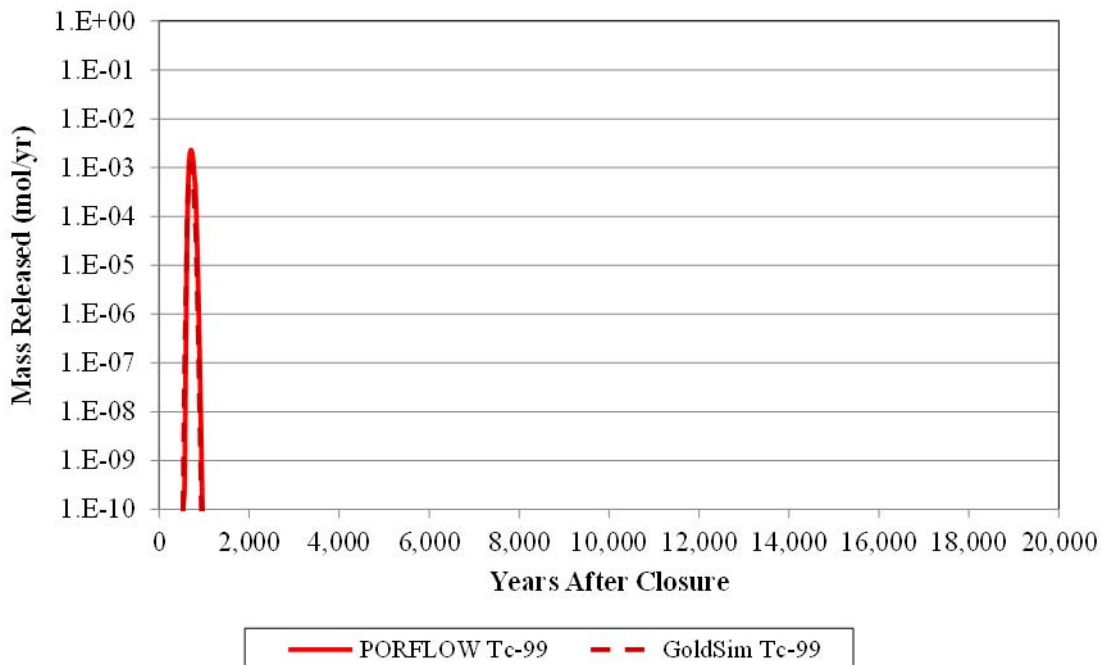


Figure A.1-53: I-129 Release from Transfer Line, Zone 3 (Case A)

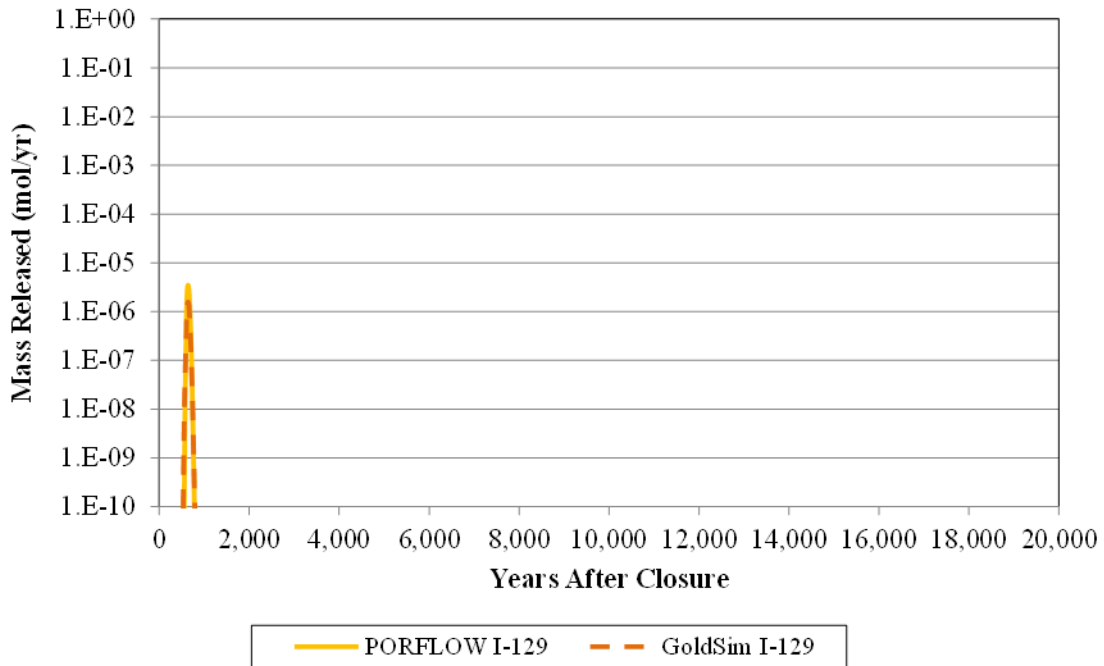


Figure A.1-54: Cs-135 Release from Transfer Line, Zone 3 (Case A)

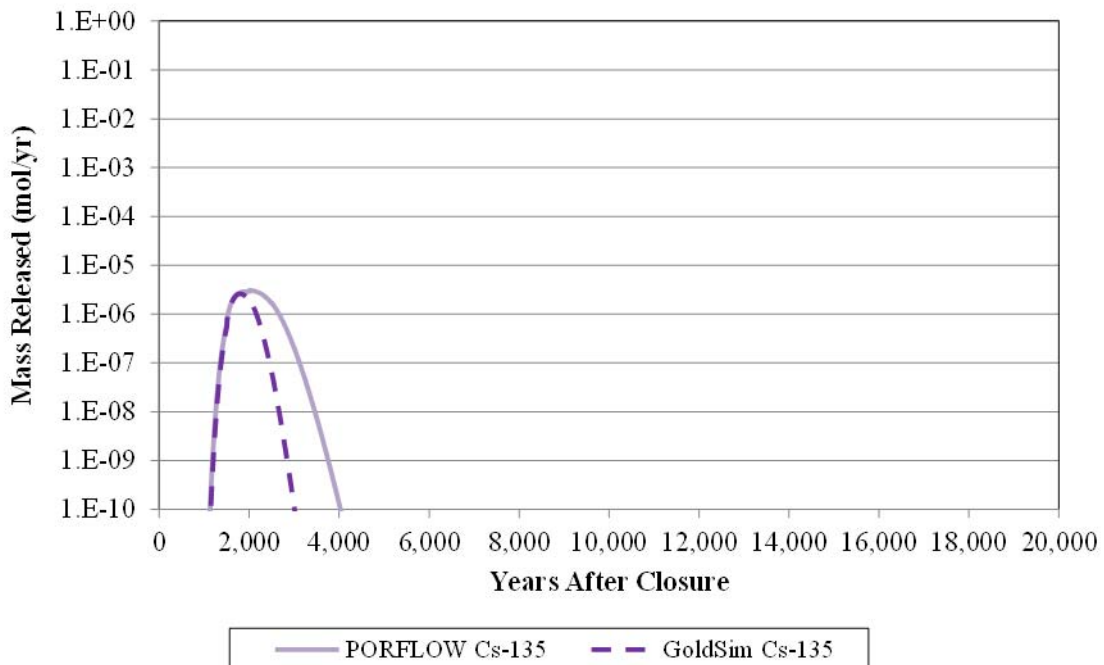


Figure A.1-55: Np-237 Release from Transfer Line, Zone 3 (Case A)

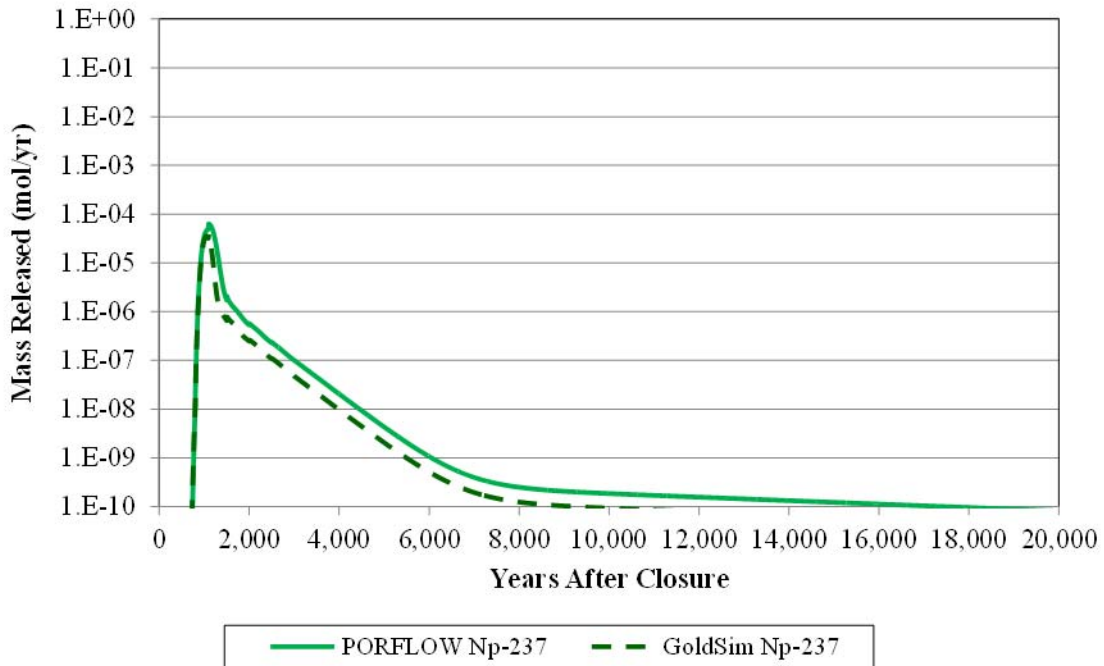


Figure A.1-56: Ra-226 Release from E242-25H (Case A)

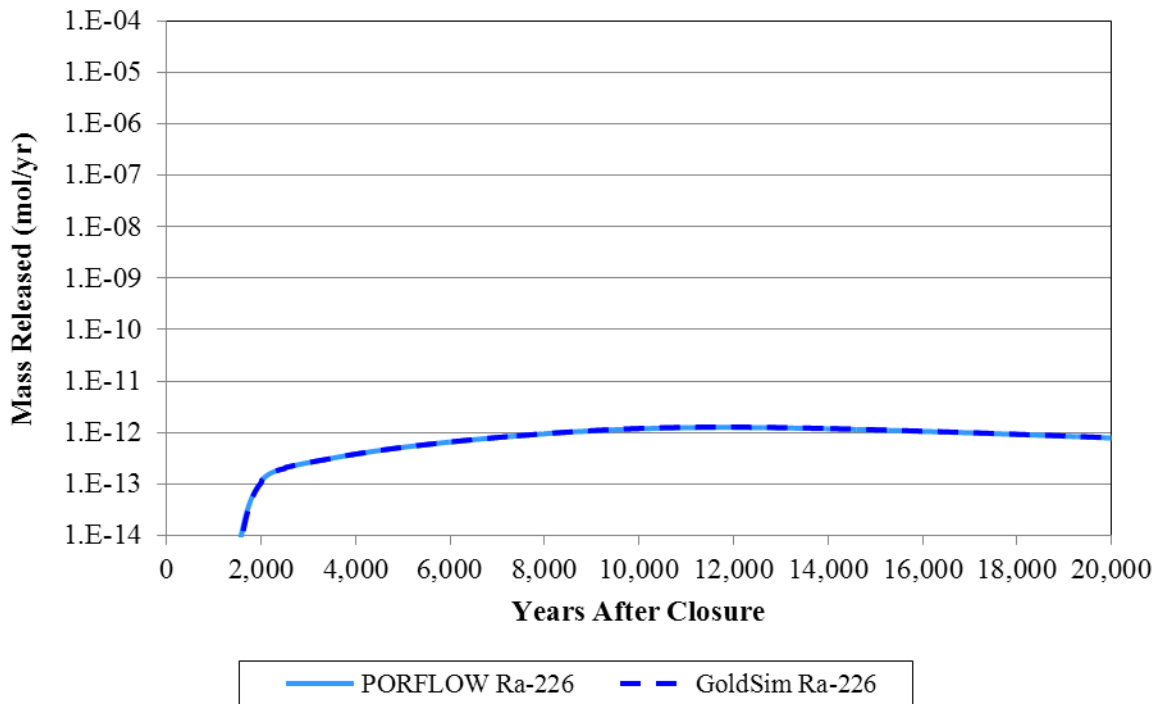


Figure A.1-57: Tc-99 Release from E242-25H (Case A)

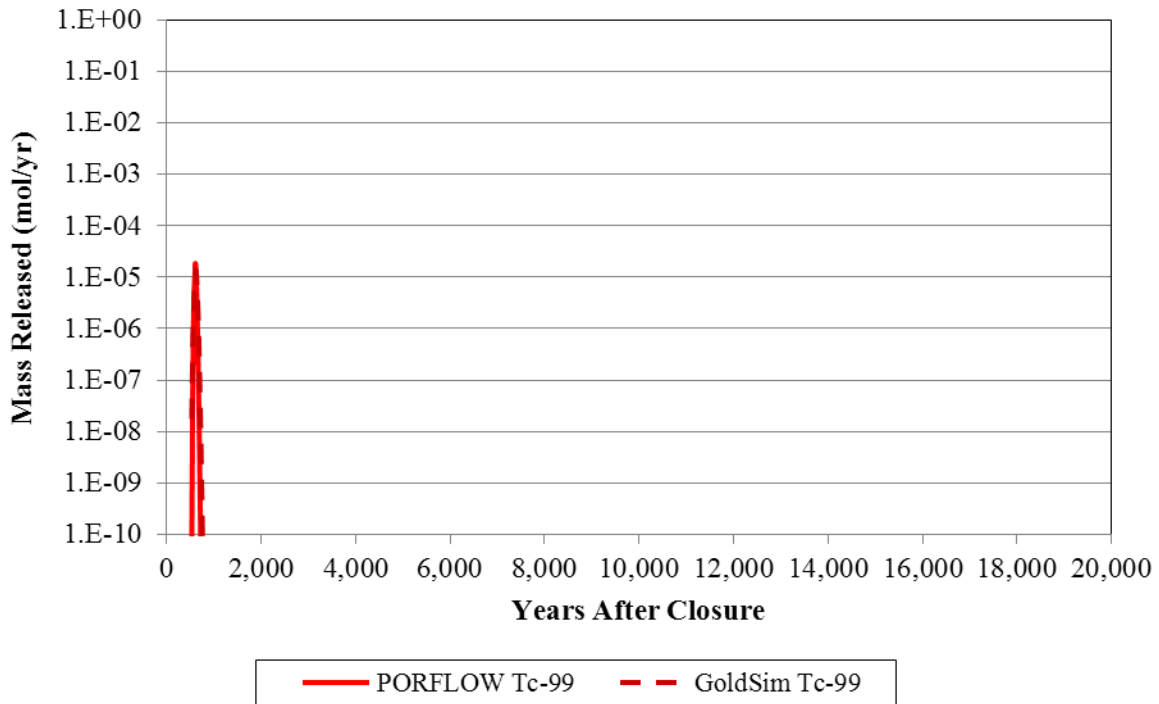
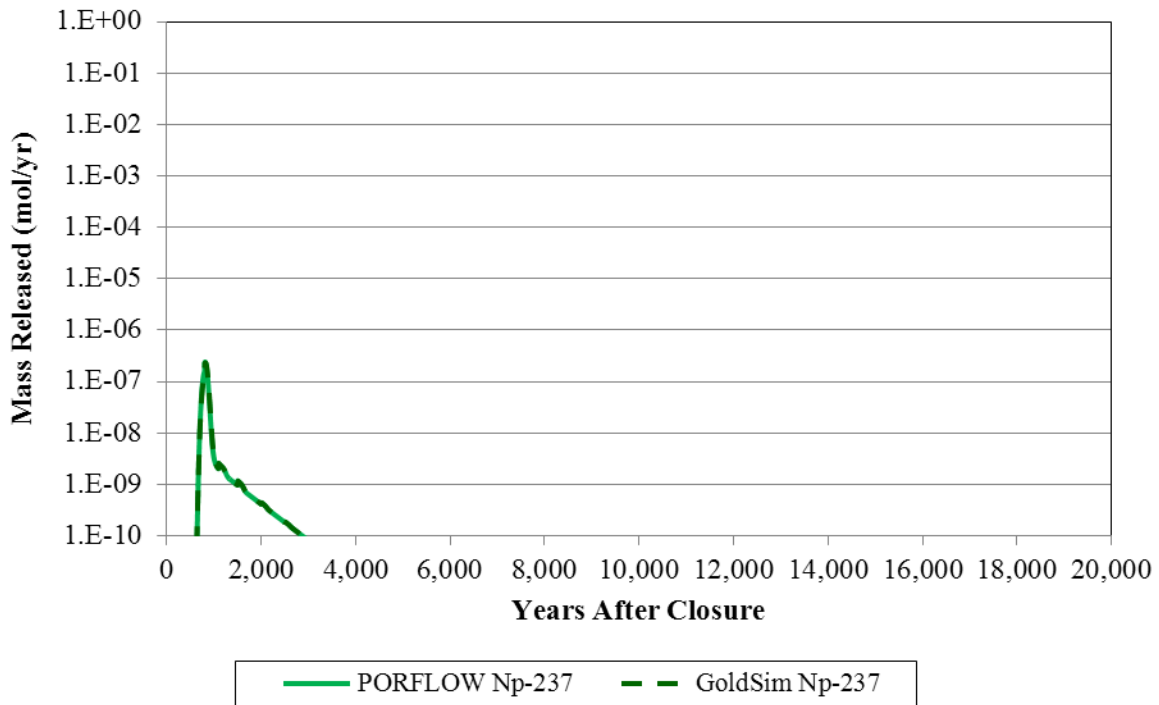


Figure A.1-58: Np-237 Release from E242-25H (Case A)



A.2 Benchmarking Stage Two

The second stage of the GoldSim benchmarking effort consisted of a comparison of species-specific PORFLOW generated dose contributions (in mrem/yr) at the 100-meter boundary in the SZ with HTF GoldSim Model generated results. The benchmarking results for the Case A HTF simulations are presented below.

Figure A.2-1: HTF PORFLOW Model Species-Specific Dose Contributions for Sector A

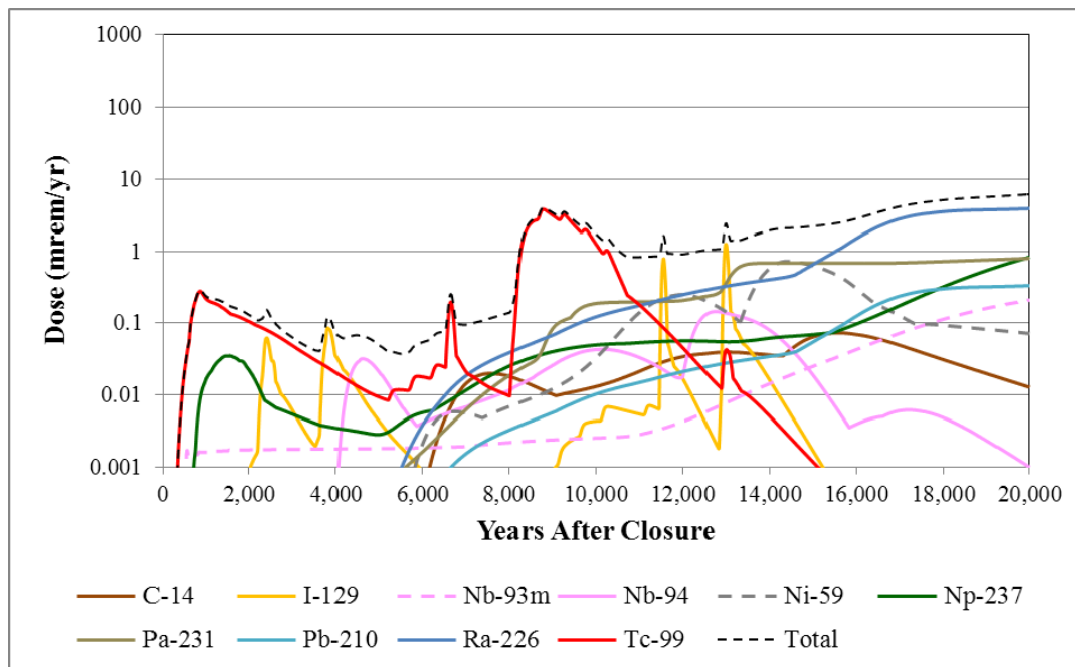


Figure A.2-2: HTF GoldSim Model Species-Specific Dose Contributions for Sector A

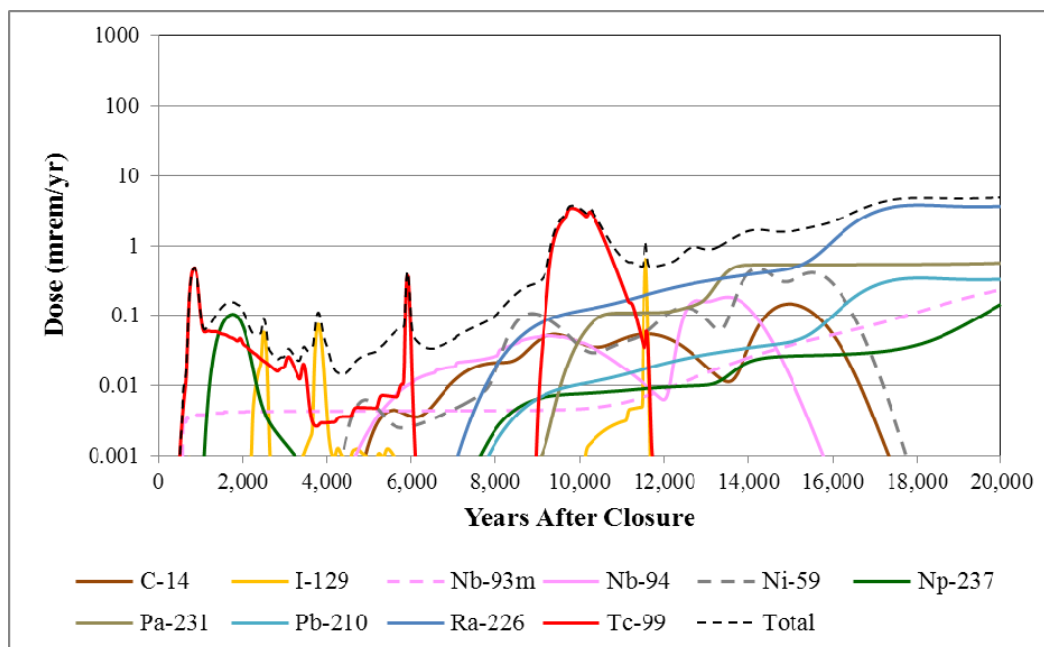


Figure A.2-3: HTF PORFLOW Model Species-Specific Dose Contributions for Sector B

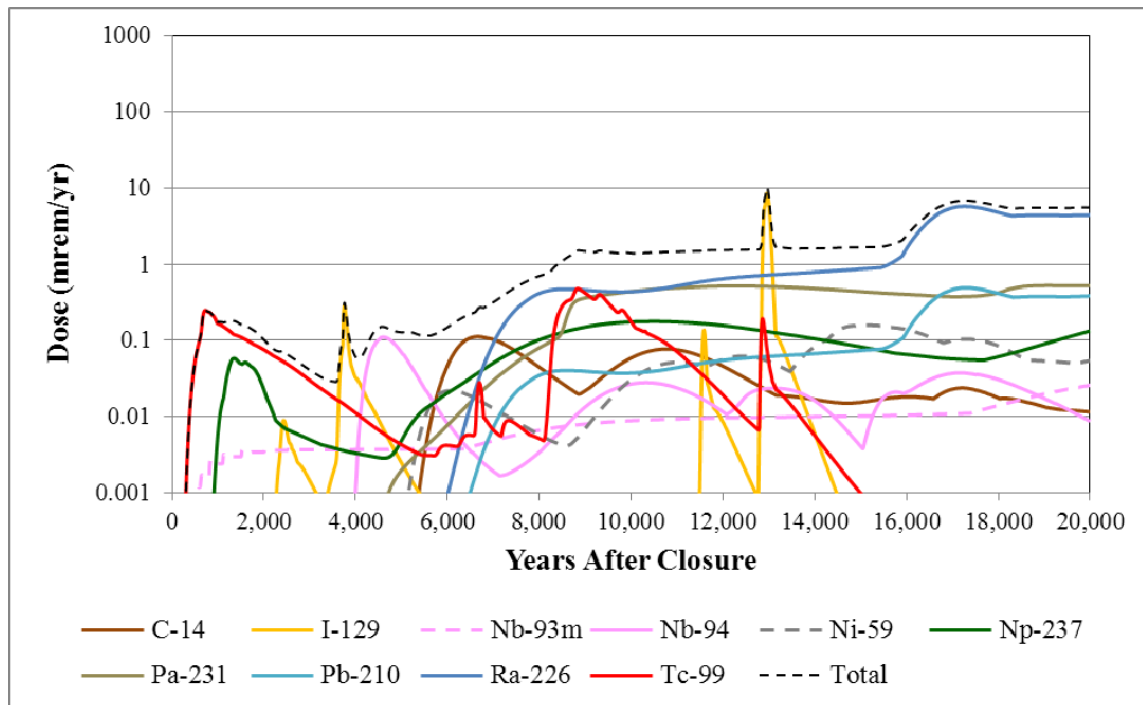


Figure A.2-4: HTF GoldSim Model Species-Specific Dose Contributions for Sector B

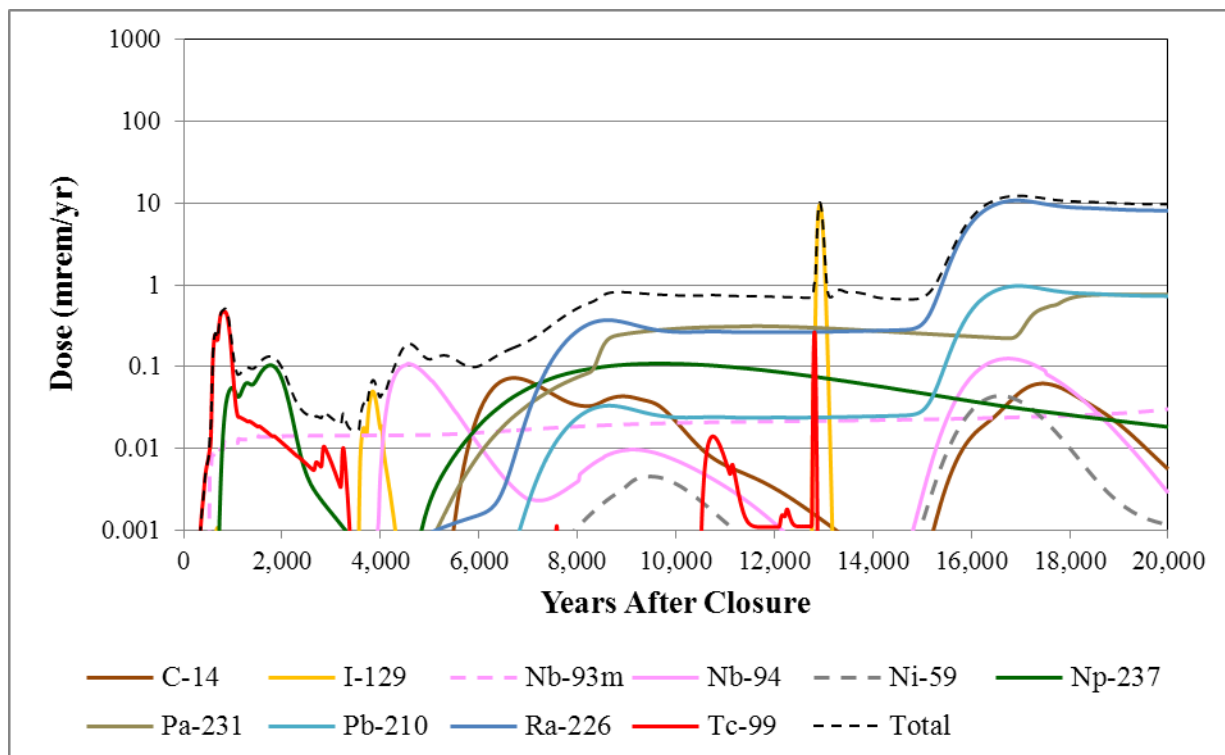


Figure A.2-5: HTF PORFLOW Model Species-Specific Dose Contributions for Sector C

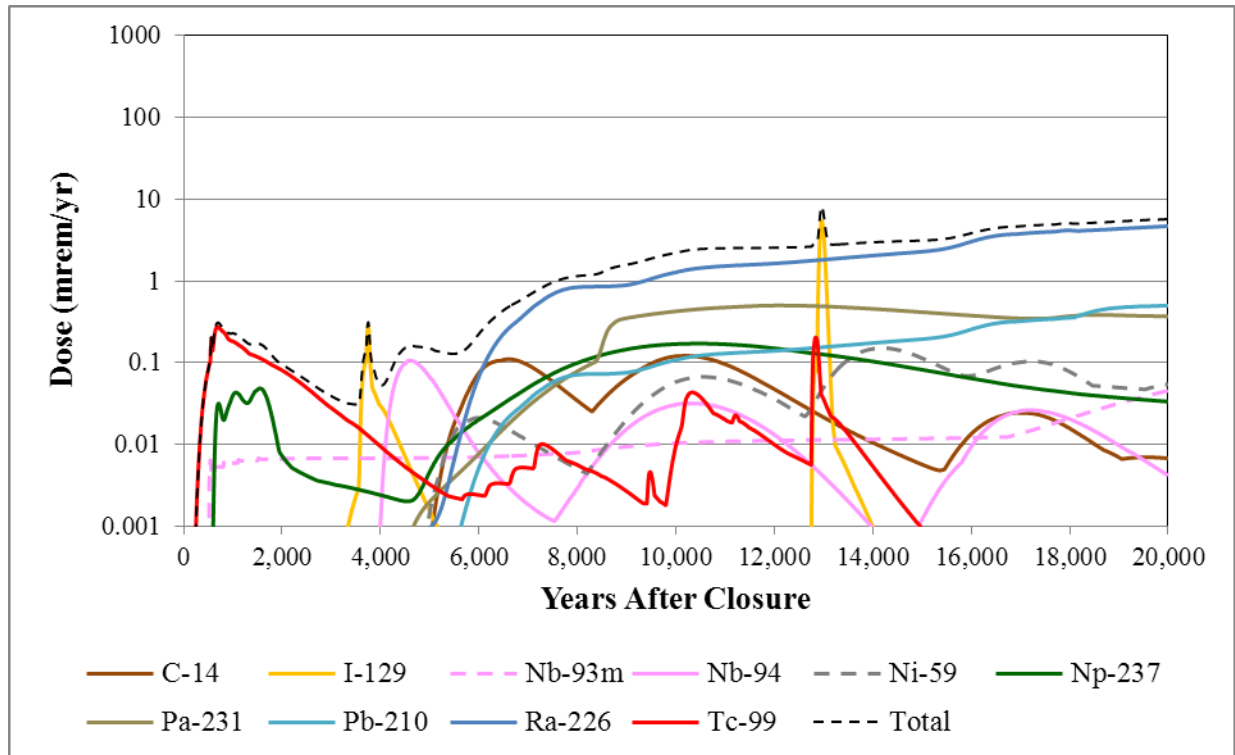


Figure A.2-6: HTF GoldSim Model Species-Specific Dose Contributions for Sector C

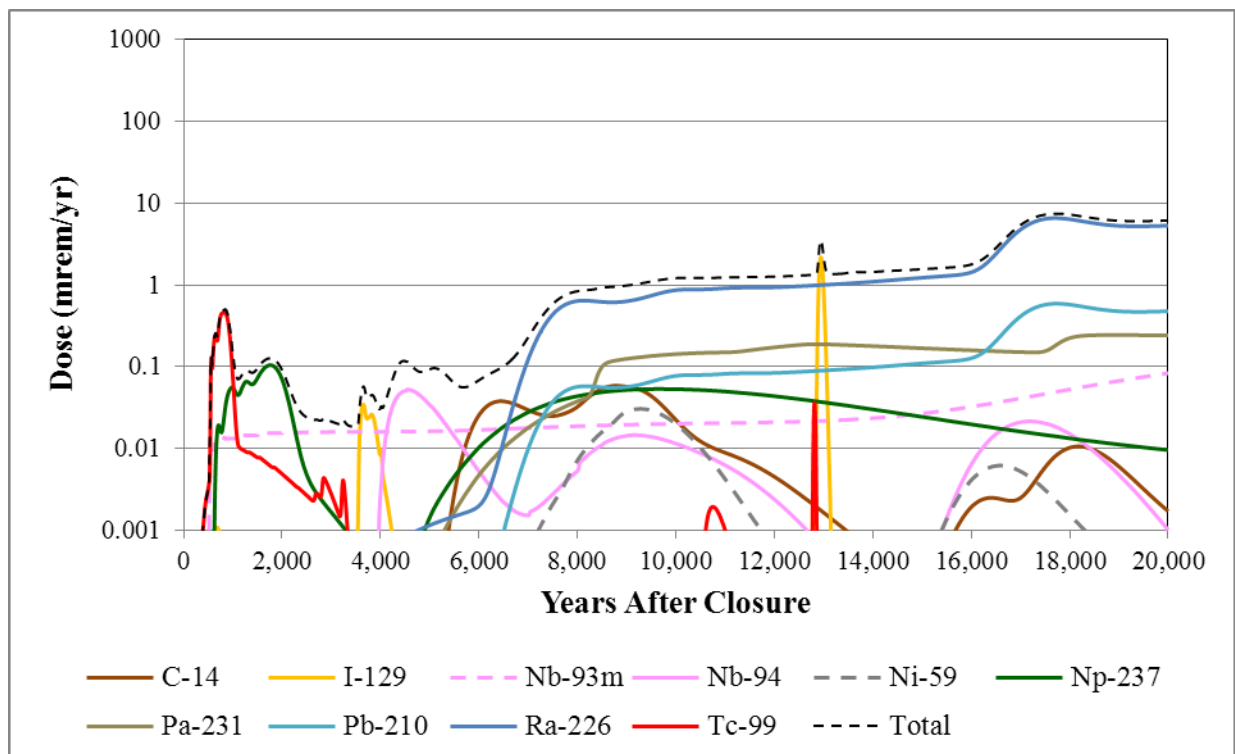


Figure A.2-7: HTF PORFLOW Model Species-Specific Dose Contributions for Sector E

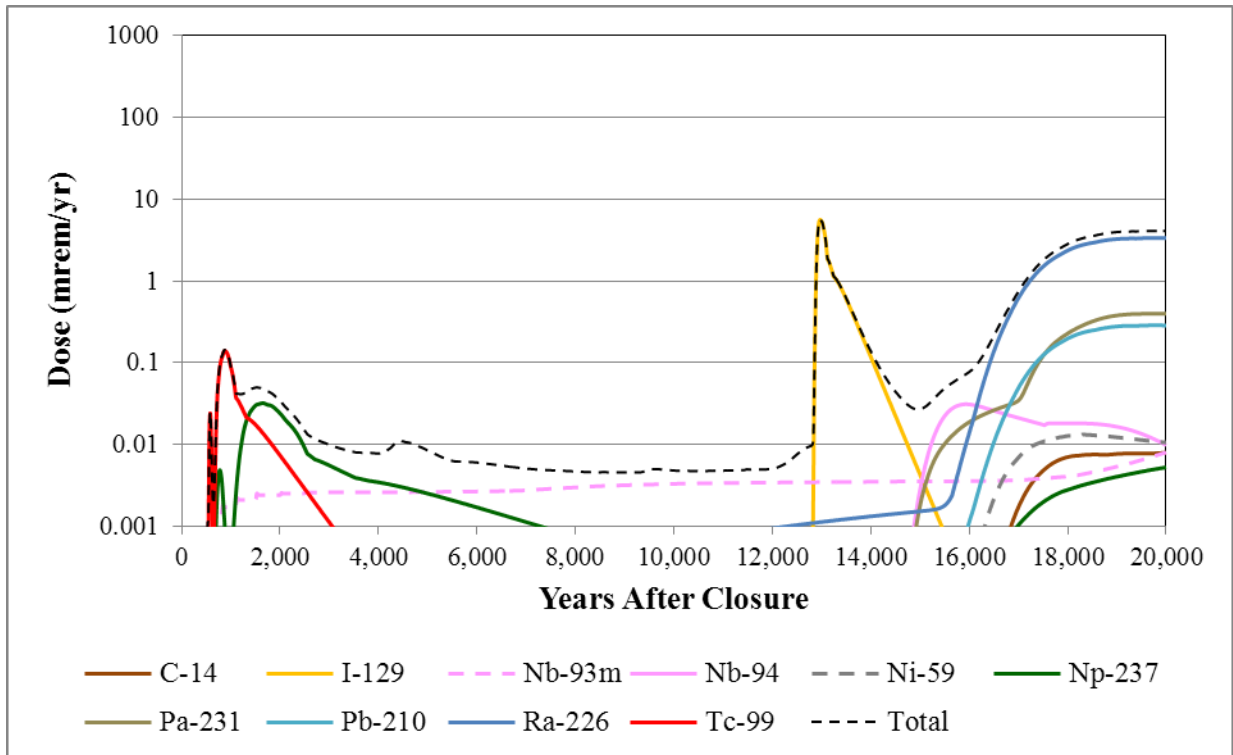


Figure A.2-8: HTF GoldSim Model Species-Specific Dose Contributions for Sector E

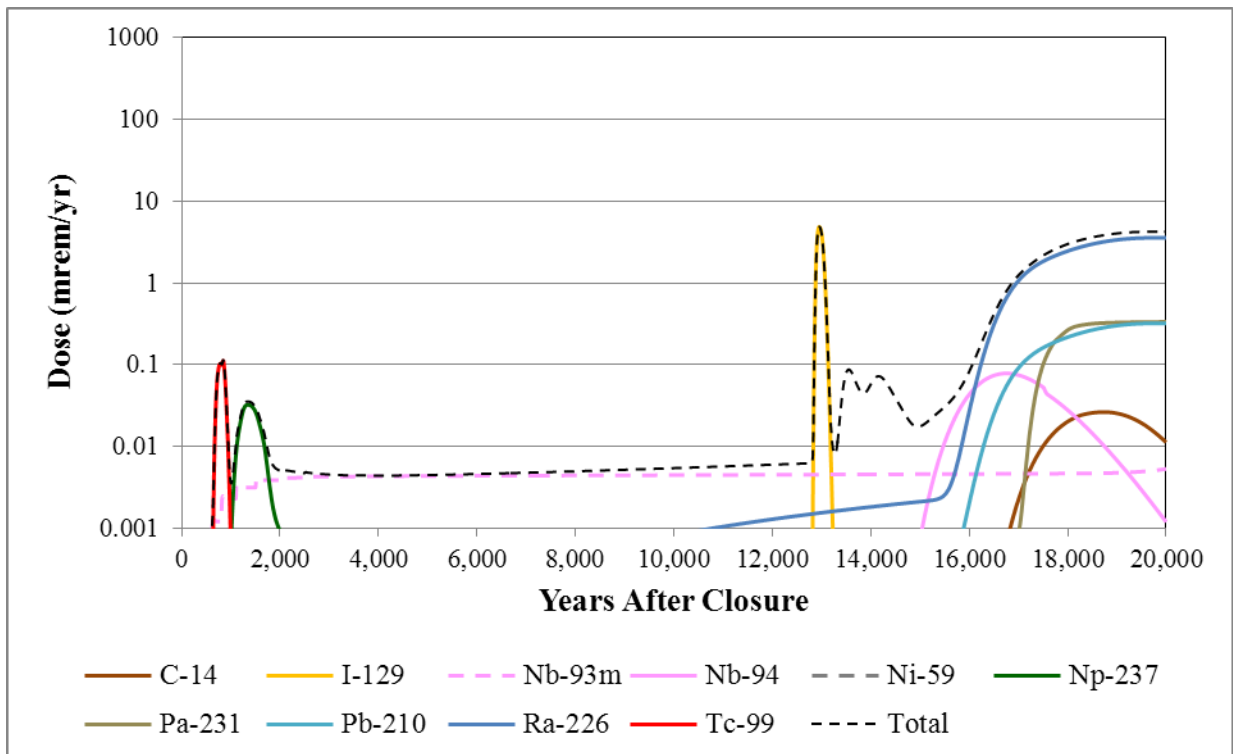


Figure A.2-9: HTF PORFLOW Model Species-Specific Dose Contributions for Sector F

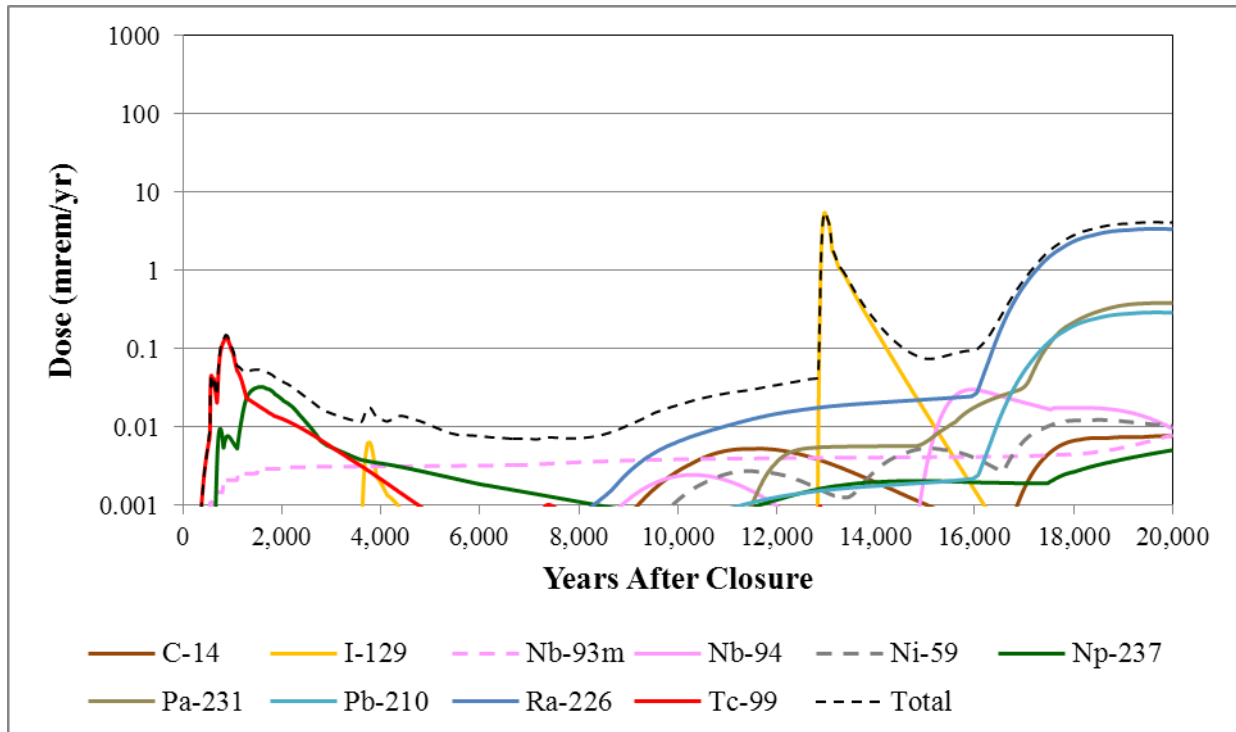
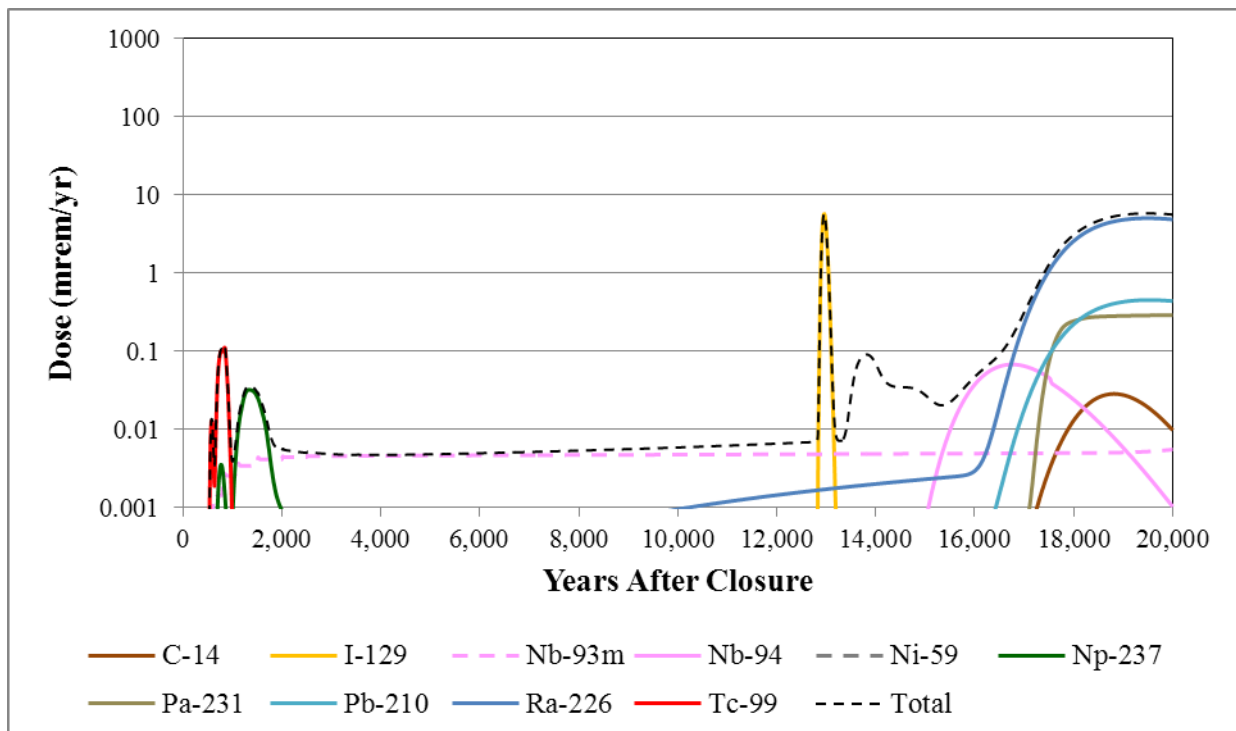


Figure A.2-10: HTF GoldSim Model Species-Specific Dose Contributions for Sector F



APPENDIX B

B.0 Errata

After this report was finished, an error was found in the original PORFLOW simulation for the Tank 12 radionuclide release to the saturated zone. The input data had a small error in the Eh and pH transition times. This error was reflected in the tank release results and was perceptible in the Tank 12 Tc-99 graphical results presented in Section A.1. Therefore, the results presented in Section A.1 were updated. In addition, this error slightly influences near-field release results presented in the IHI scenario write-up in Section 7.1.4. Therefore, the calculations and the plot presented in Section 7.1.4 were updated. A comparison of 100-meter boundary dose results for Sector A presented in Figure B.0-1 shows that only a slight difference at around 6,500 years can be discerned between the incorrect and corrected results. This difference would not be perceptible in dose results for the other sectors or in the maximum dose results. Therefore, the 100-meter boundary dose plots presented in Section 7.1.3 and A.2 were not updated.

Figure B.0-1: Comparison of Incorrect and Corrected 100-Meter Total Dose Results for Sector A

